



**Channel and Watershed Processes Research Unit
National Sedimentation Laboratory
Oxford, Mississippi**

**ACTUAL AND REFERENCE SEDIMENT YIELDS FOR THE JAMES
CREEK WATERSHED - MISSISSIPPI**



By Andrew Simon, Ronald L. Bingner, Eddy J. Langendoen, and Carlos V. Alonso

Research Report No. 31

August 12, 2002

**ACTUAL AND REFERENCE SEDIMENT YIELDS FOR THE
JAMES CREEK WATERSHED – MISSISSIPPI**

Prepared by

**Channel and Watershed Processes Research Unit
National Sedimentation Laboratory
Oxford, Mississippi**

For

Mississippi Department of Environmental Quality

August 12, 2002

ACTUAL AND REFERENCE SEDIMENT YIELDS FOR THE JAMES CREEK WATERSHED – MISSISSIPPI

ARS Designated Representative and Project Manager:

Carlos V. Alonso

Technical Direction, Data Analysis, and Report Preparation by:

Andrew Simon, Ronald L. Bingner, and Eddy J. Langendoen

Mapping, GIS and Model Execution:

Robert Wells, Yongping Yuan, Vance G. Justice, and Igor Jaramillo

Field Operations and Database Management:

Mark Griffith and Vance Justice

Field Data Collection and Data Processing:

Mark Griffith , Charlie Dawson, Brian Bell, Robert Wells, Nick Jokay, Anthony Lazell, Lauren Farrugia, Igor Jaramillo, Micah Fendiesen, Vance Justice, and Yongping Yuan

EXECUTIVE SUMMARY

At the request and support of the Mississippi Department of Environmental Quality (MDEQ), the Channel and Watershed Processes Research Unit, National Sedimentation Laboratory embarked on a 90-day study of sediment loadings in James Creek, Monroe County, Mississippi. The principal objective of the study was to determine “actual” sediment-transport rates and rates for similar, but stable or unimpaired (“reference”) streams by which MDEQ could develop water-quality targets for sediment. Without historical sediment-transport data for James Creek a combination of methods were used including empirical analysis of historic data from other sites, field reconnaissance and detailed data collection and surveying, and numerical modeling of uplands and channels.

“Reference” suspended-sediment transport rates were obtained from stable streams with historical flow and sediment-transport data in the Southeastern Plains Ecoregion. Using the discharge that occurs, on average every 1.5 years ($Q_{1.5}$) as the “effective discharge” and a flow rate that represents long-term sediment-transport conditions, an initial “general reference” of 0.31 T/d/km^2 was obtained. This value, however, is skewed towards streams with sand beds and does not accurately reflect conditions along James Creek. A refined “reference” condition was developed for stable silt/clay-bed streams in the Southeastern Plains resulting in a “reference” suspended-sediment yield of 3.23 T/d/km^2 at the $Q_{1.5}$. Although silt/clay bed substrates dominate James Creek, some reaches’ substrate are largely sands and/or gravels. A weighted-reference condition based on the percentage of the drainage area encompassed by the various bed-material types results in a reference yield at the $Q_{1.5}$ of 2.22 T/d/km^2 . This is converted to a “reference” suspended-sediment load at the watershed outlet of 249 T/d . Similarly, an equivalent weighted-reference suspended-sediment concentration of 160 mg/l was obtained.

“Actual” sediment-transport rates were obtained by three mechanisms: simulations of flow and sediment transport using the AnnAGNPS watershed model and the CONCEPTS channel-evolution model; and direct comparisons of measured cross sections from 1967 and 2002. AnnAGNPS simulations were conducted using actual precipitation data from Aberdeen, Mississippi as well as using generated precipitation data. AnnAGNPS was used in combination with CONCEPTS to take advantage of the best features of each of these models, AnnAGNPS for uplands and CONCEPTS for the main-stem channel. The resulting simulated flows were compared to peak flows recorded by the USGS at the Highway 25 bridge and showed close agreement. Sediment-transport rates are provided for the watershed outlet, at Darracott Road, and the Highway 25 bridge over the period 1967 - 2002.

Average sediment loads at the mouth of James Creek over the 35-year period are about 250,000 T/y with about 89% of this material emanating from James Creek and its tributaries with only 11 % derived from upland sources. Of this 89% eroded from the channel boundaries, about 88% comes from the channel banks. This loading value, however, is somewhat misleading in that severe channel erosion occurred between 1967-1968 following channel clearing and snagging operations over the lower 17 km of James Creek. Since this time, sediment loads have attenuated and the contributions from channels and uplands over the period 1970-2002 are 70% and 30%, respectively.

“Actual” suspended-sediment yields at the $Q_{1.5}$ as simulated by AnnAGNPS in combination with CONCEPTS show a 35-year average of 675 T/d/km^2 (3.0 tons/d/acre). However, the average over the past 10 years is 155 T/d/km^2 (0.69 tons/d/acre) and, following the installation of additional low-water crossings in 1999 further reduced yields to about 39 T/d/km^2 (0.17 tons/d/acre) Converting these values to “actual” suspended-sediment loads by multiplying by drainage area at the Highway 25 bridge gives 35-, 10- and three-year averages of 50,000 T/d, 11,500 T/d, and 2,880 T/d, respectively.

Results of this study indicate that a significant proportion of the sediment in the James Creek watershed emanates from stream channels and not from uplands and fields. Subsequent decisions regarding reducing sediment loadings will need to pay particular attention to stream-channel processes and stabilizing eroding reaches and tributaries of James Creek.

ACKNOWLEDGMENTS

This project was performed in support of the Reimbursable Cooperative Agreement number 58-6408-2-0029 funded by the Mississippi Department of Environmental Quality entitled “Actual and Reference Sediment Yields for the James Creek Watershed – Mississippi”. This intensive study of sediment loadings in the James Creek watershed could not have been accomplished in such a short timeframe without the exceptional dedication and efforts put forth by staff of the Channel and Watershed Processes Research Unit. The following individuals are to be singled out for their important role in helping to complete this project on time.

The AnnAGNPS input database for the watershed was assembled and developed by Dr. Yongping Yuan and Vance Justice, including verification of the input parameters. Additional technical support was provided by Dr. Fred Theurer of the USDA-NRCS on the selection of appropriate input parameters. Steve Holman, NRCS Monroe County District Conservationist, supplied landuse information, and Robert Wimbish provided the sequence of operations associated with the crops produced on James Creek watershed. Jackie Moore transcribed the weather data from Aberdeen, Mississippi, from printed copies to the AnnAGNPS-input digital format.

The field channel program was concluded efficiently and on time due largely to the efforts of Mark Griffith and Charlie Dawson. Robert Wells was instrumental in conducting field reconnaissance, channel surveys and providing leadership in data analysis, and performed the bulk of the channel-evolution modeling. Brian Bell, Lauren Farrugia, Tony Layzell, Nick Jokay, and Igor Jaramillo contributed weeks of efficient field support.

It is important to also acknowledge the support of Chris Zabawa, Tom Davenport and Jim Greenfield with the U.S. Environmental Protection Agency who have provided research funding at the national and regional levels to develop the “reference” methodology used in this report.

TABLE OF CONTENTS

ACKNOWLEDGMENTS	v
LIST OF TABLES	ix
LIST OF FIGURES	xi
INTRODUCTION.....	1
Background and Problem.....	1
Objectives and Scope.....	2
WATERSHED AND CHANNEL CONDITIONS	3
Basin Characteristics.....	3
Ecoregion 65: Southeastern Plains.....	3
Surficial Geology	3
Land Use	5
Climate.....	7
Channel Characteristics	7
Human Intervention	8
Channelization (1905).....	8
Clearing and Snagging (1967)	8
Low-water Crossings	8
Construction of the Tennessee-Tombigbee Waterway.....	9
Streamflow	9
Boundary Materials.....	11
OVERVIEW OF METHODOLOGY	12
Characterization of “Reference” Suspended-Sediment Loading.....	12
Characterization of “Actual” Sediment Loading	12
General Description of AGNPS Modeling Technology	13
Input Data Requirements	14
Contributions from Tributaries into the Main Channel	14
Contributions from AnnAGNPS Cells Adjacent to the Main Channel	14
General Description of CONCEPTS Modeling Technology.....	15
Hydraulics.....	15
Sediment Transport and Bed Adjustment.....	15
Streambank Erosion	15
Input Data Requirements	16
Simulation Scenarios	16
Conventional Tillage.....	17
Reduced Tillage	17
Stable and Unstable Channel Reaches.....	17
DEVELOPMENT OF DATABASES.....	18
Aerial and Ground Reconnaissance	18
Watershed Reconnaissance.....	19
Channels Reconnaissance	19
Input Database for the AGNPS Model	21
GIS Database	21
Topographic Analysis	22
DEMs	22

Modification of DEMs.....	23
Digitized Soils Maps.....	23
Digitized Landuse Maps.....	24
National Agricultural Statistics Service (NASS) Landuse.....	24
Multi-Resolution Land Characteristics (MRLC) Landuse.....	25
Landuse from the NRCS Monroe County District Conservationist Office.....	25
Landuse Derivation for Use with AnnAGNPS.....	25
Additional GIS Layers.....	28
Digital Raster Graphics (DRG's).....	28
Digital Ortho Quarter Quads (DOQQs).....	29
Perennial and Intermittent Streams.....	29
AGNPS Arcview Interface Application.....	30
Watershed Segmentation.....	31
Drainage Boundary.....	31
Subdrainage Areas: AnnAGNPS Cells.....	35
Stream Network.....	38
Generated and Digitized Drainage Network.....	38
Location of Tributary Confluences Within the James Creek Main Channel.....	39
Drainage Network Reach Hydraulic Geometry.....	40
Location of Unstable Channel Reaches.....	41
Weather Data.....	45
Landuse Data.....	45
Best Management Practices (BMPs).....	47
Impoundments.....	48
Operation Information Associated with Crops and Non-Crops.....	49
Soil Conservation Service (SCS) Runoff Curve Numbers Associated with Watershed Characteristics.....	49
Soil Properties.....	50
Vegetation Information for Crops and Non-Crops.....	50
Evaluation of Erosion from Gully Sources.....	50
Input Database for the CONCEPTS Model.....	53
1967 Channel Survey.....	53
1967 Corps of Engineers label.....	54
Distance upstream of 2002 mouth of James Creek.....	54
2002 Channel Survey.....	54
Synthesis of 1967 Upstream Cross Sections.....	55
Streambed Erodibility and Composition.....	57
Cohesive Materials.....	60
Non-Cohesive Materials.....	62
Streambank Stability.....	63
Bank-Toe Erodibility.....	63
Bank-Material Shear Strength.....	64
Borehole Shear Testing and Bulk Unit Weights.....	65
Texture of Bed and Bank Materials.....	67
DEVELOPING A “REFERENCE” SEDIMENT-TRANSPORT CONDITION FOR JAMES CREEK.....	73

Regionalization by Level III Ecoregion.....	73
Availability of Data.....	73
“Reference” Conditions	74
Stages of Channel Evolution.....	74
Rapid Geomorphic Assessments: RGA’s	76
Channel-Stability Index	76
Specific-Gage Analysis.....	76
Analysis of Suspended-Sediment Data.....	77
Calculating Effective Discharge ($Q_{1.5}$)	80
Results from Evaluations of “Reference” Sediment Loading.....	82
“Reference” Sediment-Transport Conditions	82
Empirical Relations With Stage of Channel Evolution and Channel-Stability Index	86
Refinement of Estimates of “Reference” Sediment Discharge.....	87
RESULTS FROM EVALUATIONS OF “ACTUAL” SEDIMENT LOADING.....	92
Introduction.....	92
AnnAGNPS and the Combined AnnAGNPS and CONCEPTS Simulations of the Main Upstream Tributary for Reduced Tillage Conditions	92
AnnAGNPS Simulated Streamflow and Sediment Discharge Rates.....	92
Comparison of Measured and Simulated Peak Flow Rates at the Highway 25 Gaging Station, 1967-2001	92
Simulated Runoff at the Darracott Road Bridge Crossing.....	93
Simulated Sediment Load at the Darracott Road.....	94
Combined AnnAGNPS and CONCEPTS Simulation of Main Channel Evolution and Transport Rates, 1967-2001	97
Year of construction.....	97
Changes in Thalweg Profile.....	98
Changes in Cross-Sectional Geometry	100
Comparison of Measured and Simulated Recurrence Intervals at the Highway 25 Gaging Station, 1967-2001	100
Channel Erosion 1967-2002: Measured Changes in Channel Geometry	105
Simulated Sediment Loads	108
Simulated Sediment-Transport Rates and Yields at the Highway 25 Bridge.....	109
Simulated Sediment Loads at the Watershed Outlet.....	115
SUMMARY OF RESULTS	117
Sediment Loads Under “Reference” Conditions	117
Amounts and Sources of Eroded Sediment Under “Actual” Conditions.....	117
CONCLUSIONS	120
REFERENCES.....	122
APPENDICES	125

LIST OF TABLES

Table 1 – Recurrence intervals for peak discharges at James Creek at Aberdeen: USGS station number 02437600.	11
Table 2 – The TOPAGNPS critical source area (CSA) and minimum source channel length (MSCL) parameters used for each of the five regions defined for the final subdivision of the watershed into AnnAGNPS cells.	38
Table 3 – Dates associated with precipitation that was not available at the Aberdeen, Mississippi climate station and another station’s information was used.	45
Table 4 – Landuse defined by the final GIS landuse layer and by AnnAGNPS cells.	47
Table 5 – SCS curve numbers for the James Creek watershed simulation by land cover class. .	49
Table 6 – Location of 1967 surveyed cross sections along James Creek.	54
Table 7 – The locations of all surveyed cross sections along James Creek.	56
Table 8 – Development of 1967 synthesized cross sections from relations shown in Figure 59 and Figure 60. Note: W/D is width to depth ratio. See Table 7 for drainage areas.	60
Table 9 – Critical shear stress (τ_c) and erodibility coefficient (k) values based on submerged jet tests used for input into CONCEPTS. Note: SP-GP = sand and gravel; Cross section numbers beginning with “T” refer to locations on the main tributary.	64
Table 10 – Critical shear stress (τ_c) and erodibility coefficient (k) values for bank toes based on submerged jet tests used for input into CONCEPTS.	66
Table 11 – Summary of shear-strength parameter values used for bank-stability modeling in CONCEPTS. Note: c_a = apparent cohesion; c' = effective cohesion; ϕ' = effective friction angle; U = upper; L = lower; “full” refers to a layer incorporating the remainder of the bank height below.	69
Table 12 – Distribution of bed-material particle sizes for sites along James Creek and the main tributary. See Figure 1 for site locations.	70
Table 13 – Composition of bank materials by section and layer along James Creek and the main tributary. Note: U = upper; L = lower; d_{50} = median particle size.	72
Table 14 – Source of sediment simulated by AnnAGNPS at Darracott Road by simulation scenario totals for 1967-2001.	95
Table 15 – Time and position of low-water crossing installation.	97
Table 16 – Contribution of sediments eroded from the channel boundary of James Creek between 1967 and 2002 between rkm 0.27 and rkm 17.2.	108
Table 17 – Sediment loads and yields at river kilometer 7.92 (Darracott Road) as simulated by AnnAGNPS combined with CONCEPTS.	109
Table 18 – Suspended-sediment transport relations derived from CONCEPTS output for each year of simulation showing calculated load and yield at the measured $Q_{1.5}$ of $86.8 \text{ m}^3/\text{s}$. Note: Coefficient and exponents correspond to the general equation $L = a Q^b$, where a and b are the coefficient and exponent, respectively.	110
Table 19 – Total sediment load at the outlet of the James Creek watershed for the period 1967 – 2002.	116
Table 20 – Summary table of “reference” and “actual” suspended-sediment yield showing central 50% of the data distribution and “actual” yields at the $Q_{1.5}$. Note: Q1 = first quartile; Q3 = third quartile; difference between Q1 and Q3 is the central 50% of the distribution.	118

Table 21 – Summary table of “reference” and “actual” suspended-sediment load showing central 50% of the data distribution and “actual” loads at the $Q_{1.5}$. Note: Q1 = first quartile; Q3 = third quartile; difference between Q1 and Q3 is the central 50% of the distribution. 119

LIST OF FIGURES

Figure 1 – Site location map for James Creek watershed including locations of surveys, geotechnical data and surficial geology. Note: Channel network is derived from digitized perennial and intermittent streams.	4
Figure 2 – Double cropping operation of planting soybeans into a recently harvested wheat field, James Creek watershed, June 2002.	5
Figure 3 – Soybean emergence within a field double cropped with wheat, James Creek watershed, June 2002.	6
Figure 4 – Typical soybean crop with a slight amount of residue visible between rows as a result of reduced tillage farming practices, James Creek watershed, June 2002.	6
Figure 5 – Aerial photograph of extensive corn fields within James Creek watershed, June 2002.	7
Figure 6 – Example low-water crossing along the main stem of James Creek.	9
Figure 7 – Mean-daily flows for James Creek near Aberdeen: USGS station number 02437600. Data obtained from USGS Web site.	10
Figure 8 – Annual instantaneous maximum discharges for James Creek at Aberdeen: USGS station number 02437600. Data obtained from USGS Web site.	10
Figure 9 – Carlos Alonso, Ron Bingner and Andrew Simon following completion of aerial reconnaissance of the James Creek watershed.	18
Figure 10 – Aerial photograph of extensive wheat fields that have been recently harvested in June, 2002 within James Creek watershed.	19
Figure 11 – View looking upstream from the junction of Darracott Road and James Creek located at the bridge in the lower right portion of the aerial photograph.	20
Figure 12 – Significant recent gully migration within a recently planted soybean field, as evidenced by gully headcuts moving into rows.	20
Figure 13 – One of the few corn fields using strip cropping as a best management practice.	21
Figure 14 – The Monroe County digital elevation model (DEM) obtained from MARIS at the 10 meter by 10 meter resolution with 0.3 meter elevation resolution.	23
Figure 15 – The geographic soil layer for James Creek watershed obtained from MARIS and derived from STATSGO.	24
Figure 16 – Land ownership fields on James Creek watershed as defined by NRCS.	26
Figure 17 – Land ownership boundaries with a single landuse defined for comparison of the crops.	26
Figure 18 – Landsat 7 classified landuse layer obtained for August 3, 2001.	27
Figure 19 – Cropland defined from the digitized field boundaries of the DOQQ.	27
Figure 20 – Landsat 5 landuse layer obtained from MARIS based on images from 1991-1993.	28
Figure 21 – Landuse used as the final layer defined as applied with the AGNPS Arcview interface.	28
Figure 22 – The Monroe County digital raster graphic (DRG).	29
Figure 23 – The DOQQ for Monroe County.	30
Figure 24 – The Perennial streams (purple) and intermittent streams (blue) indicated on the DRG for James Creek watershed and surrounding areas.	30
Figure 25 – A graphic drawn on the Monroe County DEM containing the James Creek watershed for use in clipping the DEM to a smaller area for analysis with the AGNPS Arcview Interface.	32

Figure 26 – The outlet determination of James Creek into the Tombigbee River using the digitized perennial streams and the DOQQ	32
Figure 27 – The outlet determination of James Creek into the Tombigbee River using the digitized perennial streams and the DRG.	33
Figure 28 – The initial James Creek watershed boundary generated from TOPAGNPS as displayed with the DRG.....	33
Figure 29 – The initial James Creek watershed boundary generated from TOPAGNPS as displayed with the DOQQ.....	34
Figure 30 – A watershed boundary problem illustrated by a channel indicated on the DRG that crosses the boundary.....	34
Figure 31 – The updated watershed boundary (red) produced from modifications of the DEM and the initial watershed boundary (black) produced without modification of the DEM. 35	
Figure 32 – The updated watershed boundary (red) produced from modifications of the DEM and the initial watershed boundary (black) produced without modification of the DEM, with the perennial streams (purple) and intermittent streams (blue).	35
Figure 33 – The first trial of the generation of AnnAGNPS cells for James Creek watershed with the correct watershed boundary.	36
Figure 34 – The delineation of TOPAGNPS regions for use with various CSA and MSCL values within TOPAGNPS to develop a more detailed subdivision of the watershed for use as AnnAGNPS cells. Region 1 is indicated with red, Region 2 with blue, Region 3 with green, and Region 4 with yellow.	37
Figure 35 – The final delineation of TOPAGNPS regions with the associated AnnAGNPS cell boundaries produced by TOPAGNPS for use with the various CSA and MSCL values. Region 1 is indicated with white, Region 2 with yellow, Region 3 with orange, Region 4 with green, and Region 5 with light red.....	37
Figure 36 – The final generation of AnnAGNPS cells used for the James Creek watershed simulations.....	38
Figure 37 – The generated stream network (red) in comparison with the digitized perennial (purple) and intermittent (blue) streams with the James Creek watershed boundary (black).	39
Figure 38 – A major confluence reflected properly by the generated stream network as indicated by the streams shown on the DOQQ.....	39
Figure 39 – The TOPAGNPS generated stream network with the main channel simulated by CONCEPTS (blue), tributaries simulated by AnnAGNPS as loadings into CONCEPTS (green), the AnnAGNPS loadings (gray) into the lower channel (red) used to determine the total loadings at the James Creek outlet.....	40
Figure 40 – Location of the reach hydraulic geometry tributary survey points used for AnnAGNPS with the main channel simulated by CONCEPTS (blue), tributaries simulated by AnnAGNPS as loadings into CONCEPTS (green), the AnnAGNPS loadings (gray) into the lower channel (red) used to determine the total loadings at the James Creek outlet.	41
Figure 41 – Reach hydraulic geometry width measured at survey location #9.	42
Figure 42 – Reach at survey location #3 looking upstream.....	42
Figure 43 – Width reach hydraulic geometry derivation based on the top width of all main channel and supplemental tributary surveys.	43

Figure 44 – Depth reach hydraulic geometry derivation based on the top width of all main channel and supplemental tributary surveys.	43
Figure 45 – The TOPAGNPS generated stream network with the main channel simulated by CONCEPTS (blue), along with the designated unstable reaches (red) and stable reaches (green) that are simulated by AnnAGNPS.	44
Figure 46 – The main tributary (blue) with stable (green) and unstable (red) reaches entering the tributary from AnnAGNPS cells (black) within a portion of James Creek watershed.	44
Figure 47 – Annual rainfall measured at the Aberdeen, Mississippi weather station from 1967-2001.	46
Figure 48 – Landuse assigned to each AnnAGNPS cell.	46
Figure 49 -- Location of terraces and impoundments shown on the DOQQ on the upper end of the main tributary of James Creek watershed.	47
Figure 50 – Location of the impoundment associated with AnnAGNPS reach 133.	48
Figure 51 – Location of the impoundment associated with AnnAGNPS reach 166.	48
Figure 52 – Soils defined by AnnAGNPS cells.	50
Figure 53 – The scanned 1960 aerial photographs over a portion of James Creek watershed with locations 1 – 3 indicated for comparison with gully sites to 1994 conditions.	51
Figure 54 – Location of the same gully for location 1 in the aerial photographs of 1960 (left) and 1994 (right).	52
Figure 55 – Location of the same gully for location 2 in the aerial photographs of 1960 (left) and 1994 (right).	52
Figure 56 – Location of the same gully for location 3 in the aerial photographs of 1960 (left) and 1994 (right).	53
Figure 57 – Surveying from the James Creek flood plain.	55
Figure 58 – Comparison of 1967 and 2002 thalweg elevations for the main stem of James Creek showing the extent of bed-level lowering during the period.	58
Figure 59 – Variation in channel cross-sectional area with distance upstream along James Creek. Note: similarity between 2002 upstream relation and interpreted line.	58
Figure 60 – 1967 and 2002 channel depths along James Creek showing the effects of the low-water crossings and the probable incision in the reach upstream of rkm 17.3.	59
Figure 61 – Depth of channel below floodplain of tributary channel entering James Creek at rkm 18.8 showing 1 – 2 m of deepening near the mouth.	59
Figure 62 – Submerged jet-tests being conducted on the streambed of the main stem of James Creek. Vertical jet test device is in the foreground.	61
Figure 63 – Results of individual jet tests on cohesive streambed materials along James Creek. Note: Dashed lines are 95% confidence limits.	62
Figure 64 – Non-vertical jet-test device used to determine erodibility of bank toes.	65
Figure 65 – Borehole shear-test device (BST) used to conduct tests of the shearing resistance of different layers of streambanks along James Creek.	67
Figure 66 – Example BST results and regression. Note: c_a is the y-intercept; ϕ' is the slope of the regression; dotted lines are 95% confidence limits.	68
Figure 67 – Longitudinal distribution of streambed texture along James Creek expressed in terms of size classes (A) and d_{50} (B).	71
Figure 68 – Six stages of channel evolution from Simon and Hupp (1986) and Simon (1989b) identifying Stages I and VI as stable, “reference” conditions.	75

Figure 69 – Channel stability ranking scheme used to conduct rapid geomorphic assessments (RGA’s). The channel stability index is the sum of the values obtained for the nine criteria.	78
Figure 70 – Development of suspended-sediment rating relation showing potential error at $Q_{1.5}$ and other high discharges without a second (A) or third (B) linear segment.	79
Figure 71 – Flood-frequency distribution for James Creek near Aberdeen showing the $Q_{1.5}$ to be used in calculating sediment loads at the effective discharge.....	80
Figure 72 – Determination of effective discharge ($Q_{1.5}$) from annual-maximum flow series (A) and suspended-sediment load at the effective discharge using the sediment-transport rating relation (B).....	81
Figure 73 – Comparison of national median suspended-sediment yields at the $Q_{1.5}$ for 84 ecoregions of the continental United States. Modified from Simon <i>et al.</i> , 2002.....	82
Figure 74 – Distribution of suspended-sediment yields at the $Q_{1.5}$ for the Southeastern Plains ecoregion.....	83
Figure 75 – Distribution of suspended-sediment concentrations at the $Q_{1.5}$ for the Southeastern Plains ecoregion.....	83
Figure 76 – Relation between stage of channel evolution and channel-stability index (I) for the Southeastern Plains ecoregion.	84
Figure 77 – Comparison of suspended-sediment yields at the $Q_{1.5}$ for stable “reference” sites and for evaluated, unstable sites. Yield shown is a general reference for the Southeastern Plains ecoregion.	85
Figure 78 – Comparison of suspended-sediment concentrations at the $Q_{1.5}$ for stable “reference” sites and for evaluated, unstable sites. Concentration shown is a general reference for the Southeastern Plains ecoregion.	85
Figure 79 – Relation between channel-stability index (I) and suspended-sediment concentration (C) at the $Q_{1.5}$ for sites in the Southeastern Plains. Coefficient of determination is low ($r^2 = 0.41$) and relation should be used with caution.	86
Figure 80 – Inter-quartile distributions of suspended-sediment yield (A) and concentration at the $Q_{1.5}$ by stage of channel evolution for 97 sites in the Southeastern Plains.	88
Figure 81 – “Reference” suspended-sediment yields at the $Q_{1.5}$ for three major textural classes of bed sediment in the Southeastern Plains.	89
Figure 82 – “Reference” suspended-sediment concentrations at the $Q_{1.5}$ for three major textural classes of bed sediment in the Southeastern Plains.	90
Figure 83 – Bed-material types along James Creek and “reference” values at $Q_{1.5}$ used for developing weighted “reference”.....	91
Figure 84 – Comparison of the AnnAGNPS and measured annual peak discharge at the Highway 25 gaging station with a best fit line (red).....	93
Figure 85 – Simulated yearly runoff by AnnAGNPS at the Darracott Road crossing and the yearly rainfall used within the simulation of the entire James Creek watershed.....	93
Figure 86 – Average annual runoff simulated from AnnAGNPS for each cell.....	94
Figure 87 – The total sediment, AnnAGNPS bed and bank contribution, and the AnnAGNPS cell contribution at the Darracott crossing.	96
Figure 88 – Average annual erosion simulated from AnnAGNPS for each cell.	96
Figure 89 – Average annual sediment yield simulated from AnnAGNPS for each cell.	97
Figure 90 – Simulated thalweg elevations for rkm 7.29 to 24.02.	98
Figure 91 – Comparison of simulated and measured thalweg profile.	99

Figure 92 – Comparison of simulated and measured thalweg elevations at cross sections surveyed in 2002.	99
Figure 93 – Simulated channel top widths for rkm 7.29 to 24.02.	101
Figure 94 – Simulated top widths comparison to measured 2002 top widths.	101
Figure 95 – Comparison of 1967 and 2002 measured and 2002 simulated cross-section 228+60.	102
Figure 96 – Comparison of 1967 and 2002 measured with 2002 simulated cross-section 294+00.	102
Figure 97 – Comparison of 1967 and 2002 measured with 2002 simulated cross-section 311+20.	103
Figure 98 – Comparison of 1967 and 2002 measured with 2002 simulated cross-section 381+23.	103
Figure 99 – Comparison of 1967 and 2002 measured with 2002 simulated cross-section 432+10.	104
Figure 100 – Comparison of 1967 and 2002 measured with 2002 simulated cross-section 548+70.	104
Figure 101 – The recurrence interval based on the annual peak discharge obtained from measurements at the Highway 25 bridge, the AnnAGNPS simulation using peak discharges that match the measured annual peak discharge event date, the AnnAGNPS simulation using the simulated annual peak discharge at whatever date it occurred, the AnnAGNPS simulated values using precipitation generated from GEM for 39 years, and the CONCEPTS simulated values using the simulated annual peak discharge at whatever date it occurred.	105
Figure 102 – Example from 1967 survey-match section 381 + 23 of calculating the amount of material eroded from the channel boundary over the period 1967 to 2002.	106
Figure 103 – Cross-sectional area of James Creek during 1967 and 2002 (A); and “Actual” sediment loading from the channel boundary over the period 1967 – 2002 based on changes in channel cross-sectional area (B). Note the greater magnitude of erosion in the downstream sinuous section.	107
Figure 104 – Annual sediment loads and relative contributions from channels and fields at Darracott Road as simulated by AnnAGNPS with CONCEPTS.	109
Figure 105 – Suspended-sediment transport relation for 1977 at the Highway 25 bridge derived from CONCEPTS modeling results with corresponding regression equation. Note: L = load (T), Q = water discharge (m^3/s).	112
Figure 106 – Calculated suspended-sediment yields at the $Q_{1.5}$ based on three-year blocks of CONCEPTS output showing non-linear decrease with time as channels and tributaries adjusted to the 1967 channel clearing and snagging operations. Note: Data are plotted arithmetically (A) to show non-linear trend of approaching “reference” and in log-space (B) to provide a more detailed view of difference between current conditions and “reference” conditions.	113
Figure 107 – Calculated annual suspended-sediment yields at the $Q_{1.5}$ based on CONCEPTS output showing non-linear decrease with time as channels and tributaries adjusted to the 1967 channel clearing and snagging operations and lowered yields following construction of low-water crossings in 1999. Note: Data are plotted arithmetically (A) and in semi-log space (B) to show “actual current” conditions.	114

Figure 108 – Differences in suspended-sediment yields for the Highway 25 bridge at the Q_{1.5} using annual peak-flow series derived by four methods. Note that the yields based on simulated peak-flow series bound those based on measured data. 115

INTRODUCTION

Excessive erosion, transport, and deposition of sediment in surface waters are major water quality problems in the United States. The 1996 National Water Quality Inventory (Section 305(b) Report to Congress) indicates that sediments are ranked as a leading cause of water-quality impairment of assessed rivers and lakes. Impairment by sediment can be separated into problems resulting from chemical constituents adsorbed onto the surface of fine-grained sediments (sediment quality), problems resulting from sediment quantities (clean sediment) irrespective of adsorbed constituents, and alteration of substrate (bed material) by erosion or deposition. The maximum allowable loadings to, or in a stream or waterbody that does not impair designated uses has been termed the “TMDL” (total maximum daily load). The 1996 list of impaired waterbodies in the state of Mississippi lists three segments along James Creek, Monroe County that have impaired conditions for aquatic life support due to sediment.

Background and Problem

Virtually the entire length of James Creek is encompassed in the three segments listed as impaired by the Mississippi Department of Environmental Quality (MDEQ). Field surveys conducted by MDEQ in May 2001 indicated biologic impairment because habitat conditions were of only fair quality due to “excessive sedimentation”. By law a TMDL must therefore, be developed by MDEQ for James Creek. Water Quality Criteria for the State of Mississippi does not contain a numerical target for sediment but is in narrative form: “Waters shall be free from materials...in such a degree as to create a nuisance, render the waters injurious to public health, recreation, or to aquatic life and wildlife...or impair the waters for any designated uses” (MDEQ, 2002, written communication). In the absence of a numerical target for sediment MDEQ seeks a percent reduction in sediment loads such that the James Creek watershed is producing sediment at rates commensurate with those in a biologically unimpaired stream. This unimpaired stream is thus termed a “reference” stream or reach.

Preliminary-reference sediment suspended-sediment transport rates have been developed for various ecoregions of the United States, including the Southeastern Plains (Ecoregion 65), which contains James Creek (Simon *et al.*, 2002). However, to produce a TMDL expressed in terms of a percent reduction, MDEQ needs to know the:

1. Sediment loads that are currently being transported in the James Creek watershed; and
2. Sources of those sediments to address future BMP's.

Because there are no historical sediment-transport data nor “reference” reaches for James Creek, alternative methods are required. More specifically, these sediment-transport data must be expressed in the same form as those data developed for reference conditions. To accomplish these tasks a combination of empirical and numerical techniques can be used. Suspended-sediment loads from typical streams in the region with historical data can be analyzed by relating the geomorphic conditions at those streams with the conditions along James Creek (Simon *et al.*, 2002). Water and sediment contributions from uplands areas can be obtained with the watershed simulation model AnnAGNPS (Cronshey and Theurer, 1998). This information is also supplied as the boundary conditions used to determine the channel contributions from main channel

streambeds and banks using the one-dimensional channel-evolution model CONCEPTS (Langendoen, 2000).

Objectives and Scope

The overall objective of this study is to determine sediment loads and sources in the James Creek watershed and to compare these to a “reference” sediment load for unimpaired streams in the region. Sediment sources can potentially include sheet and rill erosion from uplands and agricultural fields, gullies, and streambeds and banks. Specific objectives include:

1. Determine an applicable “reference” condition and sediment load for the Southeastern Plains and apply it to conditions along James Creek using geomorphic techniques;
2. Determine the sediment load emanating from James Creek by direct comparison of measured cross sections, upland flow and sediment modeling using AnnAGNPS and channel-evolution modeling using CONCEPTS;
3. Determine the contributions to sediment loads from various channel and upland sources in the James Creek watershed to identify potential areas for future remediation work.

The project encompasses the entire James Creek watershed. Aerial watershed reconnaissance, channel surveys, sampling and testing of stream boundary sediments, and rapid geomorphic assessments were conducted along the entire length of James Creek as well as along one of the main tributaries that drains from the northwestern part of the watershed. This tributary was modeled using both AnnAGNPS and CONCEPTS to provide a comparison of the sediment prediction capabilities for tributaries using AnnAGNPS only. AnnAGNPS modeling was conducted for the entire watershed in order to produce water and sediment loadings from tributaries and adjoining fields along the main channel used within CONCEPTS. Essentially, the main channel portion of the watershed simulated by AnnAGNPS was replaced through the use of CONCEPTS for improved results. Results from AnnAGNPS at selected drainage points in the watershed were compared with the results of combined ANNAGNPS and CONCEPTS simulations to demonstrate the need for higher resolution treatment of bed and bank processes. Particular attention was given to the northwest tributary and at the Highway 25 bridge southwest of Aberdeen where some historical flow data were available. CONCEPTS modeling was conducted from Darracott Road south of Aberdeen (river kilometer (rkm) 6.37) upstream to the Illinois-Central Railroad bridge west of Aberdeen (rkm 24.0). CONCEPTS modeling was not conducted in the sinuous reaches of James Creek between its confluence with the Tennessee-Tombigbee Waterway and Darracott Road, because the cross-stream variations in flow and sediment transport in meander bends can not be accurately represented by CONCEPTS.

WATERSHED AND CHANNEL CONDITIONS

Basin Characteristics

James Creek is located in Monroe County, Mississippi within the Southeastern Plains Ecoregion and drains directly to the Tennessee-Tombigbee Waterway. Characteristics of the 112 km² watershed include attributes of uplands, fields and channels.

Ecoregion 65: Southeastern Plains

Omernik (1995) defined 84 ecoregions (Level 3) in the continental United States based on regional similarities of climate, geology, topography and ecology. Ecoregion 65 extends from the eastern half of Mississippi and parts of western Tennessee, east and north through parts of Alabama, Florida, Georgia, South and North Carolina to parts of eastern Virginia and Maryland. These irregular plains generally have a mosaic of cropland, pasture, woodland, and forest. Natural vegetation is mostly oak-hickory-pine and Southern mixed forest. The Cretaceous or Tertiary-age sands, silts, and clays of the region contrast geologically to the older igneous and metamorphic rocks of the Piedmont, and the older limestone, chert, and shale found in the Interior Plateau. Streams in this area are relatively low-gradient and generally have sand beds. James Creek is somewhat unique in this context in that much of the streambed is composed of cohesive clays. In Mississippi, the Southeastern Plains are bordered to the west by the Mississippi Valley Loess Plains ecoregion, which has the greatest sediment yields in the continental United States (Simon *et al.*, 2002).

Surficial Geology

The James Creek watershed is dominated by two formations of Cretaceous age. The Selma formation also known as the Selma Chalk covers the western part of the watershed from the basin divide east to a north-south line crossing James Creek about 5.7 km west of Aberdeen (Figure 1). The survey and sampling locations shown in Figure 1 are referred to later in the report. The formation is characterized as soft, argillaceous and sandy (Vestal and McCutcheon, 1943). The impure chalk is dark bluish-gray where fresh but dries to light gray, white or yellowish. A borehole drilled in 1941 in the vicinity of the intersection of old highways 45 and 8 and within 100 m of James Creek shows about 30 cm of recent alluvium overlaying at least 3 m of gray to light brownish gray, sandy clay (Vestal and McCutcheon, 1943). This strata is typical of the Selma Chalk.

The Eutaw formation outcrops east of the Selma Chalk and is separated into two members. The upper unit, extending east to a north-south line crossing James Creek about halfway up the sinuous section near the mouth of James Creek is termed the Tombigbee Sand member. This unit is a massive sand deposit. The lower member of the formation is predominantly sandy, locally cemented with clay inter-bedded clay laminae (Vestal and McCutcheon, 1943). In places sub-angular chert gravel and bentonite clay are also included. Test holes drilled in 1941 in the vicinity of the contact of the two members of the Eutaw formation show sand or sandy loams to depths of about 9 m. Each borehole contains a layer of bentonite clay ranging from 1.0 – 1.5 m thick.

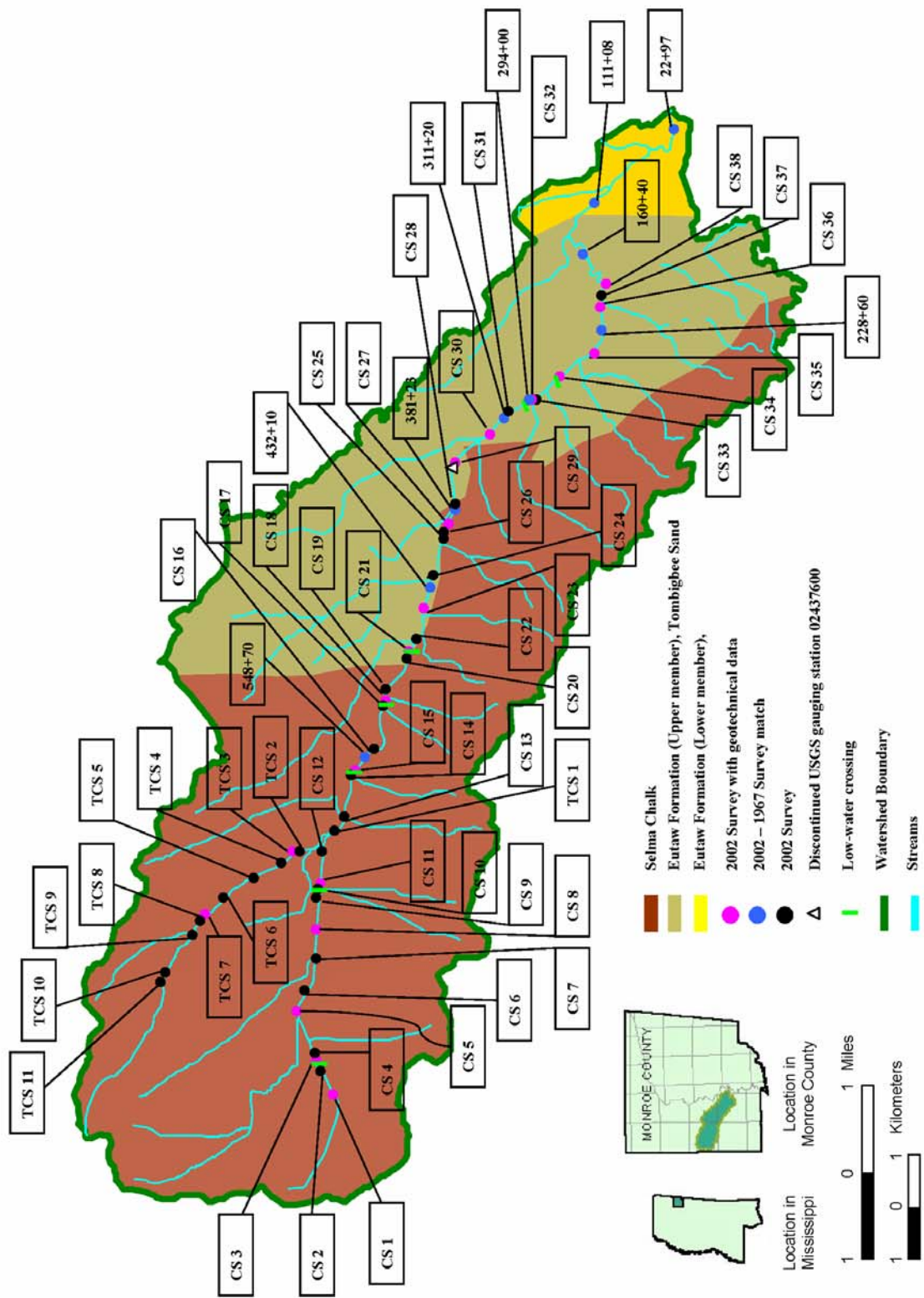


Figure 1 . Site location map for James Creek watershed including locations of surveys, geotechnical data and surficial geology. Note: Channel network is derived from digitized perennial and intermittent streams.

Recent deposits of alluvium from flood flows overlay the Cretaceous deposits along the main channels of the watershed. This material is generally brown in color and composed of mixtures of sand, silt and clay.

Land Use

The James Creek Watershed is in a highly agricultural area, with most of the watershed in cultivated croplands, pasture or fallow conditions. The predominate types of crops produced include corn, soybeans, cotton, wheat, and sorghum. Some wheat fields are also doubled cropped with soybeans (Figure 2 and Figure 3). The amount of land devoted to each crop can vary from year to year depending on the current crop prices or weather. Within the last several years, farming practices have been adopted that provide improved erosion control over conventional farming practices. Most farmers no longer plow fields by completely turning the soil over in the fall and then extensively cultivating the crops during the growing season. The adoption of pesticide use has eliminated the need to cultivate as much or to drastically plow the soil, resulting in more effective erosion control and reduced soil erosion. Some cultivation is still used with the crops resulting in the practices being defined as reduced tillage (Figure 4), as compared to an approach of no cultivation practices that are defined as no-tillage. Corn fields can also provide better erosion control than cotton or soybeans (Figure 5).



Figure 2 – Double cropping operation of planting soybeans into a recently harvested wheat field, James Creek watershed, June 2002.



Figure 3 – Soybean emergence within a field double cropped with wheat, James Creek watershed, June 2002.



Figure 4 – Typical soybean crop with a slight amount of residue visible between rows as a result of reduced tillage farming practices, James Creek watershed, June 2002.



Figure 5 – Aerial photograph of extensive corn fields within James Creek watershed, June 2002.

Heavily wooded areas are predominately located on land at the lower end of James Creek. The city of Aberdeen, outer residential and business areas represent the urban portion of the watershed. There are numerous areas containing small reservoirs, ponds or lakes, which can provide for a small amount of erosion control from the upstream drainage areas of those water bodies.

Climate

The climate for the area is typical for the Southeast region of the U.S. where generally the winter and spring months contain the highest rainfall amounts. The summer months are characterized by afternoon thunderstorms that can produce locally heavy rainfall. Average annual precipitation for Aberdeen is 1431 mm as reported by the Aberdeen climate station recorded by the US Department of Commerce, National Oceanic and Atmospheric Administration, National Environmental Satellite, Data and Information Service, National Climatic Data Center. Air temperatures are mild in the winter, resulting in minimal snowfall, and hot in the summer resulting in an average annual temperature of 18.3 degrees centigrade.

Channel Characteristics

James Creek, like many streams in Mississippi is an incised, channelized stream throughout most of its length. Only the lower 6.6 km remains in a “natural” sinuous alignment (Figure 1). As is typical in incised alluvial streams, evidence of bank erosion by mass failures is prevalent throughout the course of James Creek. Tributaries draining to James Creek have been dredged, straightened and moved at various times over the past 100 years, creating a complex scenario of channel responses. Like the trunk stream, most of the tributaries are incised and are experiencing bank failures. This network-wide pattern of bed incision and subsequent channel

widening is characteristic of streams that have been disturbed by channelization and other direct modifications (Simon and Rinaldi, 2000).

Human Intervention

Prior to the turn of the 20th century James Creek and its tributaries were probably sinuous throughout their lengths. Like other agricultural basins in the region, land clearing in the mid to late 1800's probably resulted in upland erosion and filling of channels causing frequent and prolonged flooding of adjacent croplands. In the early 1900's, drainage districts were formed to address issues related to poor land drainage caused by the loss of channel capacity.

Channelization (1905)

In an effort to reduce flooding, James Creek and many of its tributaries were dredged and straightened in about 1905 (R. Goodgame, 2002, land owner, personal communication.). Little is known of the details of this channelization project although it seems certain that the reach below rkm 6.6 was not modified and has always been sinuous. The effects of network-wide channelization projects are well documented (Daniels, 1960; Emerson, 1971; Simon, 1994; Simon and Rinaldi, 2000). Bed incision generally migrates upstream through the main stem and tributaries, deepening channels and increasing bed-material loads. Streambanks become higher and steeper through bank-toe erosion. Bank failures occur as the resistance of the bank materials to shearing is exceeded by gravitational forces. This is generally the period of peak sediment loads (Simon, 1989a). The accelerated erosion of sediments from upstream reaches causes bed deposition in downstream reaches since these downstream sections have become less competent to transport sediments because of adjustment to flatter channel gradients. Ultimately, continued bank failures flatten bank slopes and deposition decreases bank heights and may stabilize streambanks and reduce sediment loads. In the case of James Creek, the 62-year period between channelization and the next engineering works in 1967 was probably of sufficient duration for the erosion process to effect upstream reaches and for downstream reaches to fill and re-stabilize.

Clearing and Snagging (1967)

A clearing and snagging project was undertaken by the U.S. Army Corps of Engineers in 1967 from the mouth of James Creek to a point 16.7 km upstream. The purpose of this project was to restore channel capacity that had been compromised by sediment deposition, accumulation of large woody debris emanating from upstream bank failures, and the growth of riparian vegetation. In theory this type of engineering work does not involve dredging of the channel bottom, but only removal of vegetation. The consequent reduced flow resistance has the effect of increasing flow velocities, channel conveyance and sediment transport. Several landowners commented that James Creek had eroded in the years following the clearing and snagging operation.

Low-water Crossings

Seven low-water crossings have been constructed across James Creek between the 1960's and 1990's to replace small bridges that were endangered by channel incision and widening (Figure 1). These concrete structures produce an upstream backwater effect and trap sediment

with many protruding about 1.0 m above the streambed (Figure 6). In some cases, the trapping of sediment upstream from these structures results in considerable scour on their downstream ends.



Figure 6 – Example low-water crossing along the main stem of James Creek.

Construction of the Tennessee-Tombigbee Waterway

The construction of the Tennessee-Tombigbee Waterway during the early 1980's impacted James Creek in several ways. In the vicinity of the mouth of James Creek, the Tombigbee River was deepened and the lower 215 m of James Creek was cut off to align the creek with the new waterway. A dam was constructed on the waterway at Aberdeen altering the flow regime of the Tombigbee River. Evidence from surveys by the USGS at the Highway 25 bridge indicates that James Creek did not incise immediately following completion of the waterway and during the high flows of 1982 and 1983. However, erosion of sediments from the James Creek watershed during the 1980's and 1990's causes the formation of a rather persistent channel bar where the creek enters the waterway. To maintain navigation depths, the CoE dredges this material on an almost annual basis. This activity may result in an annual reactivation of bed erosion in lower James Creek.

Streamflow

Daily streamflow in James Creek was monitored by the U.S. Geological Survey (USGS) between 1963 and 1968 at the State Highway 25 bridge southwest of Aberdeen (Figure 7). The gage record shows that there are periods of no flow in James Creek. Peak flows were monitored over a much longer period: 1963 – present. Peak instantaneous discharge for the period of record is 197 m³/s and occurred on October 22, 1984. In fact four of the nine highest peak flows

occurred between January 1982 and October 1984 (Figure 8). Recurrence intervals were calculated based on an analysis of the 39-year period of peak-flow data and are shown in Table 1. These data are important in our research effort because they provide a means of validating simulated flow rates at the bridge.

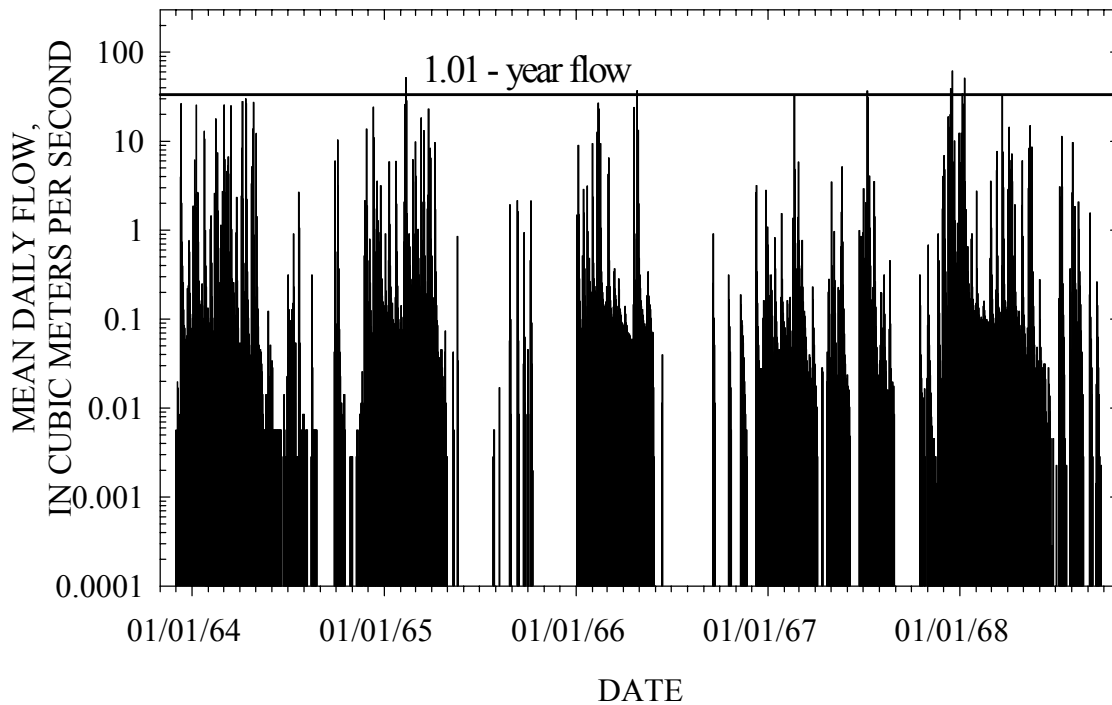


Figure 7 – Mean-daily flows for James Creek near Aberdeen: USGS station number 02437600. Data obtained from USGS Web site.

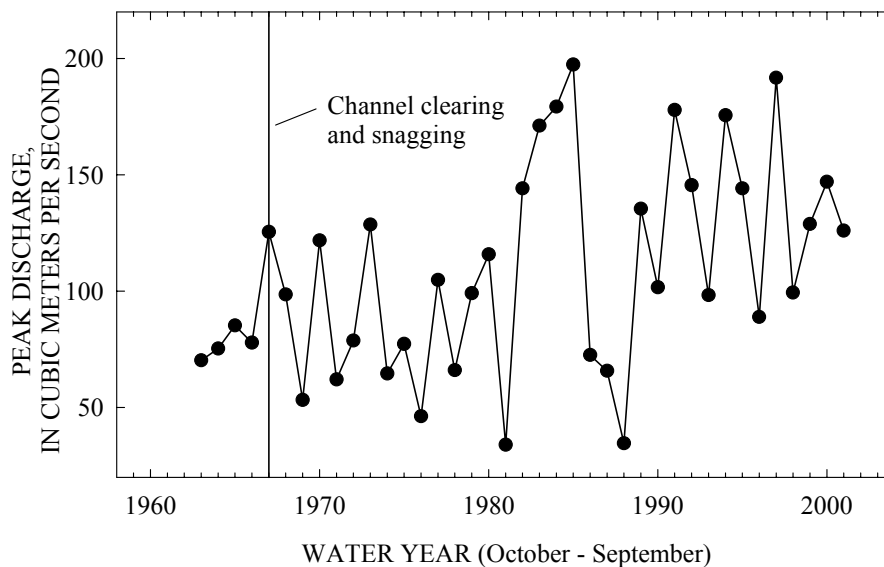


Figure 8 – Annual instantaneous maximum discharges for James Creek at Aberdeen: USGS station number 02437600. Data obtained from USGS Web site.

Table 1 – Recurrence intervals for peak discharges at James Creek at Aberdeen: USGS station number 02437600.

Recurrence interval (years)	Discharge (m³/s)
1.01	33.4
1.11	58.2
1.5	86.8
2	104
2.33	112
5	145
10	170
20	192
100	238

Boundary Materials

Channel boundary materials in James Creek are composed predominantly of silts and clays. Virtually all of the bank materials are cohesive. That the streambeds are composed of cohesive materials makes it somewhat unique in comparison to other streams in the Southeastern Plains that are generally sand or gravel bedded.

OVERVIEW OF METHODOLOGY

The methods used in this study follow a conceptual procedure aimed at developing defensible estimates of current sediment loads and sources relative to a “reference” sediment load for the James Creek watershed. Data must be acquired and analyzed to support each of the following phases of analysis, with each phase building on the previous. This methodology is outlined below as per the objectives listed in an earlier section of the report.

Characterization of “Reference” Suspended-Sediment Loading

A “reference” suspended-sediment loading condition can be defined as a concentration (in milligrams per liter; mg/l), load (in metric tonnes per day or year; T/d or T/y) or yield (in tonnes per day per square kilometer (T/d/km²) representative of “natural”, stable, or non-impaired conditions. For James Creek this means that in the absence of a stable channel analog within the watershed, data from similar watersheds in the Southeastern Plains (Ecoregion 65) must be used. The following tasks are outlined:

1. Empirically derive regional sediment loads for the Southeastern Plains using historical flow and sediment-transport data;
2. Based on diagnostic geomorphic criteria, determine relative stability of each site where historical data is available;
3. Determine regional sediment loadings by stage of channel evolution, dominant bed-material size class and relative stability;
4. Derive general “reference” and a refined “reference” for James Creek using data from the Southeastern Plains and stability conditions from James Creek.

Characterization of “Actual” Sediment Loading

“Actual” sediment loading in James Creek can be defined as the amount of sediment that is being transported through and out of the watershed outlet. Because no historical data on sediment transport is available for the James Creek watershed the only other mean possible to evaluate sediment transport is by empirical and numerical-simulation models. To characterize the actual sediment loading in James Creek, field and digital data are required as inputs to run the simulation models AnnAGNPS and CONCEPTS. The simulation period 1967-2002 was selected because this period coincides with measured channel-survey data. In general terms the work plan involves:

1. Simulate flow and sediment transport between known channel conditions 1967-2002;
2. Calculate the change in channel geometry from the 1967 and 2002 measured cross sections;
3. Simulate the contributions from uplands and tributaries (sheet, rills, gullies, tributary channels) using the non-point source pollution loading model AnnAGNPS Version 3.10;
4. Use runoff and erosion data obtained from AnnAGNPS as water and sediment inputs for CONCEPTS;
5. Simulate channel erosion along James Creek between 1967 and 2002 in the straight reach to rkm 17.2 (upstream limit of 1967 survey);

6. Simulate the contributions from the main stem of James Creek using the channel-evolution model CONCEPTS with AnnAGNPS loadings and compare these results with known changes over a shorter reach.
7. Determine sediment-transport rating relations from the combined AnnAGNPS with CONCEPTS simulations to determine “actual” sediment loadings in the same dimensions (units) as those defined for the “reference” condition.

General Description of AGNPS Modeling Technology

The Agricultural Non-Point Source Pollutant (AGNPS) watershed simulation model (Bingner and Theurer, 2001a) has been developed as a tool for use in evaluating the pollutant loadings within a watershed and the impact farming and other activities have on pollution control. Various modeling components have been integrated within AGNPS to form a suite of modules. Each module provides information needed by other modules to enhance the predictive capabilities of each. The modules in AGNPS critical to James Creek watershed include: (1) AnnAGNPS Version 3.10 (Cronshey and Theurer, 1998), a watershed-scale, continuous-simulation, pollutant loading computer model designed to quantify & identify the source of pollutant loadings anywhere in the watershed for optimization & risk analysis; and, (2) Conservational Channel Evolution and Pollutant Transport System (CONCEPTS) (Langendoen, 2000), a set of stream network, corridor, & water quality computer models designed to predict & quantify the effects of bank erosion & failures, bank mass wasting, bed aggradation & degradation, burial & re-entrainment of contaminants, and streamside riparian vegetation on channel morphology and pollutant loadings.

The Annualized Agricultural Non-Point Source Pollutant loading model (AnnAGNPS) is an advanced technological watershed evaluation tool, which has been developed through a partnering project with the United States Department of Agriculture – Agriculture Research Service (USDA-ARS) and Natural Resources Conservation Service (NRCS) to aid in the evaluation of watershed response to agricultural management practices. Through continuous simulation of surface runoff, sediment and chemical non-point source pollutant loading from watersheds, the impact of BMPs on TMDLs can be evaluated for risk and cost/benefit analyses.

AnnAGNPS is a continuous simulation, daily time step, pollutant loading model and includes significantly more advanced features than the single-event AGNPS 5.0 (Young *et al.*, 1989). Daily climate information is needed to account for the temporal variation in the weather. The spatial variability within a watershed of soils, landuse, and topography, is accounted for by dividing the watershed into many homogeneous drainage areas. These simulated drainage areas are then integrated together by simulated rivers and streams, which route the runoff and pollutants from each individual homogeneous area to downstream. From individual fields, runoff can be produced from precipitation events that include rainfall, snowmelt and irrigation. A daily soil water balance is maintained, so runoff can be determined when a precipitation event occurs. Soil loss from each field is predicted based on the Revised Universal Soil Loss Equation (RUSLE) (Renard *et al.*, 1997). The model can be used to examine the effects of implementing various conservation alternatives within a watershed such as alternative cropping and tillage systems including the effects of fertilizer, pesticide, irrigation application rate as well as point source yields and feedlot management (Bosch *et al.*, 1998).

Input Data Requirements

As part of the input data preparation process there are a number of component modules that support the user in developing the needed AnnAGNPS databases. These include: (1) the TOPographic PARAMeteriZation program (TOPAZ) (Garbrecht and Martz, 1995), to generate cell and stream network information from a watershed digital elevation model (DEM) and provide all of the topographic related information for AnnAGNPS. A subset of TOPAZ, TOPAGNPS, is the set of TOPAZ modules used within AGNPS. The use of the TOPAGNPS generated stream network is also incorporated by CONCEPTS to provide the link of where upland sources are entering the channel and then routed downstream; (2) The AGricultural watershed FLOWnet generation program (AGFLOW) (Bingner et al., 1997; Bingner et al., 2001b) is used to determine the topographic-related input parameters for AnnAGNPS and to format the TOPAGNPS output for importation into the form needed by AnnAGNPS; (3) The Generation of weather Elements for Multiple applications (GEM) program (Johnson et al., 2000) is used to generate the climate information for AnnAGNPS; (4) The program Complete Climate takes the information from GEM and formats the data for use by AnnAGNPS, along with determining a few additional parameters; (5) A graphical input editor that assists the user in developing the AnnAGNPS database (Bingner et al., 1998); (6) A visual interface program to view the TOPAGNPS related geographical information system (GIS) data (Bingner et al., 1996); (7) A conversion program that transforms a single event AGNPS 5.0 dataset into what is needed to perform a single event simulation with AnnAGNPS and, (8) An Arcview program to facilitate the use of Items 1-7. There is an output processor that can be used to help analyze the results from AnnAGNPS by generating a summary of the results in tabular or GIS format.

Contributions from Tributaries into the Main Channel

Loading information to the main channel for use with CONCEPTS is obtained by routing the AnnAGNPS water and sediment discharged by each AnnAGNPS cell through the channel system. At the outlet of each tributary that flows into the main channel AnnAGNPS provides: the flow; sediment by particle sizes of clay, silt, and sand; peak discharge; and, the time of concentration as part of an output file that can be used as an input file into CONCEPTS. This information is used in routing water and sediment by CONCEPTS in the main channel. Sediment loads for the large northwest tributary of James Creek will be also simulated using CONCEPTS to determine the applicability of the channel-erosion capabilities of AnnAGNPS for the defined unstable tributaries.

Contributions from AnnAGNPS Cells Adjacent to the Main Channel

The discharges from the tributaries provides the link between AnnAGNPS cells and CONCEPTS for the water and sediment that does not flow directly into the main channel. There are also AnnAGNPS cells that are along the main channel and deposit water and sediment directly into the main channel. These AnnAGNPS cells are also simulated and provide discharge information to CONCEPTS through an AnnAGNPS output file.

General Description of CONCEPTS Modeling Technology

CONCEPTS simulates unsteady, one-dimensional flow, transport of cohesive and cohesionless sediments in suspension and on the bed selectively by size class, and bank erosion processes in stream corridors (Langendoen, 2000). Hence, it can predict the dynamic response of flow, sediment transport and channel form ('channel evolution') to disturbances including channelization, altered hydrologic regime (e.g. by dam construction or urbanization), or instream hydraulic structures.

Hydraulics

CONCEPTS assumes streamflow to be one-dimensional along the centerline of the channel. It computes the flow as a function of time simultaneously at a series of cross sections along the stream using the Saint Venant equations (e.g. Cunge *et al.*, 1980). The governing equations are discretized using the generalized Preissmann scheme, and the resulting set of algebraic equations are solved using Gaussian elimination with partial pivoting for banded matrices (Anderson *et al.*, 1999). Four types of hydraulic structures are included in CONCEPTS: box and pipe culverts, bridge crossings, grade control (drop) structures, and any structure for which a rating curve is available.

Sediment Transport and Bed Adjustment

CONCEPTS calculates total-load sediment transport rates by size fraction from a mass conservation law, and by taking into account the differing processes governing entrainment and deposition of cohesive and cohesionless bed material (Langendoen 2000). For graded bed material, the sediment transport rates depend on the bed material composition, which itself depends on historical erosion and deposition rates. Following Hirano (1971), CONCEPTS divides the bed into a surface or active layer and a subsurface layer. These layers constitute the so-called 'mixing layer'. Sediment particles are continuously exchanged between the flow and surficial layer, whereas particles are only exchanged between the surface layer and substrate when the bed scours and fills. For cohesive materials, the erosion rate is calculated by an excess shear-stress approach while the deposition rate is calculated following the method of Krone (1962).

Streambank Erosion

CONCEPTS simulates channel width adjustment by incorporating the fundamental physical processes responsible for bank retreat: (1) fluvial erosion or entrainment of bank toe material by flow, and (2) bank mass failure due to gravity (Simon *et al.*, 1999; Langendoen 2000). Natural streambank material may be cohesive or noncohesive and may comprise numerous soil layers reflecting the depositional history of the bank materials; each layer can have physical properties quite different from those of other layers. CONCEPTS accounts for streambank stratigraphy by allowing variable critical shear-stresses to be assigned to the bank materials. An average shear-stress on each soil layer is computed, which increases with depth. Because of the resulting shear stress distribution, CONCEPTS is able to more realistically simulate streambank erosion caused by undercutting and cantilever failures.

Bank stability is analyzed via the limit equilibrium method, based on static equilibrium of forces and/or moments. Streambank failure occurs when gravitational forces that tend to move soil downslope exceed the forces that resist movement. The risk of failure is usually expressed by a factor of safety, defined as the ratio of resisting to driving forces or moments. CONCEPTS performs stability analyses of planar slip failures and cantilever failures of overhanging banks by dividing the bank into slices, and evaluating the balance of forces on each slice in vertical and horizontal directions. The slope of the failure surface is defined as that slope for which the factor of safety is a minimum. The bank's geometry, soil shear-strength (effective cohesion, c' , and angle of internal friction, ϕ'), pore-water pressure, confining pressure, and bulk unit weight determine the stability of the bank.

Input Data Requirements

CONCEPTS requires similar input data to other such models [e.g. HEC-RAS (Brunner, 2001), or GSTARS2.1 (Yang, *et al.*, 1998)]. Typical input data are: water and sediment inflow at the upstream boundary of the model channel and any tributaries; the geometry (cross sections) of the channel; Manning's n roughness coefficients; and composition of bed and bank material. In addition, the user needs to supply bank material properties for the streambank erosion component of CONCEPTS, such as the critical shear stress required to entrain bank material particles, and the shear-strength parameters effective cohesion, c' , and angle of internal friction, ϕ' . All input data can be obtained from Federal agencies such as the United States Geological Survey or can be measured *in situ*.

Simulation Scenarios

The characterization of James Creek watershed during the simulation period is critical in providing estimates of the loadings at the outlet. The AnnAGNPS model provides the capability of simulating changing landuse with time if adequate information is available. Unfortunately, for James Creek watershed, landuse information is not available for the entire simulation period, and at best has recorded information available from NRCS on the landuse applied only over the last ten years.

For James Creek watershed the channel reaches have been evolving with time, producing changing channel cross sections that affect the flow and sediment discharge. The capability of estimating channel erosion using AnnAGNPS is best suited for channels that are not evolving, since simulated channel cross sections remains fixed with time. The application of CONCEPTS on evolving channels provides the best determination of the sediment eroded from these evolving and incised channels. Since AnnAGNPS simulates the discharge from the tributaries that also may be evolving, certain assumptions are needed on how to best describe the tributary contributions.

Since accurate information is not available for all locations and for all the years simulated, then an approach that would provide the best estimate of sediment loadings at the outlet and the uncertainty of this estimate is needed. The use of simulation models provides the capability to easily simulate various scenarios that can provide meaningful upper and lower limits of an estimated actual condition by changing the characterizations of the watershed. These scenarios will be developed for use by AnnAGNPS to provide the loadings to CONCEPTS and

CONCEPTS will then provide an estimate of the sediment loadings at the downstream outlet. The worst and best case erosion control scenarios will be simulated for cropping practices and for the location of eroding channels.

Conventional Tillage

The farming practice that would have been in place from 1967 to the early 1990's would have mainly involved the use of conventional tillage for all of the crops. This is mainly because effective weed and insect control was not available through the use of chemicals, nor was the use of chemicals affordable for most farmers at that time in this area. Although, most likely some farmers would have started using some reduced tillage practices beginning in the 1980's, but the amount of land or the location on the watershed used with these practices is unknown. Conventional tillage provides the least erosion control for protecting the fields and when simulated over the entire period, would provide the upper limits of sediment loadings. The distribution of the crops will be assumed to be the same as currently applied in the watershed as of 2000 and 2001 as a two year rotation.

Reduced Tillage

Reduced tillage farming practices provides more effective erosion control than conventional tillage, but not as well as no-tillage practices. For James Creek watershed, most farmers have not adopted no-tillage, but mostly all farmers currently use reduced tillage practices. For this area, reduced tillage means that farmers would mainly only cultivate as few times as possible and no longer plow up the soil completely, but use chisel plowing. The application of reduced tillage farming practices for the entire simulation period would provide the lower limits of sediment loadings from the uplands of the watershed.

Stable and Unstable Channel Reaches

The AnnAGNPS model can be used to simulate channel erosion, but the simulated channel will not change over time and thus, can not widen, aggrade, or degrade throughout the simulation period. The application of AnnAGNPS and CONCEPTS provides the capability to effectively simulate evolving channels. For James Creek watershed, the tributaries may also be evolving, which AnnAGNPS will not effectively simulate that evolving channel process, but AnnAGNPS can be used to estimate if the channel is eroding. One assumption used for the James Creek watershed simulation will be if a channel reach is determined to be stable (not evolving), then there is no erosion from that reach simulated by AnnAGNPS. Although, sediment can still be deposited in the AnnAGNPS simulation within each reach. The second assumption will be that channels that are identified as unstable (evolving), from ground reconnaissance, then channel erosion will be allowed from that reach simulated by AnnAGNPS. The following AnnAGNPS simulation scenarios will be applied: all of the channels are stable and thus, not eroding; all of the channels are unstable, and thus, eroding; and, only the channels identified as being unstable are set to allow channel erosion, with all of the rest of the channels set to stable conditions. This will provide the upper and lower limits of the capability of estimating channel erosion with AnnAGNPS through a determination of channel stability.

DEVELOPMENT OF DATABASES

The types of data required to perform geomorphic interpretations and conduct numerical simulations is extremely diverse. This information ranges from historical accounts, maps and photographs, precipitation and flow data, digital elevation and land use coverages, first-hand observations, and numerical characterization of channel conditions and boundary sediments.

Aerial and Ground Reconnaissance

A reconnaissance of James Creek and the main tributary channels was conducted for the purpose of obtaining access for field crews and for determining the relative state of channel instability along their entire lengths. A helicopter flight was used to evaluate the magnitude and extent of channel instabilities, identify locations of hard points or grade control on the streambed, and to note the stability conditions at tributary mouths, as well general watershed characteristics (Figure 9). In any study of watershed runoff and sediment production, it is extremely important to have a first-hand look at ground conditions in as much of the watershed as possible. In addition, this provided an opportunity to obtain information from local landowners and access to properties to conduct field testing and sampling.



Figure 9 – From left, Andrew Simon, Carlos Alonso and Ron Bingner following completion of aerial reconnaissance of the James Creek watershed.

Watershed Reconnaissance

An aerial reconnaissance provided information on the general patterns of land use and best management practices (BMPs) contained within James Creek watershed. While the aerial reconnaissance provided general insight on the extent of the tributaries and the watershed boundary, ground reconnaissance was needed to confirm many features of the watershed. The land use distributions at select locations were investigated, such as the magnitude of wheat growing on the watershed (Figure 10). The locations of road crossings over James Creek and tributaries were also investigated for points of entry for surveys or erosion control (Figure 11). Locations of some problem areas associated with gullies were located by aerial reconnaissance, but confirmed later with ground reconnaissance or historical aerial photographs (Figure 12). The locations of best management practices (BMPs) were identified, such as the application of strip cropping with corn (Figure 13).



Figure 10 – Aerial photograph of extensive wheat fields that have been recently harvested in June, 2002 within James Creek watershed.

Channels Reconnaissance

Observations from the helicopter flight were that almost the entire length of James Creek had unstable banks except in those locations just upstream from the seven low-water crossings. The downstream sinuous reach appeared to be the deepest with the most active banks. The majority of tributary mouths were incised and unstable with only tributary reaches with very small drainage areas being stable. Sediment deposition on the inside of incipient meander bends was observed, particularly in the sinuous reach below rkm 6.6. Although this bed process indicates a net deposition of sediment in the section, the lateral and vertical accretion of sediments on the inside bend leads to flow deflection and bank-toe erosion, and ultimately bank failures on the opposite side of the channel. In fact, it is common in these types of incised reaches for there to be a net erosion of sediment because of the large contributions from the channel banks.



Figure 11 – View looking upstream from the junction of Darracott Road and James Creek located at the bridge in the lower right portion of the aerial photograph.



Figure 12 – Significant recent gully migration within a recently planted soybean field, as evidenced by gully headcuts moving into rows.



Figure 13 – One of the few corn fields using strip cropping as a best management practice.

Ground reconnaissance was used to establish the locations of surveying and field-testing locations and to provide us with an initial understanding of the type of bed and bank materials. From this effort an initial total of 38 cross-section locations along James Creek were selected for surveying and 17 of those were selected for sampling and materials testing (Figure 1). Eight sites were selected for surveying along the main tributary with sampling and testing at two of those sites.

Input Database for the AGNPS Model

The development of input parameters used for AnnAGNPS to describe the James Creek watershed conditions involved assembling many sources of available information, such as elevation maps, soil data, landuse and operation management data, and especially weather information. Most of the required model parameters can be selected from the available data, but there are some instances where the collection of additional measured data will improve the simulation results. Most of the measured data needs for James Creek involved collecting simple channel geometry values of various tributaries, as described in the reach geometry section. The compilation of the data into the form needed by AnnAGNPS was performed using the AGNPS Arcview Interface and the AnnAGNPS Input Editor.

GIS Database

The use of a geographic information system (GIS) is critical in gathering the needed data to perform simulations for watersheds of the size of James Creek watershed. The GIS data provides the vital link between the characteristics of the watershed and the parameters needed by the model. Fortunately, for Mississippi there is a data warehouse, Mississippi Automated Resource Information System (MARIS), which catalogs and distributes data administered by the state of Mississippi Board of Trustees / Institutions of Higher Learning's MARIS Technical

Center (MTC) that serves as a central location for much of the GIS data available for any watershed in the state. There are limits to the quality of this data and, as will be discussed for the landuse of James Creek watershed, requires other sources to obtain all of the information needed.

For the application of the entire suite of AGNPS, the basic GIS data needed are: the digital elevation models (DEMs) to describe the topography; the landuse GIS layer to describe the vegetative cover; and, a soils GIS layer, which all together can provide the spatial variation of the important characteristics of the watershed. Additional GIS data is useful in assessing the creation of model parameters and the impact various features may have on the watershed system. This can include digitized quad sheets, aerial photographs, location of streams, roads, erosion control structures on fields and in the channels, lakes, and other features impacting the watershed. For information that is not available from any source, then information may need to be digitized from other maps, or transferred from field work using global positioning system (GPS) techniques.

The projection used for the James Creek watershed analysis by all of the GIS data layers was the Mississippi Transverse Mercator (MSTM). This provided consistency among all of the layers when data was analyzed or paper maps were produced. Other GIS layers can easily be reprojected from another projection to MSTM.

Topographic Analysis

Every watershed has unique topography that is difficult to characterize without having maps that describe the elevation throughout the watershed. Topographic information is crucial in determining the watershed and subwatershed boundaries, channel locations, channel slopes, routing of flow from fields to channels to the watershed outlet, field slopes, travel time of flows, the RUSLE LS-factor, aspect and elevation of fields. The use of DEMs provides a convenient source of topographic information, but often is derived from basic topographic contours, such as from the USGS 7.5 minute quad maps. Thus, the resolution can range from 120m x 120m raster grids with 5m elevations, to 30m x 30m with 1m elevations, to 10m x 10m with 0.1m elevations, depending on the source of the DEMs. The 10m x 10m raster grid can provide a better definition of the watershed topography, but generates a much larger file size needed to store the data. Other considerations in using the 10m x 10m raster grid are that this will require more computer resources to execute the AGNPS topographic tools, such as more memory, more hard disk space, and additional computational time. Also, the 10m x 10m DEM raster grid is available from MARIS with the elevation provided in feet and requires the conversion to meters before using TOPAGNPS, while the 30m x 30m DEM already has the elevation in meters. For larger watersheds of over 200 square kilometers with homogeneous characteristics, DEM resolutions of 30m x 30m might provide adequate information when computer resources are limited.

DEMs

The MARIS Technical Center has been producing tagged vector contours at 1:24,000 scale from U.S.G.S. mylar separates. These contour line files were used to produce 10 meter resolution DEMs for each county in Mississippi. For James Creek watershed, the Monroe county 10 meter resolution DEM was obtained (Figure 14). While the 30 meter resolution DEM

was also available, with less storage space requirements on a computer, this was not a limitation for the computers available at NSL, and thus, the 30 meter resolution DEM was not used.

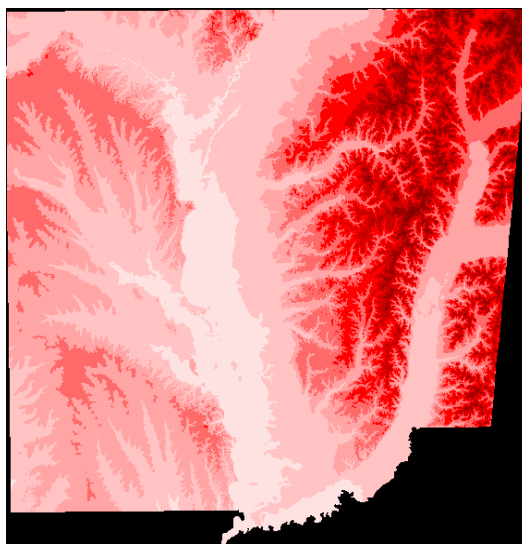


Figure 14 – The Monroe County digital elevation model (DEM) obtained from MARIS at the 10 meter by 10 meter resolution with 0.3 meter elevation resolution.

Modification of DEMs

The modification of DEMs may be required when local features within a watershed are not captured during the development of the DEM. This could be because of recent human activities that change the elevation within areas of the watershed. This includes land-leveling of fields, channel straightening, road construction, or development of field ditches to route water around fields. The generated watershed characteristics generated by AGNPS components then may not correspond to actual stream locations or watershed boundaries. In order to account for these topographic variances, the DEM may be modified to adopt the required features. Typically, areas near the watershed boundary may contain problem areas, but generally are not a major concern unless there is a noticeable problem or a feature of interest is not included in a known watershed. More likely areas that may require modification of a DEM are measures that have produced straightened channels.

Digitized Soils Maps

The soils information obtained from MARIS is a near approximation of the State Soil Geographic (STATSGO) soils database available nationwide for every state from NRCS, with some added spatial resolutions to better describe the variation of the soils. The soils from this layer was then used to determine the appropriate soils to use within the James Creek watershed (Figure 15). The Monroe County Soil Survey Geographic (SSURGO) data base from NRCS has not been completed, but when finished will provide information based on the NRCS County Soil surveys and should be used in place of STATSGO.

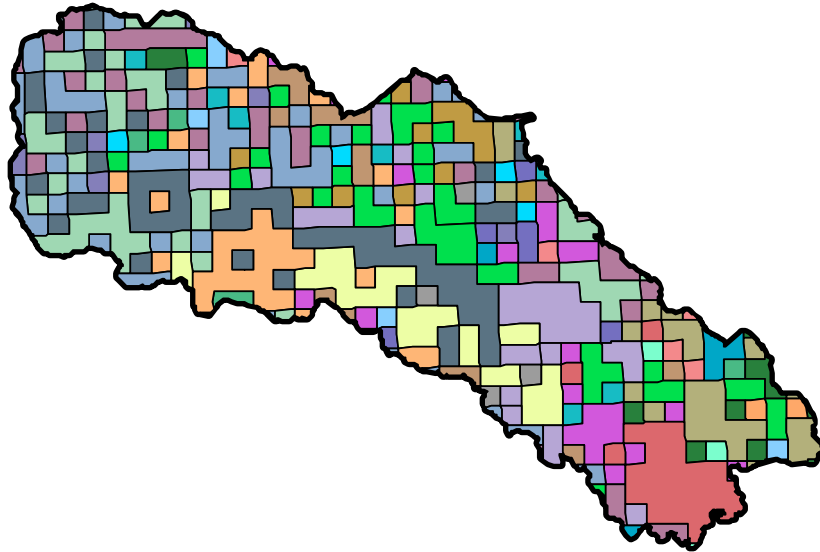


Figure 15 – The geographic soil layer for James Creek watershed obtained from MARIS and derived from STATSGO.

Digitized Landuse Maps

An accurate description of the landuse is critical in defining the impact farming management practices may have on soil erosion. The determination of the historical landuse for large watersheds such as James Creek watershed can be difficult without the use of satellite imagery. Although, local information based on documented crops and aerial photographs can be used, this often requires considerable time in analyzing and digitizing the data. Various sources were used to derive the best description of the landuse on James Creek watershed by the amount and location of the various types of vegetation.

National Agricultural Statistics Service (NASS) Landuse

The U.S. Department of Agriculture, National Agricultural Statistics Service (NASS), Research and Development Division have developed images using categorized Landsat 5 and 7 data for Mississippi. The images have been labeled as specific crop types for the cultivated cropland areas. The non-cropland areas are broadly defined to complete the watershed area coverage, and are not accurate for non-cropland land cover maps. Thus, for the cropland areas and categories, the performance statistics and the accuracy levels and measurements for the categorization are considerably more meaningful than for non-cropland areas and categories. The data layer from NASS provides a rasterized Cropland data layer for Mississippi. The data provided is projected in the UTM projection and is available through the web address:

<http://www.nass.usda.gov/research/SARS1.htm>

The NASS landuse was developed through a data sharing partnership with USDA's Foreign Agricultural Service and USDA's Farm Services Agency. The agreement provided access to Landsat 5 coverage in Mississippi. The information for James Creek watershed was determined to not be of a sufficient accuracy for use in the simulations, since the non-crop description of NASS is not accurate.

Multi-Resolution Land Characteristics (MRLC) Landuse

The Multi-Resolution Land Characteristics (MRLC) Consortium was sponsored originally in 1992 by the U.S. Geological Survey (USGS) National Mapping Division (NMD) Earth Resources Observation Systems (EROS) Data Center (EDC), the U.S. Environmental Protection Agency (EPA) Office of Research and Development (ORD) National Exposure Research Laboratory (NERL) Environmental Science Division (ESD) Landscape Characterization Branch (LCB), the National Oceanographic and Atmospheric Administration (NOAA), and the U.S. Forest Service (USFS). Additional sponsors are the National Atmospheric and Space Administration (NASA) and the Bureau of Land Management (BLM). The data can be obtained at the Internet Web address:

<http://www.epa.gov/mrlc/nlcd.html>

Land cover was mapped using general land cover classes. For example, forest is classified as either, deciduous, evergreen or mixed. Land-cover classification was based on MRLC's Landsat 5 Thematic Mapper (TM) satellite data archive and a host of ancillary sources. From the overlay of the James Creek watershed boundary the estimated MRLC cropland was 5,463 hectares.

Landuse from the NRCS Monroe County District Conservationist Office

The office of the NRCS District Conservationist for Monroe County provided information on landuse as described for James Creek watershed from aerial photographs and records of cropping patterns for the years 1999-2001. From this information, field boundaries were digitized linking the location of the field with the associated management applied on each field (Figure 16). This landuse information can then be compared with classified Landsat imagery to determine the actual landuse for that time. From the analysis of the data provided by NRCS there are approximately 4,249 hectares of cropland in James Creek watershed.

Landuse Derivation for Use with AnnAGNPS

In order to accurately determine the landuse for the year 2001, the digitized field boundaries based on land ownership (Figure 16) were compared with field boundaries observed from the DOQQ to identify fields that contained entirely a single crop (Figure 17). This provided information that was used to obtain the 'ground truthing' for the accurate classification of landuse in Landsat 7 Enhanced Thematic Mapper (ETM+) imagery. A comparison of the identified fields (Figure 17) with the Landsat 7 Enhanced Thematic Mapper (ETM+) imagery acquired on August 3, 2001 (Figure 18) provided the basis to classify the remaining crop fields for 2001, with the crop field boundaries digitized from the DOQQ (Figure 19). The resulting information on fields that have crops (Figure 19) was then combined with the MARIS Landsat 5 imagery (Figure 20) that had adequate information to describe the non-crop areas, to produce a

derived GIS landuse layer that best represented the landuse for 2001 (Figure 21). Areas that were defined as cropland in the Landsat 5 imagery (Figure 20) were either replaced with the cropland defined in (Figure 19) or redefined based on the classification of the Landsat 7 imagery (Figure 18). All non-crop areas in the final landuse used with the AGNPS Arcview interface (Figure 21) remained as defined by Landsat 5 (Figure 20).

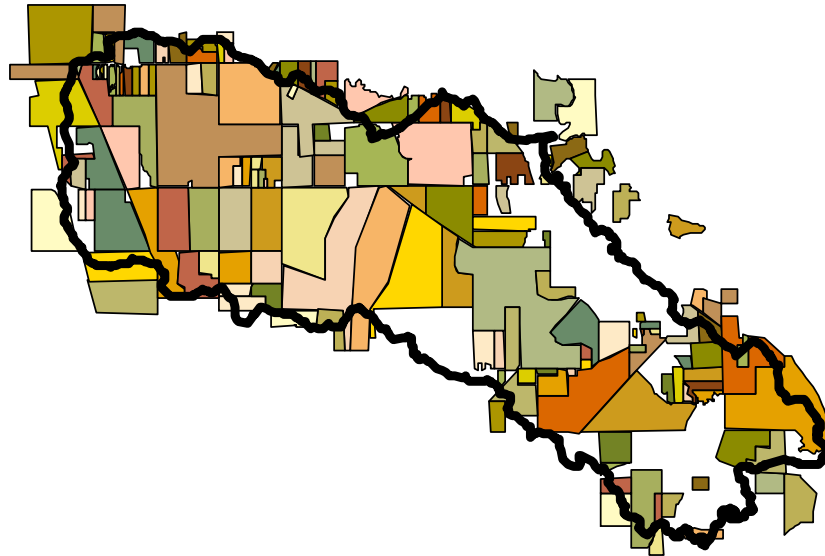


Figure 16 – Land ownership fields on James Creek watershed as defined by NRCS.

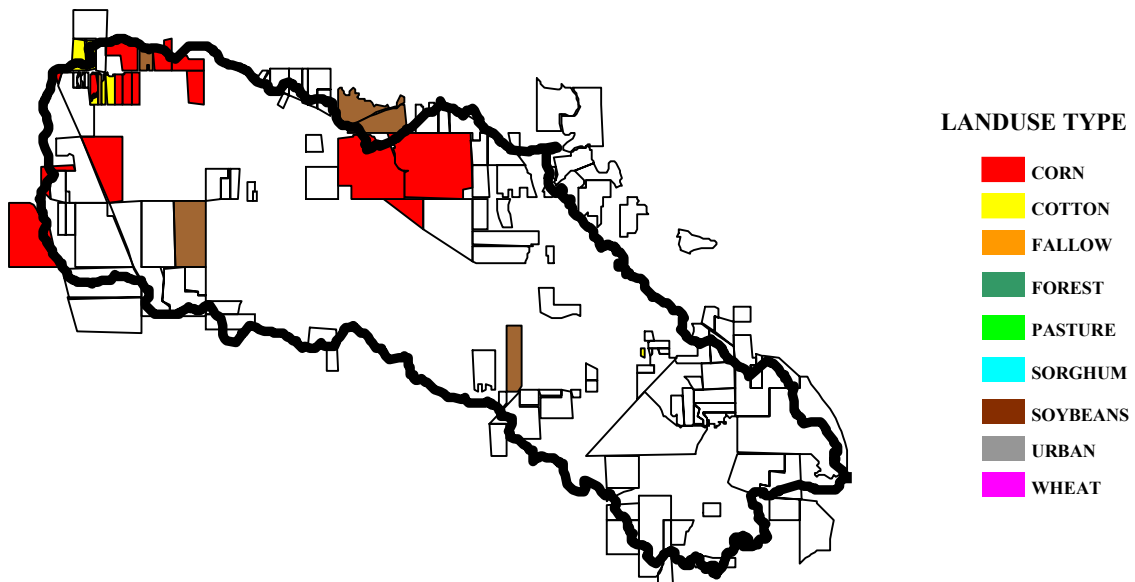


Figure 17 – Land ownership boundaries with a single landuse defined for comparison of the crops.

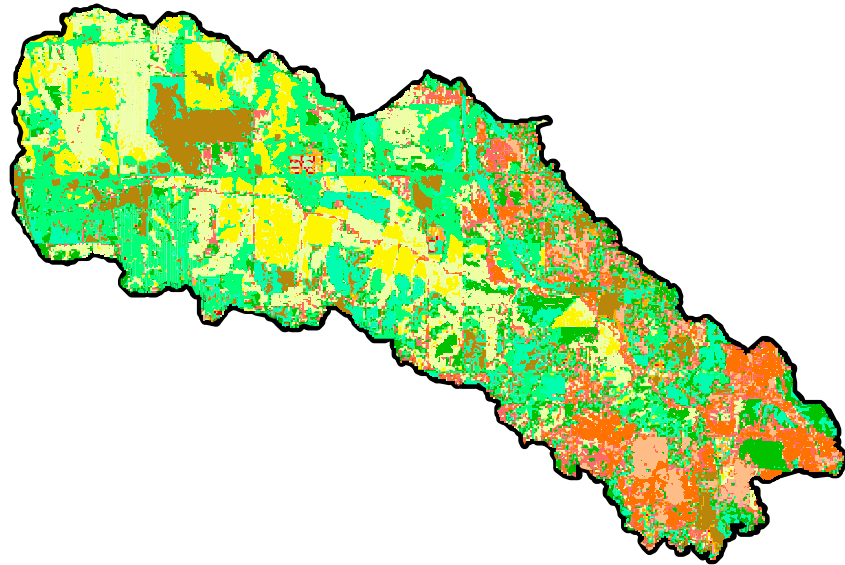


Figure 18 – Landsat 7 classified landuse layer obtained for August 3, 2001.

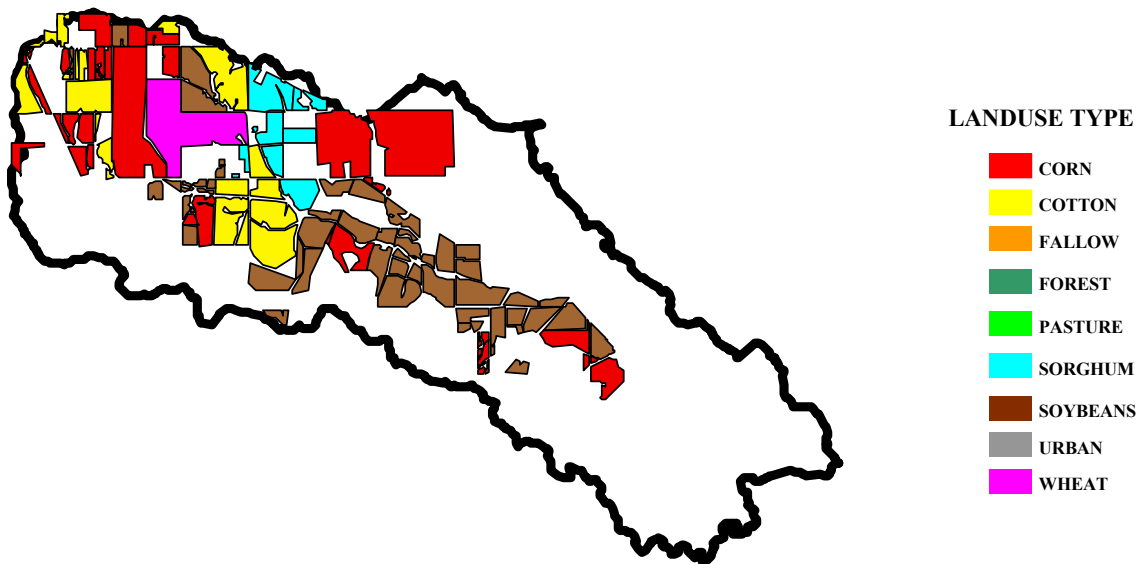


Figure 19 – Cropland defined from the digitized field boundaries of the DOQQ.

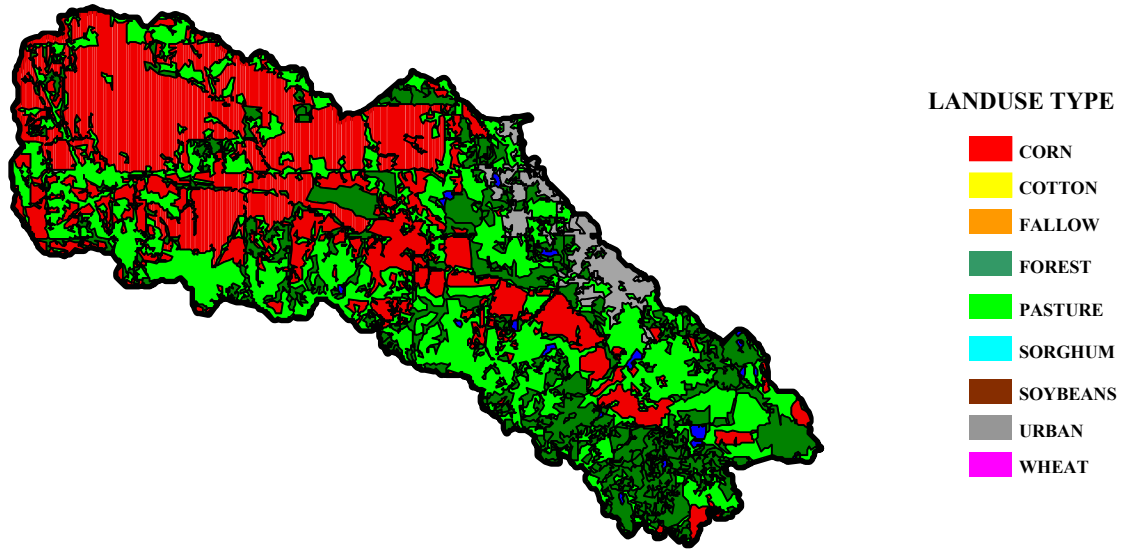


Figure 20 – Landsat 5 landuse layer obtained from MARIS based on images from 1991-1993.

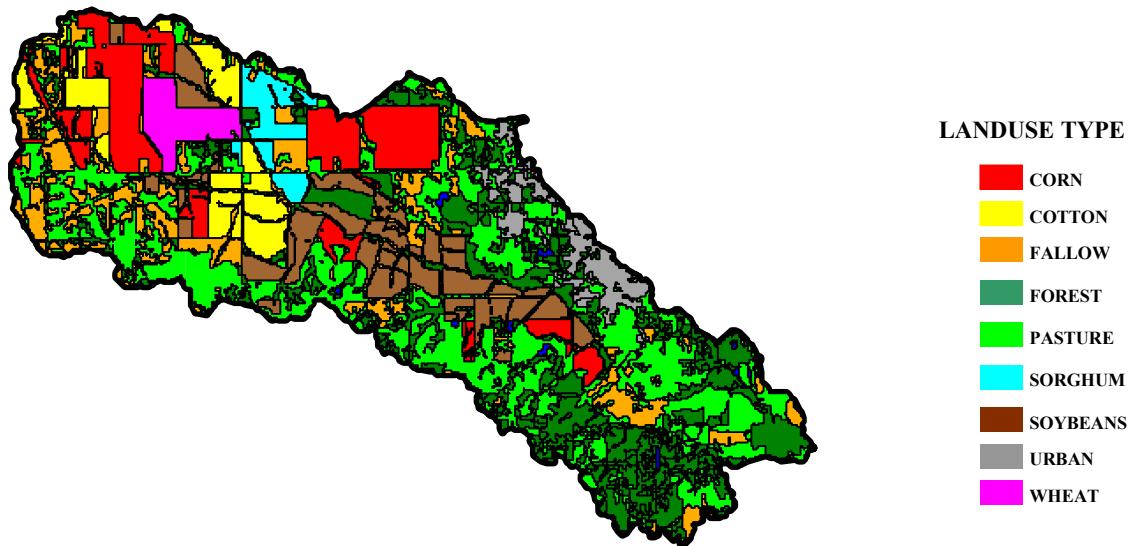


Figure 21 – Landuse used as the final layer defined as applied with the AGNPS Arcview interface.

Additional GIS Layers

Digital Raster Graphics (DRG's)

Digital Raster Graphics (DRG's) are digital copies of 7.5 minute - 1:24,000 topographic maps published by the U.S.Geological Survey. The USGS produces their DRG product by scanning paper copies of the map at 500dpi and then resampling them to 250 dpi. USGS

topographic maps covering Mississippi were published over a number of years, with the most recent original versions and updates ranging from the early 1960's to mid 1990's. The DRG's are output as geotif image files and for Monroe county the DRG was available from MARIS in the MSTM projection (Figure 22). The DRG's are very useful in evaluating the location of the watershed boundary and channels generated by TOPAGNPS.

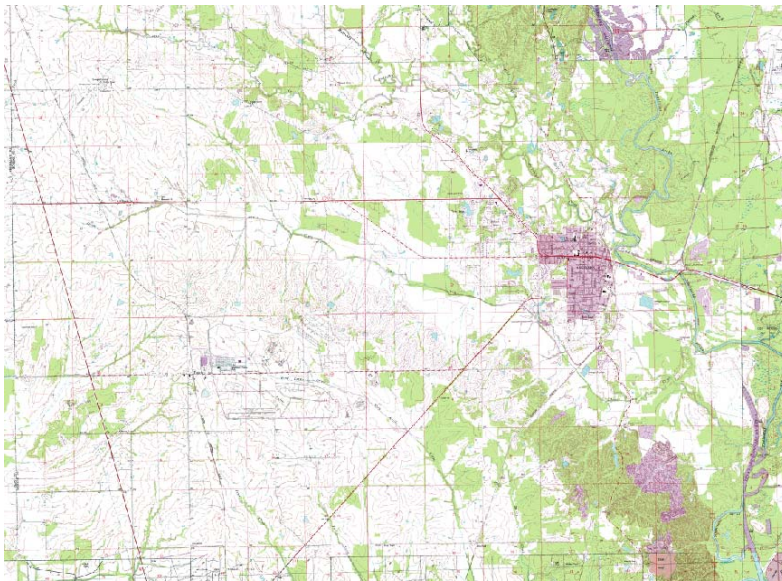


Figure 22 – The Monroe County digital raster graphic (DRG).

Digital Ortho Quarter Quads (DOQQs)

Digital Ortho Quarter Quads (DOQQs) were produced from 23 millimeter by 23 millimeter (9 x 9 inch) film images scaled at 1:40,000 and mosaiced to produce an image in MSTM projection with a ground resolution of one meter and obtained from MARIS (Figure 23). This image can then be used to investigate various features in the watershed such as the location of terraces, gullies, or ponds.

Perennial and Intermittent Streams

The location of perennial and intermittent streams is important in determining if the generated stream network by TOPAGNPS is at a sufficient accuracy for use with AnnAGNPS. The location of the streams can also provide information as to whether the watershed boundary has been determined accurately. This can be seen if a stream crosses a watershed boundary, resulting in a problem with the DEM. One technique to improve the accuracy of the location of the watershed boundary and generated streams is to adjust the DEM based on the location of the digitized streams. Whenever a digitized stream would fall onto a DEM raster then the elevation of the DEM raster can be adjusted by a set amount, such as subtracting three meters from the DEM raster value. This would help to ensure that the slope of the streams would be maintained when the TOPAGNPS module generates the stream network. For James Creek watershed the digitized perennial and intermittent streams were obtained from MARIS (Figure 24).



Figure 23 – The DOQQ for Monroe County.

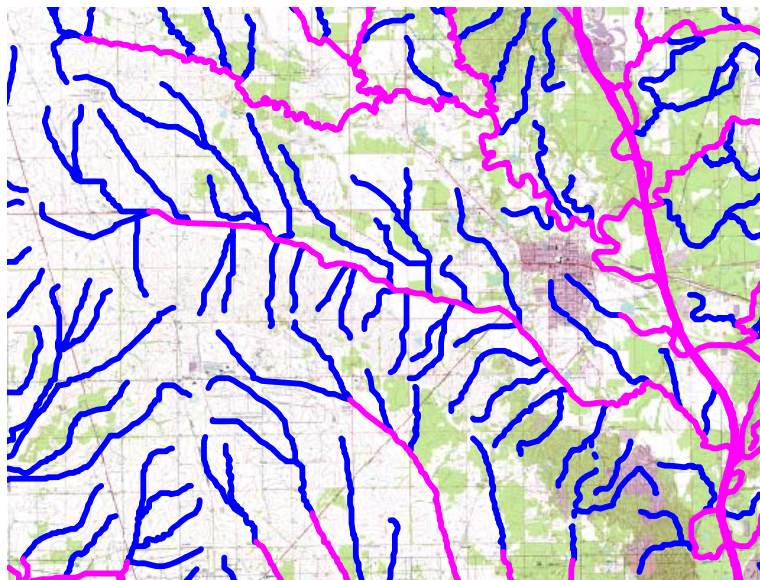


Figure 24 – The Perennial streams (purple) and intermittent streams (blue) indicated on the DRG for James Creek watershed and surrounding areas.

AGNPS Arcview Interface Application

The AGNPS Arcview interface can simplify many of the steps used in developing the needed input parameters required by AnnAGNPS. The User's Guide for the AGNPS interface details the application of the program. A summary of what was done for James Creek watershed in the development of the AnnAGNPS input dataset using the interface is provided in this report.

Watershed Segmentation

Drainage Boundary

A determination of the drainage boundary for James Creek watershed is critical before proceeding to other issues, such as using the landuse and soils GIS layers to determine the attribute identifier from each layer. Having an accurate watershed boundary focuses the area of concern so all of the important watershed characteristics can be examined. Using the AGNPS Arcview interface, which accesses the TOPAGNPS files, and the DEM, the watershed boundary file was produced. Additional files for use with AGNPS were also produced, but the use of those will be discussed in later sections. The first step in this process is to determine the watershed outlet.

For James Creek watershed the outlet coincides with the mouth of James Creek as it flows into the Tombigbee River. The exact location of the outlet in terms of the position within the DEM was determined using the perennial streams shown in Figure 24 and the DRG. This also allows the DEM to be reduced in size by clipping the drainage area that includes only James Creek watershed (Figure 25) using the AGNPS Arcview Interface. This reduces the computational time needed when using TOPAGNPS and displaying the final determinations with Arcview. The Monroe county DEM was not converted for the elevations to be in meters until after a clipped region was selected, since the main information is the location of the stream network in this step. The DEM was clipped based on the location of the confluence of James Creek and Tombigbee River, and the drainage area that would flow into the farthest upstream channel locations and then elevations were converted to meters. The watershed outlet location used with TOPAGNPS was determined by viewing the DRG and DOQQ layers with the digitized perennial streamflow locations for the entire Monroe County DEM (Figure 26 and Figure 27, respectively), and using “Step 2 Select watershed Outlet” menu item of the Interface with the “Interactively Select Outlet” option. Once the outlet was determined, AGNPS Arcview Interface Steps 3-6 were performed to generate the topographic parameters used by AnnAGNPS. The watershed boundary along with the generated stream network, and other associated files were also produced for use in analyzing the data for any noticeable problems.

The initial watershed boundary was displayed as an overlay onto the DRG and the DOQQ (Figure 28 and Figure 29, respectively). From these comparisons, there were problems identified with the watershed boundary at certain locations (Figure 30). In addition, the location of the stream network generated by TOPAGNPS did not define very well the location of the major confluences as observed from the digitized perennial and intermittent streams (Figure 24). Thus, a modification of the clipped DEM was made based on the location of the digitized perennial and intermittent stream locations, where at points that coincided with the stream network and the DEM, the DEM elevation at that raster point was reduced by three meters. This would provide information within the DEM concerning the location of concentrated flows and the generated stream network that would likely produce a stream network similar to the digitized stream network. The reduction of three meters at each stream point would ensure that the slope of the channels would be maintained.

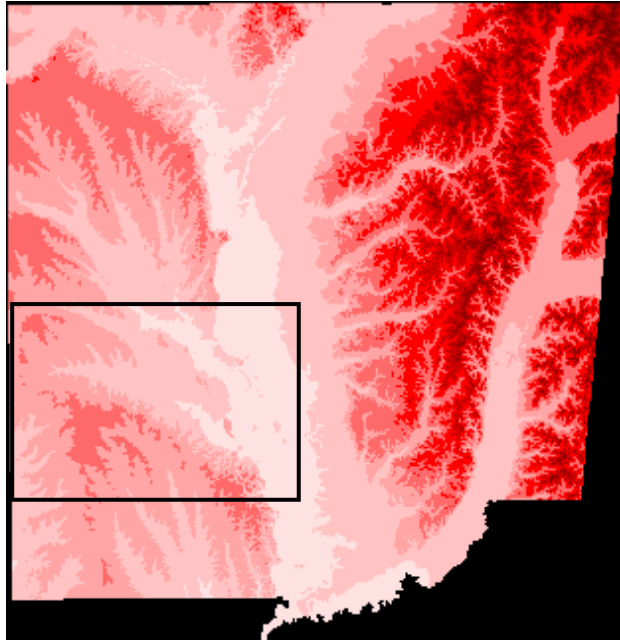
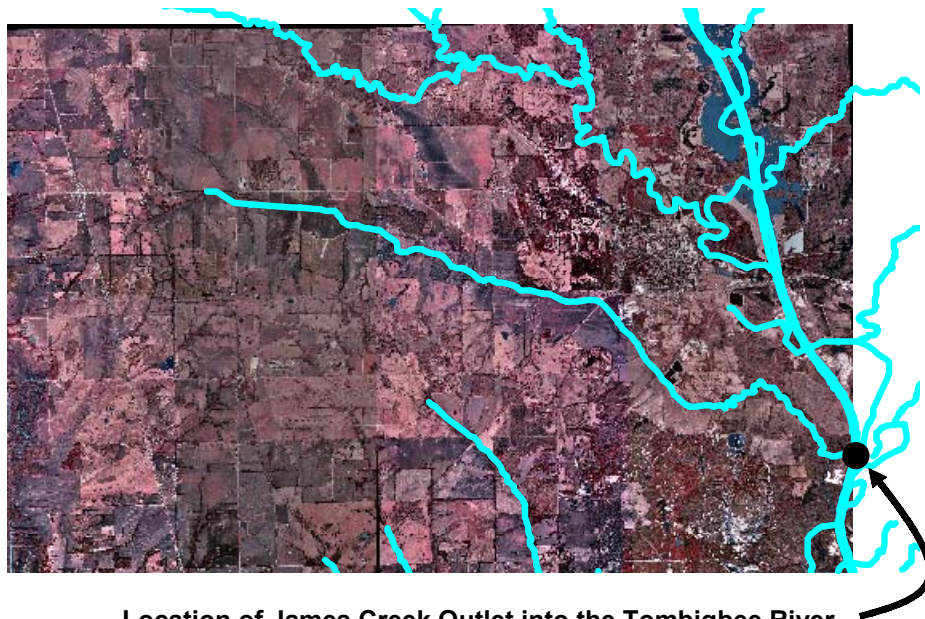
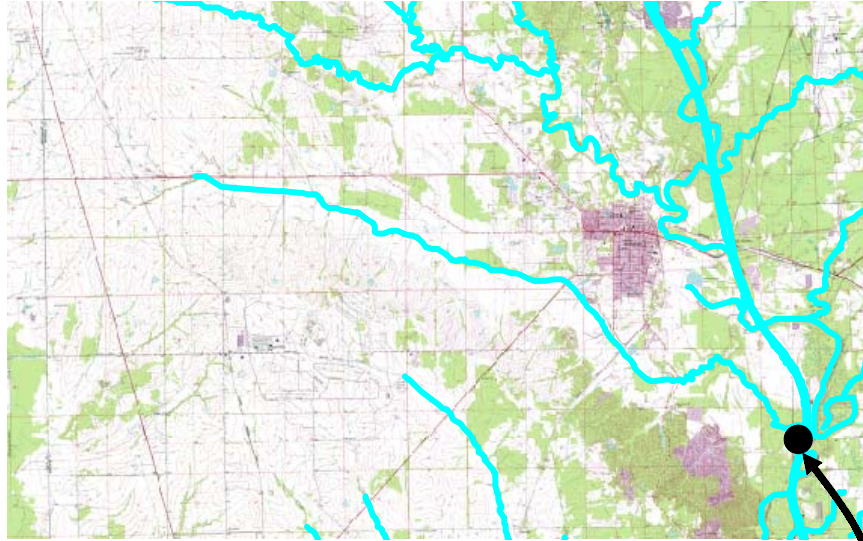


Figure 25 – A graphic drawn on the Monroe County DEM containing the James Creek watershed for use in clipping the DEM to a smaller area for analysis with the AGNPS Arcview Interface.



Location of James Creek Outlet into the Tombigbee River

Figure 26 – The outlet determination of James Creek into the Tombigbee River using the digitized perennial streams and the DOQQ



Location of James Creek Outlet into the Tombigbee River

Figure 27 – The outlet determination of James Creek into the Tombigbee River using the digitized perennial streams and the DRG.

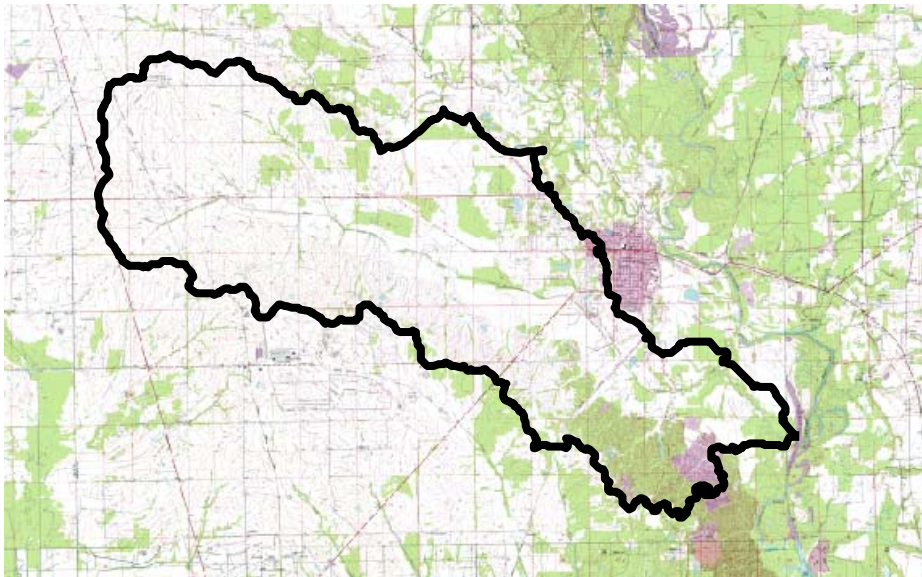


Figure 28 – The initial James Creek watershed boundary generated from TOPAGNPS as displayed with the DRG.

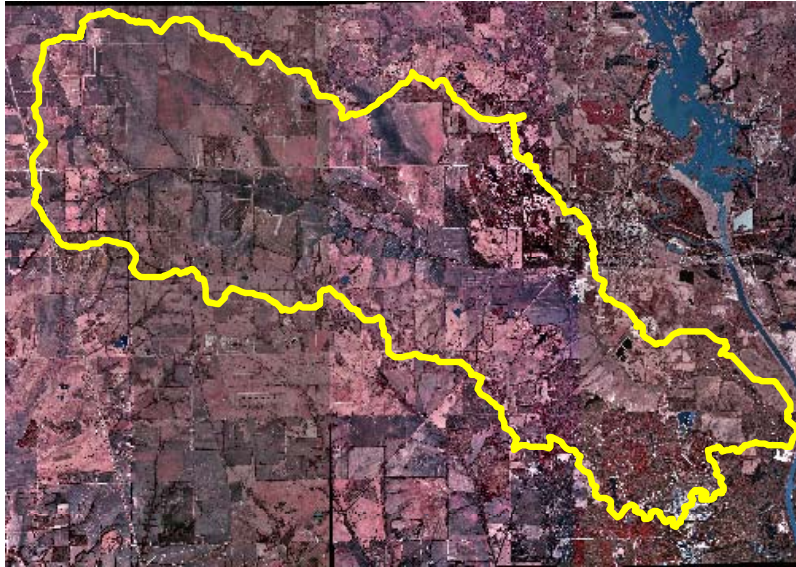


Figure 29 – The initial James Creek watershed boundary generated from TOPAGNPS as displayed with the DOQQ.

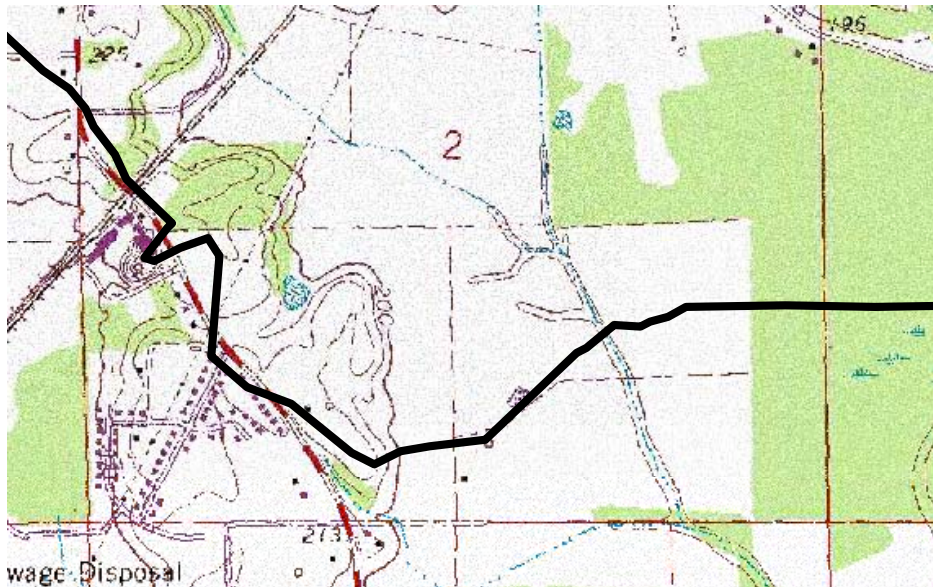


Figure 30 – A watershed boundary problem illustrated by a channel indicated on the DRG that crosses the boundary.

The AGNPS Arcview Interface procedures were then repeated with the eventual result producing a watershed boundary that better represented the drainage area of James Creek watershed (Figure 31). This was verified through an inspection of flow paths indicated on the DRG, to determine that the streams did not cross the watershed boundary (Figure 32). Once the modifications to the DEM have been completed, then the determination of the appropriate subdivision of the watershed into AnnAGNPS cells can be initiated.

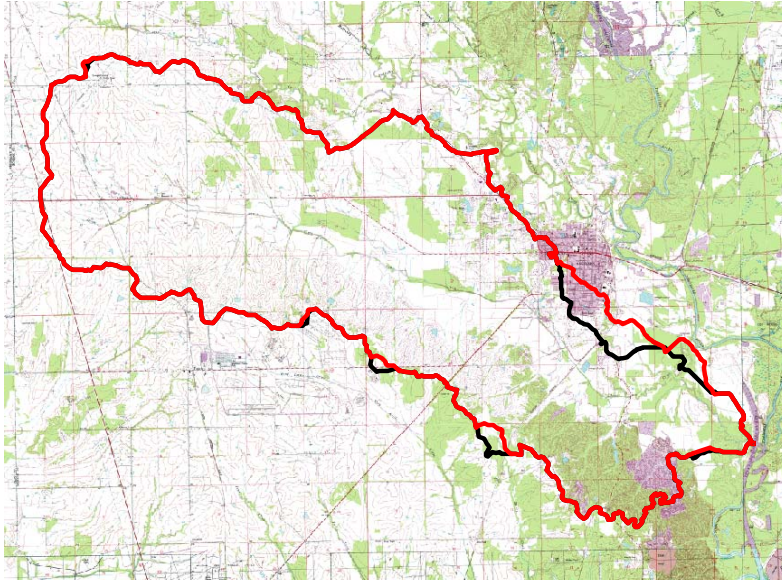


Figure 31 – The updated watershed boundary (red) produced from modifications of the DEM and the initial watershed boundary (black) produced without modification of the DEM.

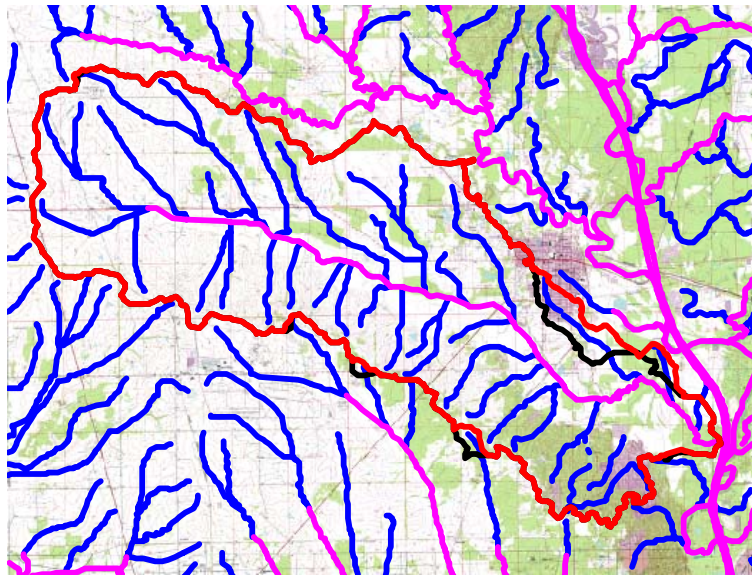


Figure 32 – The updated watershed boundary (red) produced from modifications of the DEM and the initial watershed boundary (black) produced without modification of the DEM, with the perennial streams (purple) and intermittent streams (blue).

Subdrainage Areas: AnnAGNPS Cells

The determination of the subdrainage areas of the James Creek watershed into AnnAGNPS cells was performed based on the spatial variation of landuse and the location of the digitized stream network. Additional information from the soils GIS layer is sometimes used in this determination, but was not used in this case because of the lack of reliable and detailed soil

information. The watershed was subdivided into a significant number of cells in order to reflect the landuse based on Landsat imagery, and NRCS landuse data for 2001. The process started with an assumption of the critical source area (CSA) and minimum source channel length (MSCL) required with the use of TOPAGNPS. An initial 200 hectare CSA and 800 meter MSCL values were selected to produce AnnAGNPS cells that are of significant size that individual AnnAGNPS cells can be identified for further subdivision. The process of starting with the generation of AnnAGNPS cells with large drainage areas and working to subdivide only those areas of major concern to the user's satisfaction provides the simplest approach to capturing the main features of the watershed.

The initial subdivision produced 63 AnnAGNPS cells distributed throughout the watershed (Figure 33). Since noticeable landuse areas were not adequately characterized, such as the spatial variability of cropland, various AnnAGNPS cells were selected for further subdivision using one of five various TOPAGNPS regions defined within the generation of the network region generation file (ntgcod.inp) (Figure 34). A further subdivision was also performed on the main tributary in order to characterize the lateral inflow adequately in comparing the loadings simulated by AnnAGNPS and CONCEPTS at the outlet of the main tributary discussed later. The final subdivision of James Creek watershed with TOPAGNPS produced 436 AnnAGNPS cells based on five TOPAGNPS regions (Figure 35) using CSA and MSCL values provided in Table 2, with an associated stream network of 178 reaches to produce the final subwatershed layer (Figure 36).

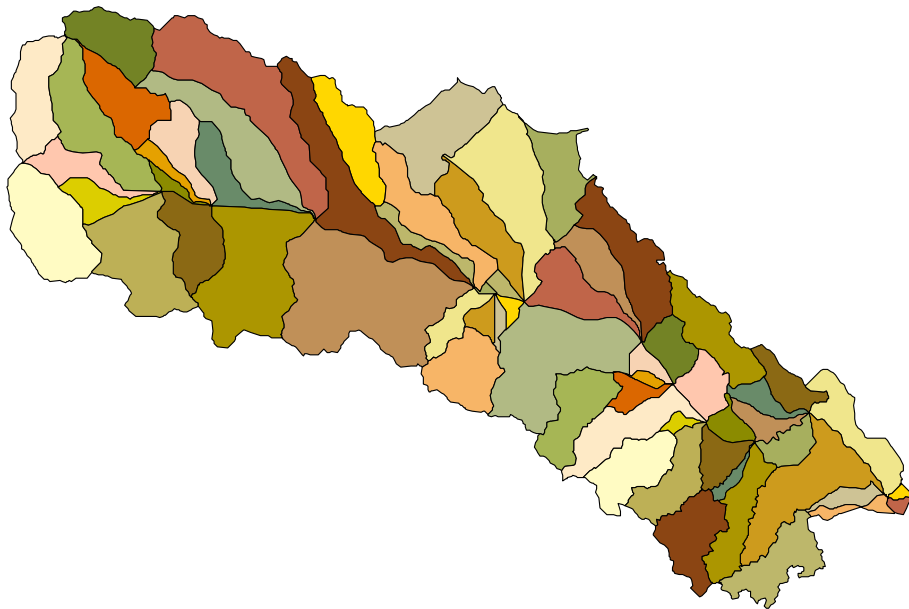


Figure 33 – The first trial of the generation of AnnAGNPS cells for James Creek watershed with the correct watershed boundary.

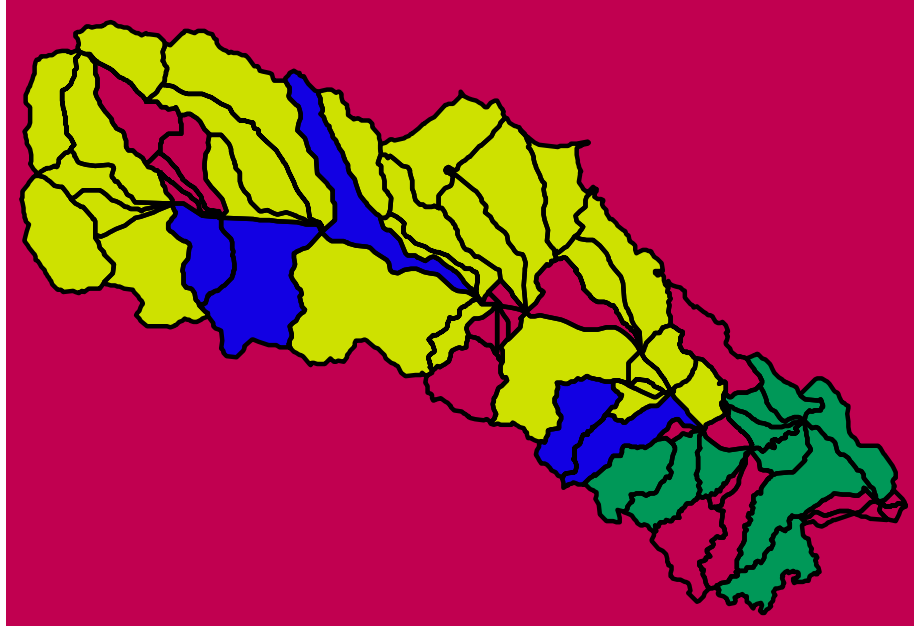


Figure 34 – The delineation of TOPAGNPS regions for use with various CSA and MSCL values within TOPAGNPS to develop a more detailed subdivision of the watershed for use as AnnAGNPS cells. Region 1 is indicated with red, Region 2 with blue, Region 3 with green, and Region 4 with yellow.

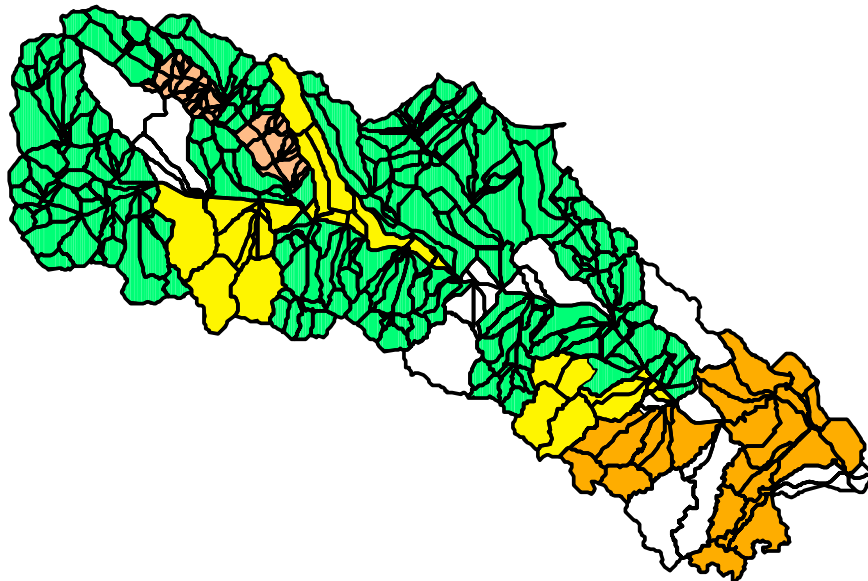


Figure 35 – The final delineation of TOPAGNPS regions with the associated AnnAGNPS cell boundaries produced by TOPAGNPS for use with the various CSA and MSCL values. Region 1 is indicated with white, Region 2 with yellow, Region 3 with orange, Region 4 with green, and Region 5 with light red.

Table 2 – The TOPAGNPS critical source area (CSA) and minimum source channel length (MSCL) parameters used for each of the five regions defined for the final subdivision of the watershed into AnnAGNPS cells.

TOPAGNPS CSA and MSCL Region	CSA Parameter (hectares)	MSCL Parameter (meters)
1	200	800
2	100	400
3	50	200
4	25	100
5	5	80

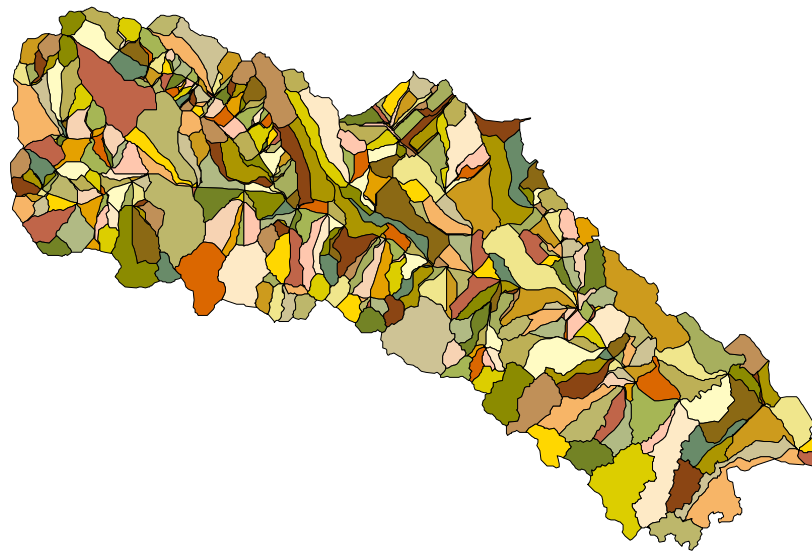


Figure 36 – The final generation of AnnAGNPS cells used for the James Creek watershed simulations.

Stream Network

Generated and Digitized Drainage Network

In order to ensure that the process of using TOPAGNPS produced an adequate stream network to link with the CONCEPTS model, the stream network was compared to the digitized location of the perennial and intermittent streams (Figure 37). Major confluences of tributaries and the main channel were examined along with the physical location of the channels as observed using the DOQQs (Figure 38). The generated stream network reflected the digitized stream network in most cases. Some of the meandering portions of the channel towards the mouth of James Creek were not entirely reproduced by TOPAGNPS, as well as some smaller tributaries.

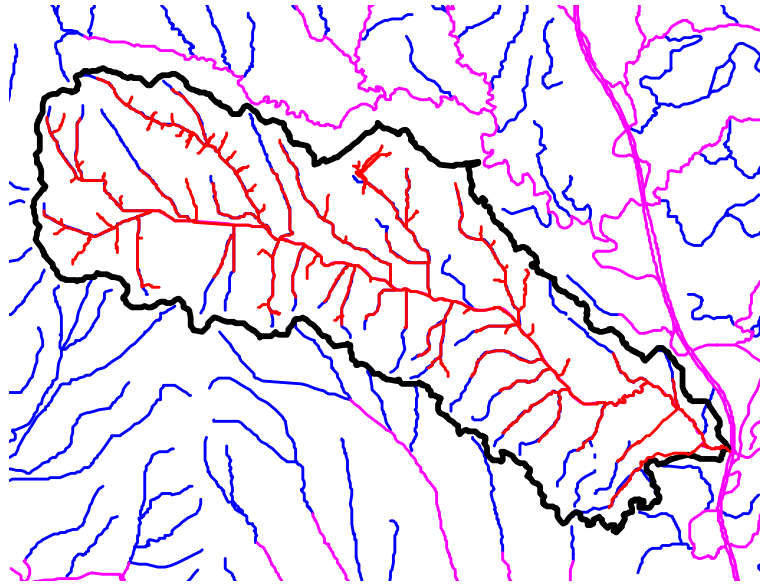


Figure 37 – The generated stream network (red) in comparison with the digitized perennial (purple) and intermittent (blue) streams with the James Creek watershed boundary (black).



Figure 38 – A major confluence reflected properly by the generated stream network as indicated by the streams shown on the DOQQ.

Location of Tributary Confluences Within the James Creek Main Channel

The confluences of the tributaries generated by TOPAGNPS that flow into the main channel of James Creek were determined from visual inspection of the generated stream network (Figure 39). Each tributary outlet reach number identifier assigned from TOPAGNPS was designated as a point that AnnAGNPS would produce information needed by CONCEPTS for each runoff event that occurred between January 1, 1967 and December 31, 2001. The tributary

confluence was then assigned as inflow to the main channel as simulated by CONCEPTS with the tributary information from AnnAGNPS produced in a single file.

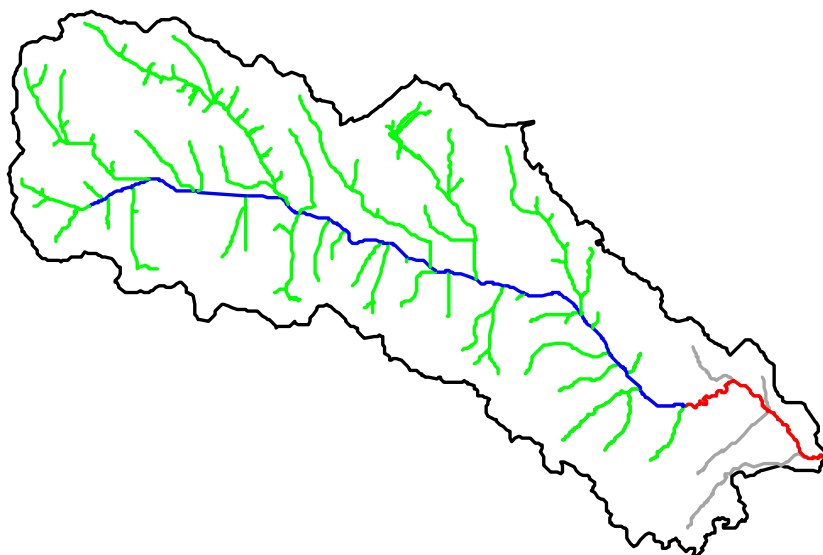


Figure 39 – The TOPAGNPS generated stream network with the main channel simulated by CONCEPTS (blue), tributaries simulated by AnnAGNPS as loadings into CONCEPTS (green), the AnnAGNPS loadings (gray) into the lower channel (red) used to determine the total loadings at the James Creek outlet.

Drainage Network Reach Hydraulic Geometry

The determination of reach hydraulic geometry provides a mechanism used within AnnAGNPS to generate cross section geometry for all of the channel reaches without having to actually measure all of them. This approach is best used on streams that not have incurred incision or channelization as the geometry will not be based on natural conditions. For most channels in a large watershed the determination of hydraulic geometry is the most feasible method available. For incised channels the width can be similar to natural condition if significant bank failure has not altered the channel significantly. Some hydraulic geometry relationships have been derived for various parts of the U.S., but the ability to derive a relationship specifically for James Creek watershed would provide better representations of the cross sections if measured data is available. Since detailed cross sections were performed on the main channel, only supplementary surveys targeted to only obtain channel widths and depths of smaller tributaries would be performed.

A supplemental tributary survey of selected reaches was undertaken to cover the smaller portion of the channel system that the main channel survey would not consider (Figure 40). This involved a very simple approach to survey the top bank width and depth at a variety of points in the channel system with varying drainage areas. Farther upstream in the tributaries, the channel became very small resulting in the ability to take very quick measurements (Figure 41). Some points in the channel system included grassed waterways, such as at location 3 (Figure 42), where hydraulic reach geometry measurements were not obtained because of the extensive

reforming of the channel for erosion control. The determination of the width portion of the hydraulic geometry was determined based on using all of the main channel survey and the supplemental tributary survey top bank widths (Figure 43). An analysis that considered only the supplemental tributary survey points of locations 1, 2, 5, 7, and 9 was also made to exclude the impact channelization or incision may have had on the determination of this parameter. The supplemental tributary survey points provided a better fit to the power series regression for top width and were thus used within AnnAGNPS (using feet and acres, the coefficient was 2.83 and an exponent of 0.314, with a coefficient of determination of 0.70). The depth measurements were taken at the same points as the width and provided an analysis using all of the cross section values (Figure 44). From this analysis the hydraulic depth parameters were derived from the power series regression for use within AnnAGNPS.

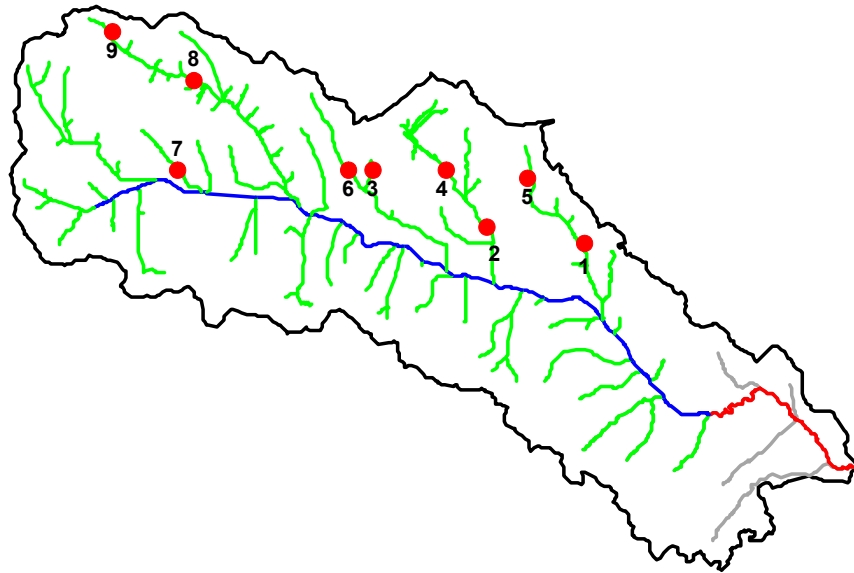


Figure 40 – Location of the reach hydraulic geometry tributary survey points used for AnnAGNPS with the main channel simulated by CONCEPTS (blue), tributaries simulated by AnnAGNPS as loadings into CONCEPTS (green), the AnnAGNPS loadings (gray) into the lower channel (red) used to determine the total loadings at the James Creek outlet.

Location of Unstable Channel Reaches

The identification of unstable tributary reaches from the personnel performing the field surveys of James Creek was performed to designate the AnnAGNPS reaches that would be allowed to have channel erosion (Figure 45). If the channel was designated as being stable then that reach was not allowed to have channel erosion to occur at any time in the simulation. Since the CONCEPTS model was not performing simulations on the tributaries, then having AnnAGNPS perform channel erosion would provide some impact of those unstable reaches on total sediment. A CONCEPTS simulation of one of the main tributaries entering the main



Figure 41 – Reach hydraulic geometry width measured at survey location #9.



Figure 42 – Reach at survey location #3 looking upstream.

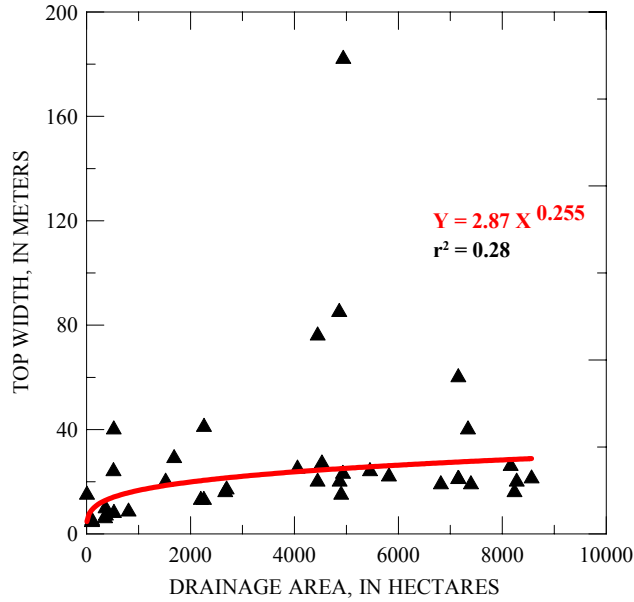


Figure 43 – Width reach hydraulic geometry derivation based on the top width of all main channel and supplemental tributary surveys.

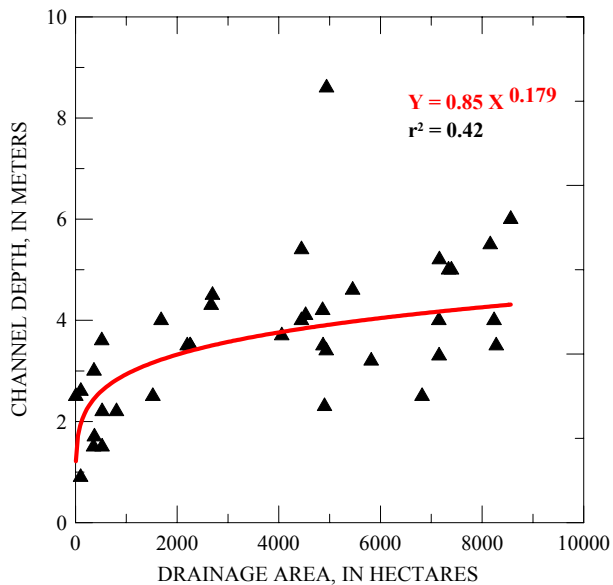


Figure 44 – Depth reach hydraulic geometry derivation based on the top width of all main channel and supplemental tributary surveys.

channel of James Creek was developed to analyze the designation of unstable reaches as eroding within the AnnAGNPS simulation (Figure 46). For the main tributary, AnnAGNPS provided information from the loadings from upland sources and the results at the outlet of the main tributary simulated by AnnAGNPS and by CONCEPTS would be compared. If the results are in general agreement, then the application of AnnAGNPS on the rest of the tributaries would

provide adequate results for an assessment of sediment loadings from those areas into the CONCEPTS model.

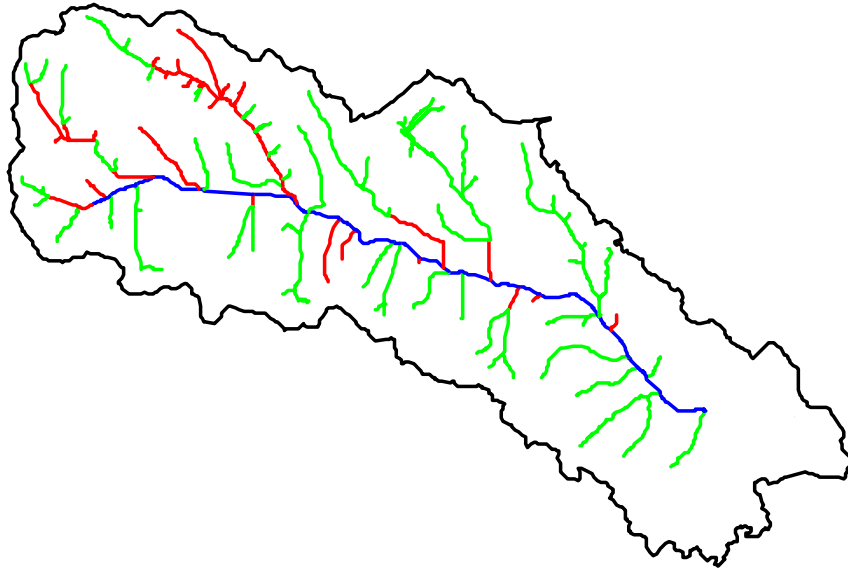


Figure 45 – The TOPAGNPS generated stream network with the main channel simulated by CONCEPTS (blue), along with the designated unstable reaches (red) and stable reaches (green) that are simulated by AnnAGNPS.

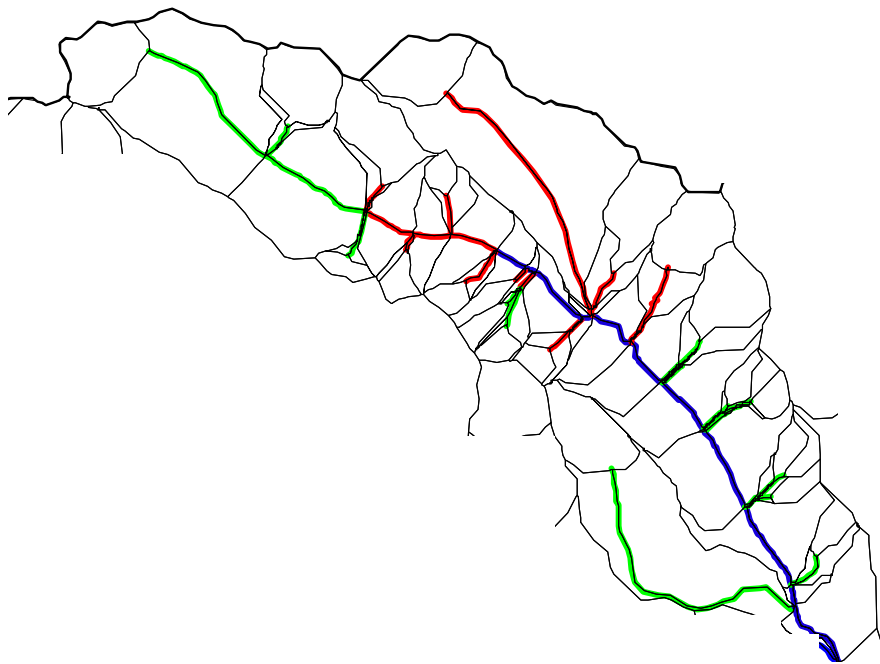


Figure 46 – The main tributary (blue) with stable (green) and unstable (red) reaches entering the tributary from AnnAGNPS cells (black) within a portion of James Creek watershed.

Weather Data

The Aberdeen, Mississippi National Weather Service (NWS) climate station was the nearest station available within the James Creek watershed. Therefore, that station was used to determine the individual event information describing measured precipitation for the years 1967-2001 needed for the AnnAGNPS simulation. For missing rainfall events indicated by the NWS, the nearest climate station was Van Vleet, Mississippi and was used for most of the missing events, and if Van Vleet was also missing, then Houston, Mississippi was used. After the mid-1980's the Amory Lock and Dam station became available, but was only used if no other source was available. The periods when data other than Aberdeen are used for the precipitation used for the AnnAGNPS simulations are shown in **Table 3**. Additional weather data was generated for 35 years using the GEM climate generator for the parameters describing maximum temperature, minimum temperature, sky cover, dew point, and wind speed, and then the actual dates and precipitation replaced the generated values. These additional weather values have a minor impact on the results, thus, no additional measured weather, other than precipitation, was used. Measured temperatures were also available, but 35 years of simulations required an extensive manual data entry process that was determined as too time consuming to complete the simulations in a timely manner. The annual rainfall measured from 1967-2001 is shown in Figure 47. Annual rainfalls are generally higher during initial years of the simulation period than later.

Table 3 – Dates associated with precipitation that was not available at the Aberdeen, Mississippi climate station and another station's information was used.

1/18/1975	10/1 – 11/30/1989
6/12/1975	12/28/1989
2/28/1978	4/1 – 4/30/1990
2/16/1981	12/8/1992
1/12/1982	2/2/1996
1/14/1982	11/8/1996
1/20/1985	9/1 - 10/6/1997
1/31/1985	11/2 – 12/4/1997
2/1 – 2/2/1985	2/3/2000
2/5/1985	5/1 – 5/31/2000
3/22 – 3/39/1989	6/1 – 6/30/2000
4/15/1989	10/1 – 10/31/2000

Landuse Data

Information pertaining to the landuse of the watershed can be defined for those areas that have a direct impact on runoff and sediment loadings. This information can be defined for best management practices (BMPs), impoundments, the crops and non-crops with the associated operations that are used, and the assignment of SCS runoff curve numbers associated with the

crops and non-crops through the operations data. The type of landuse assigned to each AnnAGNPS cell was determined using the AGNPS Arcview interface procedure. This procedure assigned a landuse to each cell based on the predominate landuse from the landuse GIS layer (Figure 21) and the subwatershed GIS layer (Figure 48). The landuse areas assigned to each AnnAGNPS cell (Table 4) closely matches the landuse defined in Figure 21.

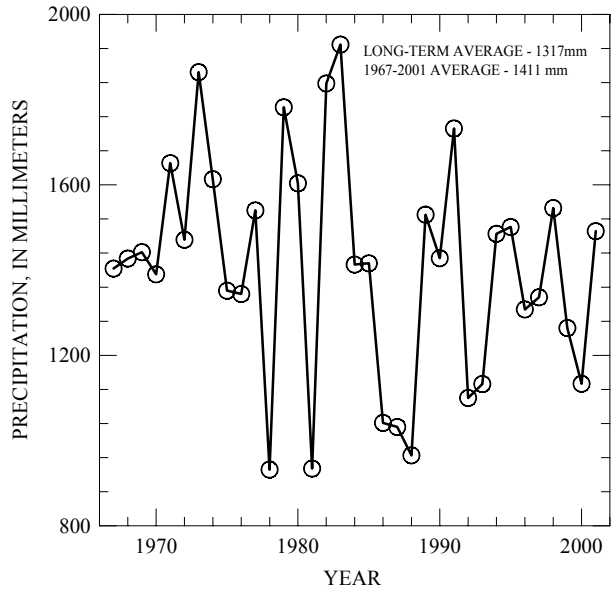


Figure 47 – Annual rainfall measured at the Aberdeen, Mississippi weather station from 1967-2001.

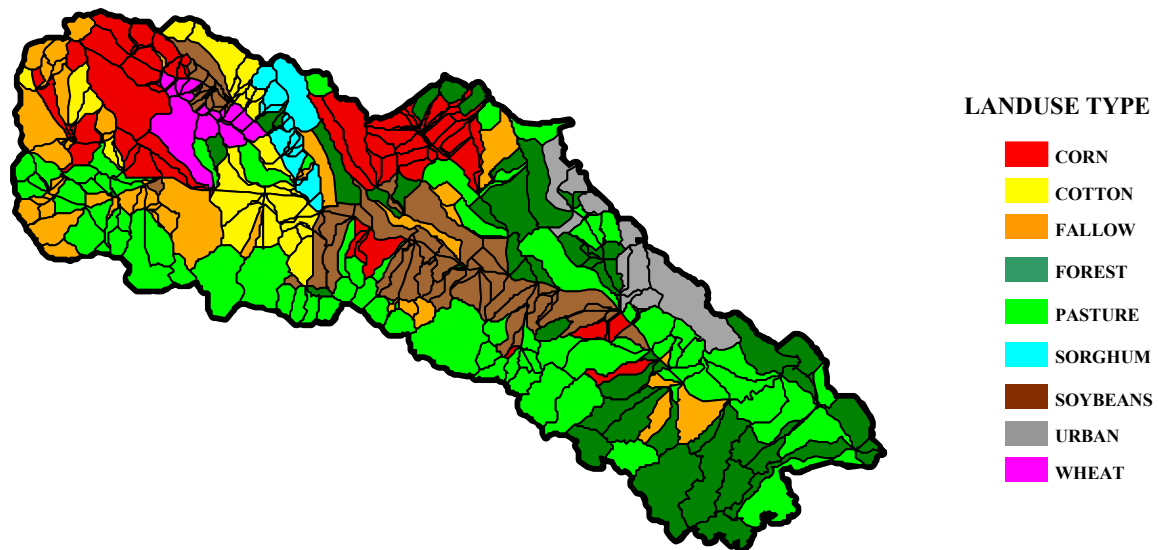


Figure 48 – Landuse assigned to each AnnAGNPS cell.

Table 4 – Landuse defined by the final GIS landuse layer and by AnnAGNPS cells.

Landuse Type	Landuse from GIS Layer (hectares)	Landuse assigned to AnnAGNPS Cells (hectares)
Corn	1252	1527
Cotton	634	740
Sorghum	268	277
Soybeans	1090	1207
Wheat	288	296
Pasture	3126	3326
Fallow	1453	1228
Forest	2454	2028
Urban	345	282

Best Management Practices (BMPs)

There are very few best management practices (BMPs) employed in the watershed. The most prominent BMP is the terraced areas that are all in the cropland areas. The characteristics of the terrace were defined by the terrace spacing measured from the DOQQ (Figure 49) and the slope along the terrace defined by the contour lines on the DRG. Terraces were defined at AnnAGNPS cells 623, 1311, and 1341.



Figure 49 -- Location of terraces and impoundments shown on the DOQQ on the upper end of the main tributary of James Creek watershed

Impoundments

There are many small impoundments within the watershed that have a minimal impact of the sediment delivery to the channels. There are two channels that have major impoundments that were simulated at AnnAGNPS cells 133 and 166 (Figure 50 and Figure 51). The characteristics of the impoundment were determined from the soils surrounding the impoundment and the elevations indicated on the DRG to determine pool depth and volume.

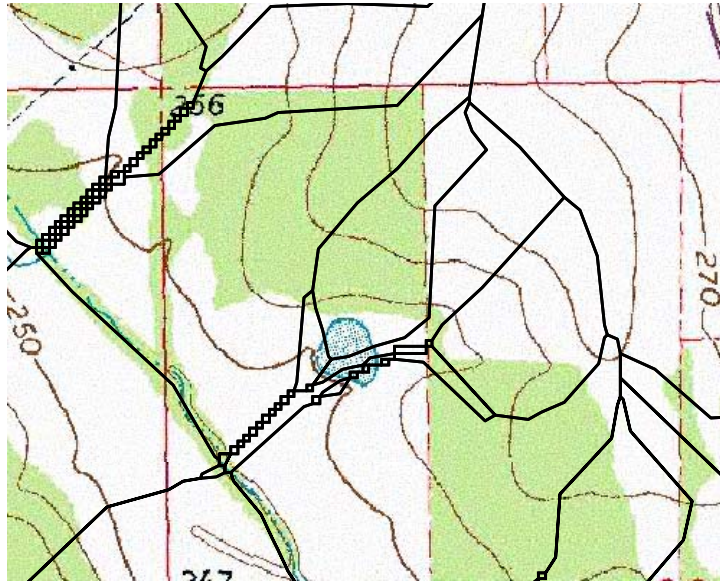


Figure 50 – Location of the impoundment associated with AnnAGNPS reach 133.

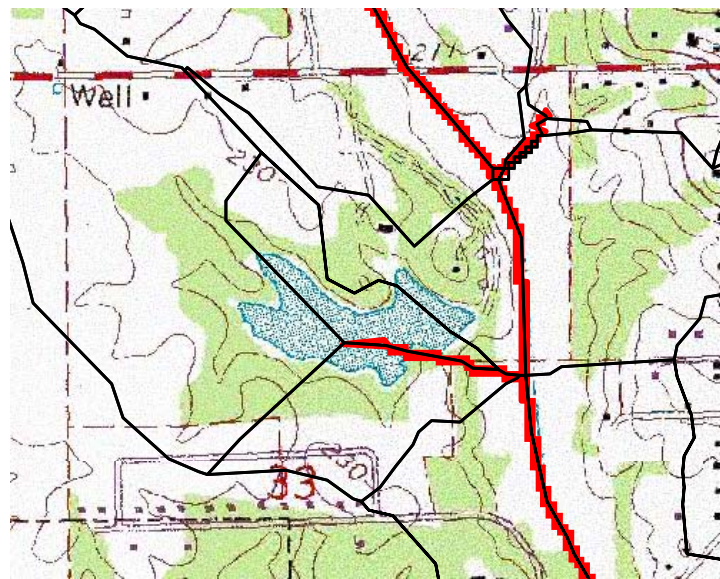


Figure 51 – Location of the impoundment associated with AnnAGNPS reach 166.

Operation Information Associated with Crops and Non-Crops

The landuse information was assigned to each cell by determining the predominant landuse area in each cell. Operation information is important to accurately determine sediment yield, but for runoff production this is not very critical unless some implemented practices would slow or capture the runoff. Typically, these would involve impoundments or terraces. Landuse, operation and operation reference information for the watershed were set up for each cell using RUSLE guidelines and databases (Renard *et al.*, 1997) and from information provided by the Mississippi NRCS personnel.

Soil Conservation Service (SCS) Runoff Curve Numbers Associated with Watershed Characteristics

The Soil Conservation Service (SCS) curve number (CN) is a key factor in obtaining an accurate prediction of runoff and sediment yields. Curve numbers were selected based on the National Engineering Handbook, Section 4 (USDA, Soil Conservation Service, 1985). CN's used in the model simulation are listed in Table 5. The CN for all cultivated fields were based as if a cotton crop was growing. Additional curve numbers were selected for forest, pasture and fallow to represent those scenarios in the simulation. Each cell assumes that the area within the cell is defined homogeneously throughout the cell.

Table 5 – SCS curve numbers for the James Creek watershed simulation by land cover class.

Land Cover Class	Curve Number			
	Hydrologic soil group			
	A	B	C	D
Row Crop Straight Row Poor	72	81	88	91
Row Crop Straight Row Good	67	78	85	89
Row Crop Straight Row Poor C	70	79	84	88
Row Crop Straight Row Good C	65	75	82	86
Row Crop Straight Row Poor C&T	66	74	80	82
Row Crop Straight Row Good C&T	62	71	78	81
Small Grain Straight Row Poor	65	76	84	88
Small Grain Straight Row Good	63	75	83	87
Fallow Bare soil	77	86	91	94
Fallow + Crop Residue Poor	76	85	90	93
Fallow + Crop Residue Good	74	83	88	90
Woods Grass Poor	57	73	82	86
Woods Grass Fair	43	65	76	82
Woods Grass Good	32	58	72	79
Woods Poor	45	66	77	83
Woods Fair	36	60	73	79
Woods Good	30	55	70	77
Pasture Poor	68	79	86	89
Pasture Fair	49	69	79	84
Pasture Good	39	61	74	80
Urban, Commercial, and Business	89	92	94	95

Soil Properties

Within James Creek watershed there are 41 separate soil types identified from the soil GIS layer. The dominate soils are silty clay that are predominately characterized by the soil types of Sumter, Leeper, Houlka, and Griffith. The other major soil types are silt loams with Kipling a dominate soil, and clays with Okolona one of the dominate soils. Along the main channel, the predominate soils are Griffith and Houlka silty clays.

Most of the soils information was derived from the NRCS Soils 5 database. Input parameters that had no impact on soil erosion were set using default parameters. These included parameters such as the soil initial organic nitrogen ratio, which was set based on AnnAGNPS guidelines as 500 PPM for the top layer and 50 PPM for the subsequent layers. The soil assigned to each AnnAGNPS cell was based on the predominant soil type within each AnnAGNPS cell (Figure 52).

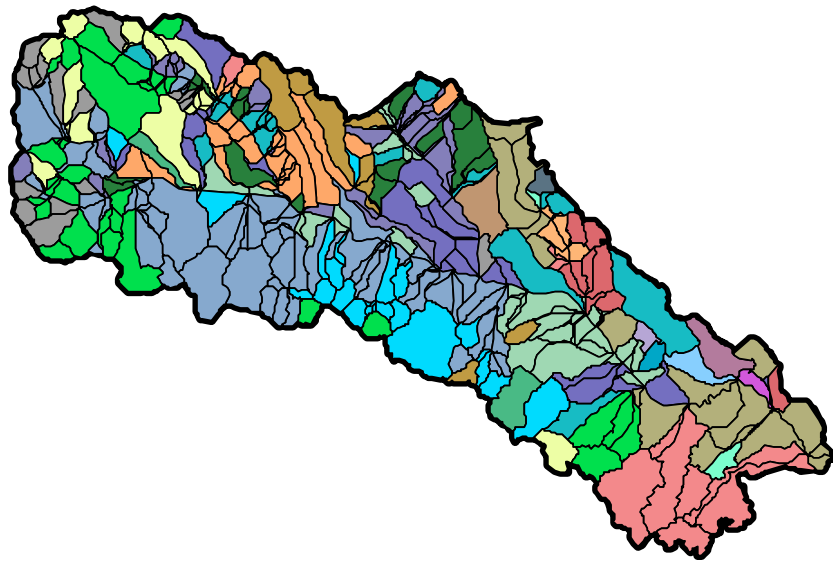


Figure 52 – Soils defined by AnnAGNPS cells.

Vegetation Information for Crops and Non-Crops

The characteristic information needed as input parameters used for AnnAGNPs assigned to each vegetation type were derived from the RUSLE database for each crop and non-crop. This included the crops defined as cotton, corn, soybeans, sorghum, and wheat. The weeds that would grow in fields after harvesting and before plowing were also defined as a crop since they would not be classified as continuously growing as non-crops are defined. The non-crop areas included pasture, fallow, forest, and urban areas.

Evaluation of Erosion from Gully Sources

An initial evaluation was commenced on the contribution of sediment from gullies. A procedure that can be used to estimate gully sediment involves a time series of aerial

photographs that have been geo-referenced over the same watershed area. For James Creek watershed the DOQQs represented the 1994 time period and paper copies of aerial photographs for 1960 were obtained from MDEQ. Each 1960 paper aerial photograph was scanned, rectified with the 1994 DOQQs, and geo-referenced to the same projection as the DOQQs using GIS software for the associated portions of the watershed (Figure 53). Most of the active gullies were observed in the upper portion of the watershed. Comparisons were made with several gullies that appeared in both the 1960 and 1994 photographs and with examples for some of the gullies shown as locations 1-3 (Figure 54, Figure 55, and Figure 56). From these comparisons the measurement of changes in the gully was not adequate to estimate the changes between the two time periods. Most of the gullies present in 1960 have healed by 1994. Any active gully that is currently apparent is too recent to be present on the available aerial photographs.

If a series of recent aerial photographs were available, then more likely discernable differences could be found, with the sediment eroded from the gully estimated by measuring the volume change between the two photographs. The flow over the gully could be estimated using the AnnAGNPS simulation for the location of the gully. Then a relationship could have been derived between the water and sediment discharge. This relationship could have then been used within AnnAGNPS for the 1967 to 2001 period for each gully identified to determine the source of sediments from gullies.

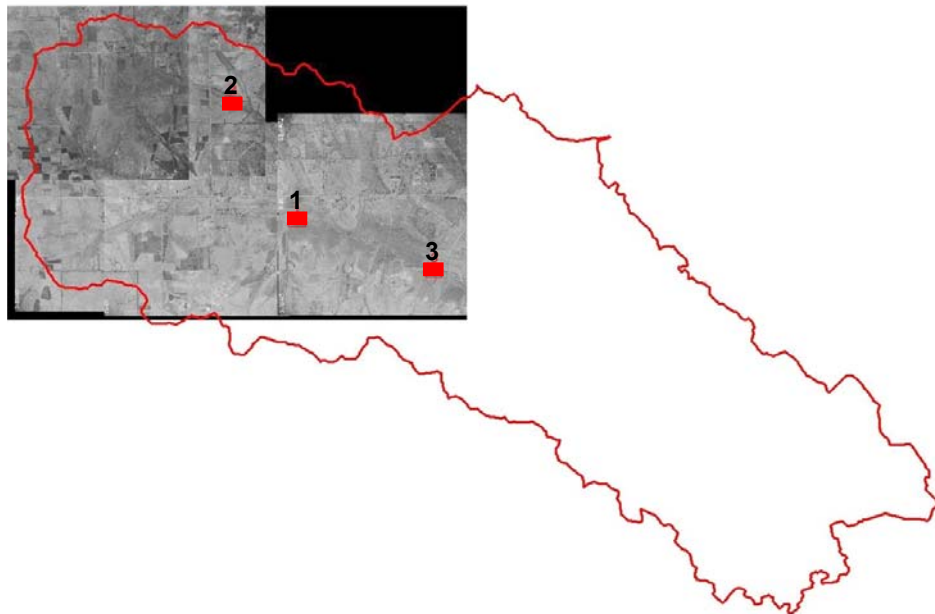


Figure 53 – The scanned 1960 aerial photographs over a portion of James Creek watershed with locations 1 – 3 indicated for comparison with gully sites to 1994 conditions.



Figure 54 – Location of the same gully for location 1 in the aerial photographs of 1960 (left) and 1994 (right).



Figure 55 – Location of the same gully for location 2 in the aerial photographs of 1960 (left) and 1994 (right).

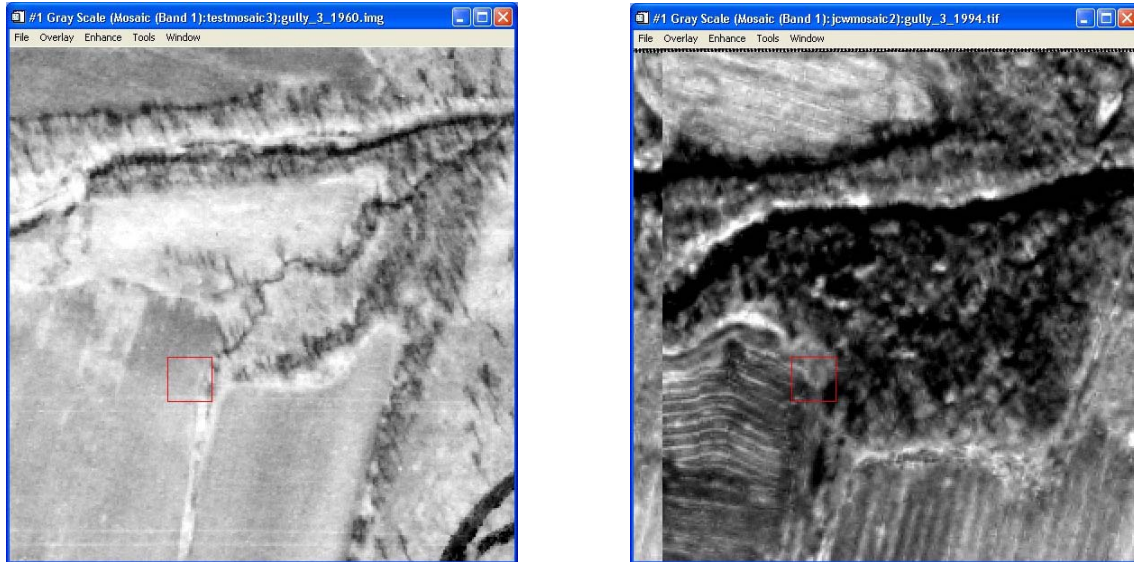


Figure 56 – Location of the same gully for location 3 in the aerial photographs of 1960 (left) and 1994 (right).

Input Database for the CONCEPTS Model

Because CONCEPTS is a deterministic model of channel evolution that incorporates processes of flow, bed-material transport, bank-toe erosion and streambank stability, it requires information about the forces provided by flow in the channel relative to the resistance of the boundary sediments to resist erosion. This includes data on channel geometry, boundary sediments, and flow. Fortunately we became aware of some channel surveys conducted in 1967 as part of a channel maintenance operation by the CoE. This survey provides a starting point by which to conduct simulations of James Creek.

1967 Channel Survey

Channel-geometry data surveyed in 1967 are available at 10 cross sections along James Creek. The locations of the sections are notated in hundreds of feet above the 1967 mouth such as 7+00 (700 feet upstream of the mouth; Table 6). This downstream-most cross section is not useable for comparative purposes because this area was located in the 1980's cutoff for the Tennessee-Tombigbee waterway. Figure 1 shows the locations of the 1967 surveys. These data were used as inputs for the initial 1967 CONCEPTS simulations and are shown in Appendix A. Additional cross sections between those surveyed in 1967 were synthesized based on the average top width and channel depth of the adjacent measured cross sections.

Table 6 – Location of 1967 surveyed cross sections along James Creek. Note: ¹This site no longer exists due to construction of the Tennessee-Tombigbee waterway.

1967 Corps of Engineers label (hundreds of feet)	Distance upstream of 2002 mouth of James Creek (rkm)
7+00 ¹	0.00
22+97	0.263
111+08	3.35
160+40	4.94
228+60	7.29
294+00	9.30
311+20	9.81
381+23	12.0
432+10	13.5
548+70	17.3

Channel depths in 1967 ranged from about 3.8 to 5.7 m deep, indicating that channel incision had taken place prior to the clearing and snagging operations in 1967. Cross-sectional areas were calculated below the floodplain/terrace surface. These data would be used to compare channel geometries in 1967 and 2002 for the purpose of establishing the contribution of channel sediments to the total sediment load in the watershed. Additionally, these data are used to synthesize 1967 cross-sections upstream of rkm 17.3.

2002 Channel Survey

A total of 47 cross sections were surveyed along James Creek in 2002 to establish current channel geometry and to provide a means of directly comparing 1967 channel geometries (Figure 1 and Figure 57). The nine locations where surveys were conducted in 1967 (Table 6) were located initially on the CoE engineering plans and then geo-referenced onto aerial-photo mosaic. GPS coordinates from these sections were then used to establish the position of the section on the ground. Since these survey locations were 35 years old and often in inaccessible locations, the 2002 re-surveys (termed “1967 match survey”) was not referenced to mean sea level geodetic datum. Instead, the “1967 survey match” sites were referenced to flood plain elevations. Additional cross sections were surveyed along the main tributary to provide input data for CONCEPTS to be used in comparison tests with the AnnAGNPS “unstable tributary” subroutine. The locations of all surveyed cross sections along James Creek are shown in Table 7 with their appropriate river kilometer (above the mouth) and drainage area. The 2002 surveys are included in Appendix B.



Figure 57 – Surveying from the James Creek flood plain.

A comparison of 1967 and 2002 thalweg elevations, showing the extent of bed-level lowering during the period along with flood plain elevations is shown in Figure 58. Bed erosion of about 2 m occurred between the mouth of James Creek and about rkm 10.5 over the 35-year period. This implies that tributaries entering the main stem in the lower 10.5 km experienced up to a 2 m overfall and much steeper slopes at their mouths resulting in re-incision. Bed erosion attenuated from 2 m to negligible amounts from rkm 10.5 upstream to the structure at rkm 12.3 (Figure 58). The low-water crossing at rkm 12.3 has the effect of retarding the headward advancement of bed-level adjustments originating in the lower reaches of James Creek such as the repeated dredging of the mouth and the loss of flow resistance from clearing and snagging operations in 1967. Other low-water crossings at rkm 20.0 and 23.3 have the same effect.

Synthesis of 1967 Upstream Cross Sections

To conduct CONCEPTS simulations for the period 1967-2002 and over the reach between river kilometers 6.37 and 24.0, initial cross sections upstream of section 548+70 (rkm 17.2) had to be synthesized from available data. To accomplish this, relations between channel geometry, distance upstream and drainage area were developed. Figure 59 shows channel cross-sectional areas for 1967 and 2002 plotted against river kilometer. Note that the 1967 “red” regression line would cross the 2002 “green” regression slightly upstream of rkm 20.0, indicating that 1967 channels were larger than 2002 channels upstream from this point. Given that this scenario is very unlikely we plotted channel depths versus river kilometer and found that in the reach above rkm 17.3, 2002 channels are probably 1 – 2 m deeper than they were in 1967 (Figure 60). The reason for this is probably related to the clearing and snagging work conducted in 1967 and terminating at rkm 17.2.

Table 7 – The locations of all surveyed cross sections along James Creek.

Cross section	River kilometer	Drainage Area (km²)
	0.00	
22+97	0.27	112
111+08	3.35	104
160+40	4.94	99.5
CS38	6.37	98.6
CS37	6.64	98.4
CS36	6.82	94.3
228+60	7.29	93.6
CS35	7.79	93.1
CS34	8.55	88.6
CS33	9.09	85.6
CS32	9.12	82.8
294+00	9.19	82.8
CS31	9.60	82.3
311+20	9.71	82.1
CS30	10.09	81.6
CS29	10.96	74.0
CS28	11.72	73.4
381+23	11.86	73.0
CS27	12.16	71.6
CS26	12.31	71.5
CS25	12.38	71.5
CS24	13.23	68.2
432+10	13.46	58.5
CS23	13.88	58.2
CS22	14.50	54.5
CS21	14.80	49.4
CS20	14.93	49.3
CS19	15.64	48.7
CS18	15.80	48.6
CS17	15.95	49.0
CS16	17.00	45.3
548+70	17.19	44.7
CS15	17.48	44.5
CS14	17.61	44.4

Table 7 (continued) – The locations of all surveyed cross sections along James Creek.		
Cross section	River kilometer	Drainage Area (km²)
CS13	18.43	40.6
CS12	19.21	27.0
CS11	19.85	26.7
CS10	19.95	22.6
CS9	20.08	22.6
CS8	20.70	22.0
CS7	21.23	16.8
CS6	21.85	15.2
CS5	22.30	14.7
CS4	23.30	5.2
CS3	23.34	5.2
CS2	23.48	5.2
CS1	24.02	3.7

The removal of riparian vegetation in the reaches downstream resulted in less form drag and consequently, lower water-surface elevations. Thus, steeper water-surface slopes and shear stresses probably occurred in the transition zone between the cleared reach downstream and the un-maintained reach upstream, leading to headward migrating incision. If during the clearing and snagging operations some dredging of channel sediments took place (which often cannot be avoided), this would have exacerbated the effect. If this interpretation were correct, we would expect to see a deepening of the main tributary (which enters James Creek in this reach) in its lower reaches, representing a more recent wave of incision. In fact we observe just that, with channel depths reaching almost 6 m near the mouth (Figure 61). By using the 2002 cross-sectional relation in Figure 59 and the 1967 depth relation in Figure 60 we obtain a range of synthesized cross-section geometries by varying bank angles between 45 and 70 degrees. With measured 1967 width-to-depth ratios being in the range of 2 – 6, we selected geometries with 45° bank angles so as to be within the range of 1967 width-to-depth ratios (Table 8). Only those in the upper two km fail to meet this criteria. The synthesized profile, therefore, shows a profile with a two-meter knickpoint at the transition between the cleared and un-maintained reach.

Streambed Erodibility and Composition

CONCEPTS requires information on the relative resistance of streambed materials for its calculations of sediment entrainment and transport. The techniques and data required for cohesive (silts and clays) are very different than those for non-cohesive materials (sands and gravels). Cohesive materials have an electro-chemical bond between particles and, therefore, erosion resistance is not simply a function of particle size and weight. Streambed erodibility was determined at 17 sites along the main stem of James Creek and at two sites along the main tributary (Figure 1). Bulk samples were also obtained at these sites to provide the distribution of bed-material particle sizes to CONCEPTS. The model uses this information to numerically sort streambed material.

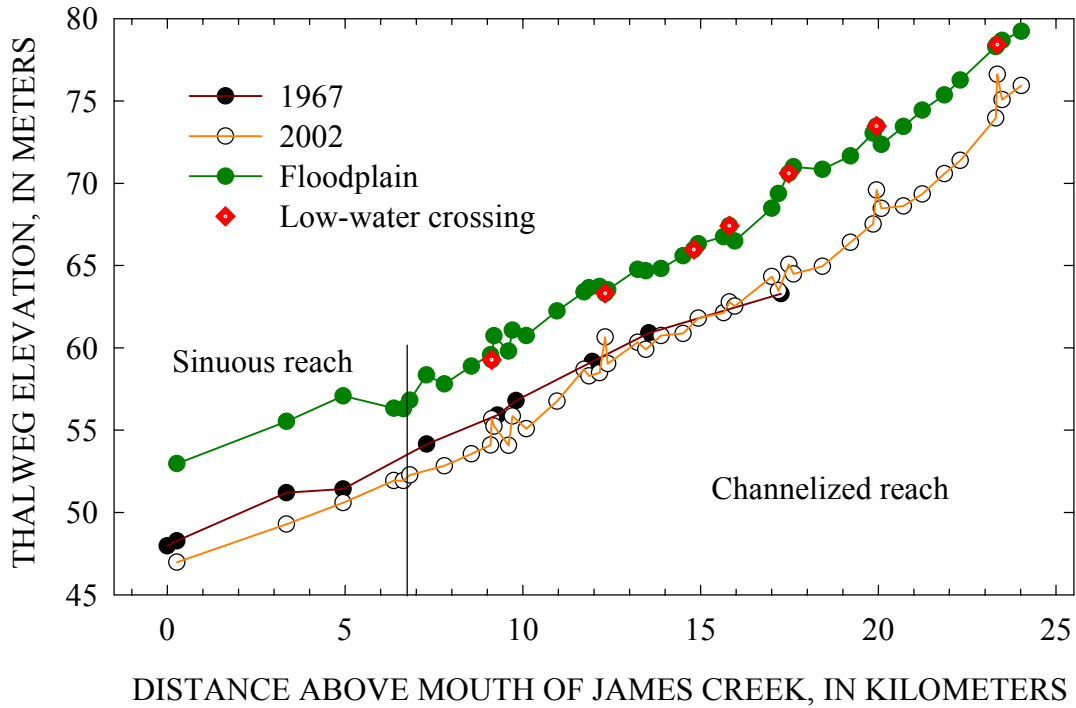


Figure 58 – Comparison of 1967 and 2022 thalweg elevations for the main stem of James Creek showing the extent of bed-level lowering during the period.

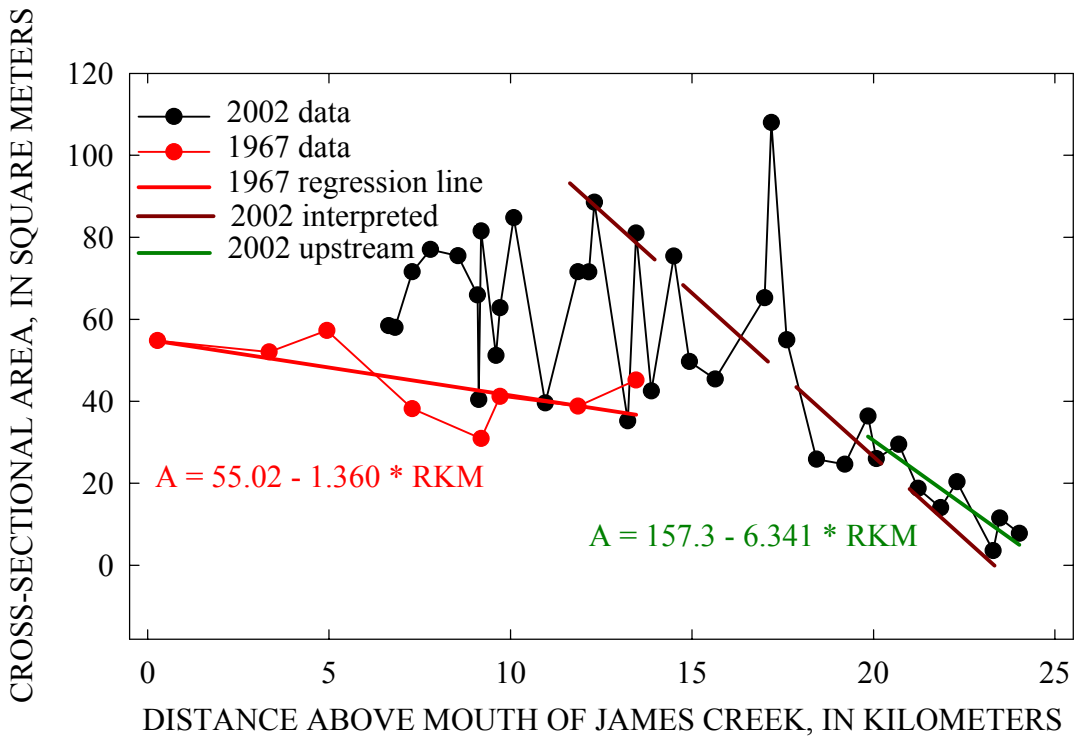


Figure 59 – Variation in channel cross-sectional area with distance upstream along James Creek. Note: similarity between 2022 upstream relation and interpreted line.

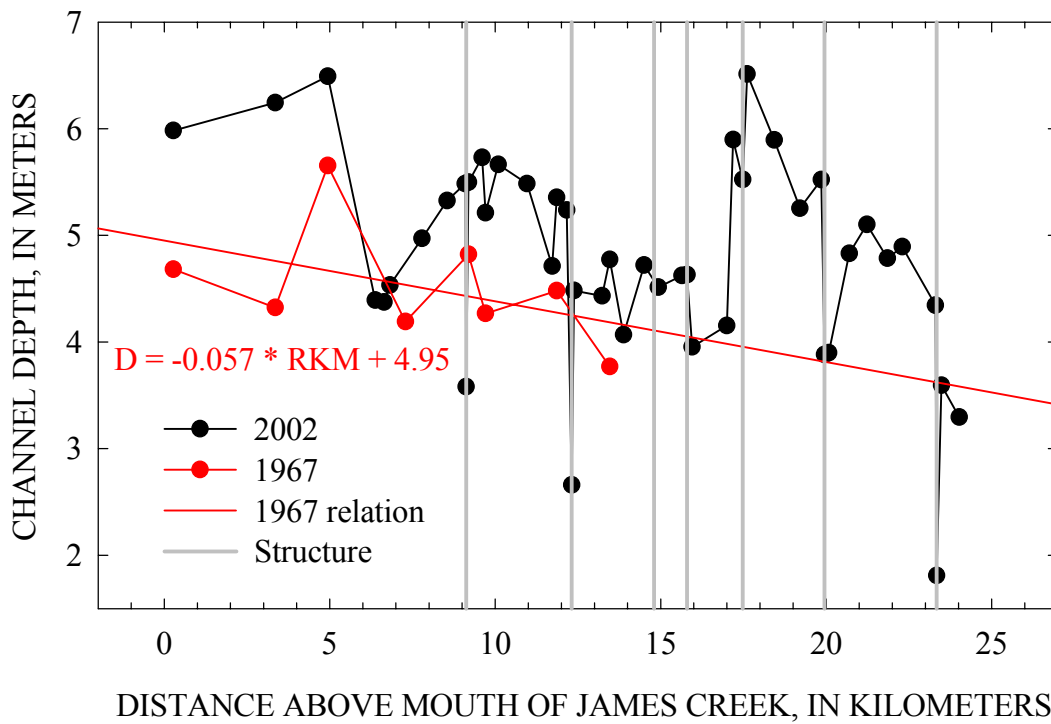


Figure 60 – 1967 and 2002 channel depths along James Creek showing the effects of the low-water crossings and the probable incision in the reach upstream of rkm 17.3.

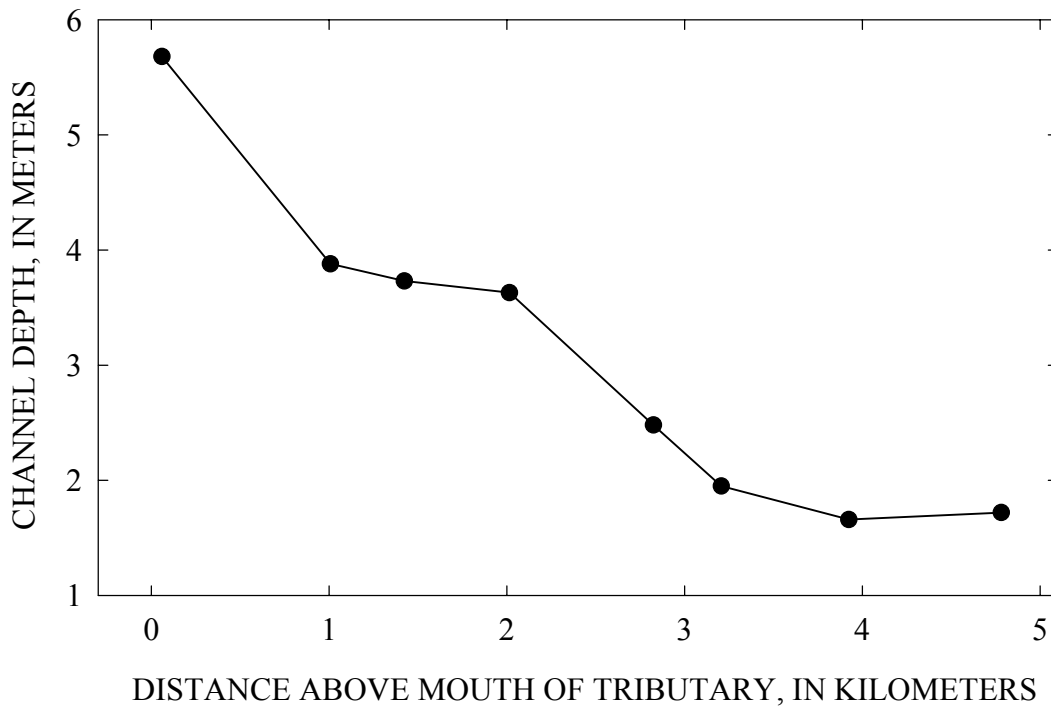


Figure 61 – Depth of channel below floodplain of tributary channel entering James Creek at rkm 18.8 showing 1 – 2 m of deepening near the mouth.

Table 8 – Development of 1967 synthesized cross sections from relations shown in Figure 59 and Figure 60. Note: W/D is width to depth ratio. See Table 7 for drainage areas.

Cross section	rkm	Cross-sectional area	Depth	Bank angle	Top width	W/D	Flood plain elevation	Thalweg elevation
		(m²)	(m)	(degrees)	(m)		(m)	(m)
548+70	17.2							
19	17.4	57.64	3.57	45	19.71	5.52	70.42	66.85
18	17.6	55.82	3.56	45	19.24	5.40	70.67	67.11
17	18.0	52.23	3.54	45	18.30	5.17	71.18	67.64
16	18.4	48.70	3.52	45	17.37	4.94	71.69	68.18
15	18.8	45.23	3.49	45	16.44	4.71	72.21	68.72
14	19.2	41.82	3.47	45	15.52	4.47	72.74	69.27
13	19.6	38.47	3.45	45	14.60	4.23	73.27	69.82
12	19.9	36.26	3.43	45	13.99	4.07	73.63	70.20
11	20.3	33.01	3.41	45	13.09	3.84	74.18	70.77
10	20.7	29.83	3.39	45	12.19	3.60	74.73	71.34
9	21.1	26.70	3.37	45	11.30	3.35	75.29	71.92
8	21.5	23.64	3.35	45	10.41	3.11	75.85	72.51
7	21.9	20.64	3.32	45	9.53	2.87	76.42	73.10
6	22.3	17.69	3.30	45	8.66	2.62	77.00	73.70
5	22.7	14.81	3.28	50	7.27	2.22	77.58	74.30
4	23.0	12.69	3.26	55	6.17	1.89	78.03	74.76
3	23.3	10.62	3.25	60	5.15	1.59	78.47	75.22
2	23.7	7.90	3.22	65	3.95	1.23	79.07	75.84
1	23.9	6.55	3.21	70	3.21	1.00	79.37	76.16

Cohesive Materials

For cohesive streambeds, a submerged jet-test device is used to estimate erosion rates due to hydraulic forces (Hanson 1990; 1991; Hanson and Simon, 2001) (Figure 62). The device shoots a jet of water at a known head (stress) onto the streambed causing it to erode at a given rate. As the bed erodes, the distance between the jet and the bed increases, resulting in a decrease in the applied shear stress. Theoretically, the rate of erosion beneath the jet decreases asymptotically with time to zero. A critical shear stress for the material can then be calculated from the field data as that shear stress where there is no erosion.



Figure 62 – Submerged jet-tests being conducted on the streambed of the main stem of James Creek. Vertical jet test device is in the foreground.

The rate of erosion ε (m/s) is assumed to be proportional to the shear stress in excess of a critical shear stress and is expressed as:

$$\varepsilon = k (\tau_o - \tau_c) = k (\tau_e) \quad (1)$$

where k = erodibility coefficient ($\text{m}^3/\text{N}\cdot\text{s}$); τ_o = average boundary shear stress (Pa); τ_c = critical shear stress; and τ_e = excess shear stress (Pa).

An inverse relationship between τ_c and k occurs when soils exhibiting a low τ_c have a high k or when soils having a high τ_c have a low k . The measure of material resistance to hydraulic stresses is a function of both τ_c and k . Based on observations from James Creek, k can be estimated as a function of τ_c (Figure 63; $r^2 = 0.64$). This is very similar to the relation derived for the Midwestern United States by Hanson and Simon (2001):

$$k = 0.2 \tau_c^{-0.5} \quad (2)$$

Two jet tests were conducted at each site where cohesive bed material was present. In general, the average value of the two tests were used to represent the cross section and for input into CONCEPTS. Those values along with indications of the presence of non-cohesive sands and gravels are shown in Table 9.

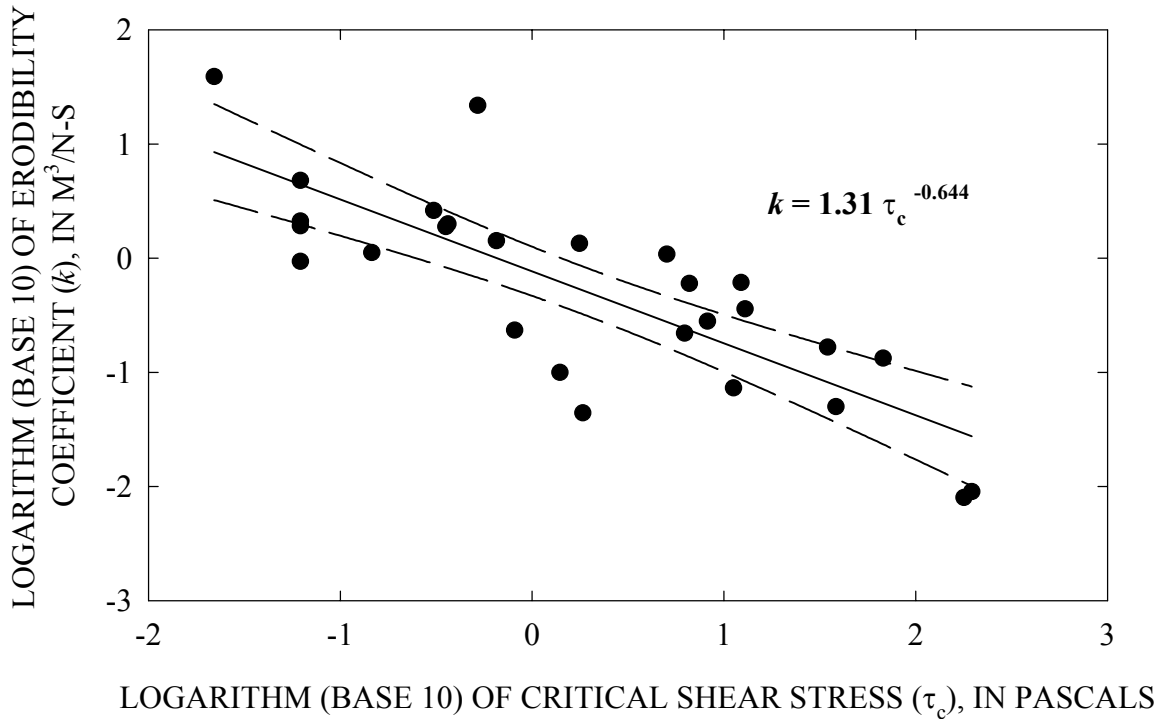


Figure 63 – Results of individual jet tests on cohesive streambed materials along James Creek. Note: Dashed lines are 95% confidence limits.

Non-Cohesive Materials

Several study sites along James Creek are characterized by streambeds composed of sand and gravel (Table 9). To provide the necessary data for input into CONCEPTS, samples of the bed material were obtained and analyzed in the laboratory for particle-size distribution. If the bed was dominated by gravel-sized material a count of a minimum of 100 particles was made to determine the distribution of particle sizes.

Resistance of non-cohesive materials is a function of bed roughness and particle size (weight), and is expressed in terms of a dimensionless critical shear stress (Shields 1936):

$$\tau^* = \tau_o / (\rho_s - \rho_w) g D \quad (3)$$

where τ^* = critical dimensionless shear stress; ρ_s = sediment density (kg/m^3); ρ_w = water density (kg/m^3); g = gravitational acceleration (m/s^2); and D = characteristic particle diameter (m). Average boundary shear stress (τ_o) is the drag exerted by the flow on the bed and is defined as:

$$\tau_o = \gamma_w R S_b \quad (4)$$

where γ_w = unit weight of water (N/m^3); and R = hydraulic radius (area/wetted perimeter)(m). Critical shear stress (τ_c) in dimensional form can be obtained by invoking the Shields criterion and, for hydrodynamically rough beds, utilizing a value of 0.06 for τ^* .

$$\tau_c = 0.06 (\rho_s - \rho_w) g D \quad (5)$$

Thus, the shear stress required to entrain a grain of diameter D can be estimated. Other commonly used values of τ^* are 0.03 and 0.047 (Vanoni 1957). CONCEPTS uses 13 particle-size classes to analyze entrainment and sorting of non-cohesive sediment by invoking the Shields' criteria (Equations 3 and 5).

Streambank Stability

The adjustment of channel width by mass-wasting and related processes represents an important mechanism of channel response and a major contributor to sediment loads in incised alluvial streams. In the loess area of the Midwest United States, for example, bank material contributes as much as 80% of the total sediment eroded from incised channels (Simon and Rinaldi, 2000). In James Creek bank failures are prevalent and appear to be a major source of sediment.

Conceptual models of bank retreat and the delivery of bank sediments to the flow emphasize the importance of interactions between hydraulic forces acting at the bed and bank toe, and gravitational forces acting on *in situ* bank (Carson and Kirkby, 1972; Thorne, 1982; Simon *et al.*, 1991). Failure occurs when erosion of the bank toe and the channel bed adjacent to the bank have increased the height and angle of the bank to the point that gravitational forces exceed the shear strength of the bank material. After failure, failed bank materials may be delivered directly to the flow and deposited as bed material, or dispersed as wash load, or deposited along the toe of the bank as intact blocks, or as smaller, dispersed aggregates (Simon *et al.*, 1991). Analysis of streambank stability within CONCEPTS is based on the ARS Bank-Toe Model and the ARS Bank-Stability Model (Simon *et al.*, 1999).

Bank-Toe Erodibility

In James Creek, *in situ* bank-toe materials are composed predominantly of cohesive materials inter-mixed with sand. As with determining the erodibility of cohesive streambed materials, a submerged jet-test device (modified to operate on inclined surfaces) is used to determine values of τ_c and k (Figure 64). The average values for each site based on two tests are shown in Table 10. Erosion of bank-toe materials is then calculated using an excess shear stress approach.

Table 9 – Critical shear stress (τ_c) and erodibility coefficient (k) values based on submerged jet tests used for input into CONCEPTS. Note: SP-GP = sand and gravel; Cross section numbers beginning with “T” refer to locations on the main tributary.

Cross-section	Bed Material		
	Values Used		
	τ_c (Pa)	k (cm ³ /N-s)	Notes
38	SP-GP	SP-GP	90 % non cohesive
36	SP-GP	SP-GP	100 % non cohesive
35	SP-GP	SP-GP	100 % non cohesive
34	SP-GP	SP-GP	90 % non cohesive
32	20	0.08	
30	1.0	2.4	
29	190	0.01	
27	6.0	0.15	
23	1.0	1.9	
21	18	0.11	
18	13	0.49	
15	1.0	30	
11	1.4	2.0	
8	7.4	0.25	
5	34	0.78	
3	1.0	2.1	20 % non cohesive
1	SP-GP	SP-GP	85 % non cohesive
T3	1.0	2.1	
T7	1.0	3.6	

Bank-Material Shear Strength

Analyzing streambank stability is a matter of characterizing the gravitational forces acting on the bank and the geotechnical strength of the *in situ* bank material. Field data are required to quantify those parameters controlling this balance between force and resistance. If we initially envision a channel deepened by bed degradation in which the streambanks have not yet begun to fail, the gravitational force acting on the bank cannot overcome the resistance (shear strength) of the *in situ* bank material. Shear strength is a combination of frictional forces represented by the angle of internal friction (ϕ'), and effective cohesion (c'). Pore-water pressures in the bank serve to reduce the frictional component of shear strength. A factor of safety (F_s) is expressed then as the ratio between the resisting and driving forces. A value of unity indicates the critical case and imminent failure.



Figure 64 – Non-vertical jet-test device used to determine erodibility of bank toes.

In the part of the streambank above the “normal” level of the groundwater table, bank materials are unsaturated, pores are filled with water and with air, and pore-water pressure is negative. The difference ($\mu_a - \mu_w$) between the air pressure (μ_a) and the water pressure in the pores (μ_w) represents the matric-suction (ψ). This force acts to increase the shear strength of the material and with effective cohesion produces Apparent cohesion (c_a). The increase in shear strength due to an increase in matric suction is described by the angle ϕ^b . This effect has been incorporated into the standard Mohr-Coulomb equation normally used for saturated soils by Fredlund *et al.*, 1978 and is often manifest in steeper bank slopes than would be indicated by ϕ' .

The advantage of the ARS Bank-Stability Model over previous models is that it combines the Mohr-Coulomb approach for saturated conditions and the Fredlund modification for unsaturated conditions and can accommodate different layers. Additionally, the model incorporates the role of matric suction, positive pore-water pressures, and confining pressure afforded by streamflow in the channel.

Borehole Shear Testing and Bulk Unit Weights

To properly determine the resistance of cohesive materials to erosion by mass movement, data must be acquired on those characteristics that control shear strength; that is cohesion, angle of internal friction, pore-water pressure, and bulk unit weight. Cohesion and friction angle data can be obtained from standard laboratory testing (triaxial shear or unconfined compression tests), or by *in-situ* testing with a borehole shear-test (BST) device (Lohnes and Handy 1968; Thorne *et al.* 1981; Little *et al.* 1982; Lutenegeger and Hallberg 1981; Simon 1989b). The BST provides, direct, drained shear-strength tests on the walls of a borehole (Figure 65). Advantages of the instrument include:

1. The test is performed *in situ* and testing is, therefore performed on undisturbed material;
2. Cohesion and friction angle are evaluated separately with the cohesion value representing apparent cohesion (c_a). Effective cohesion (c') is then obtained by adjusting c_a according to measured pore-water pressure and ϕ^b .
3. A number of separate trials are run on the same sample to produce single values of cohesion and friction angle based on a standard Mohr-Coulomb failure envelope.
4. Data and results obtained from the instrument are plotted and calculated on site, allowing for repetition if results are unreasonable; and
5. Tests can be carried out at various depths in the bank to locate weak strata (Thorne *et al.* 1981).

Table 10 – Critical shear stress (τ_c) and erodibility coefficient (k) values for bank toes based on submerged jet tests used for input into CONCEPTS.

Cross-section	Toe Material	
	Values Used	
	τ_c (Pa)	k (cm ³ /N-s)
38	1.1	2.0
36	1.0	2.1
35	3.9	0.69
34	1.0	12
32	37	0.18
30	2.7	1.7
29	7.6	0.82
27	1.0	2.4
23	1.0	1.0
21	24	1.1
18	1.7	1.3
15	1.0	45
11	1.0	1.7
8	1.0	2.1
5	1.0	0.37
3	1.0	2.1
1	1.0	3.7
T3	1.0	7.1
T7	1.0	3.4

BST tests were conducted at a minimum of two depths, representing an upper and lower unit at each of the 17 test sites (Figure 1). A borehole is augered into the bank top and samples are obtained at a prescribed depth for moisture content and bulk unit weight, pore-water pressure, and particle size. Once the samples have been removed, the shear head of the instrument is lowered into the hole and set at the desired depth. Shear stress at failure is tested in a series of trials over a range of normal stresses applied by pressurized gas at the surface. These data are plotted and c_a and ϕ' are obtained by linear regression (Figure 66).

To obtain values of effective cohesion (c') for each layer tested and for input into CONCEPTS the effects of matric suction (negative pore-water pressure) must be accounted for. A miniature, digital tensiometer was used to obtain values of matric suction from the center of small cores removed from the borehole at the approximate depth of the BST. The value obtained was then adjusted using a range of applicable ϕ^b and subtracted from the measured c_a to obtain c' .

At each testing depth, a small core of known volume was removed and sealed to be returned to the laboratory. The samples were weighed, dried and weighed again to obtain values of bulk unit weight, required for analysis of streambank stability. A summary of the shear-strength parameters used for bank-stability calculations are listed in Table 11.



Figure 65 – Borehole shear-test device (BST) used to conduct tests of the shearing resistance of different layers of streambanks along James Creek.

Texture of Bed and Bank Materials

CONCEPTS requires information on sediment texture to determine sediment routing and sorting processes. Bulk samples of streambed and bank materials were collected at the 17 sampling sites to be analyzed in the laboratory for particle-size distributions. In cases where streambeds were composed of both fine-grained cohesive materials and coarser grained sands and gravels, particle-size distributions were weighted by the percentage of the bed covered by

each type of material. These calculations had to be made at cross sections 1, 3, 34 and 38. Average bed-material particle-size distributions for each of the 17 sampled cross sections is shown in Table 12.

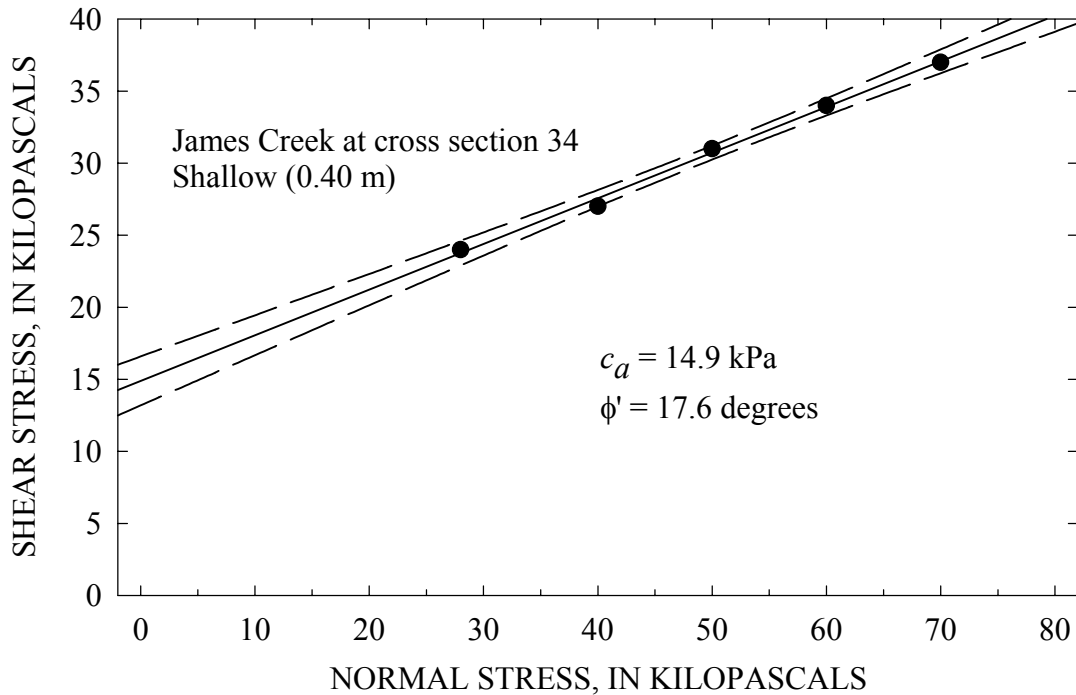


Figure 66 – Example BST results and regression. Note: c_a is the y-intercept; ϕ' is the slope of the regression; dotted lines are 95% confidence limits.

Although James Creek is considered to have a fine-grained streambed, it can be seen that in fact several sub-reaches are dominated by sand and gravel. Figure 67 shows the breakdown of bed texture by size class and d_{50} . Downstream reaches above Darracott Road are dominated by gravel transitioning to sand through rkm 12 to 13, indicating depositional conditions. The source of the gravels may be from the lower member of the Eutaw formation. The reach between rkm 13 and rkm 23 is erosional with beds dominated by fine-grained materials.

Bank materials are fine grained. The average composition of the bank materials is 12% sand, 37% silt, and 51% clay. Bank-material composition for each section and layer are shown in Table 13.

Table 11 – Summary of shear-strength parameter values used for bank-stability modeling in CONCEPTS. Note: c_a = apparent cohesion; c' = effective cohesion; ϕ' = effective friction angle; U = upper; L = lower; “full” refers to a layer incorporating the remainder of the bank height below.

Cross section	Unit	Depth (m)	c_a (kPa)	c' (kPa)	ϕ' degrees	Moisture content (%)	Sat. unit weight (kN/m ³)	Depth (layer) (m)
38	U	1.00	12.5	2.5	14.5	29.9	18.2	2.65
38	L	3.00	10.1	8.6	28.8	26.2	17.4	full
36	U	0.80	6.4	0.3	11.3	22.1	17.7	2.5
36	L	2.52	2.8	0.7	28.4	19.6	19.3	full
35	U	0.4	8.7	7.9	16.6	39.1	16.8	2.1
35	L	2.50	10.9	1.5	30.3	13.8	20.1	full
34	U	0.40	14.9	0.0	17.6	23.8	18.5	0.55
34	L	0.86	10.4	9.3	25.2	25.0	17.2	full
32	U	0.70	2.3	0.0	11.1	19.3	18.0	1.35
32	L	1.70	10.6	6.6	22.4	25.2	18.2	full
30	U	0.60	8.6	3.1	24.9	27.5	17.2	1.5
30	L	1.95	13.2	9.7	5.5	23.1	18.3	full
29	U	0.74	5.0	0.1	12.1	28.7	17.6	1.3
29	L	1.82	4.8	0.0	11.8	24.9	18.4	full
27	U	0.87	5.4	0.5	11.3	29.1	17.9	1.6
27	L	1.90	8.6	1.9	19.0	35.1	16.9	full
23	U	0.60	6.5	0.9	15.6	42.9	16.5	2.4
23	L	2.80	17.6	17.6	0.0	28.6	18.2	full
21	U	0.58	9.0	6.6	5.7	41.8	16.4	0.75
21	L	1.41	18.0	15.1	6.8	42.9	16.0	full
18	U	0.50	1.0	0.0	26.6	28.3	16.3	0.6
18	L	1.00	18.2	14.9	3.9	34.2	16.5	full
15	U	0.53	7.8	7.3	4.7	36.7	17.0	1.5
15	L	0.30	3.0	0.0	18.1	27.3	18.9	full
11	U	1.05	18.1	11.9	5.7	42.1	16.2	1.34
11	L	1.62	9.1	5.7	6.7	40.6	17.0	full
8	U	0.70	8.8	0.3	22.6	36.4	16.7	0.9
8	L	1.30	9.5	0.9	10.9	35.2	17.8	full
5	U	0.45	11.2	6.7	37.3	17.5	18.5	0.7
5	L	0.98	19.5	9.8	10.2	21.9	18.6	full
3	U	0.54	9.6	3.1	20.9	32.2	17.4	0.8
3	L	1.20	15.5	5.3	8.8	30.8	17.5	full
1	U	0.25	10.9	6.1	14.7	43.6	16.1	full
T3	U	0.95	18.6	4.4	13.9	21.7	17.5	0.5
T3	L	2.35	15.0	3.8	16.7	-	-	full
T7	U	1.20	21.9	7.3	26.0	17.9	17.9	1.7
T7	L	2.35	15.0	3.8	16.7	20.2	18.2	full

Table 12 – Distribution of bed-material particle sizes for sites along James Creek and the main tributary. See Figure 1 for site locations.

Cross section	River kilometer	% Gravel	% Sand	% Silt	% Clay	d_{50} (mm)
38	6.37	81.4	13.2	2.6	2.8	11.2
36	6.82	77.9	21.0	1.0	0.0	17.5
35	7.79	77.5	20.3	0.2	2.0	21.8
34	8.55	82.6	2.0	10.9	4.5	17.9
32	9.12	0.0	48.2	30.9	20.9	0.135
30	10.1	1.0	61.4	21.8	16.8	0.120
29	11.0	0.2	65.2	23.2	11.6	0.075
27	12.2	0.0	37.7	23.4	39.0	0.011
23	13.9	0.0	6.9	39.3	53.8	0.002
21	14.8	0.0	11.8	47.5	40.6	0.004
18	15.8	0.0	12.1	43.5	44.4	0.003
548+70	17.2	0.0	67.7	12.4	19.8	0.092
15	17.5	0.0	14.9	40.0	45.0	0.003
8	20.7	0.0	28.6	39.3	32.1	0.010
3	23.3	15.2	19.6	28.2	37.0	0.053
1	24.0	68.6	29.3	1.5	0.6	11.7
T3	19.8	0.0	9.9	40.3	49.7	0.002
T7	22.0	0.00	18.4	31.7	49.9	0.002

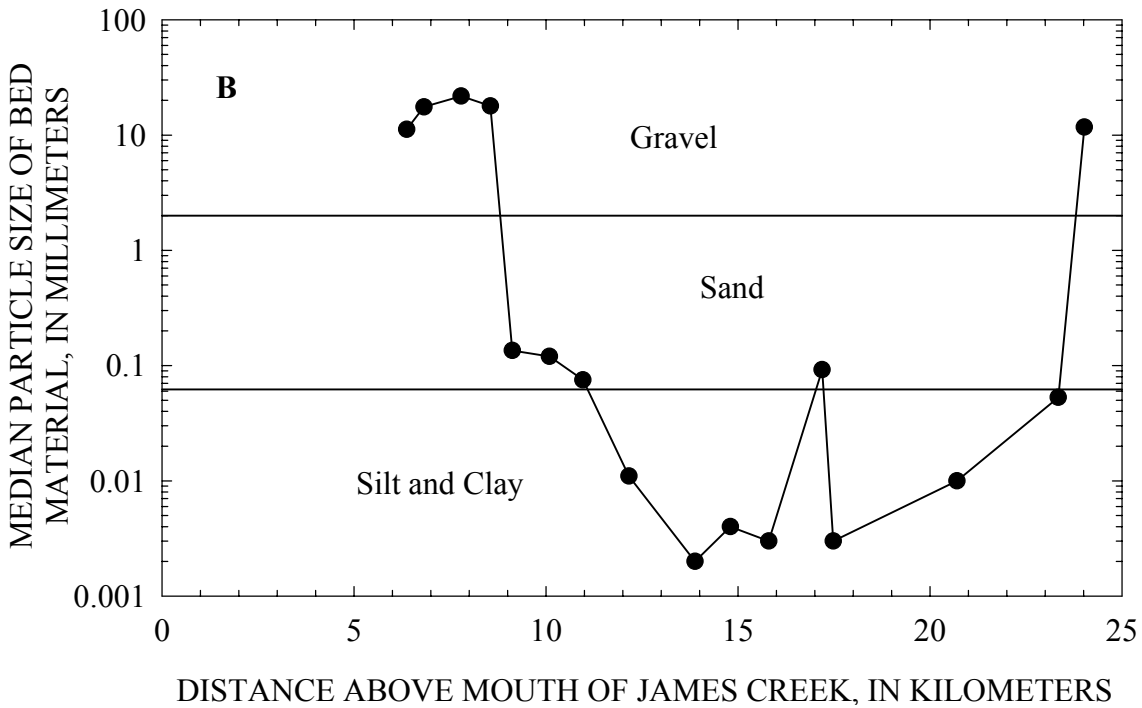
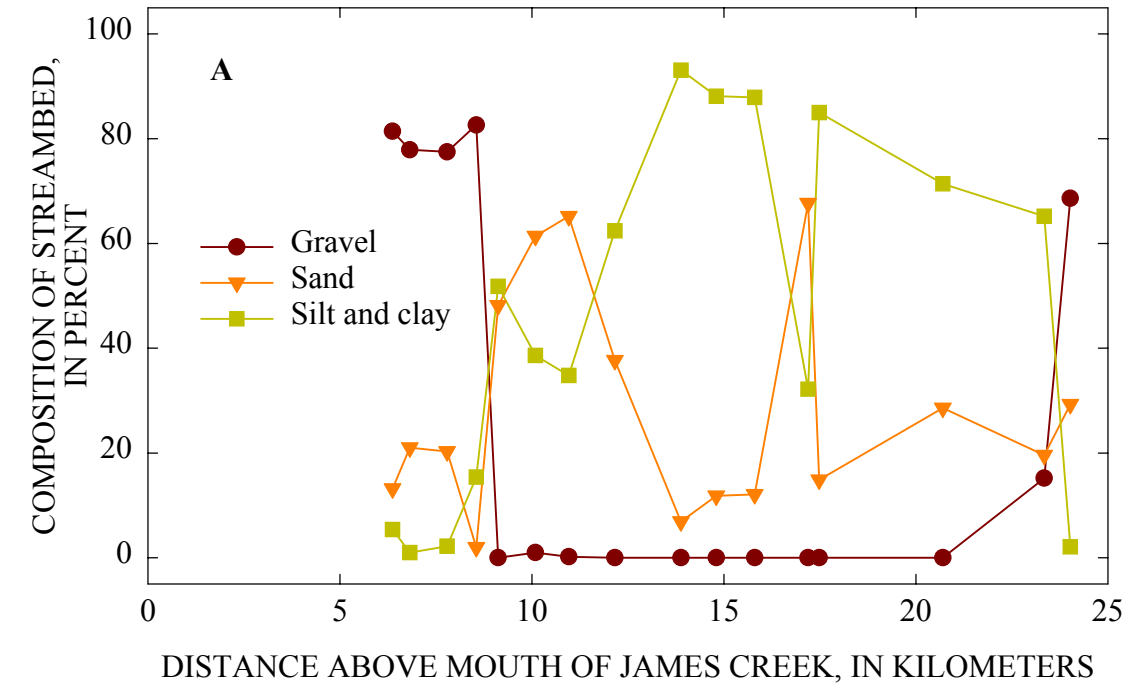


Figure 67 – Longitudinal distribution of streambed texture along James Creek expressed in terms of size classes (A) and d_{50} (B).

Table 13 – Composition of bank materials by section and layer along James Creek and the main tributary. Note: U = upper; L = lower; d_{50} = median particle size.

Cross section	Layer	% Gravel	% Sand	% Silt	% Clay	d_{50} (mm)
38	U	0.0	16.0	32.7	51.4	0.002
38	L	0.0	28.7	20.3	50.9	0.600
36	U	0.0	5.1	54.5	40.4	0.003
36	L	0.0	75.1	13.3	11.6	0.180
35	U	0.0	4.3	23.2	72.4	0.002
35	L	0.0	49.8	29.3	20.9	0.180
34	U	0.0	17.0	45.7	37.4	0.064
34	L	0.0	16.5	30.6	53.0	0.002
32	U	0.0	13.4	42.8	43.7	0.005
32	L	0.0	17.3	33.3	49.4	0.050
32	L	1.4	56.4	9.9	33.8	0.004
30	U	0.0	13.9	33.7	52.5	0.010
30	L	0.0	15.9	31.8	52.3	0.002
29	U	0.0	9.5	44.5	46.0	0.003
29	L	0.0	22.0	39.8	38.1	0.006
27	U	0.0	2.3	49.6	48.1	0.002
27	L	0.0	7.9	26.8	65.3	0.002
23	U	0.0	1.4	38.0	60.5	0.002
23	L	0.0	4.6	37.8	57.5	0.002
21	U	0.0	3.7	31.6	64.7	0.002
21	L	0.0	1.9	26.2	71.9	0.002
18	U	0.0	3.7	31.2	65.1	0.002
18	L	0.0	5.7	28.9	65.4	0.002
15	U	0.0	2.9	32.1	65.0	0.002
11	U	0.0	3.3	49.1	47.6	0.002
11	L	0.0	2.4	89.6	8.0	0.010
8	U	0.0	1.4	38.0	60.6	0.002
8	L	0.0	1.2	31.3	67.4	0.002
5	U	0.0	5.0	56.6	38.4	0.004
5	L	0.0	5.8	50.9	43.3	0.004
3	U	0.0	2.0	27.0	71.0	0.002
3	L	0.0	12.7	22.7	64.7	0.002
1	U	0.0	2.0	35.5	62.5	0.002
T3	U	0.0	5.5	49.2	45.2	0.003
T3	L	0.0	8.4	44.0	47.6	0.002
T7	U	0.0	6.6	49.2	44.3	0.003
T7	L	0.0	5.1	43.2	51.6	0.002

DEVELOPING A “REFERENCE” SEDIMENT-TRANSPORT CONDITION FOR JAMES CREEK

Sediment loads (transport rates) in streams vary by orders of magnitude over time and by location. Controls such as geology and channel-boundary materials, land use, channel stability, and the type and timing of precipitation events make prediction of sediment loads difficult and complex. Still, in order to determine the amount of sediment that impairs a given waterbody (TMDL), one must first be able to determine the sediment load that would be expected in an unimpaired stream of a given type and location. However, baseline conditions of flow, sediment concentrations, and transport rates for streams in the wide variety of physiographic provinces and under a wide variety of land uses are poorly understood. Initiating a data collection program to obtain a comprehensive data set from a sufficient number of streams from different physiographic provinces for use in developing clean sediment TMDL's is impractical from both time and monetary standpoints. A logical alternative is to make use of high-quality, historical data sets containing corresponding flow and sediment-transport information that have been collected by government and private agencies at various locations.

Regionalization by Level III Ecoregion

There is no reason to assume that “natural” or background rates of sediment transport will be consistent from one region to another. Within the context of clean-sediment TMDLs, it follows that there is no reason to assume then that “target” values should be consistent on a nationwide basis. Similarly, there is no reason to assume that channels within a given region will have consistent rates of sediment transport. For example, unstable channel systems or those draining disturbed watersheds will produce and transport more sediment than stable channel systems in the same region. This reflects differences in the magnitude and perhaps type of erosion processes that dominate a sub-watershed or stream reach.

To be useful for TMDL practitioners sediment-transport relations must be placed within a conceptual and analytic framework such that they can be used to address sediment-related problems at sites such as those along James Creek where no such data exists. To accomplish this, sediment-transport characteristics and relations need to be regionalized according to attributes of channels and drainage basins that are directly related to sediment production, transport, and potential impairment. In a general way, these attributes include among others, physiography, geology, climate and ecology, differentiated collectively as an ecoregion (Omernik, 1995). The region that includes James Creek is the Southeastern Plains (Ecoregion 65).

Availability of Data

Analysis of the impacts of suspended sediment requires a database of suspended-sediment concentrations with associated instantaneous water discharge. Data of this type permit analysis of sediment-transport characteristics and the development of rating relations (Porterfield, 1972; Glysson, 1987). Collection of suspended-sediment data is time consuming and expensive in that it must take place over a broad range of flows to accurately evaluate the sediment-transport regime at a site. However, the USGS has identified more than 2,900 sites

nationwide where at least 30 matching samples of suspended sediment and instantaneous flow discharge have been collected (Turcios and Gray, 2001). This historical database serves as the foundation for analyzing sediment-transport characteristics over the range of physiographic conditions that exist in the United States. For the Southeastern Plains, 148 sites in nine states have at least 30 matching samples of suspended sediment and instantaneous flow discharge.

“Reference” Conditions

In order to identify those sediment-transport conditions that represent impacted or impaired conditions, it is essential to first be able to define a non-disturbed, stable, or “reference” condition for the particular stream reach. In some schemes the “reference” condition simply means “representative” of a given category of classified channel forms or morphologies (Rosgen, 1985) and as such, may not be analogous with a “stable”, “undisturbed”, or “background” rate of sediment production and transport. Although the Rosgen (1985) stream classification system is widely used to describe channel form, stream types D, F, and G are by definition, unstable (Rosgen, 1996, p. 4-5). These stream reaches, therefore, would be expected to produce and transport enhanced amounts of sediment and represent impacted, if not impaired conditions. Thus, although it may be possible to define a “representative” reach of stream types D, F, and G, for the purpose of TMDL development, a “reference” condition transporting “natural” or background rates of sediment will be difficult to find.

Stages of Channel Evolution

As an alternative scheme for TMDL practitioners, the channel evolution framework set out by Simon and Hupp (1986); Simon (1989b) is proposed (Figure 68). In most alluvial channels, disruption of the dynamic equilibrium generally results in a certain degree of upstream channel degradation and downstream aggradation. If the predisturbed channel is considered as the initial stage (I) of channel evolution and the disrupted channel as an instantaneous condition (stage II), rapid channel degradation can be considered stage III (Figure 68). Degradation flattens channel gradients and consequently reduces the available stream power for given discharges with time. Concurrently, bank heights are increased and bank angles are often steepened by fluvial undercutting and by pore-pressure induced bank failures near the base of the bank. Thus, the degradation stage (III) is directly related to destabilization of the channel banks and to channel widening by mass-wasting processes (stage IV) once bank heights and angles exceed the critical conditions of the bank material (as determined by shear-strength characteristics). Channels can shift from stage III to stage IV (threshold; degradation and widening) in localized and system-wide adjustments.

As degradation migrates further upstream, aggradation (stage V) becomes the dominant trend in previously degraded downstream sites because the flatter gradient and lower hydraulic radius at the degraded site cannot transport the heightened sediment loads originating from degrading reaches upstream. This secondary aggradation occurs at rates roughly 60% less than the associated degradation rate (Simon 1992). These reduced aggradation rates indicate that bed-level recovery will not be complete and that attainment of a new dynamic equilibrium will take place through (1) further channel widening, (2) the establishment of riparian vegetation that adds roughness elements and reduces the stream power for given discharges, and (3) further gradient reduction by meander extension and elongation.

The lack of complete bed-level recovery often results in a two-tiered channel configuration with the original floodplain surface becoming a terrace. Flood flows are, therefore, constrained within this enlarged channel below the terrace level. Without proliferation of riparian vegetation within the channel, this results in a given flow having greater erosive power than if an equivalent flow could dissipate energy by spreading across the floodplain. Where vegetation does re-establish, the additional roughness limits the erosive power of flood events within the incised channel and constrains shear-stress values to near bankfull levels (Simon *et al.*, 1999). Aggrading conditions (stage V) are also common in reaches downstream from the area of maximum disturbance immediately after the disturbance is imposed on the stream channel.

With stages of channel evolution tied to discrete channel processes and not strictly to specific channel shapes, they have been successfully used to describe systematic channel-stability processes over time and space in diverse environments subject to various disturbances such as stream response to: channelization in the Southeast US Coastal Plain (Simon, 1994); volcanic eruptions in the Cascade Mountains (Simon, 1992); and dams in Tuscany, Italy (Rinaldi and Simon, 1998). Because the stages of channel evolution represent shifts in dominant channel processes, they are systematically related to suspended-sediment and bed-material discharge (Simon, 1989b; Kuhnle and Simon, 2000), fish-community structure (Simon *et al.*, 2002), rates of channel widening (Simon and Hupp, 1992), and the density and distribution of woody-riparian vegetation (Hupp, 1992).

An advantage of a process-based channel-evolution scheme for use in TMDL development is that Stages I and VI represent two true “reference” conditions. In some cases, such as in the Midwestern United States where land clearing activities near the turn of the 20th century caused massive changes in rainfall-runoff relations and land use, channels are unlikely to recover to Stage I, pre-modified conditions. Stage VI, re-stabilized conditions are a more likely target under the present regional land use and altered hydrologic regimes (Simon and Rinaldi, 2000) and can be used as a “reference” condition.

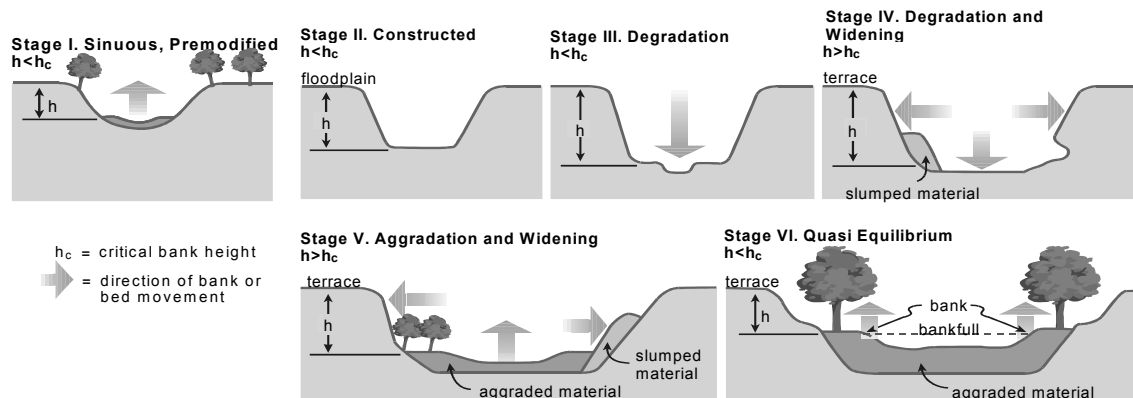


Figure 68 – Six stages of channel evolution from Simon and Hupp (1986) and Simon (1989b) identifying Stages I and VI as stable, “reference” conditions.

Rapid Geomorphic Assessments: RGA's

To determine the relative stability and stage of channel evolution for all of the sites with available sediment data in the Southeastern Plains, rapid geomorphic assessments (RGA's) are conducted. RGA techniques utilize diagnostic criteria of channel form to infer dominant channel processes and the magnitude of channel instabilities. Granted that evaluations of this sort do not include an evaluation of watershed or upland conditions, however, stream channels act as conduits for energy, flow and materials as they move through the watershed and will reflect a balance or imbalance in the delivery of flow and sediment. Given the large number of sites in the Southeastern Plains and other ecoregions where these techniques are being used, it is not feasible to perform detailed, time-consuming field surveys at every site. RGA's provide an efficient alternative to determine stability conditions.

The RGA procedure consists of four steps, which collectively take about 1.5 hours to complete on site:

1. Take photographs looking upstream, downstream and across the reach;
2. Take sample of bed material. This could be a bulk sample, a particle count if the bed is dominated by gravel and coarser fractions, or a combination of the two;
3. Make observations of channel conditions and diagnostic criteria listed on the channel-stability ranking scheme (Figure 69); and
4. Perform a survey of channel gradient, or water-surface slope if the water is too deep to wade.

RGA's were conducted at 99 sites in the Southeastern Plains and 47 sites along James Creek. None of the sites evaluated along James Creek could be considered "reference" stage I or VI. Therefore, "reference" conditions need to be obtained from stable streams elsewhere in the Southeastern Plains (Ecoregion 65).

Channel-Stability Index

A simple field form containing nine criteria is used to record observations of field conditions (Figure 69). Each criteria is ranked and all values are then summed to obtain an index of channel stability. The higher the number, the greater the instability indicated. However, the rankings are not weighted and for example, ranking of 20 does not mean that the site is twice as unstable as a site with a value of 10. Experience has shown that values of 20 or greater are indicative of significant instability; values below 10 are indicative of relative stability.

Specific-Gage Analysis

Historical gaging-station records are analyzed for those sites where channel stability conditions during the period of sampling may have been different than when the sites were evaluated by NSL field crews. The purpose of this exercise is to determine if the geometry of the channel has been changing with time and to assure that the sites representing "reference" conditions were truly stable during the period of sediment sampling. Specific-gage analysis involves obtaining the discharge measurement summary sheets from the USGS. Generally, measurements from the mid-1980's to present can be downloaded from the Worldwide Web whereas older records must be copied by the local USGS office and input by hand. These

summary sheets contain data on date of measurement, discharge, average width, average velocity, flow area, and stage (of water surface).

To investigate whether bed elevations have changed, the stage and discharge of low-water measurements are plotted and a linear regression between the two variables is established for each year of record. The water-surface elevation of a specific low-flow discharge is then determined from each regression for the period of record. Trends of these data can then be used to determine if the streambed is eroding, depositing, or stable. If the data indicate the channel bed is incising, we know it is either stage III or IV; if depositing, stage V or VI.

To refine estimates of historical stage of channel evolution the gage data are analyzed similarly but for flow width and this time, using an intermediate discharge. Regressions for each year of record are established for flow width and discharge to determine if channel width has been changing with time.

Analysis of Suspended-Sediment Data

Analysis of suspended-sediment transport data involves establishing a relation between flow and sediment concentration or load. Instantaneous-concentration data combined with either an instantaneous flow value or flow data representing the value obtained from the stage-discharge relation at 15-minute intervals are best. Mean-daily values of both flow and sediment loads, which are readily available from the USGS tend to be biased towards lower flows, particularly in flashy basins. For establishing sediment-transport rating relations, instantaneous concentration and 15-minute flow data are used from USGS and ARS gauging station records.

A suspended-sediment transport rating is developed (Porterfield, 1972; Glysson, 1987; Simon, 1989a) by plotting discharge versus concentration in log-log space and obtaining a power function by regression (Figure 70). Trends of these data (in log-log space) often increase linearly and then break off and increase more slowly at high discharges. Preliminary analyses show that although sand concentrations continue to increase with discharge, the silt-clay fraction attenuates, causing the transport relation to flatten. A transport rating developed with a single power function commonly over-estimates concentrations at high flow rates, leading to errors in calculating the effective discharge. To alleviate this problem, a second or third linear (in log-log space) segment is sometimes developed with the upper end of data set (Figure 70). This procedure was followed for each of the 148 sites in the Southeastern Plains. The next step is to determine how to best describe the transport relation in the context of developing “reference” sediment-transport relations.

Because the “effective discharge” is that discharge or range of discharges that shape channels and perform the most geomorphic work (transport the most sediment) over the long term it can serve as a useful indicator of regional suspended-sediment transport conditions for “reference” and impacted sites. In many parts of the United States, the effective discharge is approximately equal to the peak flow that occurs on average, about every 1.5 years ($Q_{1.5}$; for example, Andrews, 1980; Andrews and Nankervis, 1995) and may be analogous to the bankfull discharge in stable streams. The recurrence interval of the effective discharge calculated for 10 streams in Mississippi was about 1.5 years (Simon *et al.*, 2002). Therefore, the $Q_{1.5}$ was used as a measure of establishing the effective discharge at the remaining study sites in the ecoregion.

CHANNEL-STABILITY RANKING SCHEME

1. Primary bed material						
Bedrock	boulder/cobble	gravel	sand	silt/clay		
0	1	2	3	4		
2. Bed/bank protection						
Yes	No	(with)	1 bank	2 banks		
			Protected			
0	1	2		3		
3. Degree of incision (Relative elev. of “normal” low water; floodplain/terrace @ 100%)						
0 – 10%	11 – 25%	26 – 50%	51 – 75%	76 – 100%		
4	3	2	1	0		
4. Degree of constriction (Relative decrease in top-bank width from up to downstream)						
0 – 10%	11 – 25%	26 – 50%	51 – 75%	76 – 100%		
0	1	2	3	4		
5. Streambank erosion (Each bank)						
	None	fluvial	mass wasting (failures)			
Left	0	1	2			
Right	0	1	2			
6. Streambank instability (Percent of each bank failing)						
	0 – 10%	11 – 25%	26 – 50%	51 – 75%	76 – 100%	
Left	0	0.5	1	1.5	2	
Right	0	0.5	1	1.5	2	
7. Established riparian woody-vegetative cover (Each bank)						
	0 – 10%	11 – 25%	26 – 50%	51 – 75%	76 – 100%	
Left	2	1.5	1	0.5	0	
Right	2	1.5	1	0.5	0	
8. Occurrence of bank accretion (Percent of each bank with fluvial deposition)						
	0 – 10%	11 – 25%	26 – 50%	51 – 75%	76 – 100%	
Left	0	0.5	1	1.5	2	
Right	0	0.5	1	1.5	2	
9. Stage of channel evolution						
	I	II	III	IV	V	VI
	0	1	2	4	3	1.5

Figure 69 – Channel stability ranking scheme used to conduct rapid geomorphic assessments (RGA’s). The channel stability index is the sum of the values obtained for the nine criteria.

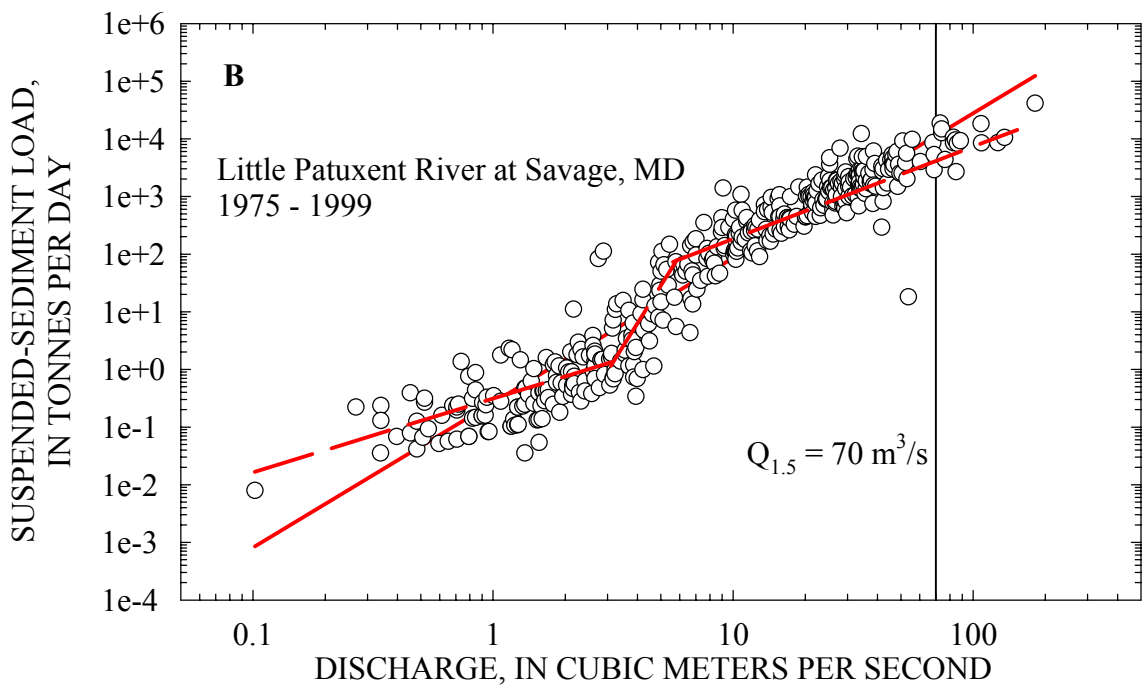
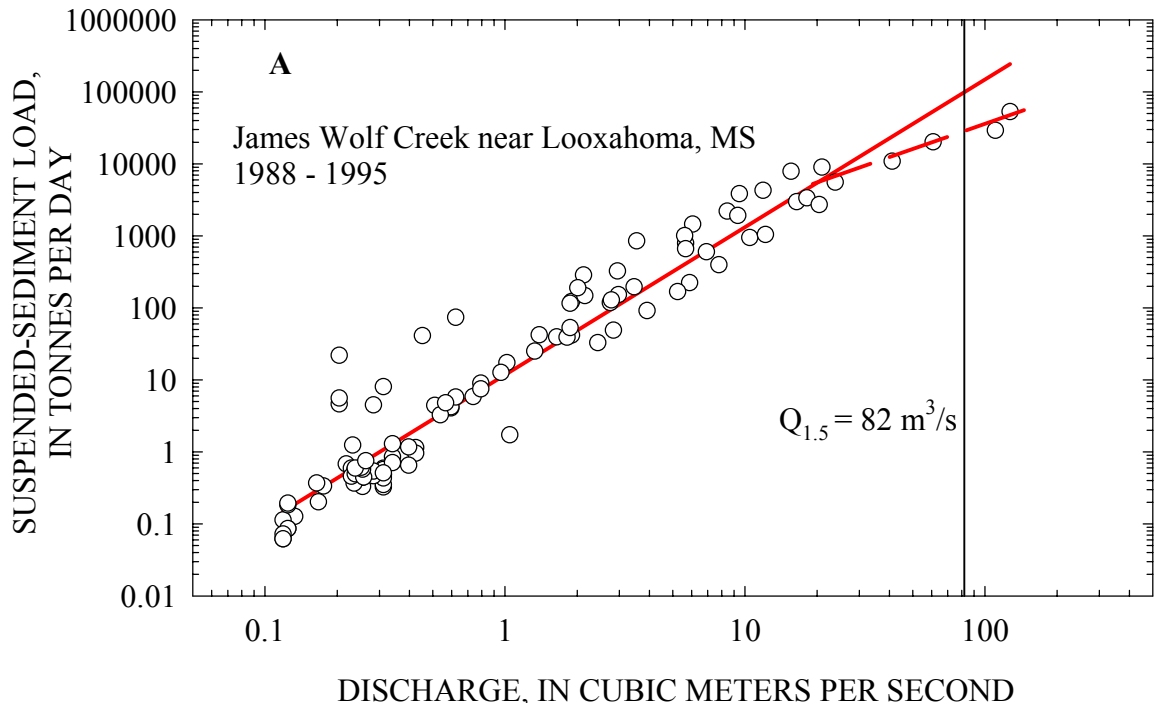


Figure 70 – Development of suspended-sediment rating relation showing potential error at $Q_{1.5}$ and other high discharges without a second (A) or third (B) linear segment.

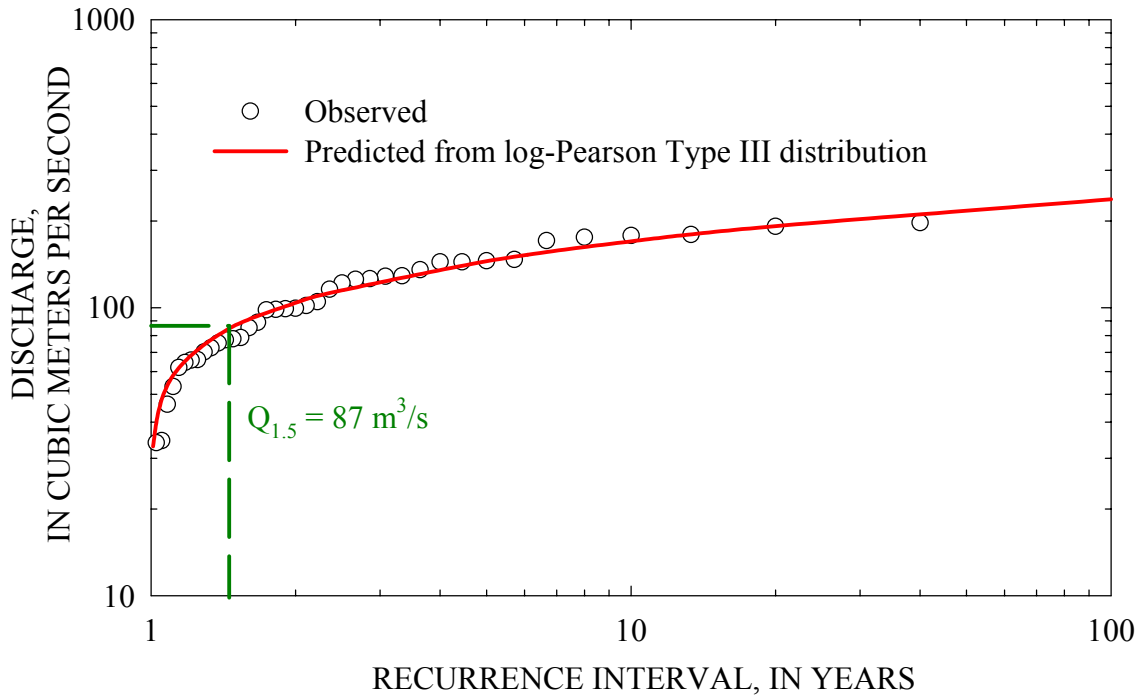


Figure 71 – Flood-frequency distribution for James Creek near Aberdeen showing the $Q_{1.5}$ to be used in calculating sediment loads at the effective discharge.

Calculating Effective Discharge ($Q_{1.5}$)

Using the annual-maximum peak-flow series for each of the sites with available data, the effective discharge ($Q_{1.5}$) was then calculated from the log-Pearson Type III distribution. The example shown in Figure 71 is for the discontinued gauge at James Creek near Aberdeen. Where peak-flow data were not available, the $Q_{1.5}$ was calculated from regional relations based on drainage area obtained from the U.S. Geological Survey (1993) and calculated in Simon and Dickerson (in press). Because these data are available for James Creek from the discontinued gauge south of Aberdeen, the $Q_{1.5}$ does not have to be estimated from regional relations. If a sediment-rating relation based on measured data were available for James Creek, concentrations or loads could be easily obtained for the effective discharge. For the 148 sites in ecoregion 65 with peak flow and sediment-transport data, sediment load at the effective discharge can be obtained directly from the rating relation.

The effective discharge ($Q_{1.5}$) was determined at all sites and applied to the transport relation to obtain the sediment load at the effective discharge. An example is shown for Town Creek near Nettleton, Mississippi where the $Q_{1.5}$ was determined to be $650\text{m}^3/\text{s}$ from the annual-maximum series (Figure 72a). The suspended-sediment load at the $Q_{1.5}$ was then obtained by using the transport rating developed for the site and by solving for $650\text{m}^3/\text{s}$ (Figure 72b). To normalize the data for watersheds of different size, the sediment load is divided by drainage area to obtain sediment yield (in $\text{T}/\text{d}/\text{km}^2$). All rating relations are checked to be sure that the $Q_{1.5}$ was within the measured bounds of the data set. If the $Q_{1.5}$ is more than 100% greater than the maximum sampled discharge, the calculated sediment yield is not included in the data set.

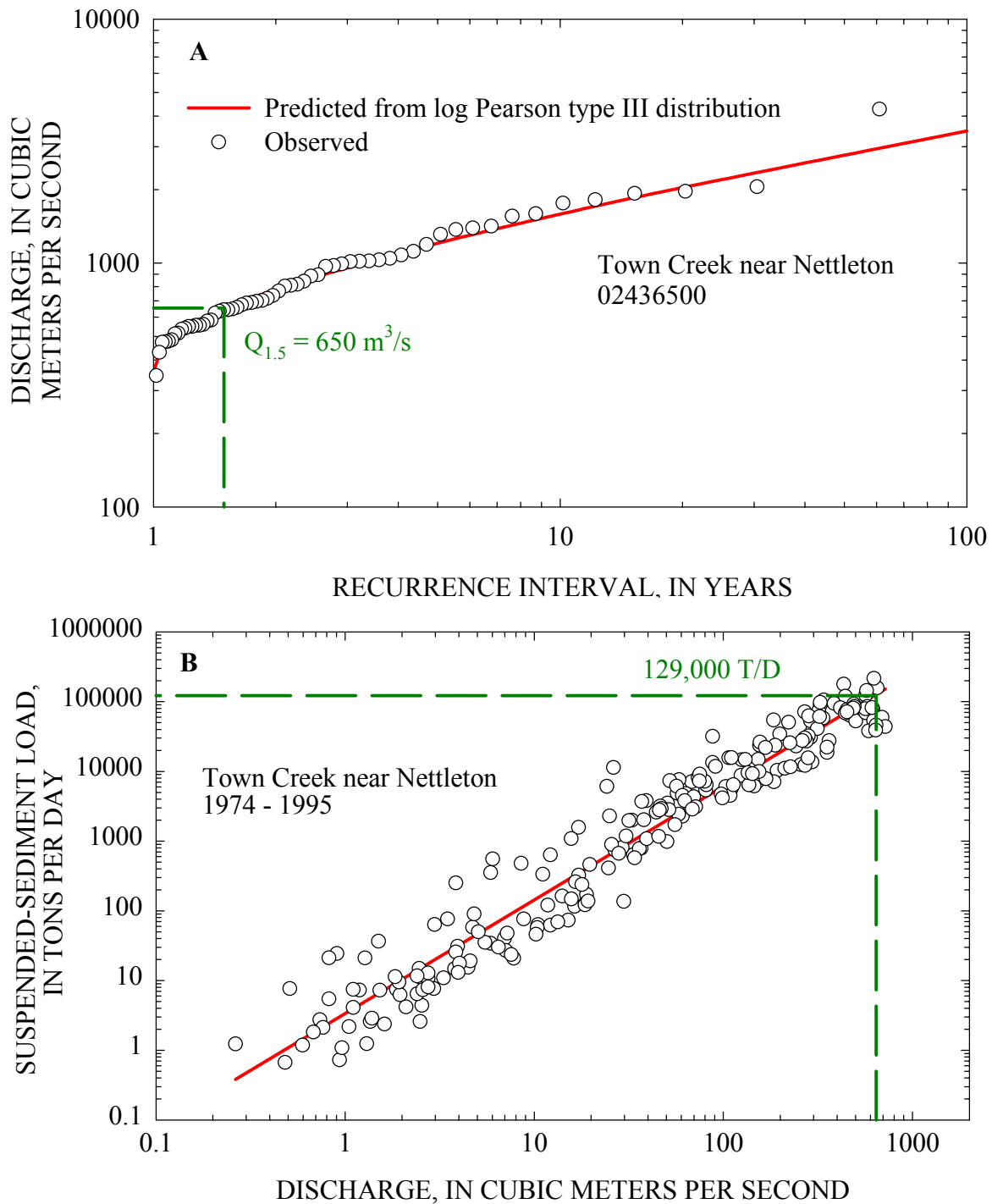


Figure 72 – Determination of effective discharge ($Q_{1.5}$) from annual-maximum flow series (A) and suspended-sediment load at the effective discharge using the sediment-transport rating relation (B).

Results from Evaluations of “Reference” Sediment Loading

Suspended-sediment yields at the effective discharge were calculated for each of the sites in the Southeastern Plains by the procedures outlined earlier. Results for each site sorted by state and station number are shown in Appendix C. The median suspended-sediment yield value at the $Q_{1.5}$ for all sites is 0.52 T/d/km^2 . This is placed in a national context in Figure 73 where median values for most of the 84 ecoregions in the continental United States are shown. The median concentration, also at the $Q_{1.5}$ is 63 mg/l . To reduce the effect of outliers on the maximum and minimum values shown in Figure 74 and Figure 75, they are calculated as the mean of the five largest, and smallest, respectively. The significance of the median values should not be overestimated in that both are derived from data throughout the ecoregion for sites of varying degrees of stability as well as for a range of bed material types. It is encouraging to note, however, that the central 50% of each distribution falls within a single order of magnitude.

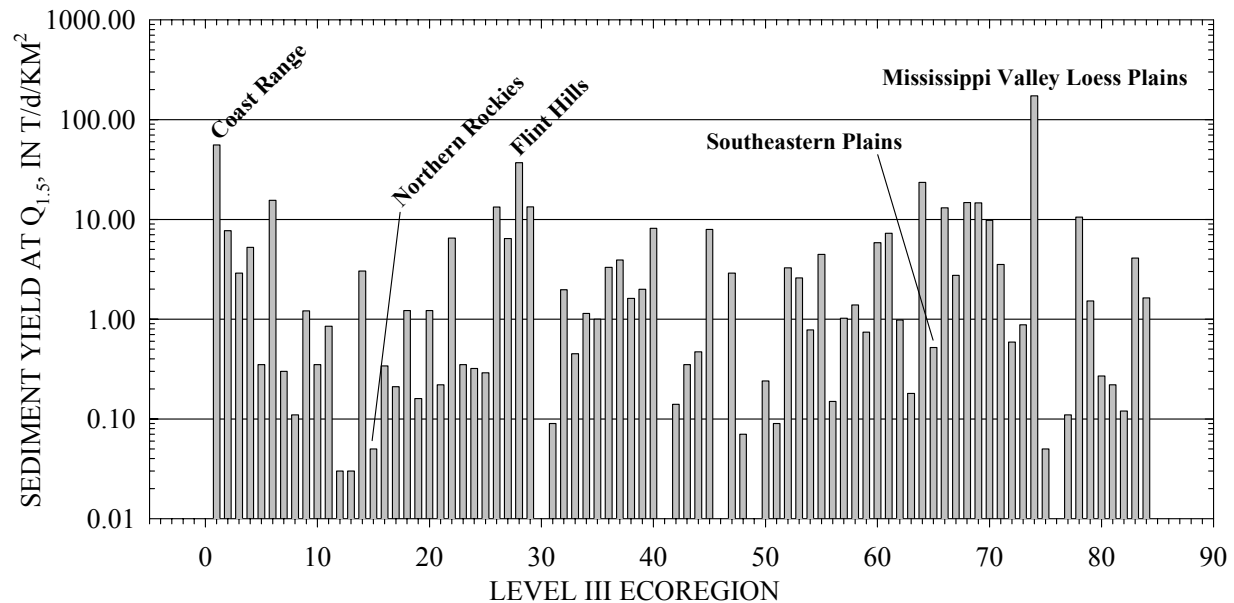


Figure 73 – Comparison of national median suspended-sediment yields at the $Q_{1.5}$ for 84 ecoregions of the continental United States. Modified from Simon *et al.*, 2002.

“Reference” Sediment-Transport Conditions

A total of 97 sites in the Southeastern Plains have been visited to determine stage of channel evolution and relative channel stability for the purpose of determining which sites can be characterized as “reference” (Figure 76). Stage I (pristine) conditions were found at 15 sites and 33 Stage VI (re-stabilized) sites were found in the region. Only one Stage VI site was found along James Creek and this was in a backwater situation directly upstream from a low-water crossing, further emphasizing the need to use “reference” conditions from elsewhere in the Southeastern Plains. All other sites along James Creek were in Stage IV or V, indicating that almost all of the streambanks along the creek showed evidence of recent failures. The mean channel-stability index for James Creek was 24, indicative of significant instabilities. The RGA summary sheet is shown in Figure 69.

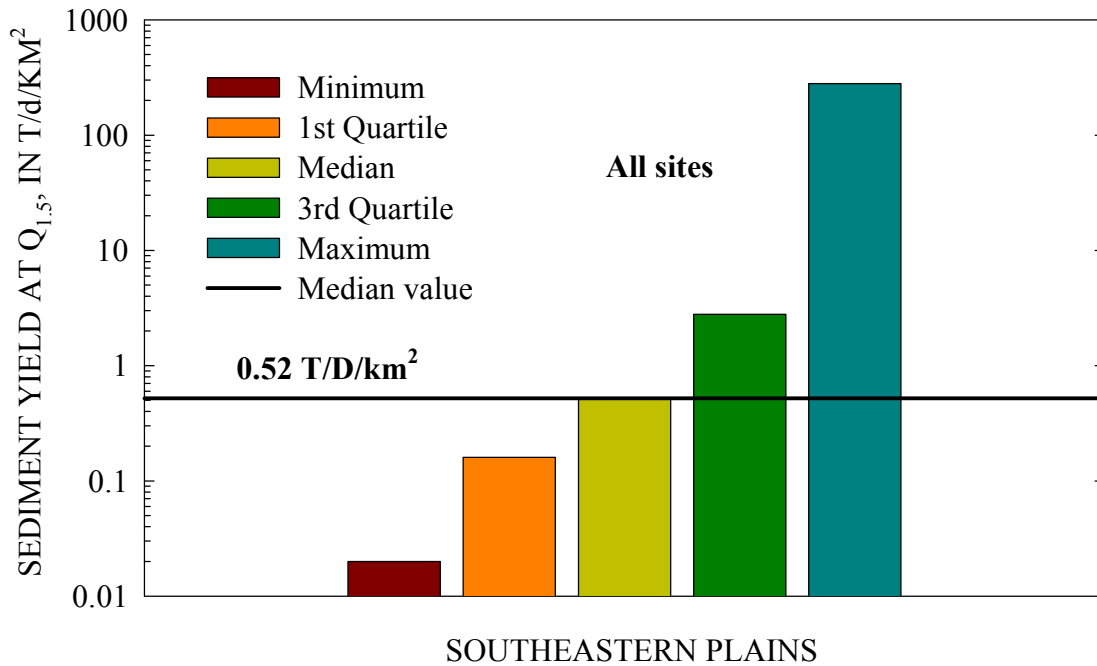


Figure 74 – Distribution of suspended-sediment yields at the Q_{1.5} for the Southeastern Plains ecoregion.

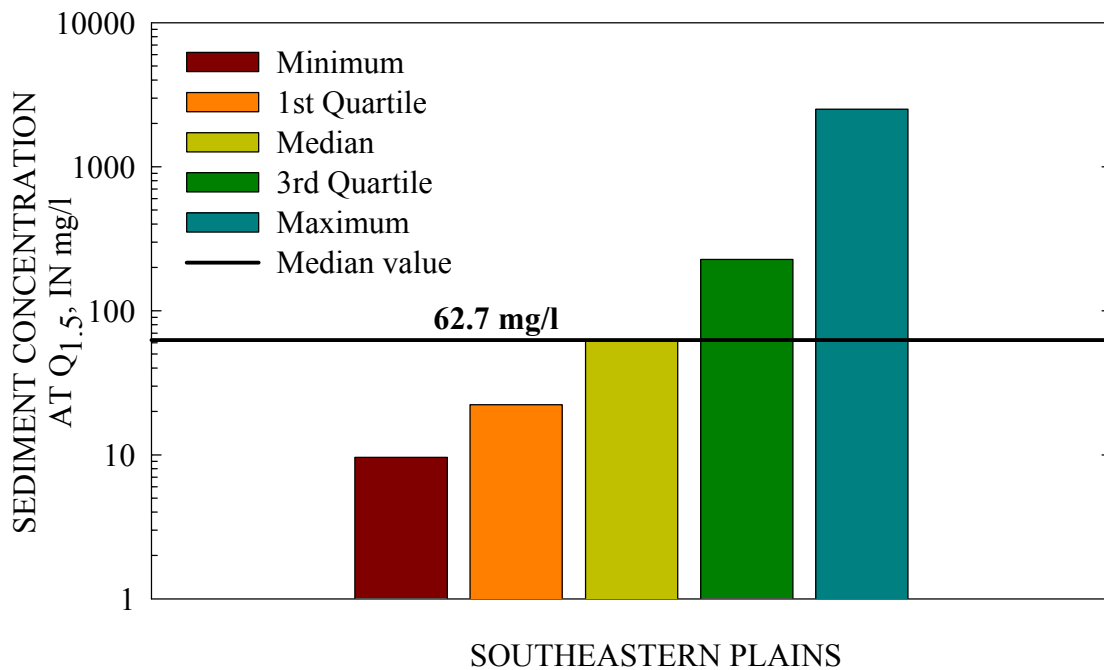


Figure 75 – Distribution of suspended-sediment concentrations at the Q_{1.5} for the Southeastern Plains ecoregion.

Suspended-sediment yield and concentration data from the 48 “reference” sites were separated from those sites that were characterized as unstable to create more meaningful sediment-transport distributions representing unstable and “reference” sites. These are shown in Figure 77 and Figure 78. The median value for the stable sites is termed the “general reference” for the particular parameter (yield or concentration) because it is not sorted by dominant bed-material particle size. It is important to note that the distributions are heavily influenced by sand-bed streams because they represent the majority of the studied sites.

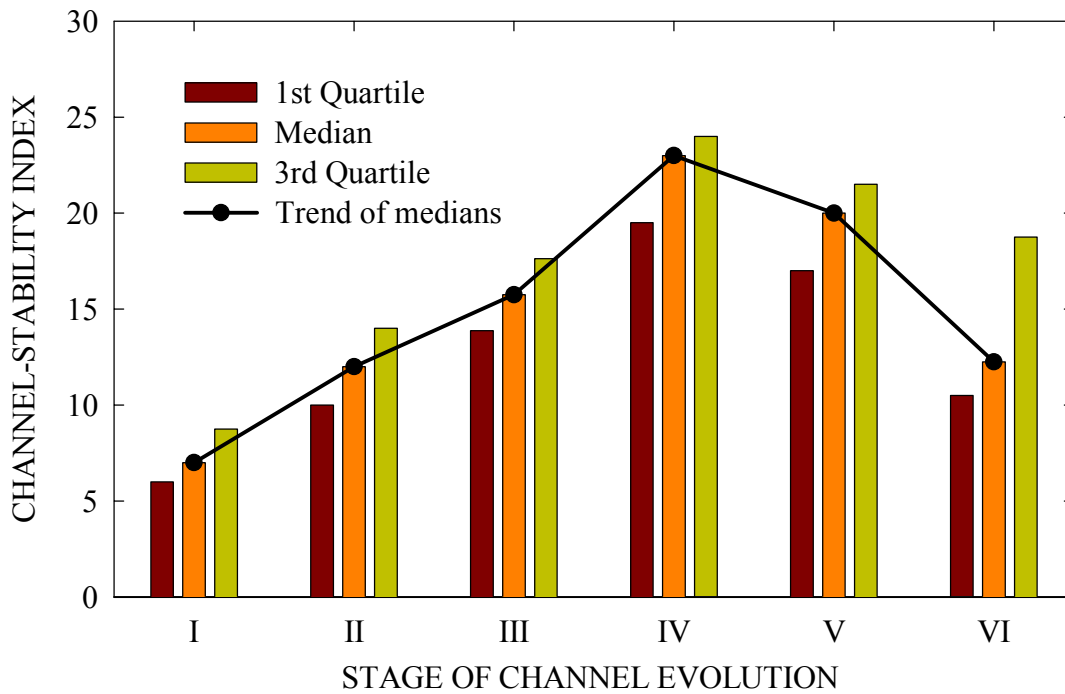


Figure 76 – Relation between stage of channel evolution and channel-stability index (*I*) for the Southeastern Plains ecoregion.

The “general reference” for suspended-sediment yield is 0.31 T/d/km^2 at the $Q_{1.5}$. For the outlet of James Creek with a drainage area of 111 km^2 , this translates into a “general reference” sediment load of 34.4 T/d at the $Q_{1.5}$. Perhaps a better way to interpret the data for the “general reference” is in terms of a range of values for the stable sites. The central 50% of the reference distribution falls within an order of magnitude ($0.17 - 1.03 \text{ T/d/km}^2$). This would provide for a “general reference” load at the mouth of James Creek of between 18.9 and 114 T/d at the effective discharge. The central 50% of the distribution for unstable sites in the Southeastern Plains ranges from 0.34 to 17 T/d/km^2 at the effective discharge. The median value for these sites is 1.53 T/d/km^2 .

A similar “general reference” transport condition can be characterized for suspended-sediment concentration at the $Q_{1.5}$ (Figure 78). Here, a median value for stable sites of 47.9 mg/l was obtained with the central 50% of the distribution ranging from 20.4 to 83.6 mg/l . This compares to a central inter-quartile range of 43.5 to 778 mg/l with a median of 127 mg/l for unstable sites in the Southeastern Plains.

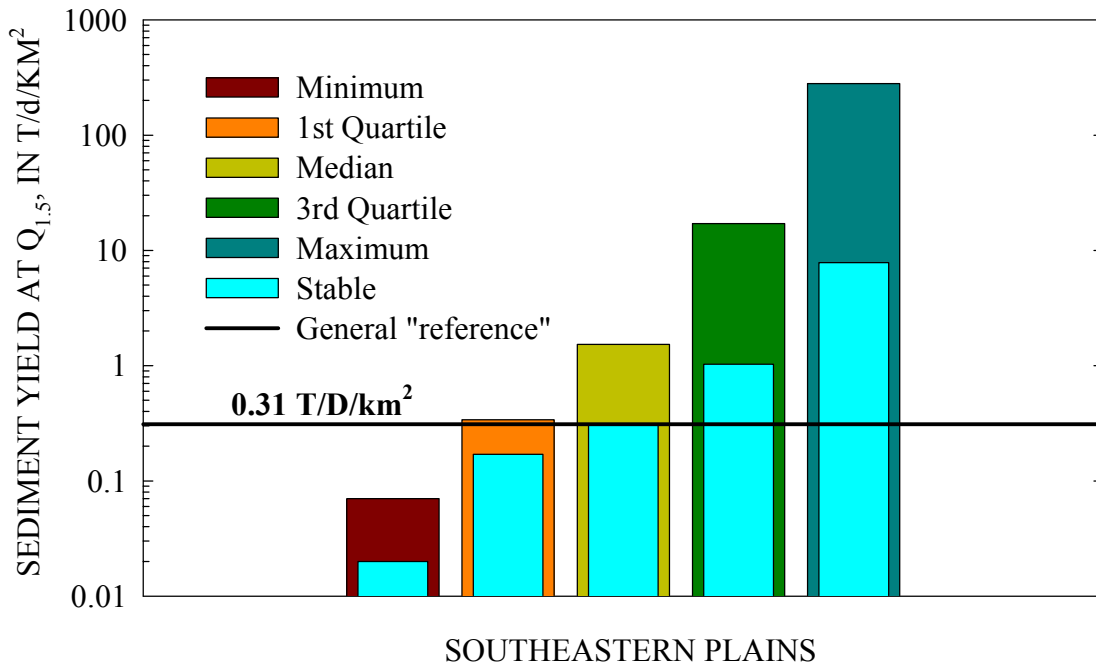


Figure 77 – Comparison of suspended-sediment yields at the Q_{1.5} for stable “reference” sites and for evaluated, unstable sites. Yield shown is a general reference for the Southeastern Plains ecoregion.

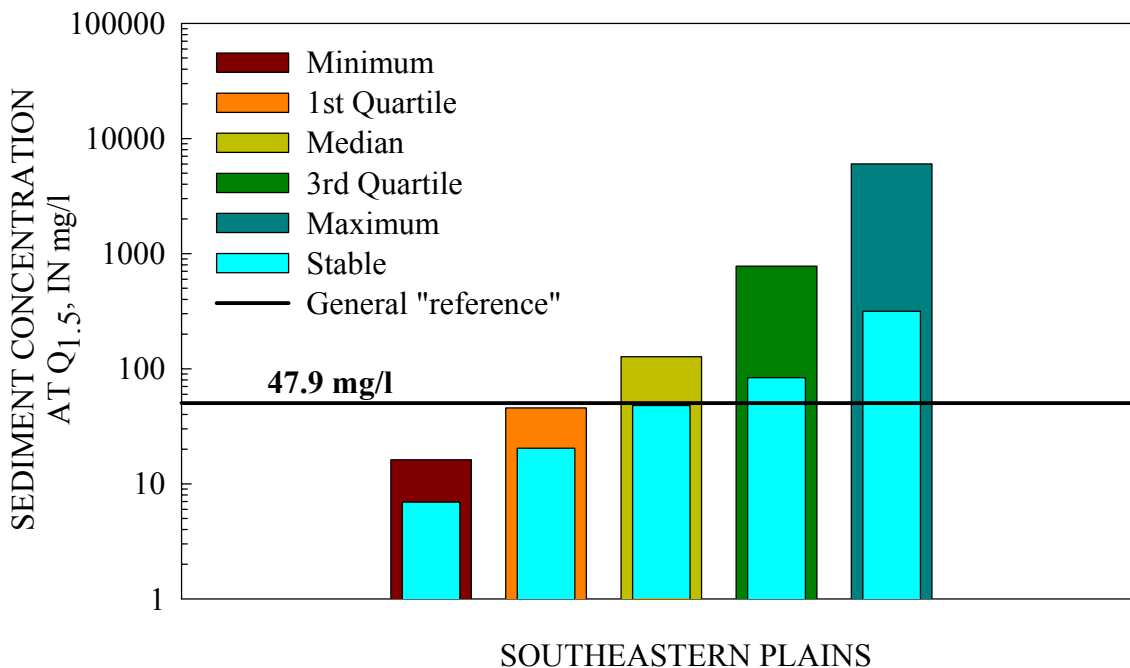


Figure 78 – Comparison of suspended-sediment concentrations at the Q_{1.5} for stable “reference” sites and for evaluated, unstable sites. Concentration shown is a general reference for the Southeastern Plains ecoregion.

Empirical Relations With Stage of Channel Evolution and Channel-Stability Index

Attempts were made to derive empirical relations between geomorphic characteristics such as stage of channel evolution and the channel-stability index for the purpose of estimating current sediment loads in ungaged streams. Various combinations using suspended-sediment yield and concentration were tried with little success in developing relations that could be used for prediction. Still, it was possible to develop two rather instructive relations. Figure 79 shows the relation between suspended-sediment concentration at the $Q_{1.5}$ and the channel-stability index (I). As one would expect concentration increases with increasing I and increasing instability. Be aware of the broad scatter around the regression line and its 95% confidence limits. The outer bands are a better descriptor (95% prediction limits) of the relative lack of certainty in the regression. We suspect that much of the problem with the relation lies with the uncertainty of channel-stability conditions (index) during the period of sediment sampling.

Suspended-sediment yields and concentrations for the Southeastern Plains were sorted by stage of channel evolution to try to identify unique distributions of these variables for each stage. Although the shape of the trend line of the medians is as expected with peak values during stages IV and V, differentiation is not as great as expected (Figure 80). However, if the data were separated solely into stable sites (Stages I and VI) and unstable sites (Stages III, IV and V) more dramatic differences would emerge. In a sense, this is the technique used to develop “reference” sediment-transport conditions. Again, we believe that the lack of complete definition of stage during periods of sediment sampling hampers the clarity of this relation.

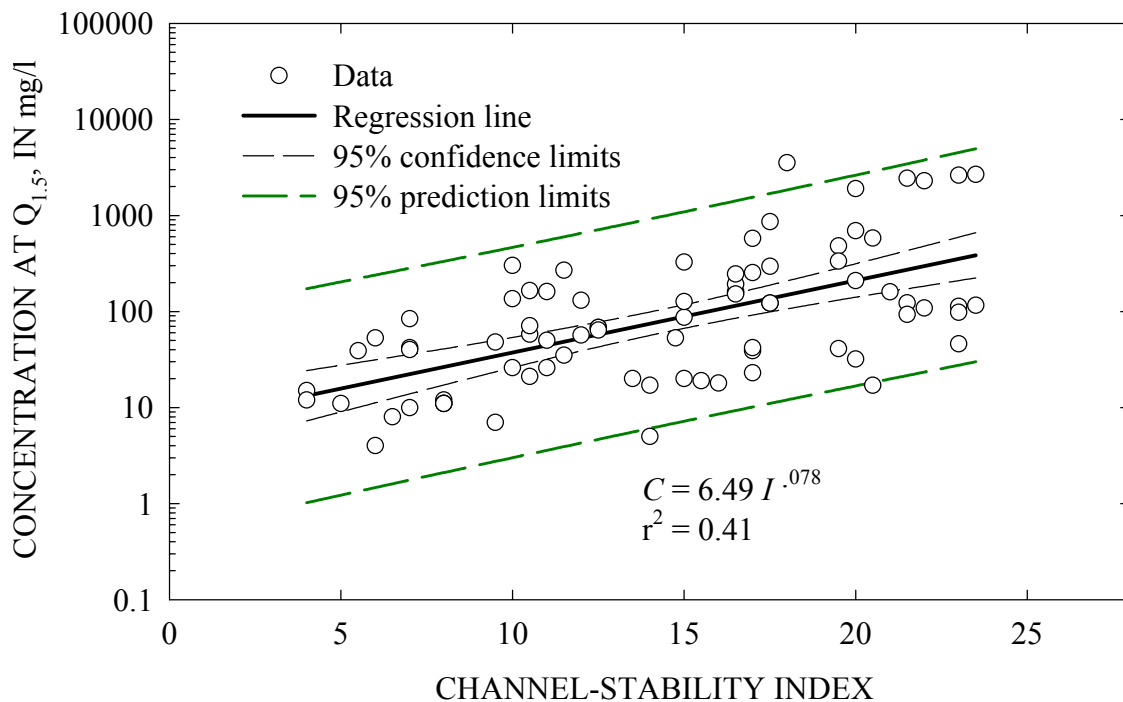


Figure 79 – Relation between channel-stability index (I) and suspended-sediment concentration (C) at the $Q_{1.5}$ for sites in the Southeastern Plains. Coefficient of determination is low ($r^2 = 0.41$) and relation should be used with caution.

Refinement of Estimates of “Reference” Sediment Discharge

In an attempt to refine the estimates of the “reference” sediment discharge, the data set for both unstable and stable sites was sorted by dominant bed-material size class: gravel, sand, and silt-clay. As stated earlier, James Creek is somewhat unique in the Southeastern Plains in that it is dominated by cohesive-bed sediments. However, of the 97 sites visited in the ecoregion, only four contained appreciable quantities of fine-grained materials on the channel bed and three of these were stable. Figure 81 and Figure 82 show the comparative distributions of suspended-sediment yield and concentration at the $Q_{1.5}$ for the three principle size classes of sediment. “Reference” suspended-sediment yields for gravel-, sand- and fine-bed streams are 0.27, 0.42, and 3.23 T/d/km², respectively (Figure 81). Only the distribution of suspended-sediment yields for stable fine-bed streams are shown in the lower-most plot in Figure 81 because of the lack of unstable streams with this type of bed material. Note that the calculated reference for streams with silt-clay beds such as much of James Creek (Figure 81) is about an order of magnitude higher than for streams with coarse-grained beds. By multiplying the “reference” sediment yield by the drainage area at the mouth of James Creek (112 km²), we obtain a “reference” sediment load of 362 T/d at the $Q_{1.5}$. By comparison, downstream of about rkm 11 where sand and gravel sediment are the dominant bed-material size classes on James Creek it is reasonable to use either the “general reference” of 0.31 T/d/km² or the appropriate “reference” for the given textural class of bed sediment (Figure 81). A similar rationale can be followed for application of the “reference” condition using concentration at the $Q_{1.5}$ as the clean-sediment parameter.

The best estimate of the “reference” suspended-sediment yield or concentration “reference” for James Creek should be based on weight-meaning of the reference- parameter values by drainage area. For example, utilizing the particle-size data shown in Table 12 and mapped in Figure 83 we can identify those reaches that are dominated by the major textural size classes (gravel, sand and fines) and determine the percentage of the drainage area that is encompassed by those reaches. The total drainage area of James Creek is 112 km². By assuming that tributaries entering the main stem have the same bed-material characteristics as the trunk stream we find that 65% is silt and clay, 21% is sand and 14% is gravel. The respective suspended-sediment yield and suspended-sediment concentration reference values for each size class are then multiplied by the percent area encompassed by that size class. The resulting “reference” values are **2.22 T/d/km²** and **160 mg/l** at the $Q_{1.5}$ or the effective discharge. Again if we multiply the reference yield by the drainage area of James Creek we obtain a “reference” load at the outlet of **249 T/d** at the $Q_{1.5}$.

The “reference” values reported here represent median values of data distributions for stable streams. Given the great variability in suspended-sediment transport even at a constant discharge, it is perhaps more appropriate to provide a range of “reference” values. We do so by taking the central 50% of the data distributions (the first and third quartiles) for both suspended-sediment yield and concentration at the $Q_{1.5}$. Values for each of the quartile measures are applied in the weighting procedure described above to calculate the range for the reference suspended-sediment yield and concentration. For the weighted, suspended-sediment reference yield, **2.22 T/d/km²** represents the center of the inter-quartile range bounded by **1.5** and **3.83 T/d/km²**. Thus, the range of the weighted, reference suspended-sediment load at the outlet of James Creek is between **168** and **429 T/d** at the $Q_{1.5}$. For suspended-sediment concentration, **160 mg/l** represents the center of the inter-quartile range bounded by **130** and **209 mg/l**.

It is important to bear in mind that sediment-transport relations based on measured data from even the most rigorous storm-event sampling program have inherent variability due to seasonality, variable source areas and hysteresis effects. Transport relations with coefficients of determination (r^2 values) as high as 0.9 may display order of magnitude variation in concentration or load for a given discharge. That the “reference” sediment-transport estimates provided in this report show the same magnitude of variability as high-quality measured data is encouraging and supportive of the technique.

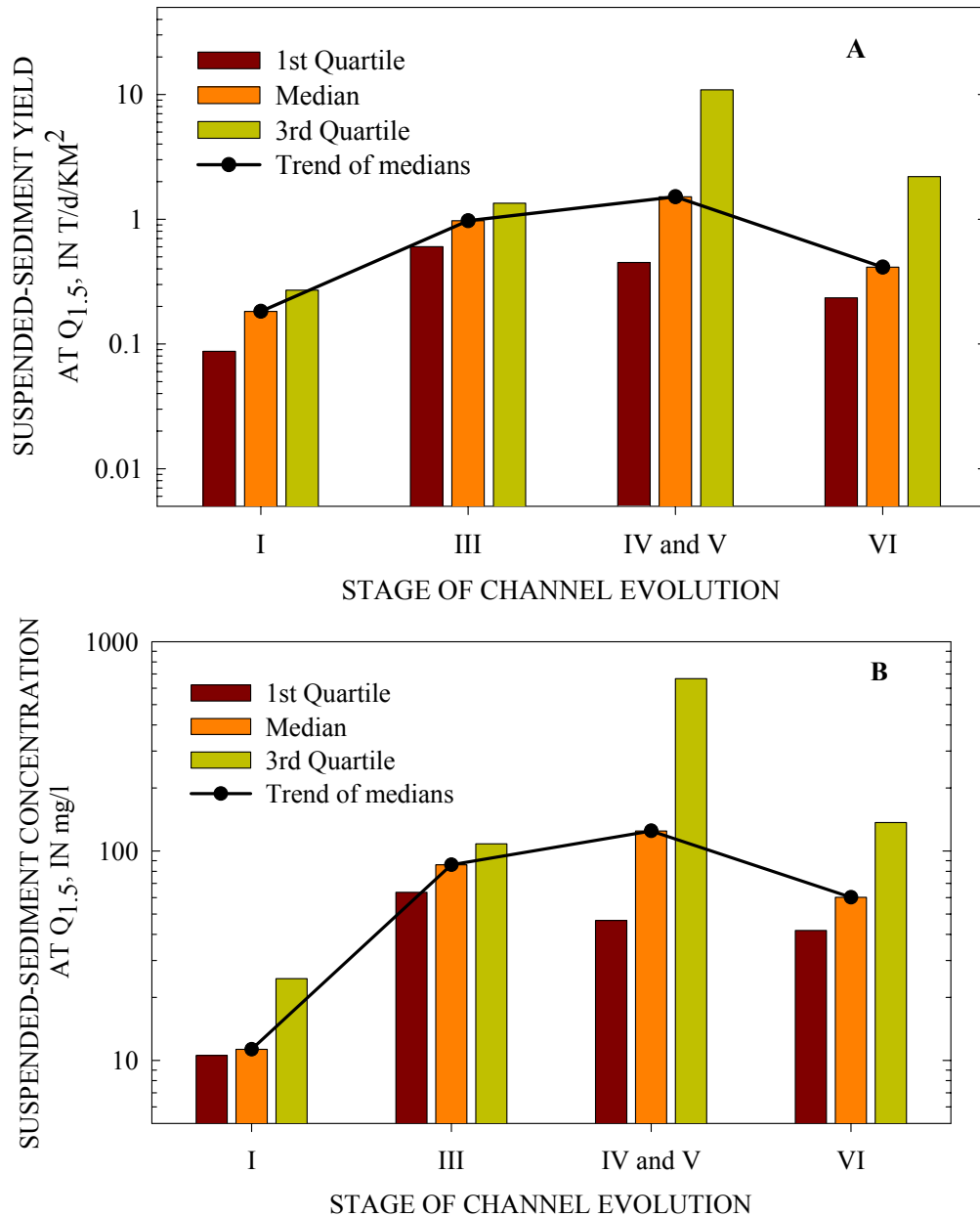


Figure 80 – Inter-quartile distributions of suspended-sediment yield (A) and concentration at the Q_{1.5} by stage of channel evolution for 97 sites in the Southeastern Plains.

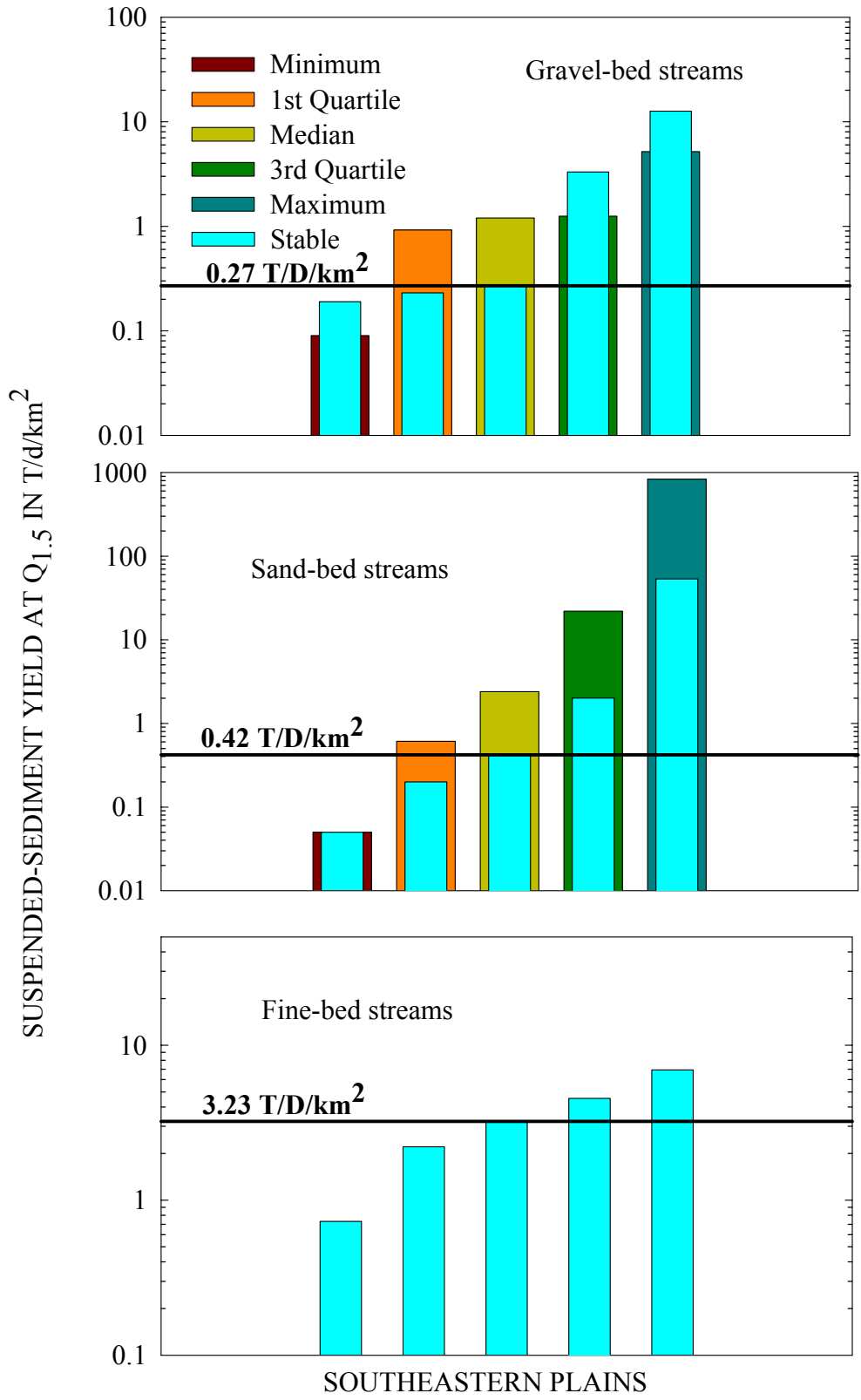


Figure 81 – “Reference” suspended-sediment yields at the $Q_{1.5}$ for three major textural classes of bed sediment in the Southeastern Plains.

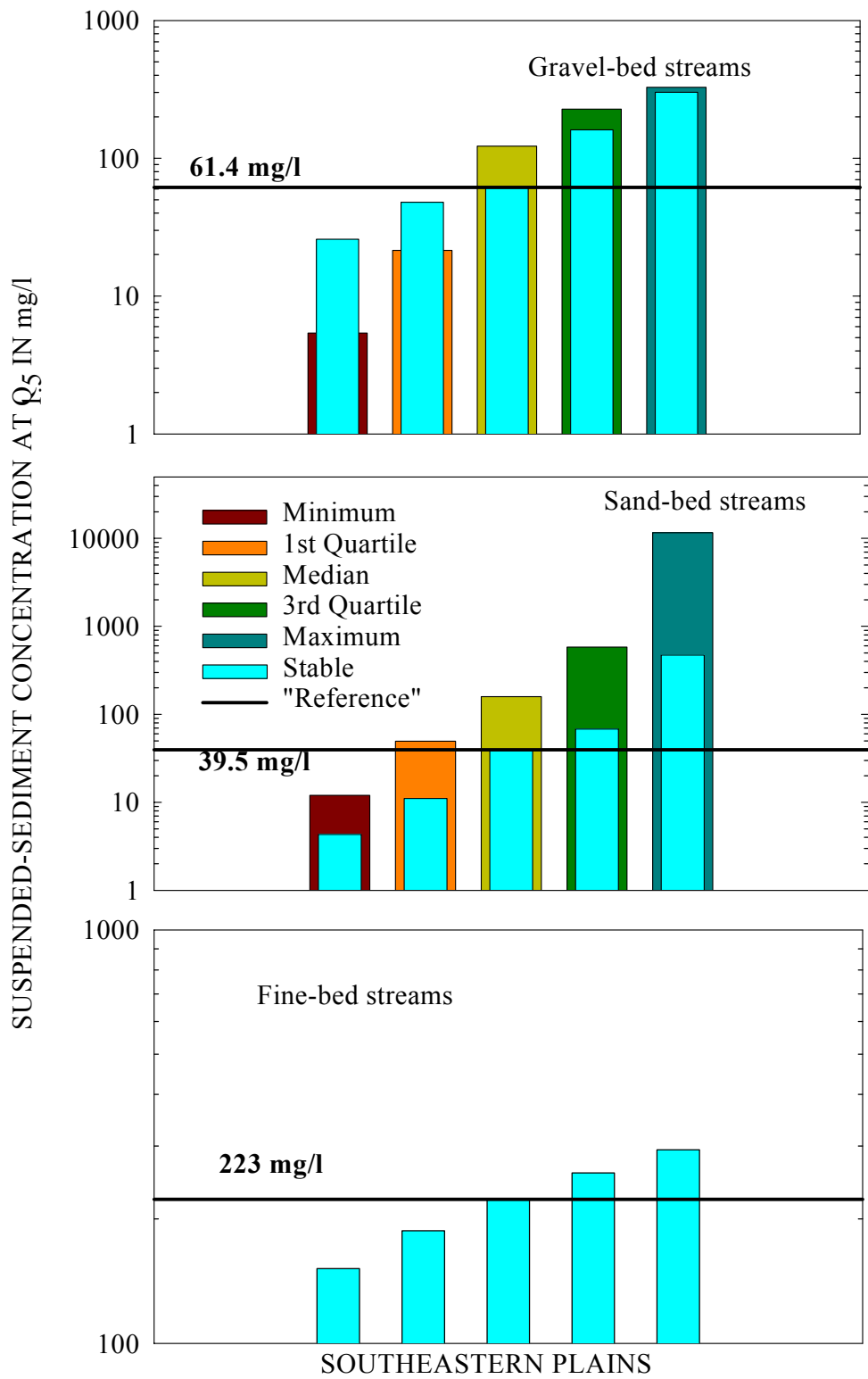


Figure 82 – “Reference” suspended-sediment concentrations at the Q_{1.5} for three major textural classes of bed sediment in the Southeastern Plains.

RESULTS FROM EVALUATIONS OF “ACTUAL” SEDIMENT LOADING

Introduction

Evaluations of “actual” sediment loadings from James Creek are based from several sources. Results from AnnAGNPS provide loadings data from gullies, fields and tributaries. Direct comparison of measured cross-sections between 1967 and 2002 provide a strong evidence of the contribution from channel sources over the period. These data are compared with simulated channel contributions over the same reach and time period by CONCEPTS. Together, the AnnAGNPS and CONCEPTS simulations provide total loadings values for the James Creek watershed. Results are determined for several locations along James Creek, including the Highway 25 bridge, Darracott Road, and the watershed outlet. These results emphasize the need for grade control in disturbed or modified channels to prevent excessive incision that leads to destabilizing of the channel banks.

AnnAGNPS and the Combined AnnAGNPS and CONCEPTS Simulations of the Main Upstream Tributary for Reduced Tillage Conditions

An evaluation was performed at one of the main tributaries (Figure 46) entering James Creek in order to assess the capability of AnnAGNPS simulations of the tributary loadings into CONCEPTS used for the entire James Creek watershed. The simulation scenario of reduced tillage with determined stability was used to compare the simulation models at the outlet of the simulated main tributary chosen. For the 1967-2001 simulation period AnnAGNPS produced 17,780 tonnes per year at the main tributary outlet. For the CONCEPTS simulation, 24,331 tonnes per year were produced at the main tributary outlet. This was within an acceptable range for the application of AnnAGNPS to supply the sediment loadings from all of the other tributaries. In order to maintain the consistency of AnnAGNPS simulated water and sediment loadings for the entire James Creek watershed, the AnnAGNPS loadings were used from this main tributary simulation to CONCEPTS for the simulation of the main channel of James Creek, instead of using the CONCEPTS simulated loadings from the main tributary for this simulation.

AnnAGNPS Simulated Streamflow and Sediment Discharge Rates

Comparison of Measured and Simulated Peak Flow Rates at the Highway 25 Gaging Station, 1967-2001

An evaluation of the capability of AnnAGNPS to reproduce the measured peak flow rates was performed using data obtained at the Highway 25 USGS gaging station for dates that corresponded to the highest peak in a water year (October-September). Measured annual peaks values from water year 1967 to water year 2001 were used to compare the AnnAGNPS simulated peak discharge for each corresponded event (Figure 84). The results of the AnnAGNPS peak values are generally lower than the measured, but with a high coefficient of determination of 0.80. The capability of AnnAGNPS to simulate peak runoff rates is dependent on the quality of the precipitation records. AnnAGNPS simulates rainfall events, which may not coincide with the dates that peak runoff events may occur, such as several days later from the rainfall.

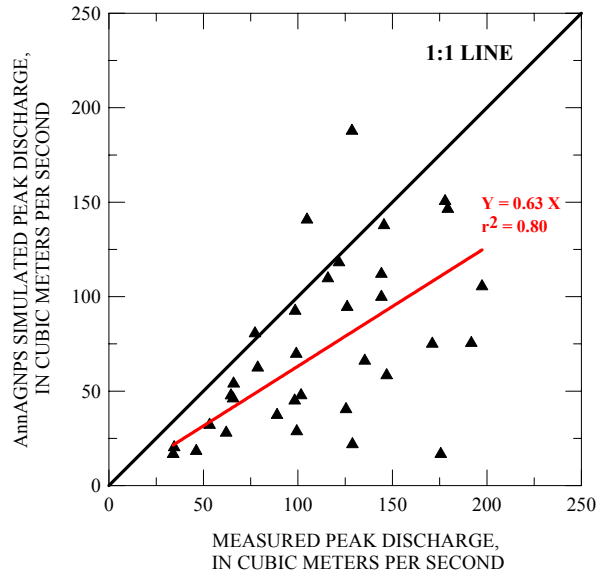


Figure 84 – Comparison of the AnnAGNPS and measured annual peak discharge at the Highway 25 gaging station with a best fit line (red).

Simulated Runoff at the Darracott Road Bridge Crossing

The simulated runoff was determined from 1967 to 2001 at the junction of the main channel and the Darracott Road crossing. The simulated runoff can be compared with the yearly rainfall to show that nearly a third of the rainfall was eventually produced as runoff (Figure 85). The simulated runoff by AnnAGNPS cells can be used to describe the degree of runoff from the various cells within the watershed (Figure 86). A significant amount of runoff occurs in the upper end of the watershed where the landuse is mostly cropland.

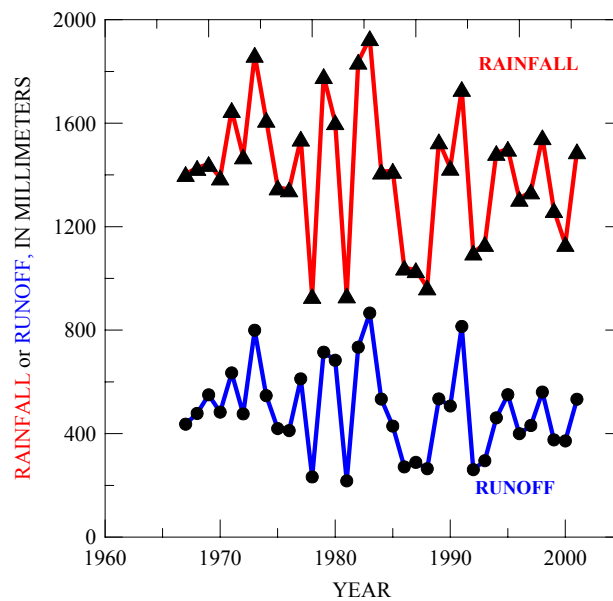


Figure 85 – Simulated yearly runoff by AnnAGNPS at the Darracott Road crossing and the yearly rainfall used within the simulation of the entire James Creek watershed.

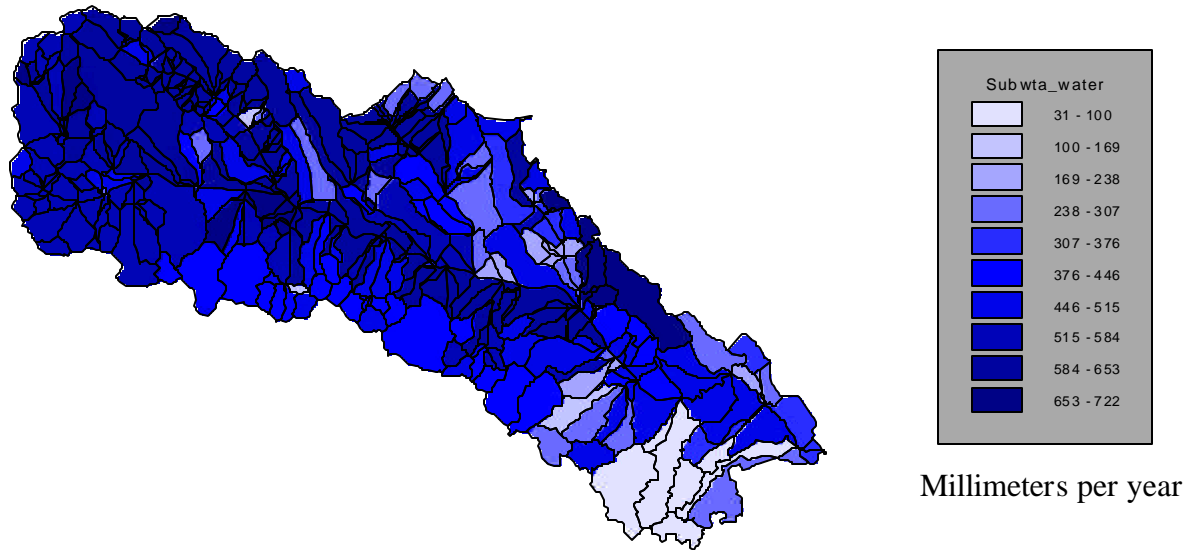


Figure 86 – Average annual runoff simulated from AnnAGNPS for each cell.

Simulated Sediment Load at the Darracott Road

Sediment from each scenario was simulated by AnnAGNPS to produce loadings at the Darracott Road crossing point in the main channel. These scenarios represented the two types of landuse employed as reduced tillage and conventional tillage, and for the degree of channel erosion that occurred as indicated by either: all of the channels being unstable and, thus, channel erosion occurs; all of the channels being stable and, thus, no channel erosion occurs; or channel stability indicated from the field survey investigation. Each of the scenarios simulated produced a significant amount of sediment from the AnnAGNPS cells, but for the scenarios that had unstable conditions, the sediment from the channels, indicated as bed and bank erosion by AnnAGNPS, was nearly seven times greater than the sediment produced by the fields (Table 14). The total sediment load simulated by AnnAGNPS at the outlet of James Creek for the reduced tillage for indicated unstable reaches was 109,717 T/y. The yearly total sediment, bed and bank contribution of the total sediment and the AnnAGNPS cell contribution are shown in Figure 87. The AnnAGNPS simulated erosion produced from each cell (Figure 88) and the sediment yield that enters the channel from each cell (Figure 89), can be derived using the AGNPS Arcview interface. From the scenarios, the sediment loadings from the AnnAGNPS cells were all very similar and since the reduced tillage condition reflected better the current condition, thus, this was used for the loadings into CONCEPTS. The comparison of the various stability conditions of the channels demonstrated a significant difference between the stable and unstable conditions. The difference in sediment loadings from the scenarios of stability selected based on channel survey techniques and all channels unstable demonstrated no major difference in sediment totals. This indicated that the selection of the unstable reaches represented a majority of the actual sediment producing sections of the channels. Thus, the scenario using the indicated channel stability would adequately represent the actual loadings into the main channel.

The contributions from individual fields as defined by AnnAGNPS cells provides the loadings into channels that are tributaries to the main channel or as cells that directly enter the main

channel. A significant portion of the sediment loadings from AnnAGNPS seems to occur from cells that are along the main channel that have landuse defined as soybeans and corn (Figure 48 and Figure 89). The soils along the main channel represent typical floodplain soils that are silty clay and clay that can have a high amount of runoff occurring on erosive soils that would produce a high amount of sediment.

The sediment loadings produced from the AnnAGNPS cells are fairly consistent between the simulated scenarios. The channel erosion simulated by AnnAGNPS shows a very high contribution from the reaches compared to the AnnAGNPS cells. This reflects the inability of AnnAGNPS to include the changing conditions of the channel, including the construction of structures that serve to control erosion and produce deposition upstream of the structure. The results show that conventional tillage produces about a third more sediment than reduced tillage practices, but that the channel systems dominant as sources of sediment.

Table 14 – Source of sediment simulated by AnnAGNPS at Darracott Road by simulation scenario totals for 1967-2001.

Scenario	Total Sediment (T/y)	Sediment Produced from AnnAGNPS Cells (T/y)	Sediment Produced from the Bed and Bank Contributions of AnnAGNPS (T/y)
Reduced Tillage with Indicated Channel Stability	158,084	24,807	133,277
Reduced Tillage with All Channels Unstable	177,198	24,579	152,620
Reduced Tillage with All Channels Stable	20,053	20,053	0
Conventional Tillage with Indicated Channel Stability	160,677	25,599	135,078
Conventional Tillage with All Channels Unstable	179,960	25,375	154,585
Conventional Tillage with All Channels Stable	26,666	26,666	0

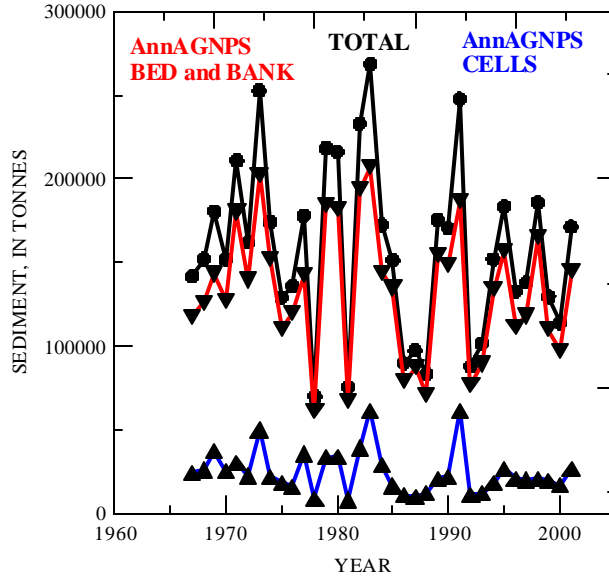


Figure 87 – The total sediment, AnnAGNPS bed and bank contribution, and the AnnAGNPS cell contribution at the Darracott crossing.

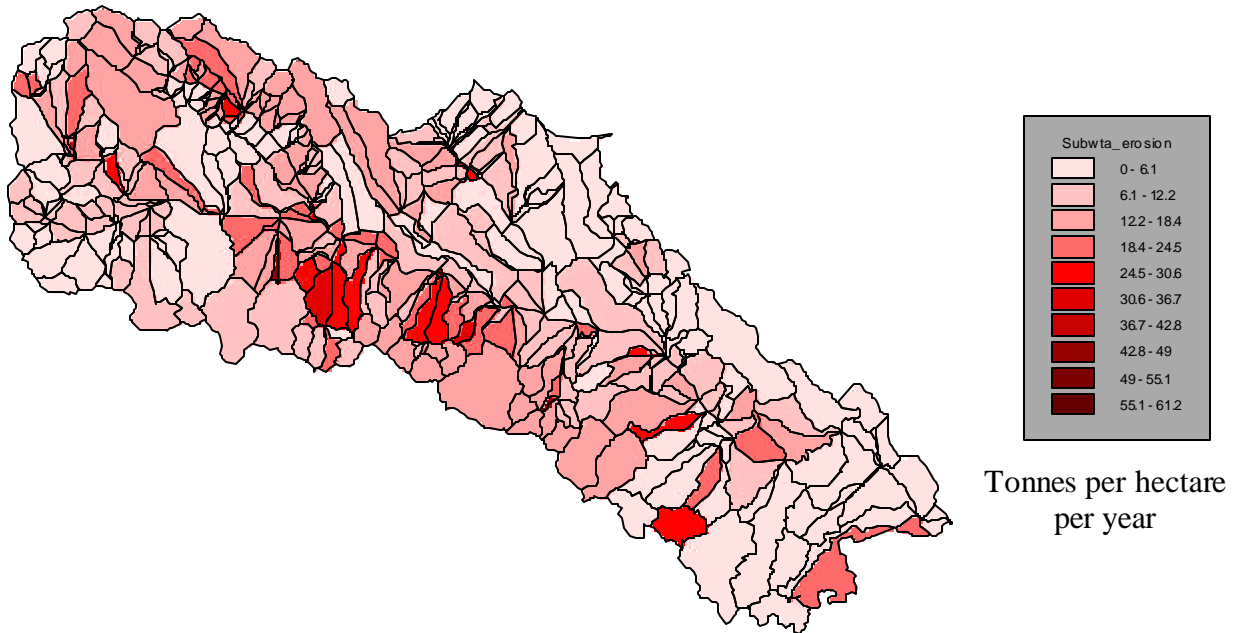


Figure 88 – Average annual erosion simulated from AnnAGNPS for each cell.

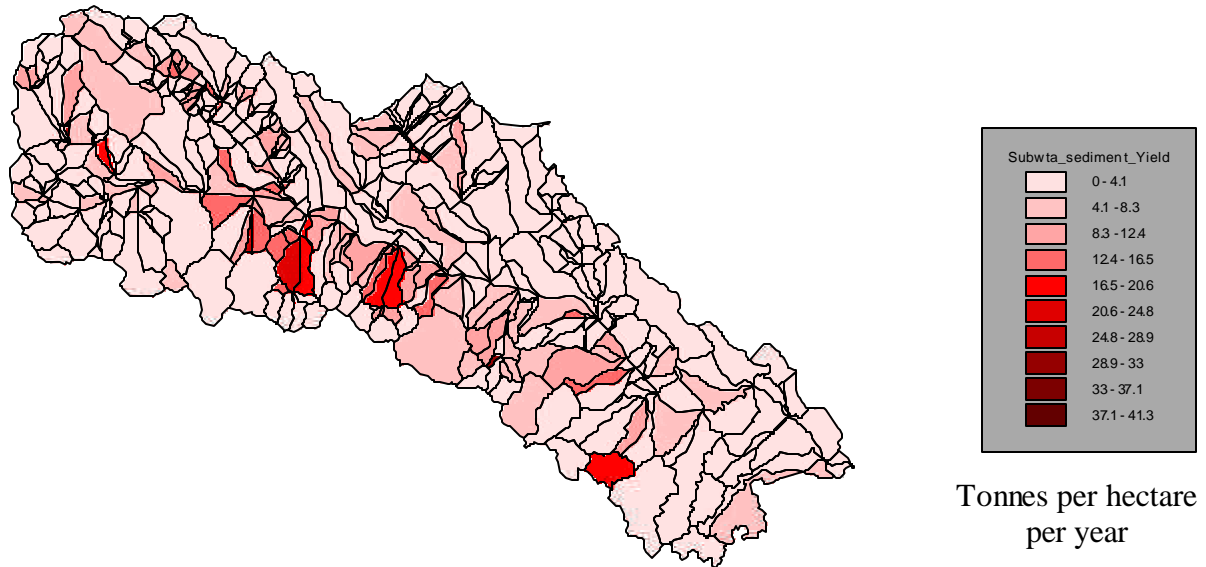


Figure 89 – Average annual sediment yield simulated from AnnAGNPS for each cell.

Combined AnnAGNPS and CONCEPTS Simulation of Main Channel Evolution and Transport Rates, 1967-2001

CONCEPTS was used to simulate channel hydraulics and morphology of James Creek between rkm 7.29 and 24.02. Flow and sediment data, output from AnnAGNPS for the period January 1, 1967 through December 31, 2001, were imposed at the upstream boundary (rkm 24.02), at the mouths of tributaries, and at the downstream end of fields adjacent to the channel. The simulation was separated into three time periods, each delineated by the construction of low-water crossings (LWC). Table 15 lists the year of construction, river kilometer of the structure, and 2002 survey cross-section identification.

Table 15 Time and position of low-water crossing installation.

Year of construction	River kilometer (rkm)	2002 Survey cross-section
1967	12.31	26
1982	19.95	10
1982	14.80	21
1990	23.34	3
1999	17.48	15
1999	15.80	18
1999	9.12	32

Changes in Thalweg Profile

In the first 10 years, large amounts of sediment were eroded above and including the transition zone, between the measured and synthesized 1967 cross-sections, at the upper end of the 1967 clearing and snagging work (Figure 90). The simulated thalweg profile is in good agreement with the measured 2002 measured thalweg profile (Figure 91 and Figure 92). Up to three meters of incision in the upstream reach initiated mass-bank instabilities (Figure 93). Figure 90 and Figure 91 show the effects of the LWCs on the evolution of the thalweg. The LWCs act as grade control. Sediment is deposited upstream of the structures and eroded at their downstream side. Hence, channel slope is reduced while minimizing the amount of incision. CONCEPTS overpredicts the amount of sediment deposited upstream of the LWC at rkm 19.95, and the amount of sediment eroded downstream of the LWC at rkm 12.31. The downstream end of the modeled reach (rkm 7.29) is affected by processes occurring between this location and the Tennessee-Tombigbee Waterway; specifically, the continuous dredging of the Tennessee-Tombigbee. These processes are not included in the simulation. A comparison between measured and predicted thalweg elevations in this area is therefore indeterminate. Figure 92 compares the 2002 measured and predicted thalweg elevations ($r^2 = 0.99$). Deviations from the line of perfect agreement are most pronounced near the LWC's.

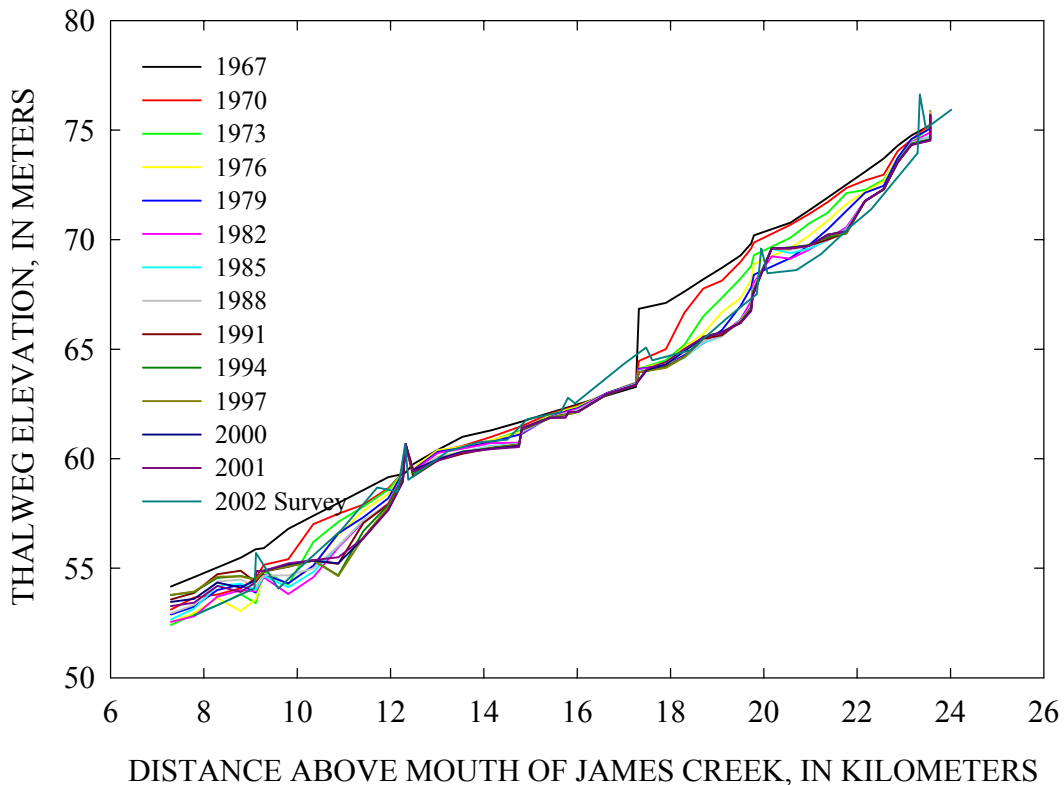


Figure 90 – Simulated thalweg elevations for rkm 7.29 to 24.02.

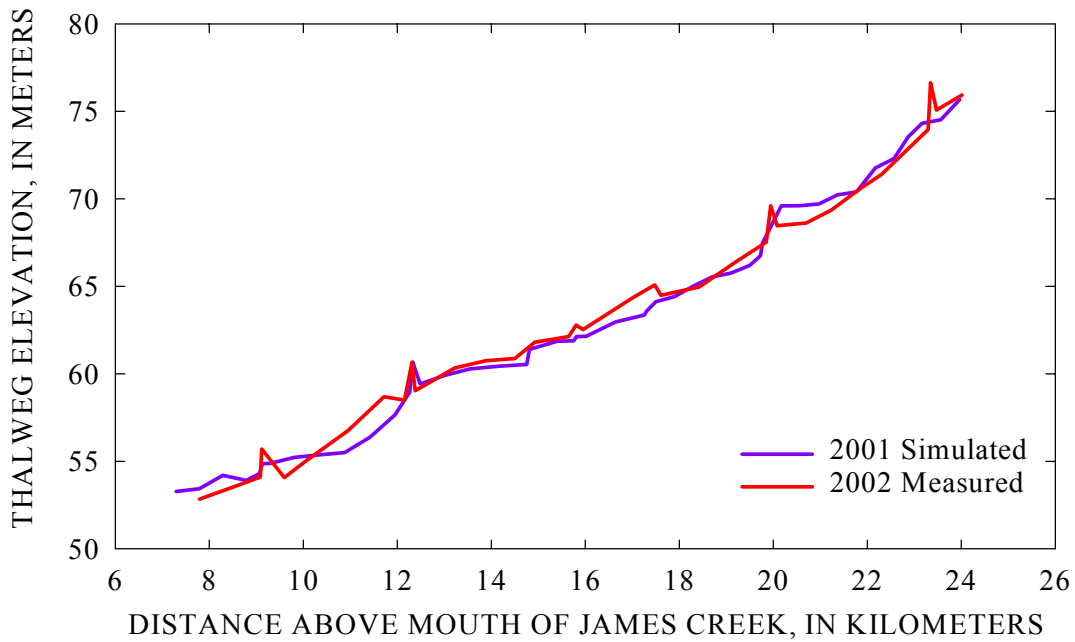


Figure 91 – Comparison of simulated and measured thalweg profile.

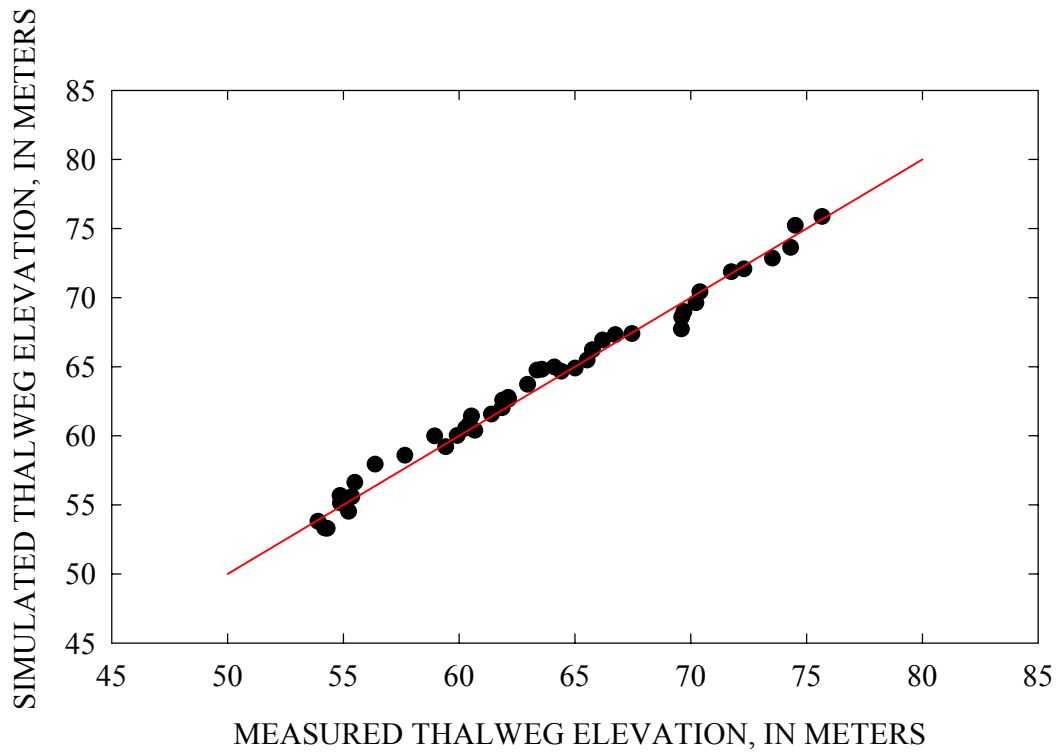


Figure 92 – Comparison of simulated and measured thalweg elevations at cross sections surveyed in 2002.

Changes in Cross-Sectional Geometry

Stable channels are, by definition, those channels where the bed and banks are in dynamic equilibrium and channel geometry does not change with time. James Creek exhibits typical characteristics of an unstable channel where changes in channel depth and top width are significant. Figure 93 shows the simulated temporal adjustment of the channel top bank width. At the upper end of the reach (between rkm 22 and 24), CONCEPTS underestimates the top bank width of the channel (Figure 94). This may be in large part due to the technique used to synthesize the upper cross-sections (rkm 17 to 24). The 2002 channel survey (Appendix A) shows that the cross-sections between rkm 17.6 and 24 are relatively narrow across the bottom half of the channel depth and widen rapidly across the top half of the channel depth. This possibly indicates failures induced by saturation of the top part of the streambank due to infiltrating rainfall. Predicted cross-sectional area, however, agrees well with that measured between rkm 22 and 24. The top width between rkm 17 and 22 is overpredicted (Figure 94). This is due to too much erosion at the toe of the bank. The applied critical shear stresses and erodibility coefficients were not calibrated against the observed widening, and were probably too small. Between rkm 12 and 17, CONCEPTS underestimates the top bank widths near the LWCs (Figure 94). Continued maintenance of the vehicle-access lane across the channel at the LWCs greatly increases local channel widths at those locations. Between rkm 9 and 12, CONCEPTS overestimates the top bank width (Figure 94). Figure 95 to Figure 100 compares measured and simulated geometries at the Corps cross-section locations. These figures again show that the simulated top width between rkm 9 and 12 is too large. This can be attributed to an overestimation of erosion of the channel bed and bank toe.

Because of the overpredicted channel top width and channel area, the resulting contribution of sediments scoured from the channel to total sediment load or yield at the channel outlet will be too large. Figure 90 and Figure 93, however, show that thalweg and top width adjustment mainly occurs between 1967 and 1980. Hence, the too large simulated channel contributions do not affect present sediment loadings.

Comparison of Measured and Simulated Recurrence Intervals at the Highway 25 Gaging Station, 1967-2001

A comparison of the capability of AnnAGNPS and CONCEPTS to estimate the recurrence interval was compared to the values determined from measured annual peak discharges at the Highway 25 gaging station (Figure 101) for the years 1967 to 2001. The recurrence interval determined using AnnAGNPS simulated annual peak discharges were based on using the annual peak discharges: from the corresponding event dates used with the measured peaks; determined for each year based on what the peak value actually was, irregardless of the date the event occurred; and, from climate generated for a 39 year period. The recurrence interval was determined by CONCEPTS from the annual peaks simulated based on whenever the peak occurred within each year. The results show the AnnAGNPS simulated values as lower than measured and CONCEPTS simulated values as higher than measured. Generated precipitation in lieu of measured precipitation used by AnnAGNPS for ungaged watersheds can be used to adequately determine the recurrence interval. This is critical in determining the $Q_{1.5}$ used in evaluating the reference conditions for ungaged watersheds.

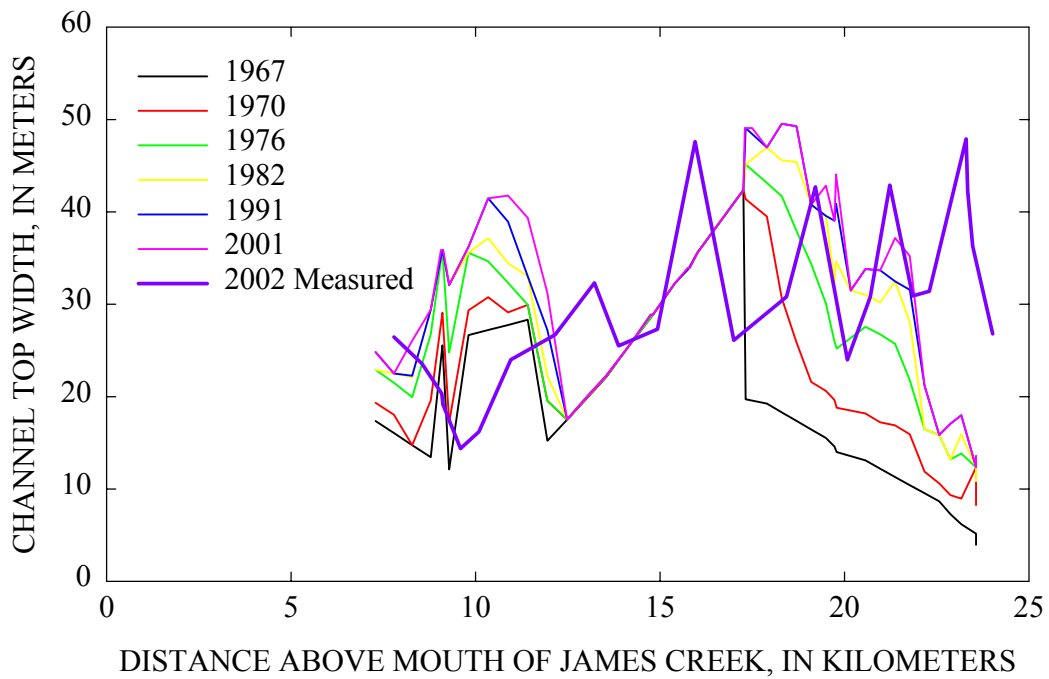


Figure 93 – Simulated channel top widths for rkm 7.29 to 24.02.

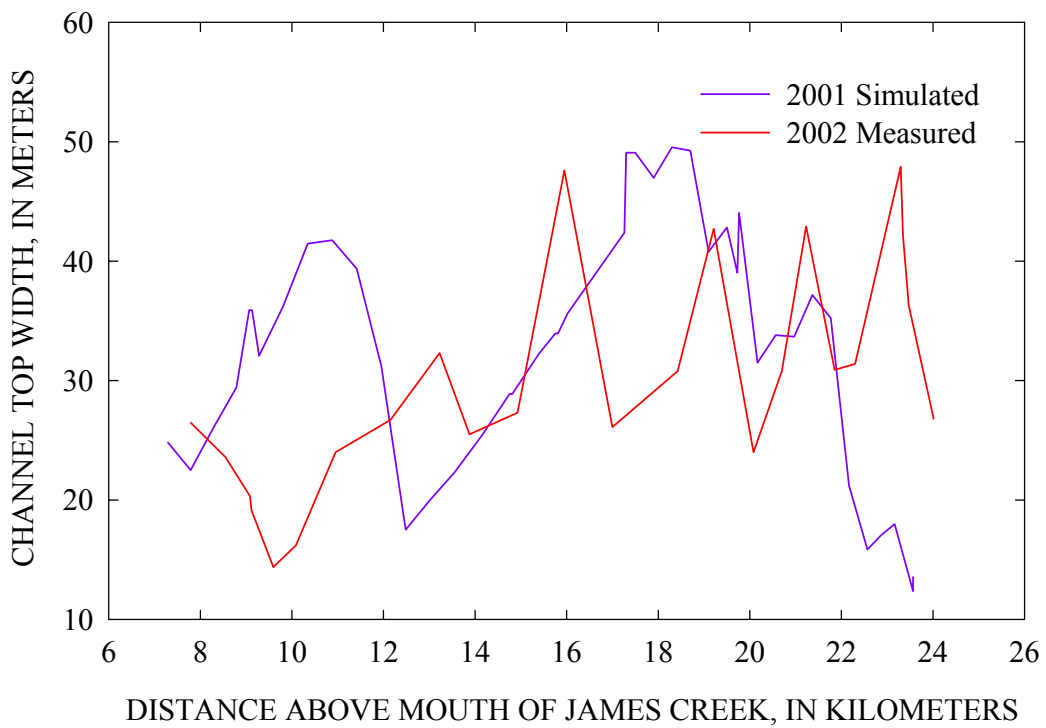


Figure 94 – Simulated top widths comparison to measured 2002 top widths.

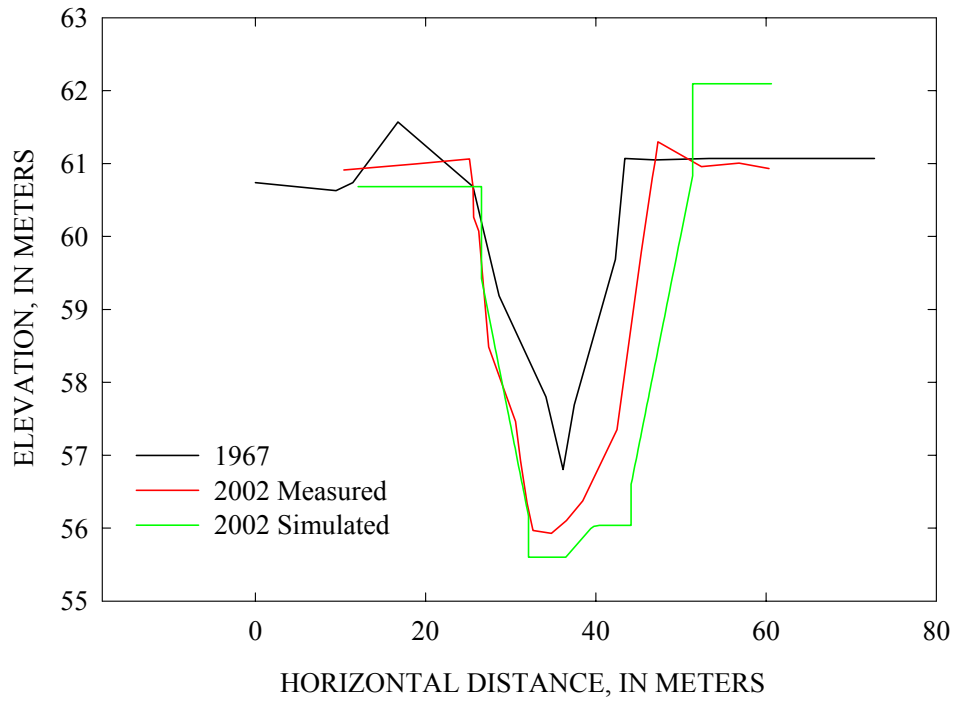


Figure 95 – Comparison of 1967 and 2002 measured and 2002 simulated cross-section 228+60.

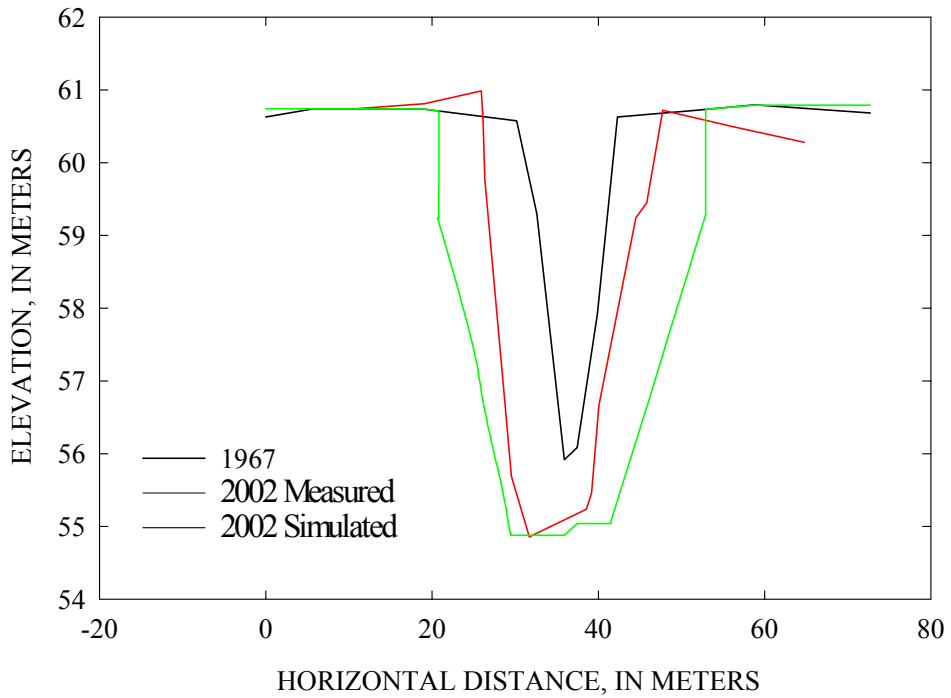


Figure 96 – Comparison of 1967 and 2002 measured with 2002 simulated cross-section 294+00.

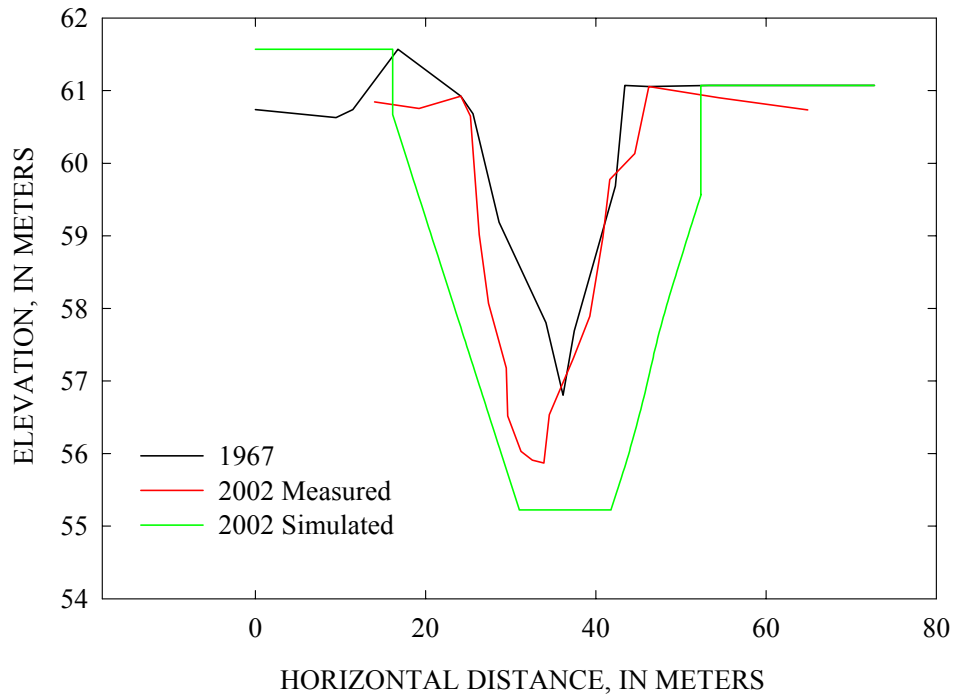


Figure 97 – Comparison of 1967 and 2002 measured with 2002 simulated cross-section 311+20.

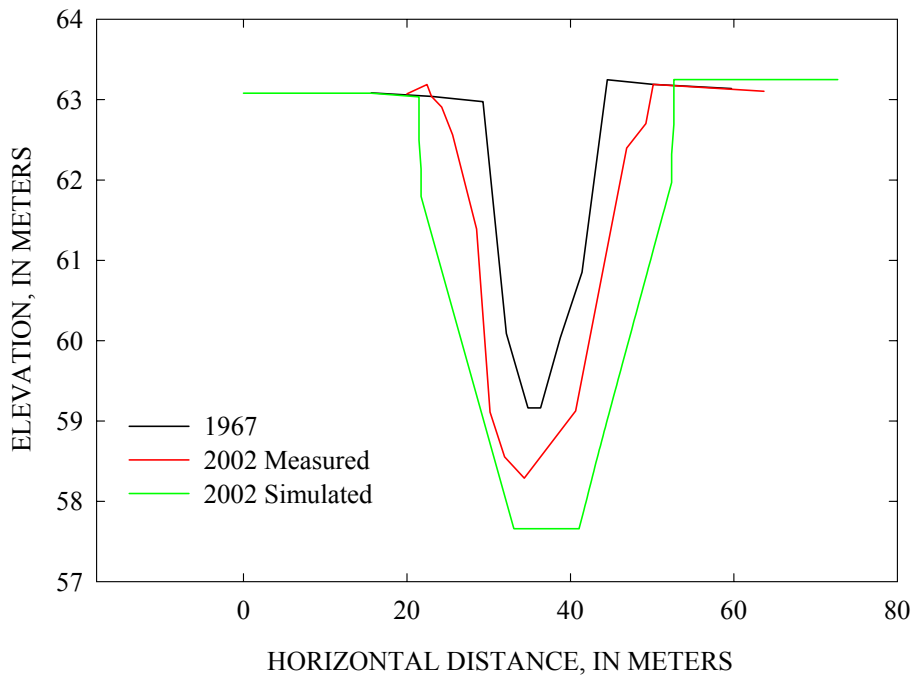


Figure 98 – Comparison of 1967 and 2002 measured with 2002 simulated cross-section 381+23.

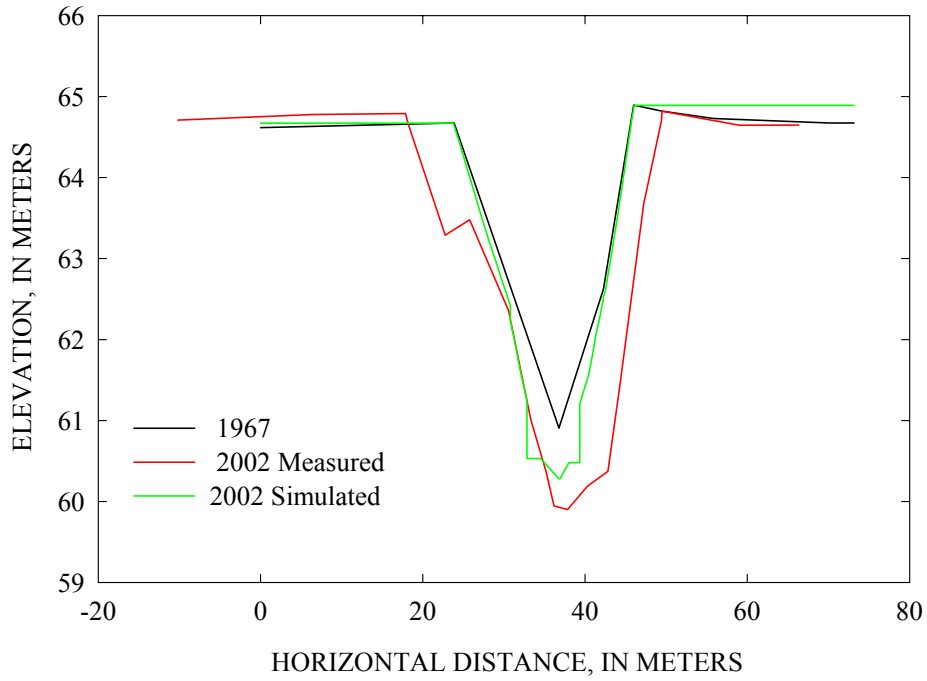


Figure 99 – Comparison of 1967 and 2002 measured with 2002 simulated cross-section 432+10.

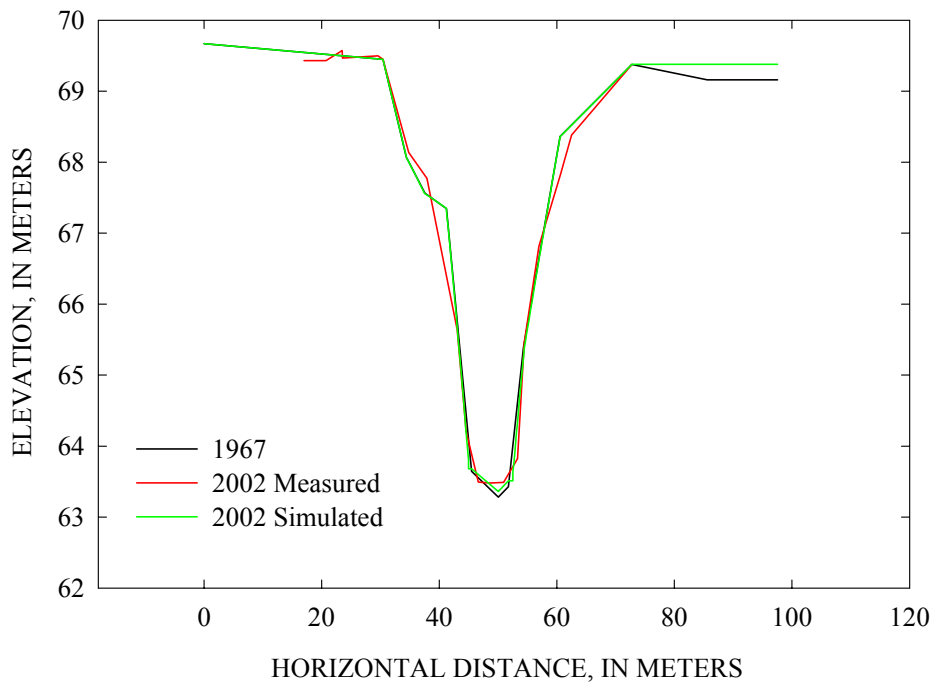


Figure 100 – Comparison of 1967 and 2002 measured with 2002 simulated cross-section 548+70.

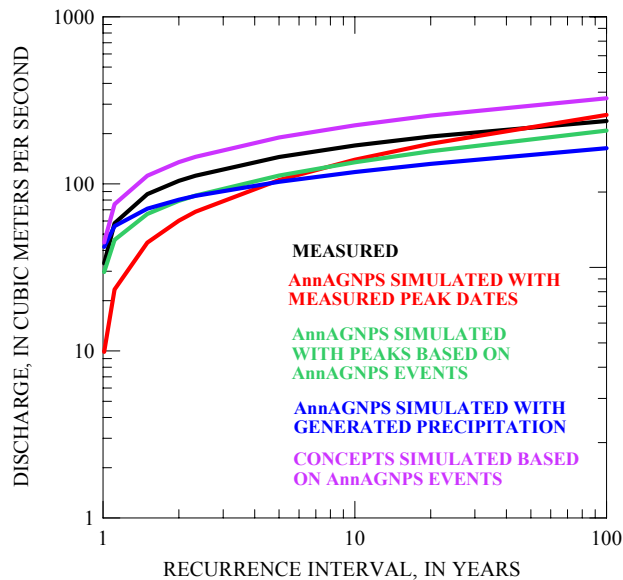


Figure 101 – The recurrence interval based on the annual peak discharge obtained from measurements at the Highway 25 bridge, the AnnAGNPS simulation using peak discharges that match the measured annual peak discharge event date, the AnnAGNPS simulation using the simulated annual peak discharge at whatever date it occurred, the AnnAGNPS simulated values using precipitation generated from GEM for 39 years, and the CONCEPTS simulated values using the simulated annual peak discharge at whatever date it occurred.

Channel Erosion 1967-2002: Measured Changes in Channel Geometry

Special surveys were conducted in 2002 to match as closely as possible the locations of cross-section surveys conducted by the Corps of Engineers in 1967 (Figure 1). In doing so, we created a means of comparing changes in channel geometry at individual cross sections. By integrating the changes in cross-sectional area over the length of the channel encompassed by the surveys, we obtain a volume of sediment eroded over the period between rkm 0.27 and 17.2. Figure 102 provides an example of how individual cross-sections were overlain and analyzed to determine the amount eroded over the 35-year period. The area of each section was initially plotted against river kilometer for each period (Figure 103a). The area between the plotted lines was then calculated to determine the total volume of material eroded from the channel boundary between 1967 and 2002 (Figure 103b).

Over the period 1967 to 2002, about 624,000 m³ of channel sediments were eroded from James Creek between river kilometers 0.27 and 17.2. This was converted to 1,136,000 tonnes (T) using the average saturated density of 1,820 kg/m³. Dividing by 35 years we obtain an average-annual load of eroded channel materials of 32,500 T/y over this reach. Dividing by the length of the reach gives unitized channel-erosion values of 1,910 T/y/km or 1.91 T/y/m of channel.

To be able to compare measured channel erosion with that simulated by CONCEPTS a shorter reach is used. Recall that CONCEPTS simulations do not include the lower sinuous section

below Darracott Road. The reach used for comparative purposes extends between river kilometers 7.29 and 17.3. Using the same techniques and conversion factors as previously we obtain the following erosion values for this approximate 10 km reach: 252,000 m³; 459,000 T; 13,100 T/y; 1,320 T/y/km; and 1.31 T/y/m.

To determine the relative contribution from the bed and banks, the 1967 and 2002 cross-sections were again overlain with 1967 bed surfaces extended down to meet the 2002 survey. Distinction was made between bed and banks by projecting the 1967 bed surface to either a survey point on the 2002 survey representing the bank toe, or normal to the 2002 bed surface (Figure 102). The area encompassed between the 1967 bed profile and the 2002 bed profile represents the amount eroded from the channel bed in m². This was converted to a percent by comparing the value calculated for the bed with the total amount eroded from the section. On average, about 12% of the materials eroded from the channel came from the channel bed, with 88% coming from the banks. (Table 16). These results emphasize the need for grade control in disturbed or modified channels to prevent excessive incision that leads to destabilizing of the channel banks.

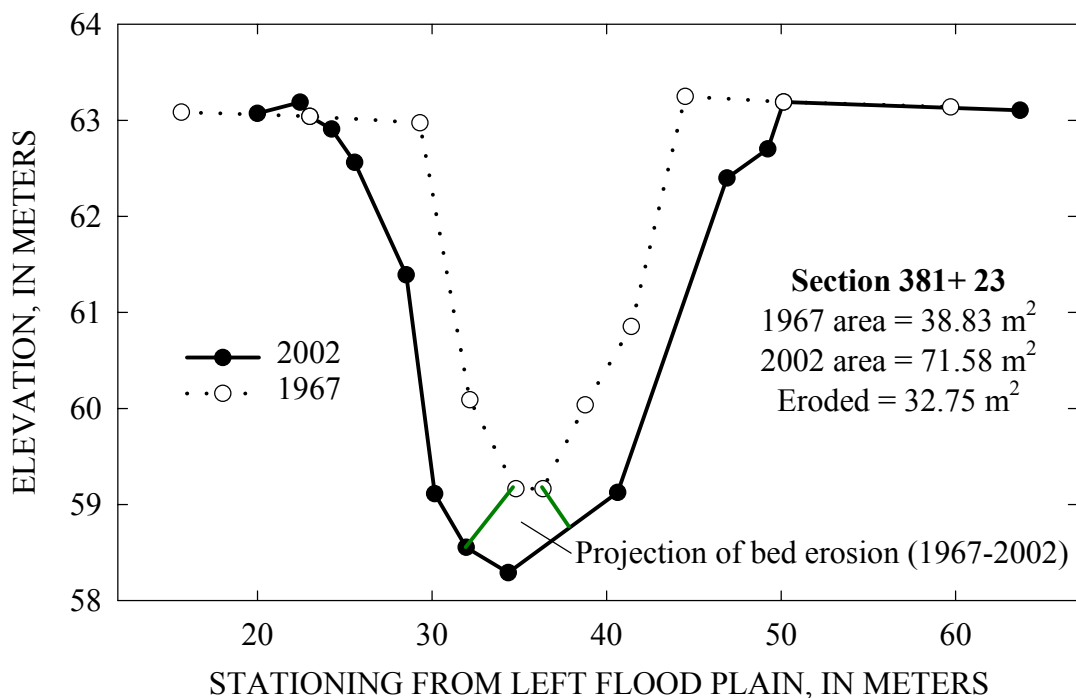


Figure 102 – Example from 1967 survey-match section 381 + 23 of calculating the amount of material eroded from the channel boundary over the period 1967 to 2002.

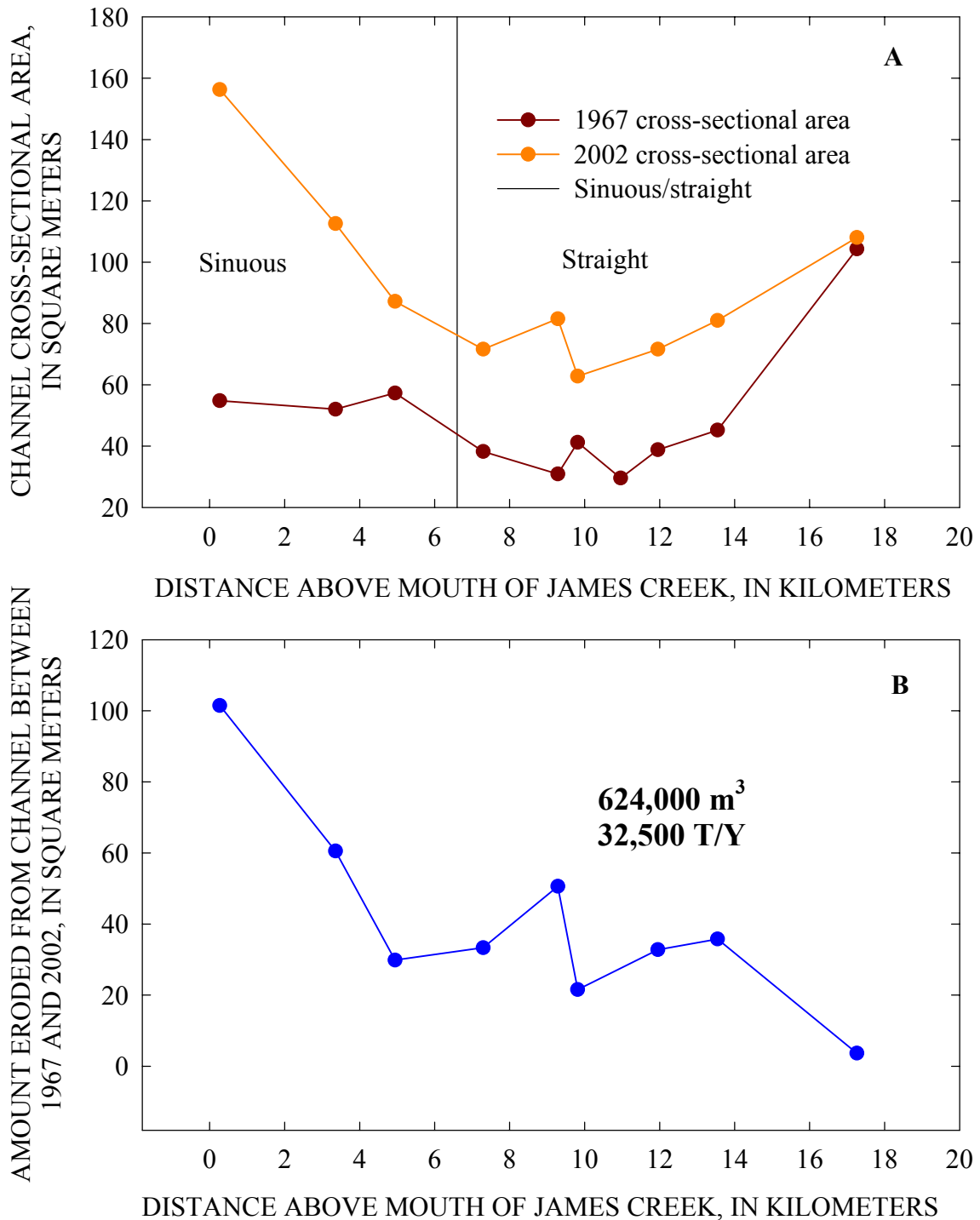


Figure 103 – Cross-sectional area of James Creek during 1967 and 2002 (A); and “Actual” sediment loading from the channel boundary over the period 1967 – 2002 based on changes in channel cross-sectional area (B). Note the greater magnitude of erosion in the downstream sinuous section.

Table 16 – Contribution of sediments eroded from the channel boundary of James Creek between 1967 and 2002 between rkm 0.27 and rkm 17.2.

Cross section	Total erosion (m²)	Bed erosion (m²)	Bank contribution (%)	Bed contribution (%)
22+97	102	10.5	89.7	10.3
111+08	60.5	8.4	86.1	13.9
160+40	27.8	4.1	85.3	14.7
228+60	33.4	5.6	83.2	16.8
294+00	50.6	4.8	90.4	9.6
311+20	21.6	2.9	86.6	13.4
381+23	32.8	2.3	93.0	7.0
432+10	35.8	4.0	88.8	11.2
548+70	3.5	0.0	-	-
Average			88	12

Simulated Sediment Loads

“Actual” sediment loads for James Creek were simulated using the combined results of AnnAGNPS and CONCEPTS as well as by using direct comparisons between measured cross sections in 1967 and 2002. Results from these simulations represent best estimates because they combine the best attributes of each of the models; AnnAGNPS for uplands and CONCEPTS for channels. Recall that AnnAGNPS produced results throughout the entire watershed to the confluence of James Creek with the Tennessee-Tombigbee waterway but that CONCEPTS simulations extend from rkm 7.29 (Darracott Road) to 24.02. All of the techniques, however, produced results for the Darracott Road bridge.

Total sediment loads passing Darracott Road over the 35-year period are about 8,130,000 tonnes, representing an average annual load of 232,000 T/y. Loads generally have decreased over the period as channels adjusted with time (Figure 104) with increase in the 1980’s probably reflecting both the high-flow years of 1982-1984 and the repeated dredging of the mouth of James Creek. The average annual yield represented by this load is about 2,360 T/y/km² (Table 17). On average, almost than 89% of this material emanated from main stem and tributary channels in the watershed while about 11% was derived from sheet and rill erosion. This breakdown may be somewhat misleading in that massive channel erosion in upstream reaches occurred in the years shortly after the completion of the clearing and snagging operations and, there are some years where the contribution from sheet and rill erosion exceeds that coming from the channels (Figure 104). A more reasonable breakdown for the James Creek watershed is obtained by taking the last 10 years of simulated loads which show that about 70% of the sediment is derived from channels and 30% from sheet and rill erosion. Similarly, average annual loads over the past 10 years at Darracott Road probably provide a better picture of “actual current” conditions and are about **71,700 T/y**, representing an annual yield of **727 T/y/km²**.

Table 17 – Sediment loads and yields at river kilometer 7.92 (Darracott Road) as simulated by AnnAGNPS combined with CONCEPTS.

AnnAGNPS with CONCEPTS			
	Channel	Sheet and Rill	Total
Total Load (T)	7220388	910212	8130600
Average Load (T/y)	206297	26006	232303
Average Yield (T/y/km²)	2093	264	2357
Contribution (%)	88.8	11.2	-

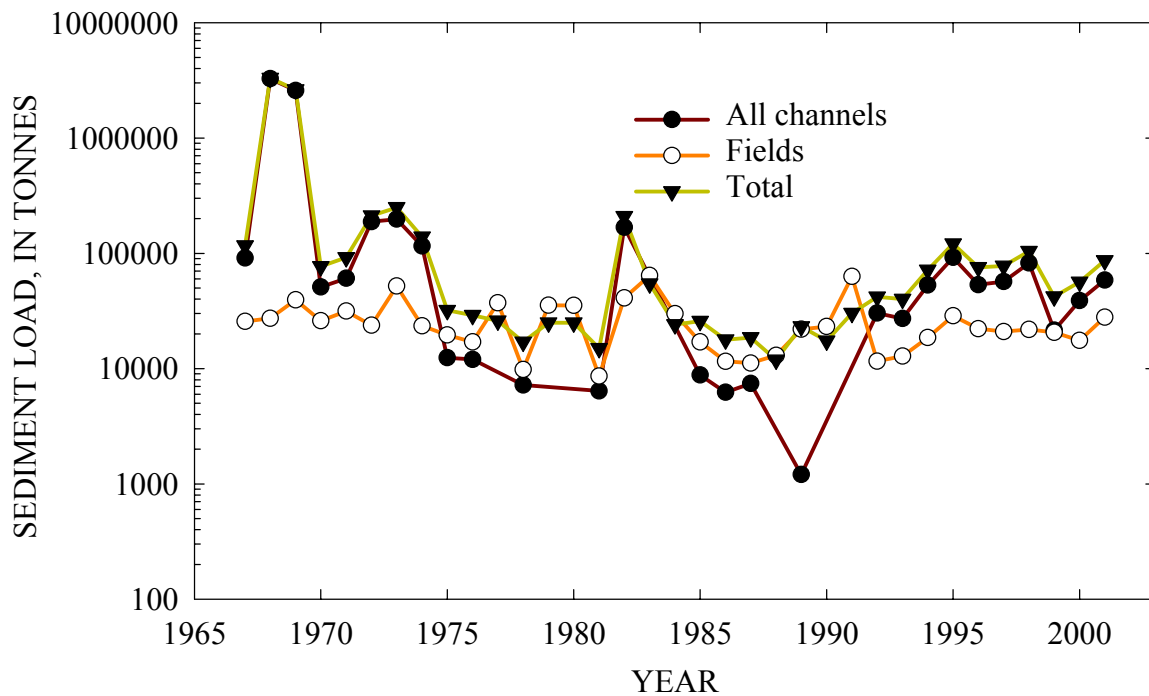


Figure 104 – Annual sediment loads and relative contributions from channels and fields at Darracott Road as simulated by AnnAGNPS with CONCEPTS.

Simulated Sediment-Transport Rates and Yields at the Highway 25 Bridge

CONCEPTS provides detailed concentration and load estimates at 10-minute time intervals that can be associated with the discharge values to produce sediment-transport relations for each of the modeled cross sections. Results are output for each time step by size class. To provide a consistent comparison between “actual” loads and “reference” loads we subtract the gravel portion from the total transport rate to obtain an estimate of suspended-sediment transport. Sediment-transport results are provided for the highway 25 bridge because this is the location where simulated results are validated with measured flow and channel geometry data and, where

reference sediment-transport conditions are established. A transport curve was developed for the highway 25 bridge encompassing the entire 35-year period of record, resulting in ($r^2 = 0.60$):

$$L = 105 Q^{1.237} \quad (6)$$

where L = suspended-sediment load (T), and Q = water discharge in m^3/s . Using the measured $Q_{1.5}$ of $86.8 m^3/s$ (Figure 71) at the site gives an average load at the effective discharge of about 26,400 T. Converting this to yield by dividing by the drainage area of $74 km^2$ gives an average suspended-sediment yield of $355 T/d/km^2$ at the $Q_{1.5}$. Recalling that the reference yield for James Creek is $2.22 T/d/km^2$ at the $Q_{1.5}$ suggests that average yields over the past 35 years are more than two orders of magnitude greater than the reference condition. However, because (1) rapid channel and tributary erosion occurred during the period of channel adjustment following the clearing and snagging operations (see 1968-1969 in Figure 104), and (2) channel responses are generally the greatest following a disturbance and rapidly decrease non-linearly, a better estimate of current conditions was obtained by analyzing the transport data on an annual basis.

CONCEPTS sediment-transport output for the highway 25 bridge was sorted by year and individual sediment-transport relations were derived for each year of simulation. Regression techniques were used to establish a transport relation for each year (1967-2001) and suspended-sediment loads and yields were calculated by substituting the $Q_{1.5}$ ($86.8 m^3/s$) into each equation (Table 18). An example suspended-sediment transport curve is shown in Figure 105 for the year 1977 with its associated 95% prediction limits. Similar transport-relations were established using three-year blocks of data to minimize annual variability.

Table 18 – Suspended-sediment transport relations derived from CONCEPTS output for each year of simulation showing calculated load and yield at the measured $Q_{1.5}$ of $86.8 m^3/s$. Note: Coefficient and exponents correspond to the general equation $L = a Q^b$, where a and b are the coefficient and exponent, respectively.

Year	Coefficient	Exponent	Load (T/d)	Yield (T/d/km ²)
1967	189.6	1.440	117000	1580
1968	109.2	1.910	551000	7440
1969	76.9	1.724	169000	2280
1970	76.8	1.483	57600	778
1971	104.3	1.473	74700	1010
1972	79.2	1.534	74500	1010
1973	82.2	1.487	62700	847
1974	83.0	1.457	55400	749
1975	107.6	1.348	44200	597
1976	108.0	1.368	48300	653

Table 18 (continued) – Suspended-sediment transport relations derived from CONCEPTS output for each year of simulation showing calculated load and yield at the measured $Q_{1.5}$ of $86.8 \text{ m}^3/\text{s}$. Note: Coefficient and exponents correspond to the general equation $L = a Q^b$, where a and b are the coefficient and exponent, respectively.

Year	Coefficient	Exponent	Load (T/d)	Yield (T/d/km²)
1977	108.5	1.345	43900	593
1978	110.9	1.335	42900	579
1979	101.7	1.375	47100	636
1980	80.9	1.416	44900	606
1981	84.1	1.382	40200	544
1982	50.9	1.433	30500	412
1983	49.5	1.406	26300	355
1984	67.0	1.283	20500	278
1985	99.8	1.162	17800	241
1986	125.8	1.042	13100	178
1987	151.0	0.938	9950	134
1988	151.7	0.940	10100	136
1989	161.8	0.926	10100	136
1990	188.6	0.880	9570	129
1991	189.5	0.941	12600	170
1992	173.4	0.942	11600	157
1993	123.8	1.036	12600	171
1994	119.6	1.111	17100	231
1995	129.1	1.140	21000	283
1996	127.1	1.042	13300	180
1997	99.7	1.113	14300	194
1998	86.1	1.176	16400	222
1999	120.3	0.680	2500	34
2000	102.5	0.770	3190	43
2001	116.2	0.724	2950	40

Suspended-sediment yields at the $Q_{1.5}$ calculated for three-year blocks (ie. 1967-1969, 1970-1972) are shown in Figure 106 along with the yield that was derived using all data from the 35-year period (blue line). Given that the majority of sediment eroded from the James Creek watershed is derived from channel sources, it is not surprising that sediment yields at the effective discharge decrease non-linearly with time. In fact, it appears that suspended-sediment yields are approaching “reference” conditions (Figure 106a). However, plotting the data in log-

space (Figure 106b) provides a clearer comparison of “actual-current” and “reference” suspended-sediment yields with a 2000-2001 value of 41 T/d/km². In looking at Figure 106b it can be seen that the last data point (2001-2002) represents a minimum value for the 35-year period. Moreover, the last three data points representing the period 1994 to 2001 appear to show a decreasing trend. To provide more confidence in the “actual-current” suspended-sediment yield and thereby the required percent reduction to meet the “reference” condition, the data set was broken out further by year as described above.

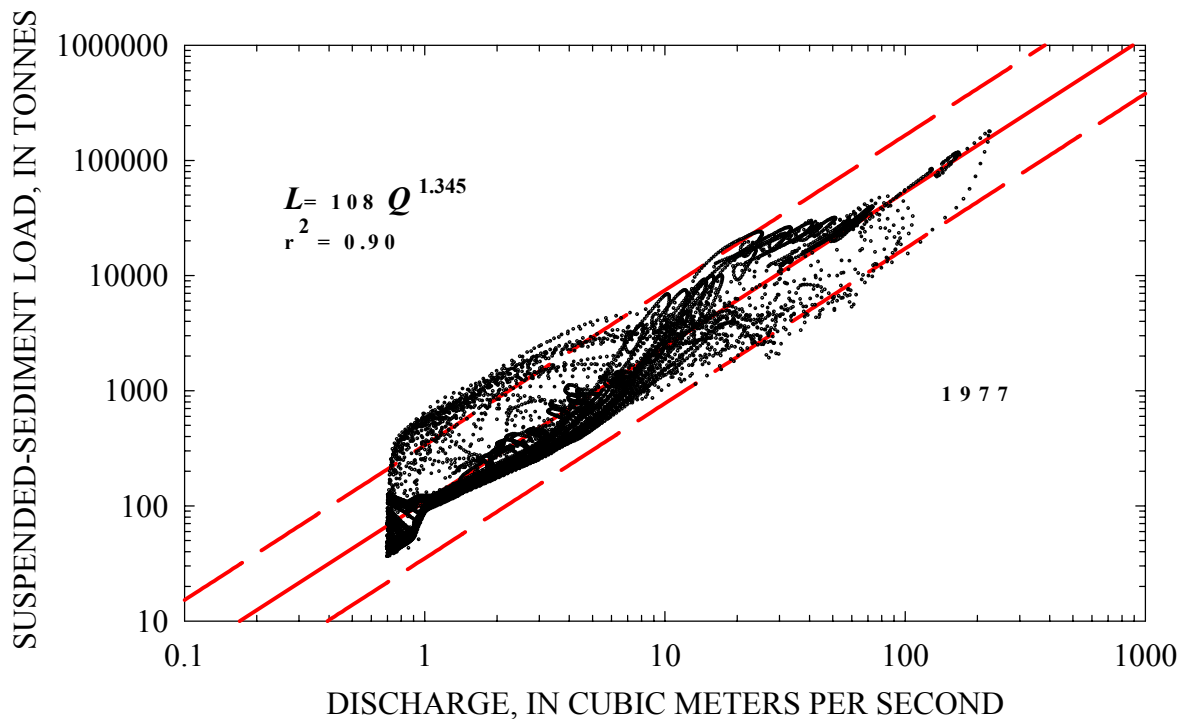


Figure 105 – Suspended-sediment transport relation for 1977 at the Highway 25 bridge derived from CONCEPTS modeling results with corresponding regression equation. Note: L = load (T), Q = water discharge (m³/s).

Annual suspended-sediment yields at the $Q_{1.5}$ are shown in Figure 107 for the highway 25 bridge. Again, yields are shown to approach the “reference” (Figure 107a) but are plotted in log-space (Figure 107b) for greater detail. The minimum value shown by the last data point in Figure 107b representing a trend of decreasing yields is in fact, representative of relatively consistent sediment transport rates over the last three years (1999 – 2001) (Figure 107b). These lower rates of sediment transport beginning in 1999 at the highway 25 bridge can be attributed to the construction of several low-water crossings that year whose effects are reflected in the CONCEPTS simulations. Thus, we can state with greater certainty that the “actual current” suspended sediment yield at the $Q_{1.5}$ is in this range. Taking the average for the most-recent three-year period gives an “actual current” yield of **38.9 T/d/km²** at the $Q_{1.5}$ (Figure 107b).

The suspended-sediment yields shown in Figure 107, and in Table 18 are based on measured peak-flow calculations of the $Q_{1.5}$. In the absence of measured data on James Creek an alternative means of calculating the $Q_{1.5}$ would have been required. The modeling system used in this project can provide peak-flow estimates in a number of ways. AnnAGNPS can be used to derive

the peak-flow series based on actual-precipitation data, generated precipitation data and, in combination with CONCEPTS (Figure 101). Extracting the $Q_{1.5}$ from each of these three methods provides a range of estimates bounding the value obtained from measured data, which is $86.8 \text{ m}^3/\text{s}$. These are 66.2 , 71.1 , and $112 \text{ m}^3/\text{s}$ for AnnAGNPS calculations using actual precipitation, generated precipitation, and AnnAGNPS plus CONCEPTS, respectively.

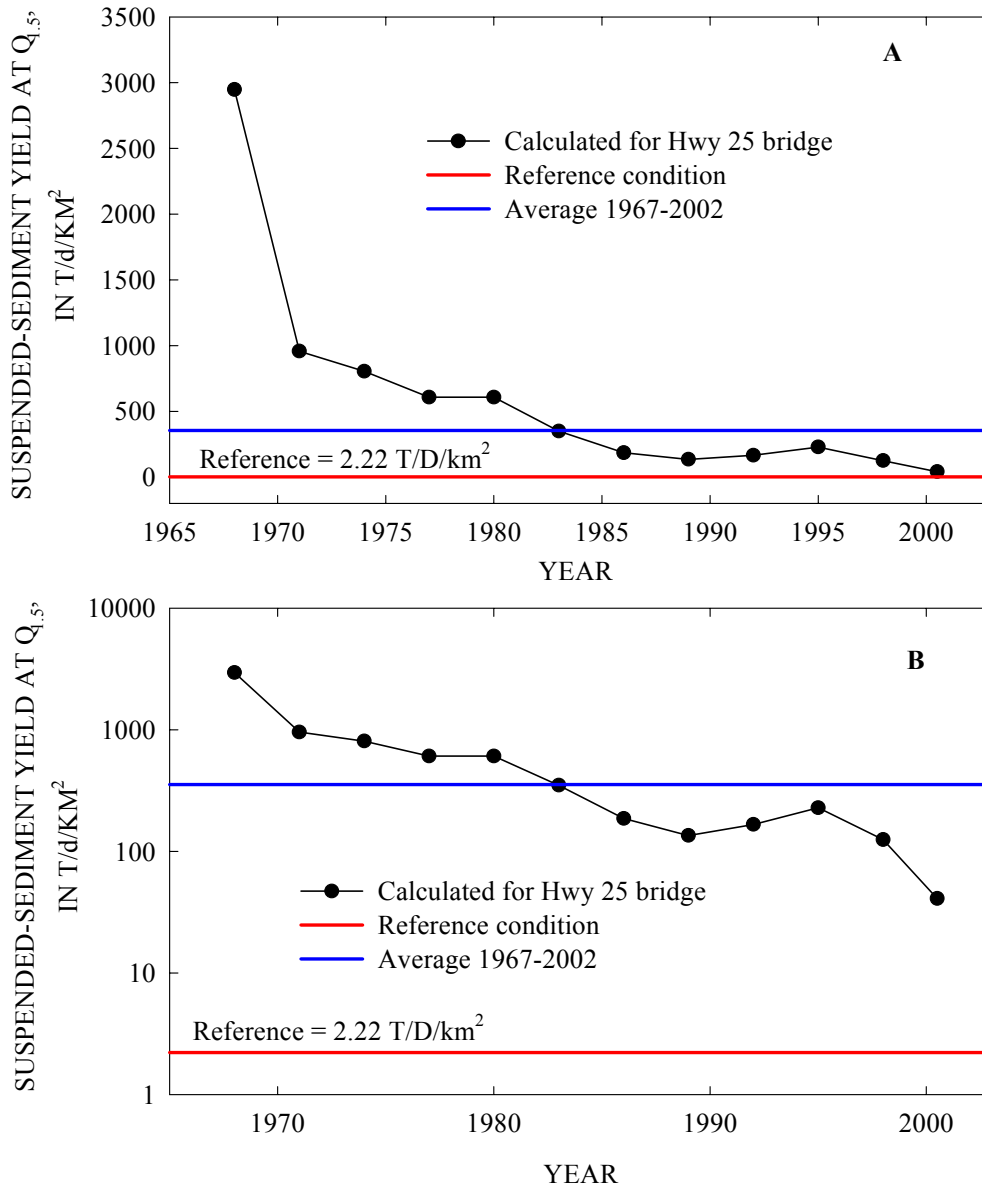


Figure 106 – Calculated suspended-sediment yields at the $Q_{1.5}$ based on three-year blocks of CONCEPTS output showing non-linear decrease with time as channels and tributaries adjusted to the 1967 channel clearing and snagging operations. Note: Data are plotted arithmetically (A) to show non-linear trend of approaching “reference” and in log-space (B) to provide a more detailed view of difference between current conditions and “reference” conditions.

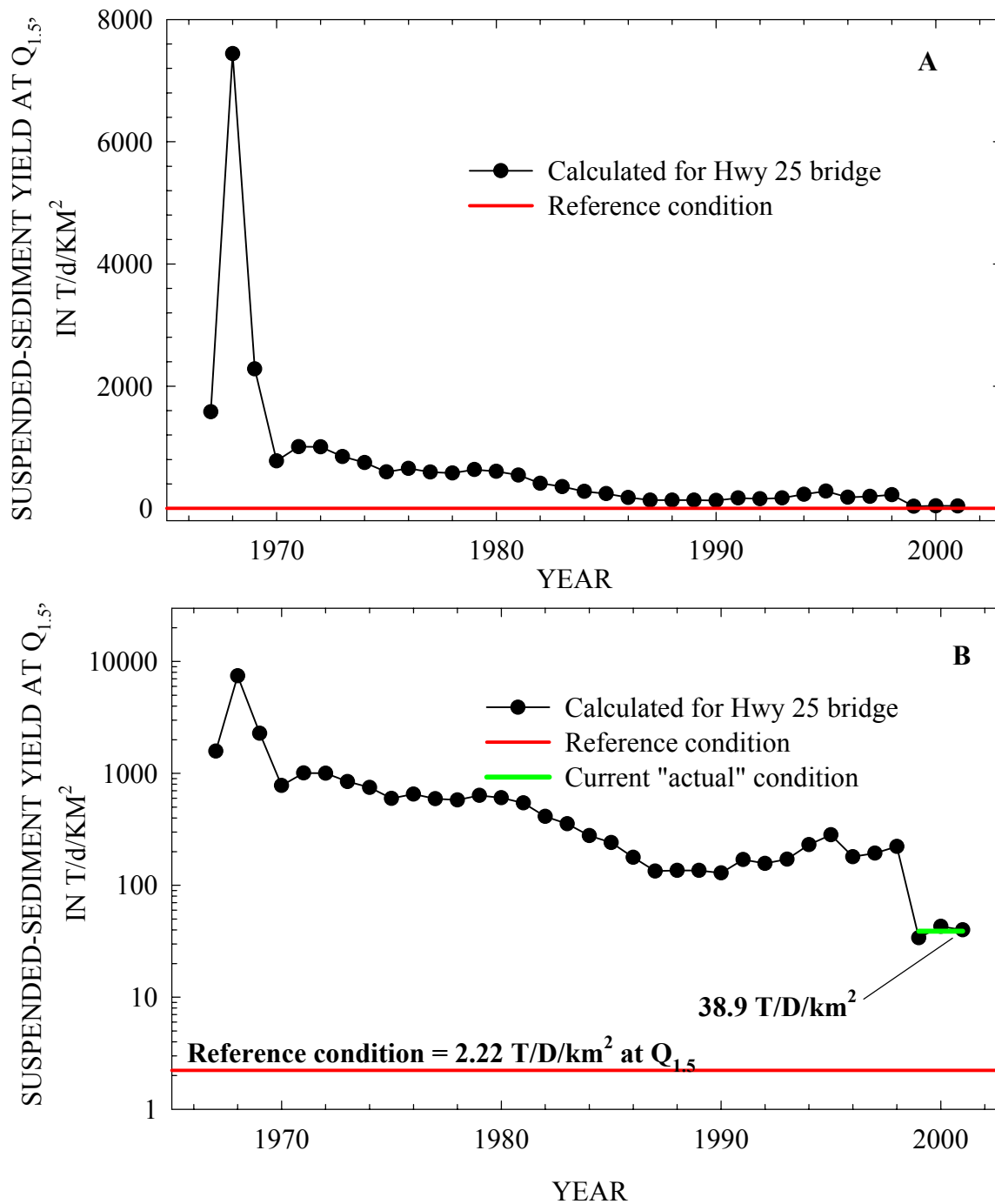


Figure 107 – Calculated annual suspended-sediment yields at the $Q_{1.5}$ based on CONCEPTS output showing non-linear decrease with time as channels and tributaries adjusted to the 1967 channel clearing and snagging operations and lowered yields following construction of low-water crossings in 1999. Note: Data are plotted arithmetically (A) and in semi-log space (B) to show “actual current” conditions.

Substituting these values into the annual regression equations shown in Table 18 provides a range of estimates of “actual” suspended-sediment yield at the $Q_{1.5}$ (Figure 108). Estimates of the “current actual” suspended-sediment yield for the period 1999 – 2001 range from 34 T/d/km² to 47 T/d/km² at the $Q_{1.5}$, with AnnAGNPS representing the lower bound and, the higher bound when in combination with CONCEPTS main-channel routing. This represents a variation of only 33% around the suspended-sediment yield obtained (38.9 T/d/km²) using the $Q_{1.5}$ obtained from the measured peak-flow series and indicates that reasonable results can be obtained without measured peak-flow data.

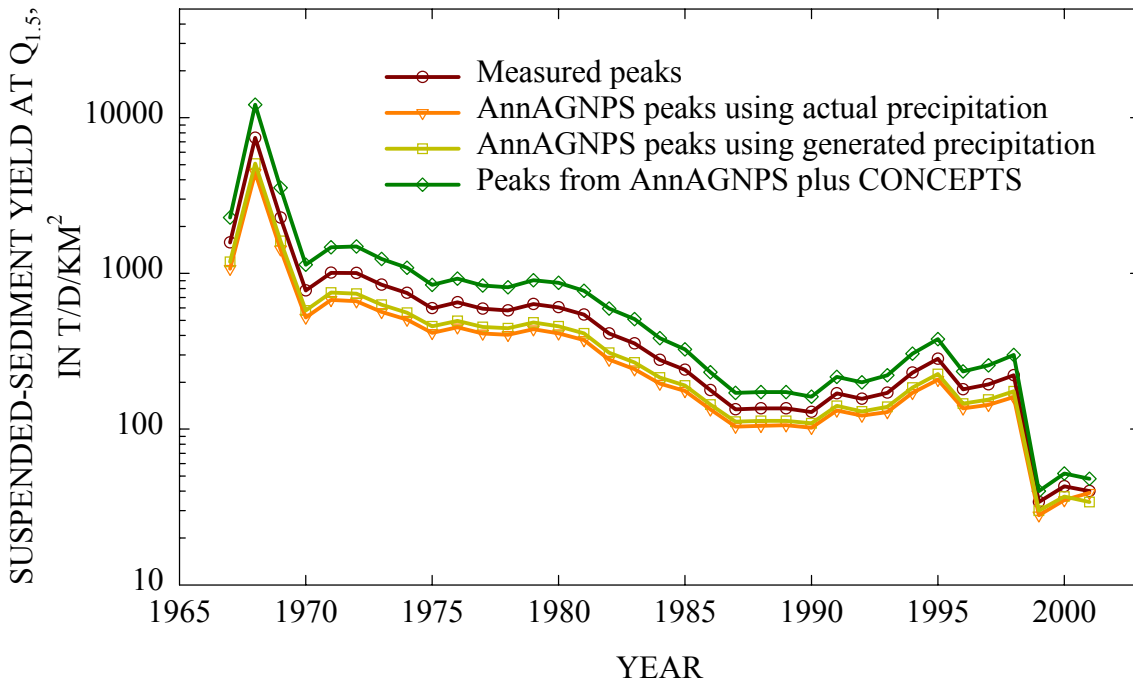


Figure 108 – Differences in suspended-sediment yields for the Highway 25 bridge at the $Q_{1.5}$ using annual peak-flow series derived by four methods. Note that the yields based on simulated peak-flow series bound those based on measured data.

Simulated Sediment Loads at the Watershed Outlet

In the absence of CONCEPTS simulations in the sinuous reach of James Creek, sediment loads at the watershed outlet cannot be calculated on an annual basis but only as a total over the 35-year period. The resulting values are obtained by summing (1) the loads provided by AnnAGNPS with CONCEPTS at rkm 7.92 (Darracott Road), (2) the measured changes in channel geometry in the reach between 1967 and 2002, and (3) the contributions from tributaries, sheet and rill erosion provided by AnnAGNPS. Total sediment loads at the watershed outlet are summarized in Table 19. The average annual load is slightly greater than 253,000 T/y, representing a total-sediment yield at the mouth of James Creek of 2,260 T/y/km². Contributions from the various erosion sources, integrated over the entire watershed show about the same proportions: 89% from channels and 11% from uplands. This occurs in spite of the fact that considerable channel erosion has occurred along James Creek in the sinuous section due to

repeated dredging of its mouth. Although, annual data are not available, we assume that the relative contributions over the past 10 years are similar to those calculated at Darracott Road: 70% channels; 30% uplands.

Table 19 – Total sediment load at the outlet of the James Creek watershed for the period 1967 – 2002.

Reach	Total Sediment Load		
	Channel (T)	Sheet and Rill (T)	Total (T)
Above rkm 7.92	7220388	910212	8130600
Below rkm 7.92	677000	53340	730340
Total Load (T)	7897388	963552	8860940
Average Load (T/y)	225640	27530	253170
Average Yield (T/y/km²)	2015	246	2260
Contribution (%)	89	11	-

SUMMARY OF RESULTS

The results presented in this report have focused on establishing numerical values for “actual” and “reference” sediment-transport rates for the James Creek watershed in the absence of historical sediment data. This work was done with the express purpose of supplying the Mississippi Department of Environmental Quality with scientifically defensible results for the development of water-quality targets for sediment. Using field and numerical-simulation techniques in the James Creek watershed, and historical flow and sediment-transport data from similar watersheds in the same ecoregion (Southeastern Plains), we have produced reliable estimates of sediment-transport rates over the period 1967 – 2002.

Sediment Loads Under “Reference” Conditions

“Reference” sediment-transport conditions for the James Creek watershed were developed from historical-flow and sediment-transport data from streams in the Southeastern Plains ecoregion. Suspended-sediment transport ratings were developed for all sites with available data and the $Q_{1.5}$ for each site was used as the effective discharge, representing long-term sediment-transport conditions. Resulting sediment loads at the $Q_{1.5}$ were normalized by drainage area to express the “reference” sediment-transport parameter in terms of $T/d/km^2$ at the $Q_{1.5}$. Data from the Southeastern Plains are dominated by streams with sand beds. The median yield for all sites is $0.52 T/d/km^2$, the median concentration is $62.7 mg/l$, with the central 50% of these distributions varying by about an order of magnitude.

General “reference” conditions for the ecoregion are derived from stable streams as determined by stage of channel evolution and have a median yield of **$0.31 T/d/km^2$** and a concentration of **$47.9 mg/l$** . To refine these estimates, particularly in light of the fact that James Creek is dominated by cohesive streambeds, “reference” conditions are defined by dominant bed-material type. In doing so we find that stable channels composed of fine-grained bed materials produce about an order of magnitude more sediment per unit area than sand and gravel-bed streams: **3.23 , 0.42 , and $0.27 T/d/km^2$** , respectively. The “reference” yield for James Creek is calculated by multiplying the reference value for each bed-material type by the respective proportion of area represented by given stream lengths. The resulting value for James Creek from its mouth to rkm 24.02 is **$2.22 T/d/km^2$ ($160 mg/l$)**.

Amounts and Sources of Eroded Sediment Under “Actual” Conditions

“Actual” sediment-transport conditions for the James Creek watershed were developed from a combination of techniques including direct comparison of measured cross-sections between 1967 and 2002, numerical simulation using AnnAGNPS, and numerical simulation of AnnAGNPS with CONCEPTS. Sediment erosion in the James Creek watershed comes from a variety of sources including sheet and rills, gullies, and channel bed and banks (main stem and tributaries). Over the 35-year period 1967 – 2002, 8.86 million tonnes of sediment have been discharged from the James Creek watershed. This represents an average annual sediment load of about **$253,000 T/y$ ($2,260 T/y/km^2$)**. However, this value is somewhat misleading for “actual current” conditions because the greatest rates of sediment transport occurred in the late 1960’s following the channel clearing and snagging operations. A more reliable estimate of “actual

current” loads is based on the last 10 years of data from Darracott Road, having an average annual load of **71,700 T/y**, representing an annual yield of **727 T/y/km²**. Given that the drainage area at Darracott Road is 12% less than the area at the mouth of James Creek, we can adjust these loadings over the past 10 years to provide “actual current” loads at the mouth over this period: **80,300 T/y**.

To compare “actual” sediment-transport conditions to those calculated as “reference” the data must be expressed in similar terms, specifically as T/d/km² at the Q_{1.5}. Using load data obtained from AnnAGNPS with CONCEPTS and the Q_{1.5} from measured data at the highway 25 bridge (discontinued USGS gage) we obtain an average “actual” yield for the 35-year period of **355 T/d/km²**, suggesting that current loads are two orders of magnitude above the calculated reference. However, more detailed (annual) analysis of sediment-transport at the Q_{1.5} disclosed that rates have been generally decreasing with time (since 1968) and that the average yield over the last three years has been consistently lower at about **39 T/d/km²**. This value represents the “actual current” suspended-sediment yield at the effective discharge and should be used to develop strategies for best management practices in terms of percent reductions.

A summary of “reference” and “actual” suspended-sediment yields at the Q_{1.5} is provided in Table 20. The general reference is based on all stable sites in the Southeastern Plains Ecoregion. The refined reference represents stable sites with silt/clay beds in the ecoregion, while the weighted reference is particular to the bed-material conditions along James Creek. In addition, the central 50% of the reference-condition distribution is shown to be within an order of magnitude or less. Note that the general “reference” is an order of magnitude lower than both the refined and weighted reference values. This is due to the fact that the majority of streams in the Southeastern Plains have non-cohesive beds.

Table 20 – Summary table of “reference” and “actual” suspended-sediment yield showing central 50% of the data distribution and “actual” yields at the Q_{1.5}. Note: Q1 = first quartile; Q3 = third quartile; difference between Q1 and Q3 is the central 50% of the distribution.

"Reference" Yield (T/d/km²) at Q_{1.5}									
	General			Refined (silt/clay beds)			Refined-weighted		
	Q1	Median	Q3	Q1	Median	Q3	Q1	Median	Q3
Hwy 25 Bridge	0.17	0.31	1.03	2.21	3.23	4.55	1.5	2.22	3.8
"Actual" Yield (T/d/km²) at Q_{1.5}									
	35-Year Average			1992 - 2001			1999-2001		
Hwy 25 Bridge		675			155		38.9		

“Reference” yields are used to derive “reference” loads at the Highway 25 bridge, Darracott Road, and the watershed outlet and these are compared with “actual” loads at the Highway 25 bridge (**Table 21**). It is important to note that whether we compare suspended-sediment yields or loads, “actual” values are about an order of magnitude greater than the “reference” values.

Table 21 – Summary table of “reference” and “actual” suspended-sediment load showing central 50% of the data distribution and “actual” loads at the Q_{1.5}. Note: Q1 = first quartile; Q3 = third quartile; difference between Q1 and Q3 is the central 50% of the distribution.

"Reference" Load (T/d) at Q_{1.5}									
Location	General			Refined (silt/clay beds)			Refined-weighted		
	Q1	Median	Q3	Q1	Median	Q3	Q1	Median	Q3
Hwy 25 Bridge	12.6	22.9	76.2	164	239	337	111	164	283
Darracott Road	16.7	30.5	101	217	318	447	148	218	377
Watershed Outlet	19	34.7	115	248	362	510	168	249	429
"Actual" Load (T/d) at Q_{1.5}									
	35-Year Average			1992 - 2001			1999-2001		
Hwy 25 Bridge		50,000			11,500			2,880	

The dominant source of sediment in the James Creek watershed is channels. Over the 35-year period, about 89% of the eroded sediment leaving the system comes from streambeds and banks with the balance coming from upland sources. Granted that this value is somewhat inflated because of the massive channel erosion during the period 1967 – 1969 following channel clearing and snagging but even with channel-adjustment processes attenuating somewhat into the 1990’s, channel contributions still represent 70% of the eroded materials. Of the sediment eroded from the channel boundary, about 88% of this material comes from the channel banks, meaning that between 62 and 78% of all eroded materials in the watershed come from unstable streambanks. These results have important implications for managing similar streams in the ecoregion that have undergone the same types of channel maintenance over the past 100 years. Similarly, these results provide evidence as to where restoration efforts and best management practices will have the greatest effect.

CONCLUSIONS

James Creek, Monroe County, Mississippi is a typical watershed for the region having been dredged and straightened near the turn of the 20th century. Located in the Southeastern Plains Ecoregion, this mostly agricultural watershed is, however, somewhat unique in being dominated by silt/clay streambeds. At present, much of the main-stem channel and tributaries are unstable and are characterized by unstable streambanks. This instability, stemming from the original channelization and the associated elevation in sediment loads has probably been exacerbated by clearing and snagging operations in 1967, and repeated dredging of the mouth of James Creek where it enters the Tennessee-Tombigbee waterway.

To develop water-quality targets for sediment in James Creek and in the absence of sediment-transport data in the watershed, historical flow and sediment transport data from similar streams in the Southeastern Plains were used to develop “reference” or unimpaired sediment-transport rates. These values are expressed in terms of the “channel-forming” or effective discharge because the effective discharge represents the flow that transports the most sediment over the long term. That flow rate occurs, on average, every 1.5 years ($Q_{1.5}$). To normalize the transport rate (load) by drainage area, the “reference” is expressed either as a suspended-sediment yield, in tonnes/day/kilometer squared ($T/d/km^2$) or as a concentration, in milligrams/liter (mg/l). A general “reference” for the Southeastern Plains was determined to be about $0.3 T/d/km^2$ and 48 mg/l by using the median value for stable sites in the region. Improved values were obtained by sorting the data by dominant bed-material size class, obtaining the median “reference” value by bed-material size class and by taking the weighted mean based on the percentage of drainage area encompassed by channels of particular bed-material types. The resulting “weighted-reference” values for James Creek are about $2.2 T/d/km^2$ and 160 mg/l at the $Q_{1.5}$.

Direct comparison of measured cross sections from 1967 and 2002, combined with numerical modeling using AnnAGNPS for uplands and CONCEPTS for the main stem of James Creek were used to determine “actual” sediment loads in the watershed. Peak-flow data generated independently by AnnAGNPS using actual precipitation data was in very close agreement with the annual-maximum flow series obtained for a discontinued gaging station on James Creek. Flows generated by AnnAGNPS in combination with CONCEPTS were also in close agreement with the measured data.

Average sediment loads at the mouth of James Creek over the 35-year period are about 250,000 T/y with about 89% of this material emanating from James Creek and its tributaries with only 11 % derived from upland sources. Of this 89% eroded from the channel boundaries, about 88% comes from the channel banks. This loading value, however, is somewhat misleading in that severe channel erosion occurred between 1967-1968 following channel clearing and snagging operations over the lower 17 km of James Creek. Since this time, sediment loads have attenuated and the contribution from channels and uplands over the period 1970-2002 is 70% and 30%, respectively.

“Actual” suspended-sediment yields at the $Q_{1.5}$ as simulated with AnnAGNPS in combination with CONCEPTS show a 35-year average of $675 T/d/km^2$. However, the average over the past

10 years is 155 T/d/km² and, following the installation of additional low-water crossings in 1999 further reduced yields to about 39 T/d/km².

The combination of empirical analysis of historical data, detailed field reconnaissance and data collection, and numerical simulation with AnnAGNPS for uplands and CONCEPTS for tributaries has been shown to be powerful tools in determining “actual” and “reference” sediment transport rates in James Creek where no historical sediment-transport data exist. Results of this study indicate that a significant proportion of the sediment in the James Creek watershed emanates from stream channels. Subsequent decisions regarding reducing sediment loadings will need to pay particular attention to stream-channel processes and stabilizing eroding reaches and tributaries of James Creek.

REFERENCES

- Anderson, E., Bai, Z., Bischof, C., Blackford, S., Demmel, J., Dongarra, J., Du Croz, J., Greenbaum, A., Hammarling, S., McKenney, A., Sorensen, D., 1999. LAPACK Users' Guide. 3rd Ed., Society for Industrial and Applied Mathematics (SIAM), Philadelphia, PA.
- Andrews, E.D., 1980, Effective and bankfull discharge of streams in the Yampa River Basin, Colorado and Wyoming. *Journal of Hydrology*, 46, 311-330.
- Andrews, E.D., and Nankervis, J.M., 1995, Effective discharge and the design of channel maintenance flow for gravel-bed rivers. In, Costa, J.E., Miller, A.J., Potter, and Wilcock, P. R., (Eds.), *Natural and Anthropogenic Influences in Fluvial Geomorphology*, Geophysical Monograph 89, p. 151-164. American Geophysical Union.
- Bingner, R. L., C. V. Alonso, R. W. Darden, R.G. Cronshey, F. D. Theurer, W. F. Getter, 1996, Development of a GIS-based flownet generator for AGNPS. *Proceedings of the Sixth Federal Interagency Sedimentation Conference*, Las Vegas, NV, March 10-14, p. Poster-52-55.
- Bingner, R. L., R. W. Darden, F. D. Theurer, and J. Garbrecht, 1997, GIS-Based Generation of AGNPS Watershed Routing and Channel Parameters. ASAE Paper No. 97-2008, St. Joseph, Michigan. 4 pp.
- Bingner, R. L., R.W. Darden, F.D. Theurer, C.V. Alonso, and P. Smith, 1998, AnnAGNPS Input Parameter Editor Interface. *First Federal Interagency Hydrologic Modeling Conference*, April 19 - 23, 1998, Las Vegas, Nevada, p. 8-15-18.
- Bingner, R. L. and F. D. Theurer, 2001a, AGNPS 98: A Suite of water quality models for watershed use. In *Proceedings of the Sediment: Monitoring, Modeling, and Managing*, 7th Federal Interagency Sedimentation Conference, Reno, NV, 25-29 March 2001. p. VII-1 - VII-8.
- Bingner, R. L. & F. D. Theurer, 2001b, Topographic factors for RUSLE in the continuous-simulation, watershed model for predicting agricultural, non-point source pollutants (AnnAGNPS). Presented at: 3-5 January 2001, *Soil Erosion for the 21st Century - An International Symposium Honolulu, Hawaii*, Paper No. in press, ASAE, 2950 Niles Road, St. Joseph, MI 49085-9659 USA. 4 pp.
- Bosch, D., F. Theurer, R. Bingner, G. Felton and I. Chaubey, 1998, Evaluation of the AnnAGNPS Water Quality Model. ASAE Paper No. 98-2195, St. Joseph, Michigan. 12 p.
- Brunner, G.W., 2001. HEC-RAS, River Analysis System User's Manual. Rep. No. CPD-68, US Army Corps of Engineers, Hydrologic Engineering Center, Davis, CA.
- Carson, M.A., and Kirkby, 1972, *Hillslope Form and Process*. Cambridge University Press, 475p.
- Cronshey, R.G and F. D. Theurer, 1998, AnnAGNPS—Non-Point Pollutant Loading Model. In *Proceedings First Federal Interagency Hydrologic Modeling Conference*, 19-23 April 1998, Las Vegas, NV, p. 1-9 to 1-16.
- Cunge, J.A., Holly Jr., F.M., Verwey, A., 1980. *Practical Aspects of Computational River Hydraulics*. Pitman Publishing Inc, Boston, MA.
- Daniels, R.B., 1960, Entrenchment of the Willow Drainage Ditch, Harrison County, Iowa. *American Journal of Science*. v. 258, pp. 161-176.
- Emerson, J.W., 1971, Channelization: A case study. *Science*, v. 172, pp. 325-326.

- Fredlund, D.G., N.R. Morgenstern, and R.A. Widger 1978. The shear strength of unsaturated soils. *Canadian Geotechnical Journal* 15: 313-321.
- Garbrecht, J. and L. W. Martz, 1995, *Advances in Automated Landscape Analysis*. In *Proceedings of the First International Conference on Water Resources Engineering*, Eds. W. H. Espey and P. G. Combs, American Society of Engineers, San Antonio, Texas, August 14-18, 1995, Vol. 1, pp. 844-848.
- Glysson, G.D., 1987, *Sediment-transport curves*. U.S. Geological Survey Open-File Report 87-218, 47 p.
- Hanson, G.J. 1990. Surface erodibility of earthen channels at high stresses. Part II - Developing an in-situ testing device. *Transactions of the ASAE* 33(1):132-137.
- Hanson, G.J. 1991. Development of a jet index to characterize erosion resistance of soils in earthen spillways. *Transactions of the ASAE*, 36(5).
- Hanson, G.J. and A. Simon 2001. Erodibility of cohesive streambeds in the loess area of the midwestern USA. *Hydrological Processes* 15 (1): 23-38.
- Hirano, M., 1971. River bed degradation with armoring. *Proceedings, Japan Society of Civil Engineers*, 195, 55-65.
- Hupp, C.R. 1992. Riparian vegetation recovery patterns following stream channelization: A geomorphic perspective. *Ecology* 73:1209-1226.
- Johnson, G. L., C. Daly, G. H. Taylor and C. L. Hanson, 2000, Spatial variability and interpolation of stochastic weather simulation model parameters. *J. Appl. Meteor.*, 39, 778-796.
- Kuhnle R., and Simon, A. (2000), *Evaluation of Sediment Transport Data for Clean Sediment TMDL's*. National Sedimentation Laboratory Report 17, Oxford, Mississippi, 65 p.
- Krone, R.B., 1962. Flume studies of the transport of sediment in estuarine shoaling processes. Final Report, Hydraulic Engineering Laboratory, University of California, Berkeley.
- Langendoen, E. J. 2000. "CONCEPTS - CONservational Channel Evolution and Pollutant Transport System," *Report*, U.S. Department of Agriculture, Agricultural Research Service, National Sedimentation Laboratory, Oxford, MS.
- Little, W.C., Thorne, C.R., and Murphy, J.B., 1982. Mass bank failure analysis of selected Yazoo Basin streams. *Trans. Amer. Soc. Agric. Eng.*, 25, 1321-1328.
- Lohnes, R.A., and R.L. Handy 1968. Slope angles in friable loess. *Journal of Geology* 76 (3), 247-258.
- Lutenegger, J.A., and Hallberg, B.R., 1981. Borehole shear test in geotechnical investigations. *ASTM Spec. Publ.* 740, 566-578.
- Omerik, J.M., 1995, *Ecoregions: A framework for environmental management*, In, Davic, W., and Simon, T., (Eds.), *Biological Assessment and Criteria: Tools for Water Resource Planning and Decision Making*, Lewis Publishers, Chelsea, Michigan.
- Porterfield, G., 1972, *Computation of fluvial sediment discharge*. U.S. Geological Survey, *Techniques in Water Resources Investigations*, Book 3, Chapter C3, 66 p.
- Renard, K. G., G. R. Foster, G. A. Weesies, D. K. McCool, and D. C. Yoder, coordinators, 1997, *Predicting Soil Erosion by Water: A Guide to Conservation Planning with the Revised Universal Soil Loss Equation (RUSLE)*. U.S. Department of Agriculture, Agriculture Handbook No. 703, 404 pp.
- Rinaldi, M., and Simon, A., 1998, Adjustments of the Arno River, Central Italy, *Geomorphology*, 22, 57-71.
- Rosgen, D.L., 1985, A classification of natural rivers. *Catena*, 22, 169-199.

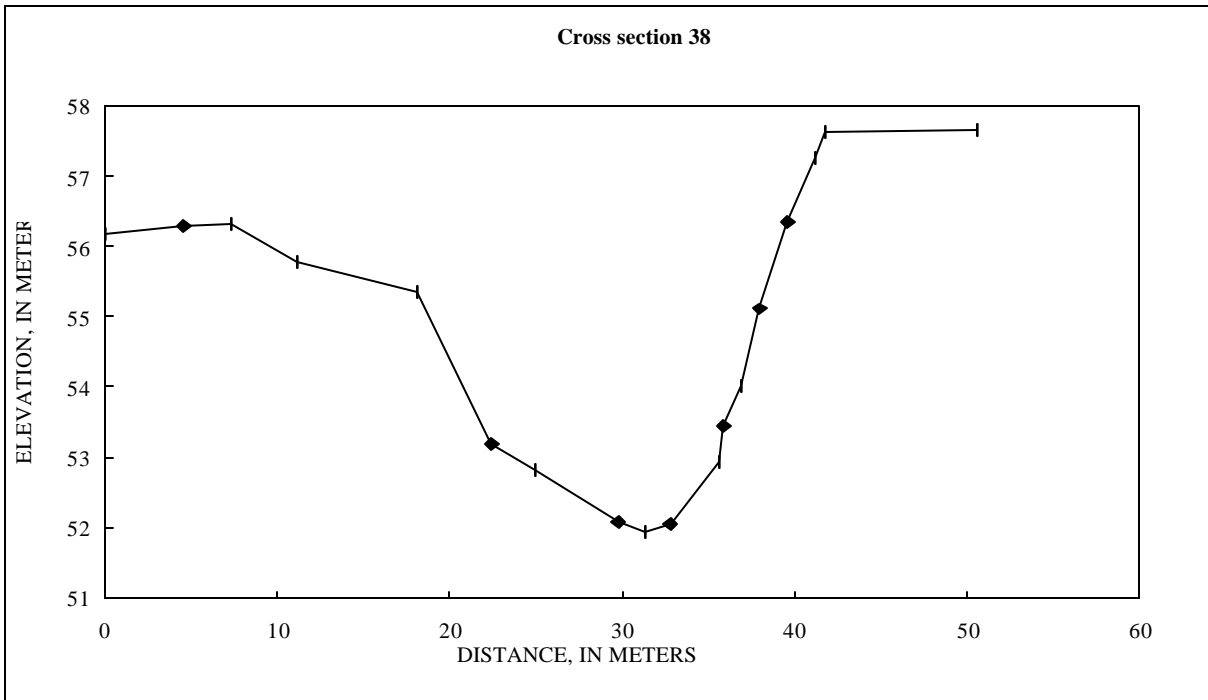
- Rosgen, D.L, 1996, Applied River Morphology, Wildland Hydrology, Pagosa Springs, Colorado.
- Shields, A. 1936. Anwendung der ahnlichkeitsmechanik und turbulenz forschung auf die geschiebebewegung. Mitteil. Preuss. Versuchsanst. Wasser, Erd, Schiffsbau, Berlin, Nr. 26.
- Simon, A., 1989a, The discharge of sediment in channelized alluvial streams, Water Resources Bulletin, v. 25, no. 6, 1177-1188.
- Simon, A., 1989b, A model of channel response in disturbed alluvial channels. Earth Surface Processes and Landforms, 14(1): 11-26.
- Simon, A. 1992. Energy, time, and channel evolution in catastrophically disturbed fluvial systems. Geomorphology, 5: 345-372 in Geomorphic Systems: J.D. Phillips and W.H. Renwick eds.
- Simon, A., 1994, Gradation processes and channel evolution in modified West Tennessee streams: Process, response and form. U.S. Geological Survey Professional Paper 1470, 84p.
- Simon, A., Curini, A., Darby, S.E. and Langendoen, E.J. 1999. Streambank mechanics and the role of bank and near-bank processes in incised channels, In Darby, S.E. and Simon, A. (Eds), Incised River Channels: Processes, Forms, Engineering and Management, John Wiley and Sons, London, 123-152.
- Simon, A., and Dickerson, W., Bankfull/Effective flow and sediment-transport rates in the United States. Geomorphology, in press.
- Simon, A., and Hupp, C. R., 1986, Channel evolution in modified Tennessee channels, Proceedings of the Fourth Interagency Sedimentation Conference, March 1986, Las Vegas, Nevada, v. 2, Section 5, 5-71 to 5-82.
- Simon, A., and Hupp, C. R., 1992, Geomorphic and vegetative recovery processes along modified stream channels of West Tennessee. U. S. Geological Survey Open-file Report 91-502, 142 p.
- Simon, A., Kuhnle, R., and Dickerson, W., 2002, Reference sediment-transport rates for Level III ecoregions for use in developing clean-sediment TMDLs, in Proc. Water Resources Planning and Management, EWRI-ASCE, May 19-22, 2002, Roanoke, 10 p.
- Simon A., and Rinaldi, M., 2000, Channel instability in the loess area of the Midwestern United States Journal of American Water Resources Association, 36(1): 133-150.
- Simon, A., Wolfe, W. J., and Molinas, A. 1991. Mass wasting algorithms in an alluvial channel model, Proc. 5th Federal Interagency Sedimentation Conference, Las Vegas, Nevada, 2, 8-22 to 8-29.
- Thorne, C.R., 1982, Processes and mechanisms of river bank erosion. In. R.D. Hey, J.C., Bathurst and C.R., Thorne, (eds.), Gravel-Bed Rivers, John Wiley and Sons, Chichester, England, 227-271.
- Thorne, C.R., J.B. Murphey, and W.C. Little 1981. Stream channel stability, Appendix D, Bank stability and bank material properties in the bluffline streams of northwest Mississippi: Oxford, Mississippi, U.S. Department of Agriculture Sedimentation Laboratory, 257 pp.
- Turcios, L.M., and Gray, J.R., 2000, U.S. Geological Survey sediment and ancillary data on the world wide web. 7th Federal Interagency Sedimentation Conference, vol. 1, Poster 31, Reno Nevada.
- USDA, Soil Conservation Service, 1972, National Engineering Handbook. Hydrology Section 4, Chapters 4-10, 16, 19. Washington, DC.

- U.S. Geological Survey, 1993, Nationwide summary of U.S. Geological Survey regional regression equations for estimating magnitude and frequency of floods for ungaged sites. Compiled by M.E. Jennings, W.O. Thomas, Jr., and H.C. Riggs, U.S. Geological Survey Water-Resources Investigations Report 94-4002.
- Vanoni, V.A., 1975, Sedimentation Engineering. ASCE Manuals and Reports on Engineering Practice - No. 54, 745 pp
- Vestal, F.E., and McCutcheon, T.E., 1943, Monroe County mineral resources, Mississippi State Geological Survey, Bull. 57.
- Yang, C.T., Trevino, M.A., Simoes, F.J.M., 1998. User's Manual for GSTARS 2.0. US Department of the Interior, Bureau of Reclamation, Technical Service Center, Sedimentation and River Hydraulics Group, Denver, Co.
- Young, R. A., C. A. Onstad, D. D. Bosch and W. P. Anderson, 1989, AGNPS: A nonpoint-source pollution model for evaluating agricultural watersheds. *Journal of Soil and Water Conservation* 44(2): 168-173.

APPENDIX A - DATA FROM 2002 CROSS-SECTION SURVEYS

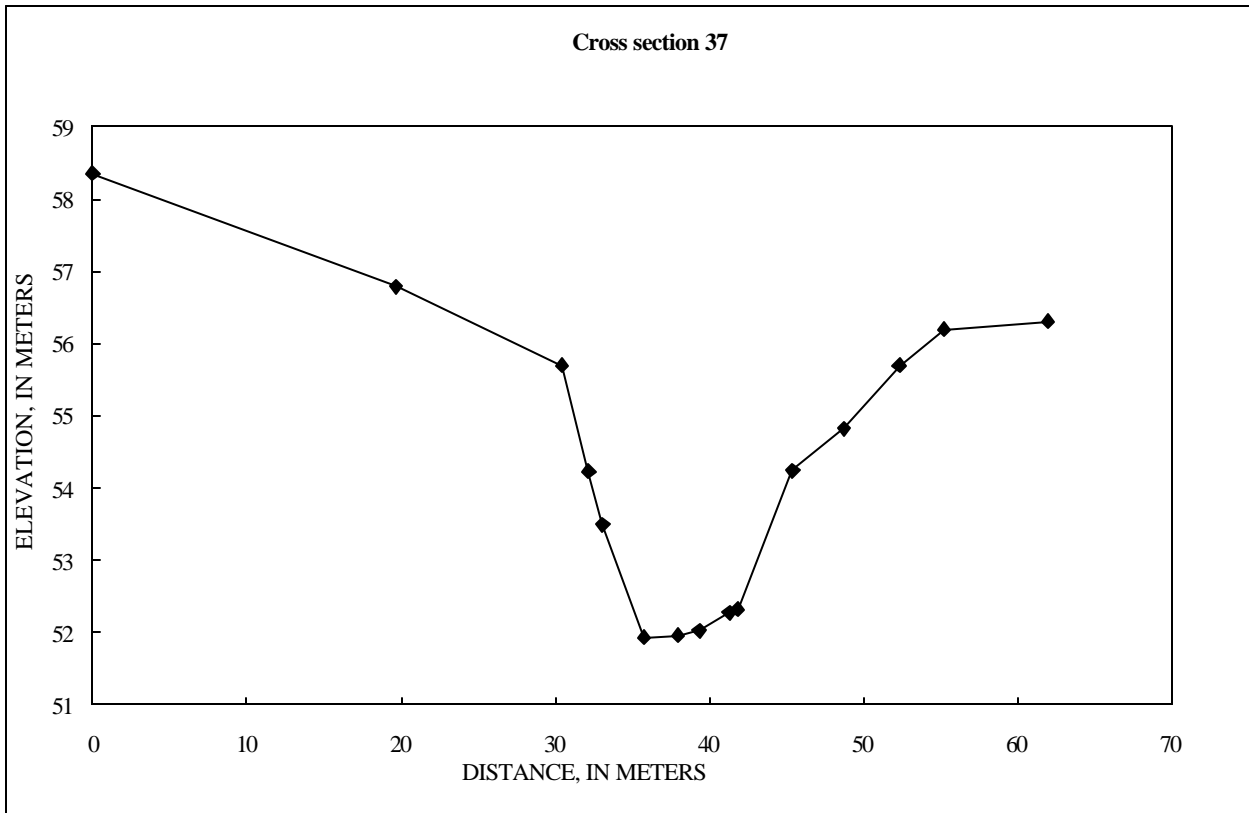
CROSS SECTION 38

SHOT #	PCODE	NORTHING (N)	EASTING (E)	ELEVATION (Z), IN METERS	DISTANCE, IN METERS	CUMULATIVE DISTANCE, IN METERS
1	START	0	0	100		
2	CS	-10589.10	12060.44	56.175	0	0
3	CS	-10593.61	12059.85	56.294	4.56	4.56
4	CS	-10596.27	12059.27	7.273	2.72	7.27
5	CS	-10599.95	12058.19	55.784	3.83	11.11
6	CS	-10606.89	12057.27	55.341	7.00	18.11
7	CS	-10611.19	12057.05	53.195	4.31	22.41
8	CS	-10613.69	12056.98	52.806	2.50	24.91
9	CS	-10618.40	12055.83	52.081	4.85	29.76
10	CS	-10619.95	12055.45	51.941	1.59	31.36
11	CS	-10621.33	12055.14	52.055	1.42	32.77
12	CS	-10624.07	12054.50	52.936	2.82	35.59
13	CS	-10624.36	12054.45	53.439	0.29	35.88
14	CS	-10625.34	12054.20	54.013	1.01	36.89
15	CS	-10626.30	12053.73	55.106	1.07	37.96
16	CS	-10627.74	12052.98	56.354	1.62	39.59
17	CS	-10629.28	12052.55	57.257	1.60	41.19
18	CS	-10629.84	12052.51	57.615	0.56	41.75
19	CS	-10638.48	12050.77	57.661	8.81	50.56



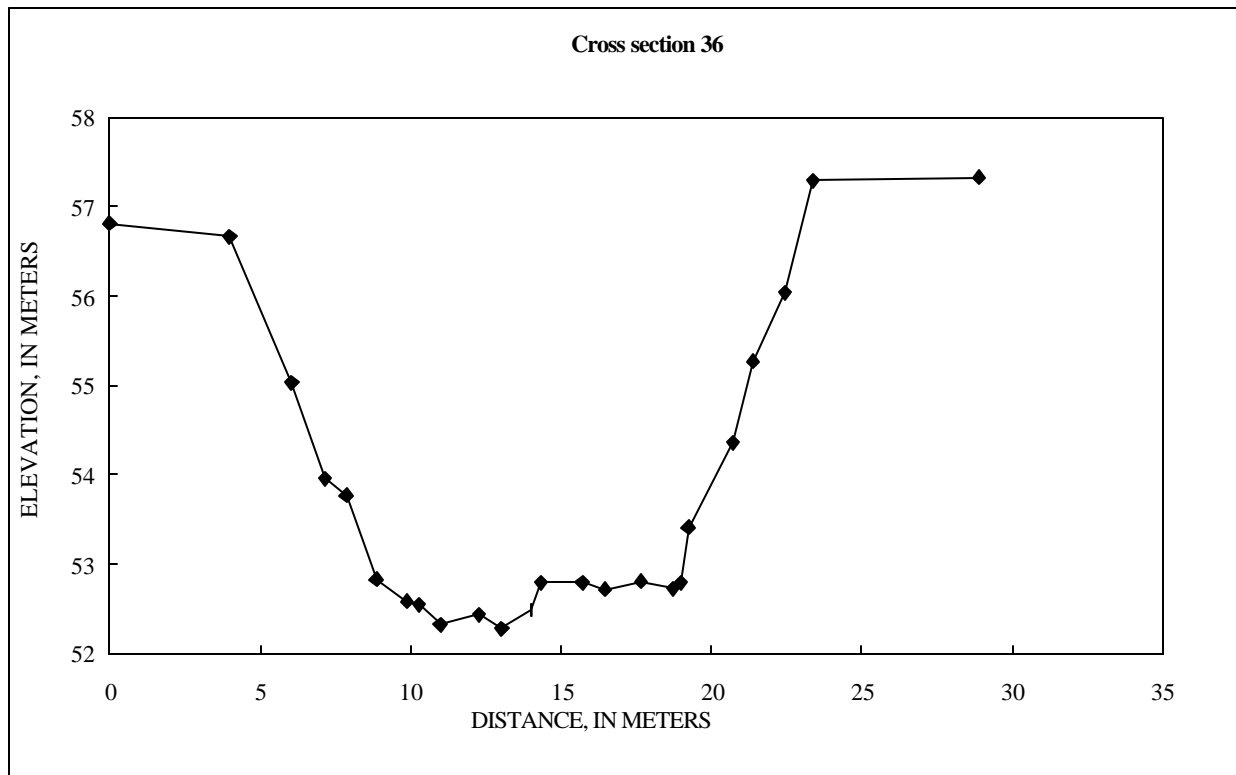
CROSS SECTION37

SHOT #	PCODE	NORTHING (N)	EASTING (E)	ELEVATION (Z), IN METERS	DISTANCE, IN METERS	CUMULATIVE DISTANCE, IN METERS
1	START	0	0	100		
2	CS	-10417.41	11910.49	58.357	0	0
3	CS	-10436.19	11904.67	56.795	19.66	19.66
4	CS	-10446.22	11900.83	55.697	10.74	30.40
5	CS	-10447.87	11900.20	54.230	1.77	32.17
6	CS	-10448.74	11899.98	53.493	0.90	33.07
7	CS	-10451.28	11899.20	51.930	2.66	35.72
8	CS	-10453.39	11898.42	51.968	2.25	37.97
9	CS	-10454.66	11897.90	52.033	1.38	39.34
10	CS	-10456.44	11897.19	52.280	1.92	41.26
11	CS	-10456.96	11897.29	52.328	0.53	41.79
12	CS	-10459.54	11894.82	54.248	3.57	45.36
13	CS	-10462.80	11894.00	54.822	3.36	48.72
14	CS	-10466.07	11892.64	55.699	3.55	52.27
15	CS	-10468.85	11891.61	56.200	2.96	55.23
16	CS	-10474.74	11888.41	56.305	6.70	61.93



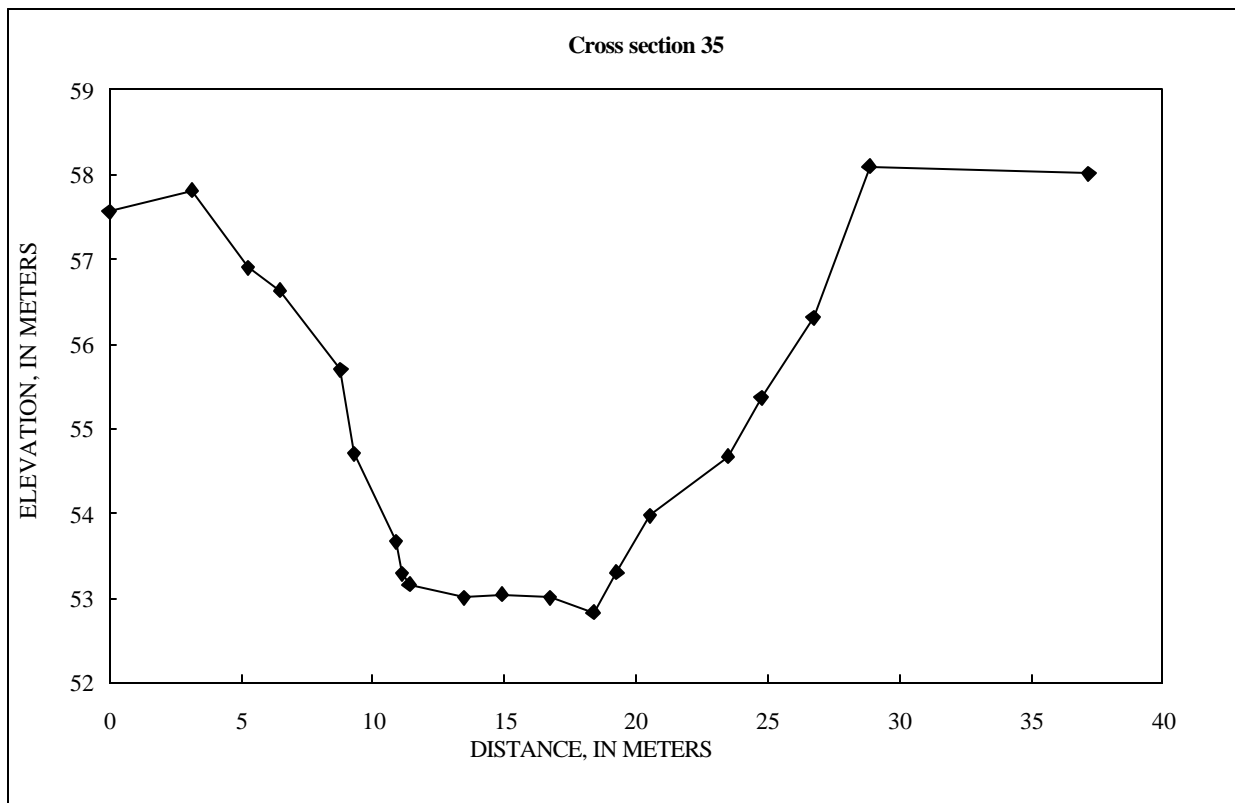
CROSS SECTION 36

SHOT #	PCODE	NORTHING (N)	EASTING (E)	ELEVATION (Z), IN METERS	DISTANCE, IN METERS	CUMULATIVE DISTANCE, IN METERS
1	START	0	0	100		
2	CS	-10386.07	11735.99	56.812	0	0
3	CS	-10389.36	11733.73	56.669	4.00	4.00
4	CS	-10390.77	11732.23	55.038	2.06	6.05
5	CS	-10391.74	11731.72	53.955	1.10	7.15
6	CS	-10392.22	11731.21	53.773	0.70	7.85
7	CS	-10392.88	11730.45	52.825	1.00	8.86
8	CS	-10393.71	11729.90	52.575	1.00	9.85
9	CS	-10393.63	11729.50	52.552	0.41	10.26
10	CS	-10394.10	11728.95	52.324	0.72	10.98
11	CS	-10395.00	11728.04	52.431	1.29	12.27
12	CS	-10395.53	11727.50	52.278	0.75	13.02
13	CS	-10395.93	11726.63	52.485	0.96	13.98
14	CS	-10396.08	11726.30	52.794	0.36	14.34
15	CS	-10396.96	11725.26	52.794	1.37	15.70
16	CS	-10397.53	11724.78	52.716	0.74	16.44
17	CS	-10398.28	11723.84	52.804	1.20	17.65
18	CS	-10399.11	11723.19	52.729	1.06	18.71
19	CS	-10399.33	11723.04	52.794	0.26	18.97
20	CS	-10399.50	11722.86	53.415	0.25	19.22
21	CS	-10400.70	11721.98	54.360	1.49	20.70
22	CS	-10401.32	11721.73	55.269	0.66	21.37
23	CS	-10402.23	11721.16	56.037	1.08	22.44
24	CS	-10402.93	11720.54	57.291	0.93	23.38
25	CS	-10407.60	11717.65	57.324	5.49	28.87



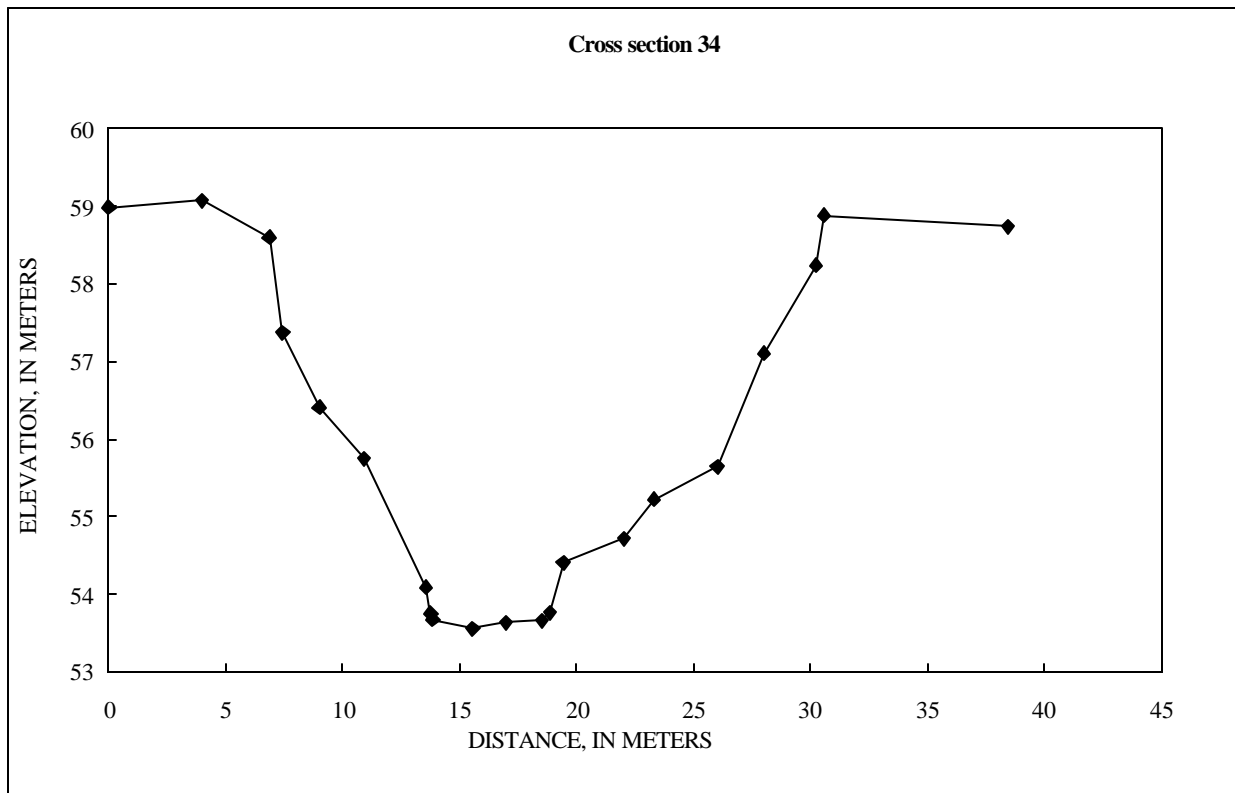
CROSS SECTION 35

SHOT #	PCODE	NORTHING (N)	EASTING (E)	ELEVATION (Z), IN METERS	DISTANCE, IN METERS	CUMULATIVE DISTANCE, IN METERS
1	START	0	0	100		
2	CS	-9846.70	10978.89	57.567	0	0
3	CS	-9848.01	10976.07	57.809	3.12	3.12
4	CS	-9848.73	10974.06	56.908	2.13	5.25
5	CS	-9849.31	10972.97	56.638	1.24	6.49
6	CS	-9850.61	10971.07	55.702	2.30	8.78
7	CS	-9850.88	10970.67	54.706	0.49	9.27
8	CS	-9851.60	10969.21	53.669	1.63	10.90
9	CS	-9851.60	10969.01	53.292	0.21	11.10
10	CS	-9851.74	10968.76	53.160	0.28	11.39
11	CS	-9852.86	10967.00	53.006	2.09	13.47
12	CS	-9853.60	10965.79	53.046	1.42	14.89
13	CS	-9854.71	10964.30	53.012	1.86	16.75
14	CS	-9855.20	10962.75	52.838	1.62	18.37
15	CS	-9855.42	10961.87	53.303	0.91	19.28
16	CS	-9856.11	10960.83	53.972	1.25	20.53
17	CS	-9857.71	10958.32	54.668	2.98	23.50
18	CS	-9858.09	10957.12	55.372	1.25	24.76
19	CS	-9858.96	10955.36	56.315	1.97	26.73
20	CS	-9859.40	10953.27	58.091	2.13	28.86
21	CS	-9862.59	10945.57	58.015	8.34	37.20



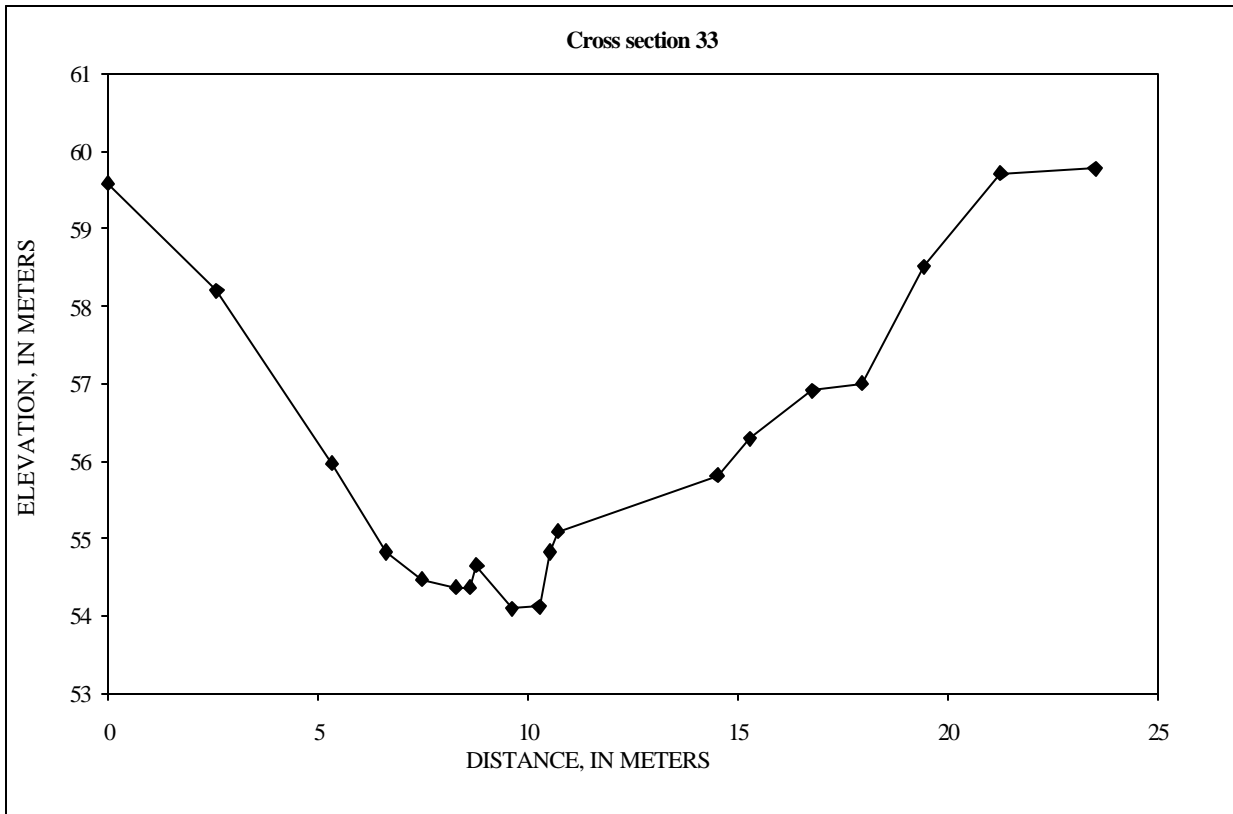
CROSS SECTION 34

SHOT #	PCODE	NORTHING (N)	EASTING (E)	ELEVATION (Z), IN METERS	DISTANCE, IN METERS	CUMULATIVE DISTANCE, IN METERS
1	START	0	0	100		
2	CS	-9176.13	10793.51	58.982	0	0
3	CS	-9178.07	10790.06	59.077	3.96	3.96
4	CS	-9179.67	10787.65	58.593	2.89	6.84
5	CS	-9180.16	10787.33	57.370	0.59	7.43
6	CS	-9180.72	10785.88	56.408	1.55	8.99
7	CS	-9181.97	10784.45	55.751	1.91	10.89
8	CS	-9183.42	10782.21	54.095	2.67	13.56
9	CS	-9183.46	10781.99	53.752	0.22	13.78
10	CS	-9183.48	10781.93	53.682	0.07	13.85
11	CS	-9184.60	10780.60	53.563	1.74	15.58
12	CS	-9185.08	10779.27	53.640	1.42	17.00
13	CS	-9185.73	10777.87	53.667	1.55	18.55
14	CS	-9185.85	10777.60	53.768	0.29	18.84
15	CS	-9186.12	10777.08	54.411	0.59	19.43
16	CS	-9187.49	10774.83	54.717	2.63	22.06
17	CS	-9187.94	10773.64	55.226	1.27	23.33
18	CS	-9189.47	10771.45	55.641	2.68	26.00
19	CS	-9190.44	10769.71	57.095	1.99	27.99
20	CS	-9191.44	10767.69	58.236	2.25	30.25
21	CS	-9191.39	10767.34	58.889	0.35	30.60
22	CS	-9195.72	10760.78	58.736	7.87	38.46



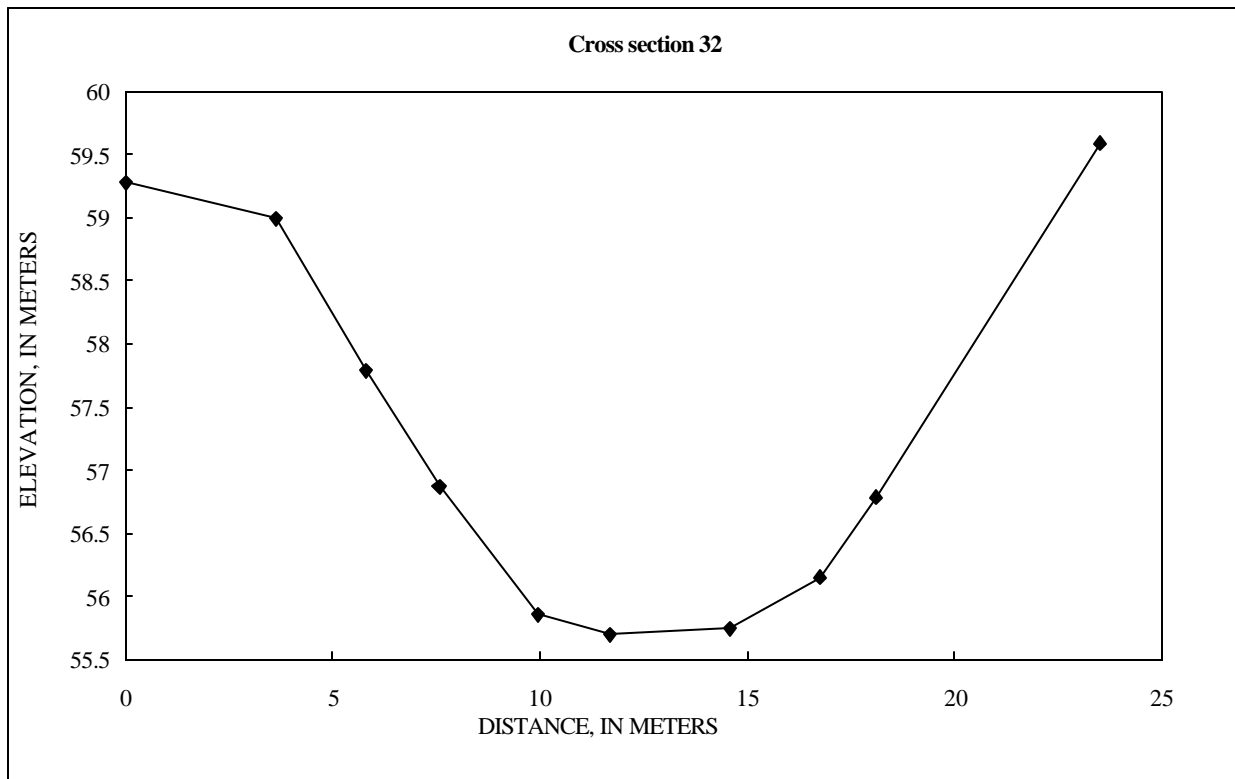
CROSS SECTION 33

SHOT #	PCODE	NORTHING (N)	EASTING (E)	ELEVATION (Z), IN METERS	DISTANCE, IN METERS	CUMULATIVE DISTANCE, IN METERS
1	START	0	0	100		
2	CS	-8615.59	10592.93	59.579	0	0
3	CS	-8615.90	10590.37	58.211	2.58	2.58
4	CS	-8616.53	10587.70	55.968	2.75	5.32
5	CS	-8617.16	10586.58	54.824	1.28	6.61
6	CS	-8617.33	10585.74	54.468	0.85	7.46
7	CS	-8617.70	10585.03	54.361	0.80	8.26
8	CS	-8617.84	10584.72	54.369	0.35	8.61
9	CS	-8617.84	10584.56	54.650	0.15	8.76
10	CS	-8617.94	10583.73	54.093	0.84	9.60
11	CS	-8618.01	10583.08	54.126	0.65	10.25
12	CS	-8618.13	10582.87	54.828	0.25	10.50
13	CS	-8618.16	10582.67	55.084	0.20	10.70
14	CS	-8619.02	10578.97	55.816	3.80	14.49
15	CS	-8618.68	10578.26	56.292	0.79	15.28
16	CS	-8618.85	10576.78	56.911	1.49	16.77
17	CS	-8619.11	10575.64	57.000	1.17	17.94
18	CS	-8618.89	10574.20	58.518	1.46	19.40
19	CS	-8619.63	10572.51	59.714	1.84	21.24
20	CS	-8619.62	10570.26	59.779	2.25	23.49



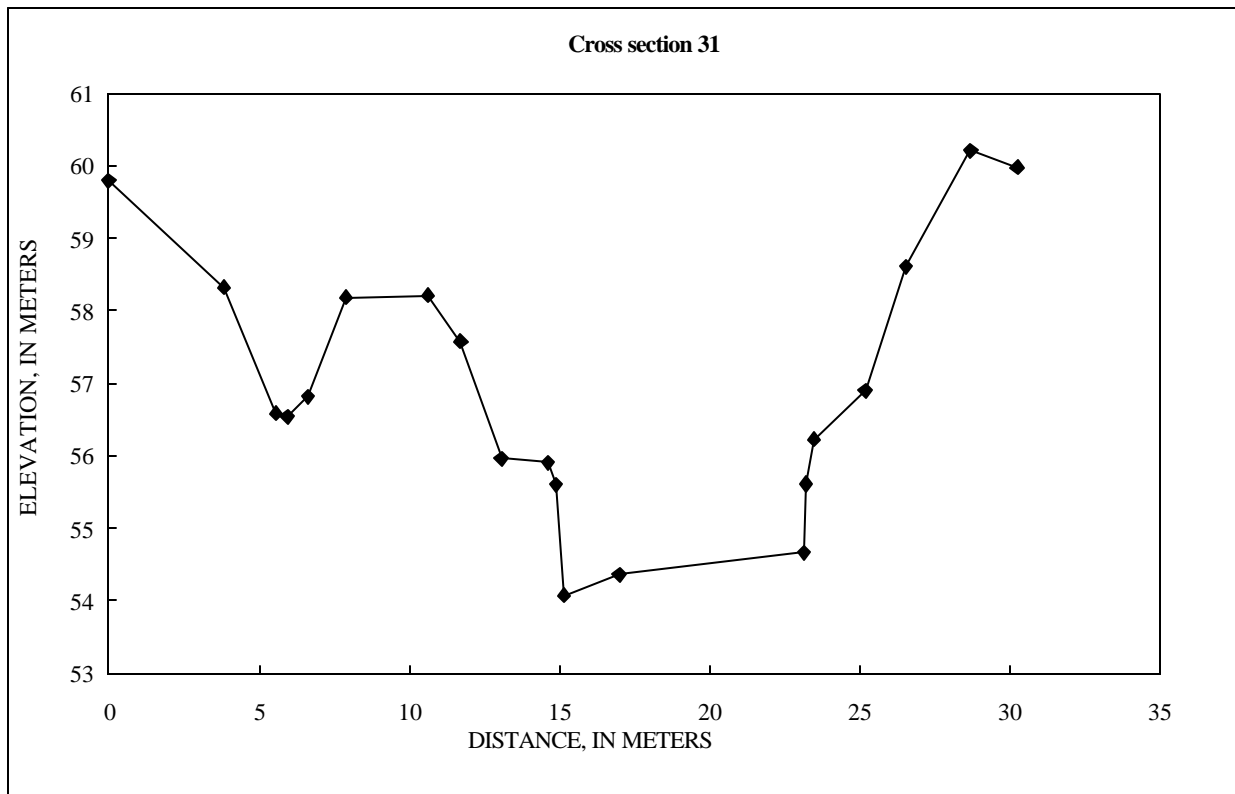
CROSS SECTION 32

SHOT #	PCODE	NORTHING (N)	EASTING (E)	ELEVATION (Z), IN METERS	DISTANCE, IN METERS	CUMULATIVE DISTANCE, IN METERS
1	START	0	0	100		
2	CS	-8581.69	10587.02	59.278	0	0
3	CS	-8582.66	10583.51	58.989	3.65	3.65
4	CS	-8583.77	10581.67	57.786	2.15	5.79
5	CS	-8584.24	10579.96	56.870	1.77	7.57
6	CS	-8584.84	10577.67	55.854	2.37	9.93
7	CS	-8585.66	10576.12	55.698	1.76	11.69
8	CS	-8586.36	10573.31	55.749	2.89	14.58
9	CS	-8586.81	10571.19	56.149	2.17	16.75
10	CS	-8587.13	10569.87	56.786	1.35	18.11
11	CS	-8589.71	10565.14	59.585	5.39	23.50



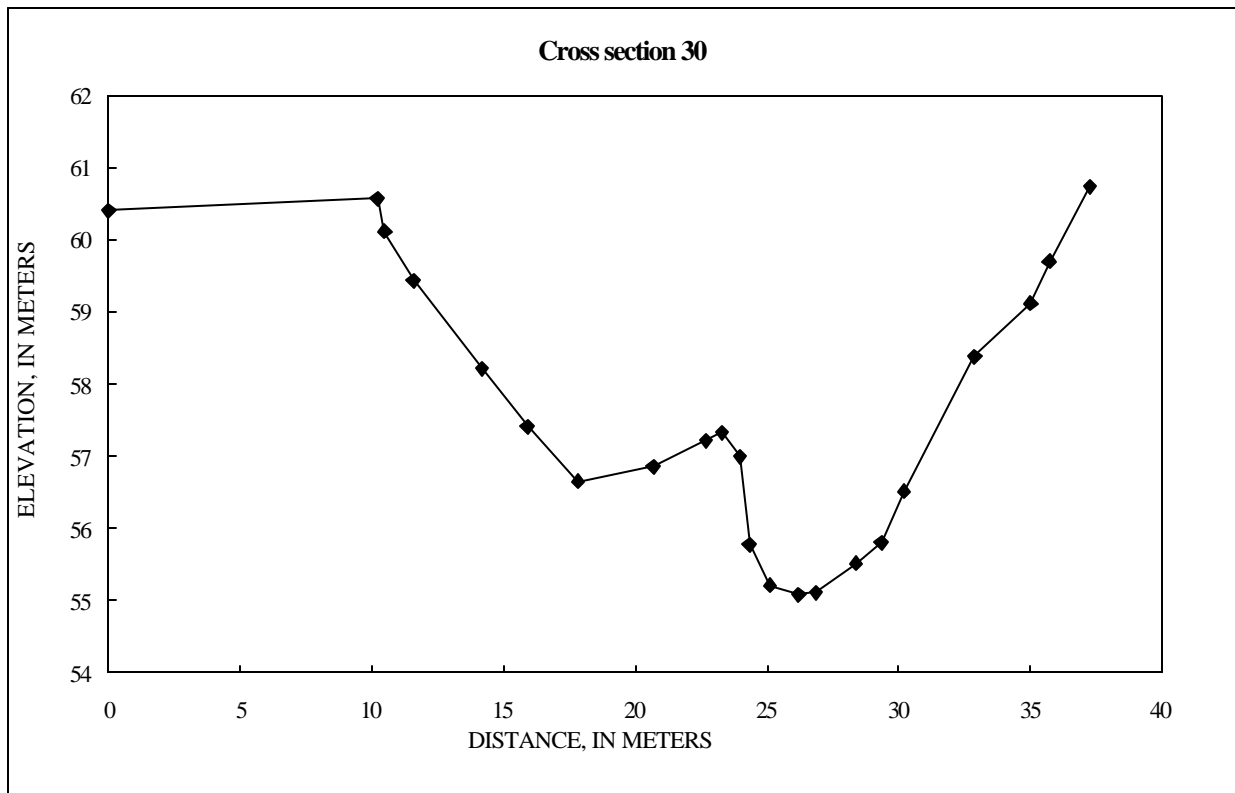
CROSS SECTION 31

SHOT #	PCODE	NORTHING (N)	EASTING (E)	ELEVATION (Z), IN METERS	DISTANCE, IN METERS	CUMULATIVE DISTANCE, IN METERS
1	START	0	0	100		
2	CS	-8106.71	10535.80	59.800	0	0
3	CS	-8108.28	10532.31	58.325	3.83	3.83
4	CS	-8108.85	10530.68	56.589	1.73	5.56
5	CS	-8108.97	10530.33	56.539	0.37	5.93
6	CS	-8108.94	10529.62	56.815	0.71	6.64
7	CS	-8109.25	10528.42	58.187	1.24	7.88
8	CS	-8110.07	10525.82	58.218	2.72	10.60
9	CS	-8110.46	10524.78	57.581	1.11	11.71
10	CS	-8110.47	10523.43	55.966	1.35	13.07
10	CS	-8111.00	10521.96	55.899	1.56	14.63
11	CS	-8111.02	10521.71	55.600	0.25	14.88
12	CS	-8111.09	10521.44	54.069	0.28	15.16
13	CS	-8109.37	10520.81	54.366	1.84	16.99
14	CS	-8112.07	10515.29	54.670	6.15	23.14
15	CS	-8112.08	10515.20	55.611	0.09	23.23
16	CS	-8112.04	10514.96	56.232	0.24	23.47
17	CS	-8112.45	10513.30	56.897	1.71	25.18
18	CS	-8113.14	10512.13	58.611	1.36	26.54
19	CS	-8113.97	10510.14	60.208	2.16	28.70
20	CS	-8114.49	10508.67	59.976	1.56	30.26



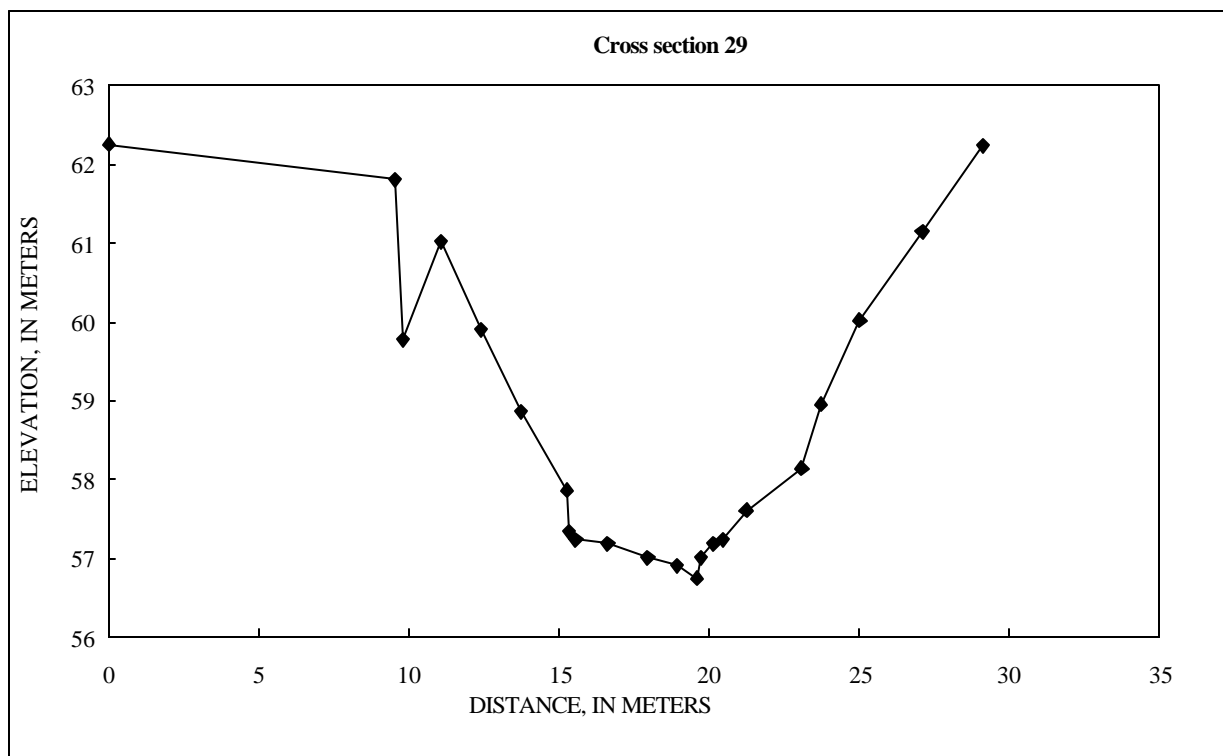
CROSS SECTION 30

SHOT #	PCODE	NORTHING (N)	EASTING (E)	ELEVATION (Z), IN METERS	DISTANCE, IN METERS	CUMULATIVE DISTANCE, IN METERS
1	START	0	0	100		
2	CS	-7692.53	10319.75	60.405	0	0
3	CS	-7685.87	10327.47	60.580	10.19	10.19
4	CS	-7685.65	10327.65	60.122	0.29	10.49
5	CS	-7684.81	10328.29	59.448	1.06	11.54
6	CS	-7683.03	10330.26	58.218	2.65	14.19
7	CS	-7682.05	10331.63	57.411	1.69	15.88
8	CS	-7680.60	10332.86	56.652	1.91	17.79
9	CS	-7678.25	10334.53	56.865	2.88	20.66
10	CS	-7676.73	10335.81	57.213	1.99	22.66
11	CS	-7676.39	10336.33	57.334	0.61	23.27
12	CS	-7675.95	10336.83	56.994	0.67	23.94
13	CS	-7675.69	10337.11	55.769	0.38	24.32
14	CS	-7674.95	10337.37	55.211	0.79	25.10
15	CS	-7674.14	10338.10	55.084	1.10	26.20
16	CS	-7673.78	10338.66	55.114	0.66	26.86
17	CS	-7672.79	10339.79	55.509	1.51	28.37
18	CS	-7672.06	10340.41	55.810	0.96	29.33
19	CS	-7671.99	10341.29	56.516	0.89	30.21
20	CS	-7669.52	10342.30	58.378	2.67	32.88
21	CS	-7667.68	10343.38	59.123	2.13	35.01
22	CS	-7667.40	10344.00	59.707	0.69	35.69
23	CS	-7665.94	10344.62	60.746	1.59	37.28



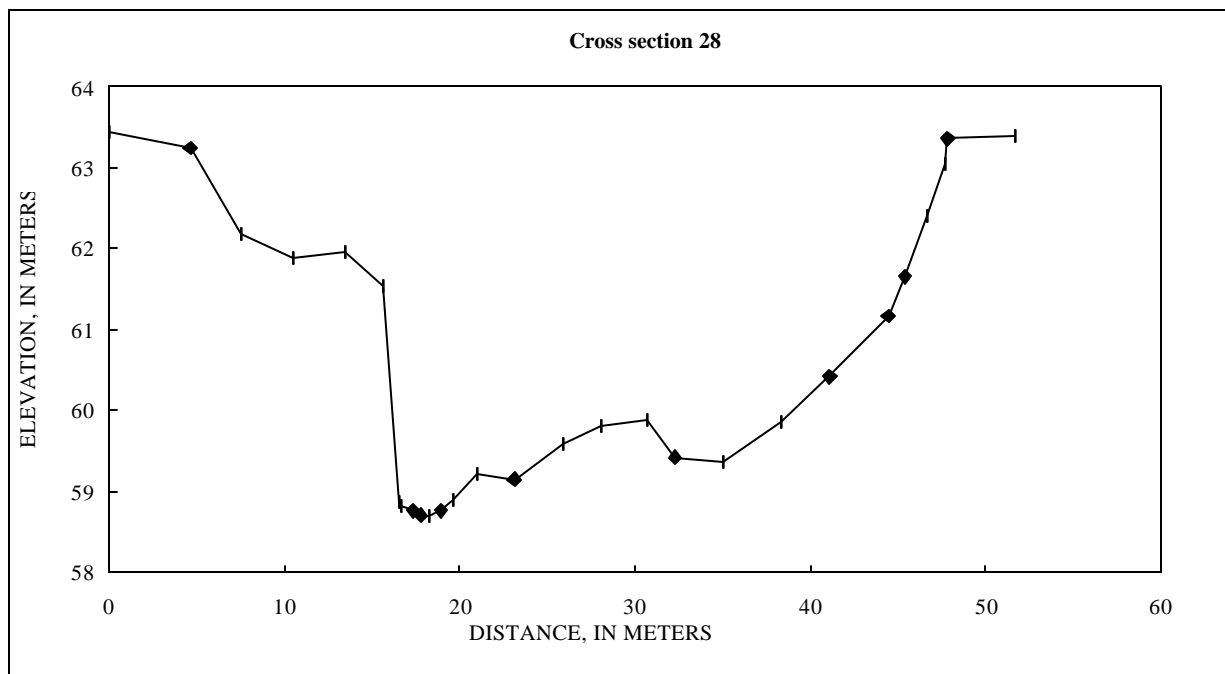
CROSS SECTION 29

SHOT #	PCODE	NORTHING (N)	EASTING (E)	ELEVATION (Z), IN METERS	DISTANCE, IN METERS	CUMULATIVE DISTANCE, IN METERS
1	START	0	0	100		
2	CS	-6874.83	10056.18	62.252	0	0
3	CS	-6879.22	10047.73	61.807	9.53	9.53
4	CS	-6879.35	10047.47	59.773	0.29	9.81
5	CS	-6880.02	10046.43	61.019	1.24	11.05
6	CS	-6880.78	10045.33	59.903	1.34	12.39
7	CS	-6881.79	10044.47	58.864	1.33	13.72
8	CS	-6882.14	10042.97	57.864	1.53	15.25
9	CS	-6882.19	10042.95	57.345	0.06	15.31
10	CS	-6882.34	10042.76	57.247	0.25	15.56
11	CS	-6882.86	10041.82	57.191	1.07	16.63
12	CS	-6883.30	10040.56	57.011	1.33	17.96
13	CS	-6883.88	10039.80	56.908	0.96	18.92
14	CS	-6884.29	10039.28	56.754	0.66	19.58
15	CS	-6884.37	10039.16	57.017	0.15	19.72
16	CS	-6884.58	10038.78	57.189	0.44	20.16
17	CS	-6884.71	10038.53	57.239	0.28	20.44
18	CS	-6885.12	10037.87	57.614	0.78	21.22
19	CS	-6886.00	10036.22	58.145	1.87	23.09
20	CS	-6886.22	10035.63	58.952	0.63	23.71
21	CS	-6886.64	10034.39	60.019	1.31	25.02
22	CS	-6887.82	10032.70	61.141	2.06	27.09
23	CS	-6888.91	10030.99	62.239	2.03	29.11



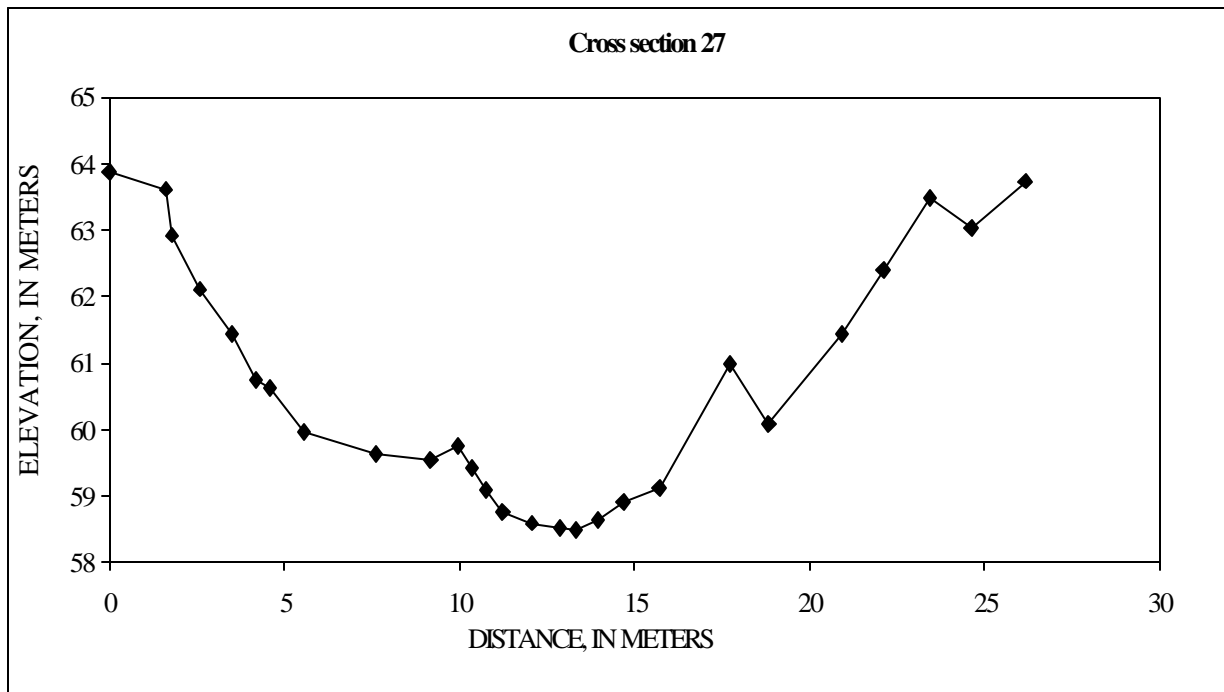
CROSS SECTION 28

SHOT #	PCODE	NORTHING (N)	EASTING (E)	ELEVATION (Z), IN METERS	DISTANCE, IN METERS	CUMULATIVE DISTANCE, IN METERS
1	START	0	0	100		
2	CS	-6587.94	9366.60	63.441	0	0
3	CS	-6592.55	9366.35	63.246	4.61	4.61
4	CS	-6595.44	9366.07	62.179	2.90	7.51
5	CS	-6598.36	9366.36	61.877	2.94	10.45
6	CS	-6601.17	9367.54	61.963	3.04	13.49
7	CS	-6603.30	9367.58	61.530	2.13	15.62
8	CS	-6603.88	9366.90	58.861	0.90	16.52
9	CS	-6604.00	9366.92	58.821	0.12	16.65
10	CS	-6604.70	9367.00	58.757	0.70	17.35
11	CS	-6605.11	9367.13	58.702	0.42	17.77
12	CS	-6605.59	9367.05	58.687	0.49	18.26
13	CS	-6606.23	9366.92	58.753	0.66	18.92
14	CS	-6606.94	9366.89	58.896	0.71	19.63
15	CS	-6608.23	9367.15	59.207	1.31	20.94
16	CS	-6610.36	9366.86	59.148	2.15	23.10
17	CS	-6613.16	9367.03	59.576	2.81	25.90
18	CS	-6615.31	9367.12	59.800	2.15	28.05
19	CS	-6617.94	9367.36	59.878	2.64	30.69
20	CS	-6619.52	9367.51	59.420	1.58	32.28
21	CS	-6622.25	9367.56	59.355	2.73	35.01
22	CS	-6625.59	9367.63	59.851	3.34	38.35
23	CS	-6628.37	9367.71	60.411	2.78	41.13
24	CS	-6631.56	9366.81	61.157	3.31	44.44
25	CS	-6632.49	9366.58	61.652	0.96	45.40
26	CS	-6633.72	9366.46	62.395	1.23	46.63
27	CS	-6634.81	9366.39	63.045	1.10	47.73
28	CS	-6634.94	9366.42	63.360	0.13	47.86
29	CS	-6638.72	9365.93	63.397	3.81	51.67



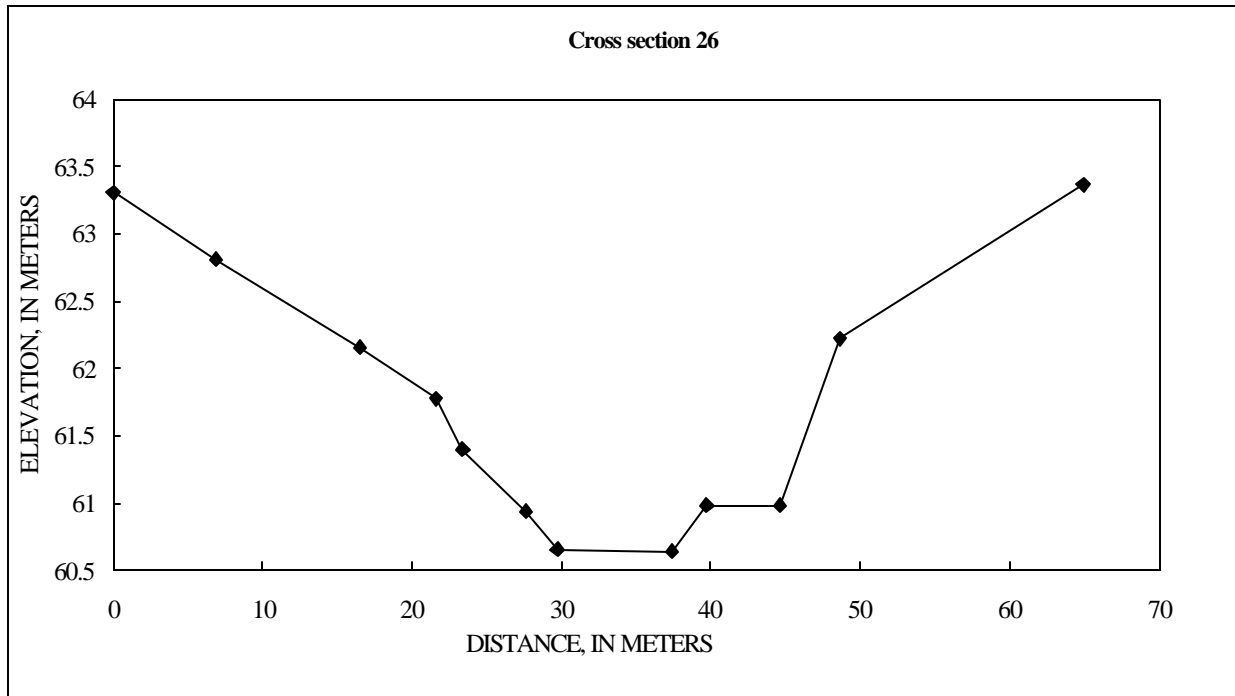
CROSS SECTION 27

SHOT #	PCODE	NORTHING (N)	EASTING (E)	ELEVATION (Z), IN METERS	DISTANCE, IN METERS	CUMULATIVE DISTANCE, IN METERS
1	START	0	0	100		
2	CS	-6338.51	9057.47	63.879	0	0
3	CS	-6339.08	9055.95	63.613	1.62	1.62
4	CS	-6339.20	9055.80	62.920	0.18	1.81
5	CS	-6339.68	9055.16	62.110	0.80	2.60
6	CS	-6339.91	9054.30	61.439	0.90	3.50
7	CS	-6340.15	9053.63	60.739	0.71	4.21
8	CS	-6340.51	9053.53	60.634	0.38	4.58
9	CS	-6340.78	9052.60	59.969	0.97	5.55
10	CS	-6341.40	9050.63	59.625	2.07	7.62
11	CS	-6341.86	9049.13	59.546	1.56	9.19
12	CS	-6342.03	9048.39	59.748	0.77	9.95
13	CS	-6342.17	9048.00	59.421	0.41	10.37
14	CS	-6342.34	9047.66	59.091	0.38	10.74
15	CS	-6342.56	9047.21	58.748	0.50	11.25
16	CS	-6342.78	9046.39	58.590	0.85	12.09
17	CS	-6342.94	9045.62	58.514	0.79	12.88
18	CS	-6343.01	9045.16	58.495	0.47	13.35
19	CS	-6343.03	9044.55	58.650	0.61	13.96
20	CS	-6343.15	9043.83	58.921	0.73	14.69
21	CS	-6343.40	9042.84	59.110	1.02	15.71
22	CS	-6343.74	9040.84	60.983	2.03	17.74
23	CS	-6343.76	9041.94	60.085	1.11	18.84
24	CS	-6343.83	9039.85	61.431	2.10	20.94
25	CS	-6343.87	9038.68	62.405	1.17	22.11
26	CS	-6343.96	9037.37	63.487	1.32	23.42
27	CS	-6344.04	9036.17	63.027	1.20	24.63
28	CS	-6344.44	9034.68	63.733	1.54	26.16



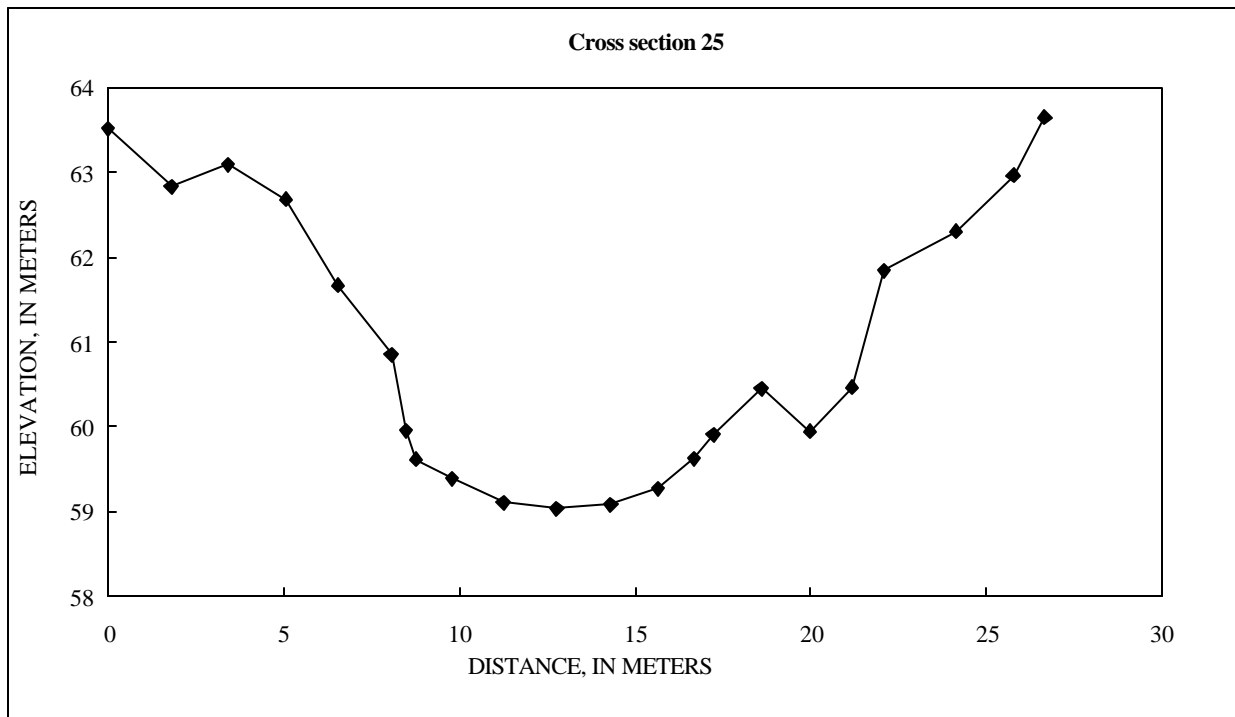
CROSS SECTION 26

SHOT #	PCODE	NORTHING (N)	EASTING (E)	ELEVATION (Z), IN METERS	DISTANCE, IN METERS	CUMULATIVE DISTANCE, IN METERS
1	START	0	0	100		
2	CS	-6199.52	8977.10	63.307	0	0
3	CS	-6204.62	8972.46	62.810	6.89	6.89
4	CS	-6211.34	8965.55	62.158	9.65	16.53
5	CS	-6214.98	8962.00	61.776	5.08	21.61
6	CS	-6216.32	8960.82	61.404	1.79	23.40
7	CS	-6219.71	8958.22	60.944	4.28	27.67
8	CS	-6221.37	8957.01	60.657	2.05	29.72
9	CS	-6227.67	8952.67	60.648	7.65	37.37
10	CS	-6229.59	8951.32	60.983	2.35	39.72
11	CS	-6233.58	8948.48	60.989	4.90	44.62
12	CS	-6236.44	8945.61	62.223	4.05	48.67
13	CS	-6249.80	8936.37	63.369	16.25	64.92



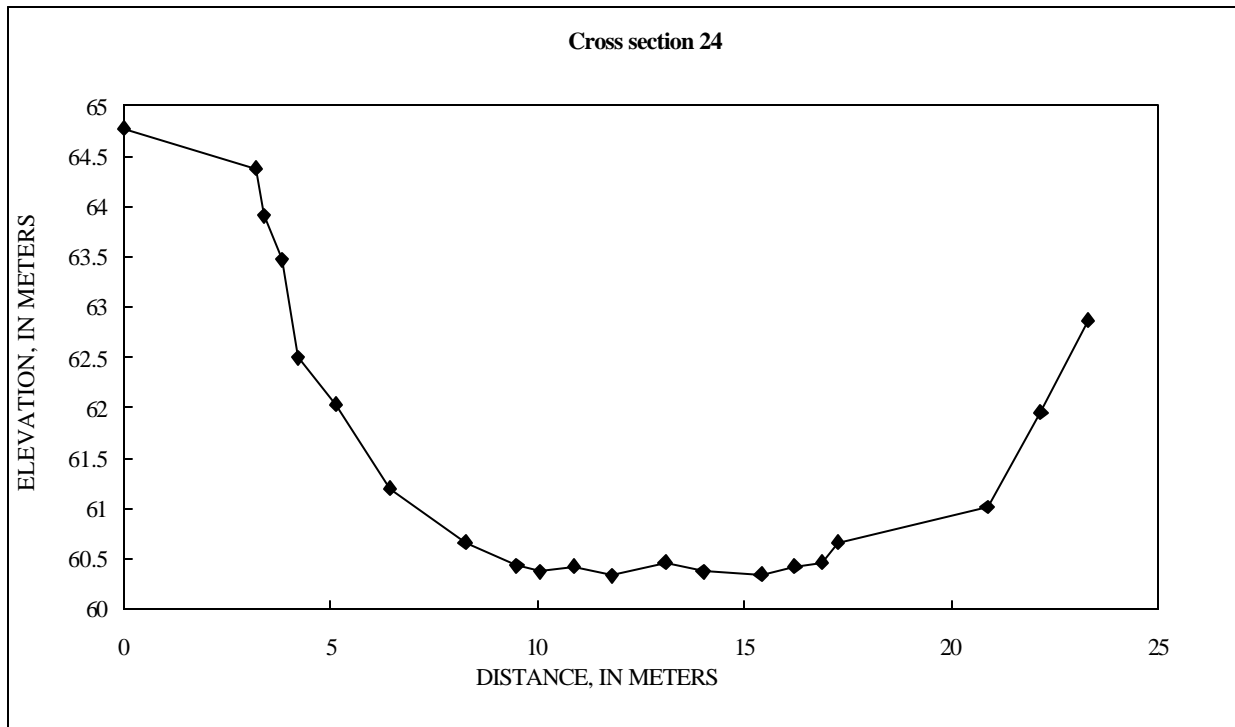
CROSS SECTION 25

SHOT #	PCODE	NORTHING (N)	EASTING (E)	ELEVATION (Z), IN METERS	DISTANCE, IN METERS	CUMULATIVE DISTANCE, IN METERS
1	START	0	0	100		
2	CS	-6176.05	8905.96	63.521	0	0
3	CS	-6177.69	8905.25	62.839	1.78	1.78
4	CS	-6179.05	8904.40	63.091	1.60	3.39
5	CS	-6180.52	8903.58	62.688	1.69	5.07
6	CS	-6181.72	8902.75	61.668	1.45	6.53
7	CS	-6182.88	8901.78	60.860	1.52	8.04
8	CS	-6183.18	8901.50	59.964	0.42	8.46
9	CS	-6183.41	8901.32	59.609	0.29	8.75
10	CS	-6184.44	8901.31	59.388	1.03	9.78
11	CS	-6185.78	8900.72	59.114	1.47	11.24
12	CS	-6187.14	8900.02	59.040	1.52	12.77
13	CS	-6188.57	8899.48	59.080	1.54	14.30
14	CS	-6189.83	8898.99	59.278	1.35	15.65
15	CS	-6190.39	8898.15	59.625	1.01	16.67
16	CS	-6190.69	8898.60	59.907	0.55	17.21
17	CS	-6191.95	8898.05	60.448	1.38	18.59
18	CS	-6193.34	8897.88	59.944	1.40	19.99
19	CS	-6194.44	8897.44	60.463	1.19	21.17
20	CS	-6195.36	8897.47	61.842	0.92	22.10
21	CS	-6197.01	8896.28	62.309	2.03	24.13
22	CS	-6198.38	8895.40	62.968	1.63	25.76
23	CS	-6199.09	8894.83	63.647	0.92	26.67



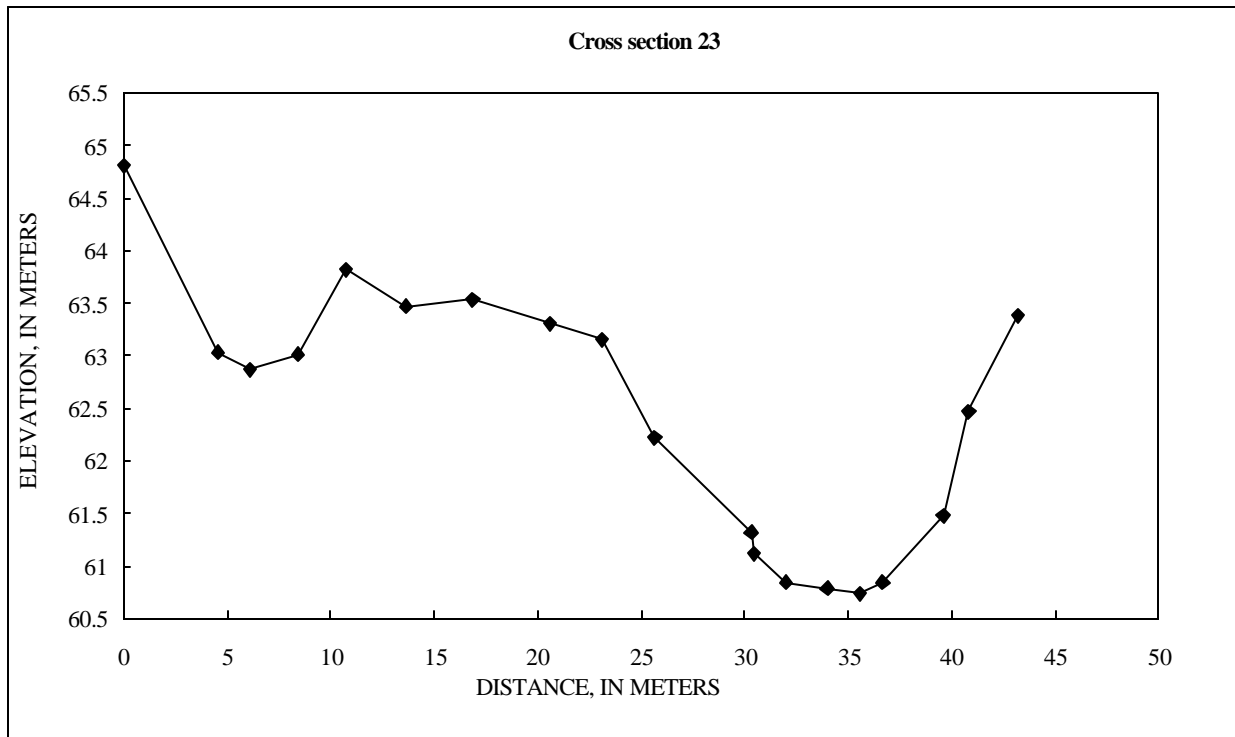
CROSS SECTION 24

SHOT #	PCODE	NORTHING (N)	EASTING (E)	ELEVATION (Z), IN METERS	DISTANCE, IN METERS	CUMULATIVE DISTANCE, IN METERS
1	START	0	0	100		
2	CS	-5770.35	8245.85	64.768	0.00	0.00
3	CS	-5771.36	8242.84	64.382	3.18	3.18
4	CS	-5771.39	8242.66	63.914	0.19	3.37
5	CS	-5771.50	8242.23	63.473	0.44	3.81
6	CS	-5771.69	8241.88	62.500	0.39	4.20
7	CS	-5771.86	8240.98	62.036	0.92	5.12
8	CS	-5772.39	8239.78	61.196	1.31	6.44
9	CS	-5772.86	8238.03	60.654	1.81	8.24
10	CS	-5773.19	8236.83	60.429	1.25	9.49
11	CS	-5773.38	8236.30	60.371	0.56	10.05
12	CS	-5773.71	8235.56	60.423	0.81	10.86
13	CS	-5774.09	8234.70	60.338	0.94	11.80
14	CS	-5774.75	8233.61	60.461	1.27	13.07
15	CS	-5775.09	8232.76	60.368	0.92	13.99
16	CS	-5775.59	8231.45	60.342	1.40	15.40
17	CS	-5775.87	8230.69	60.420	0.81	16.21
18	CS	-5776.05	8230.06	60.459	0.65	16.86
19	CS	-5776.10	8229.67	60.661	0.40	17.26
20	CS	-5776.98	8226.17	61.012	3.61	20.87
21	CS	-5777.34	8224.92	61.958	1.30	22.17
22	CS	-5777.44	8223.80	62.868	1.12	23.29



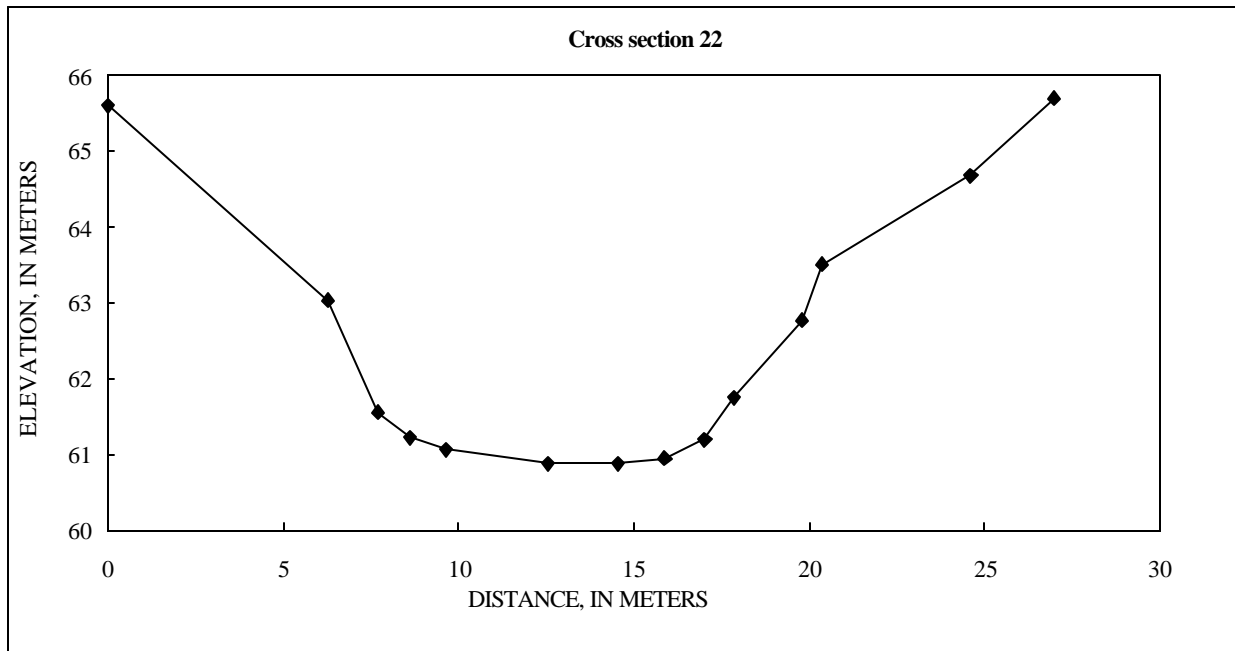
CROSS SECTION 23

SHOT #	PCODE	NORTHING (N)	EASTING (E)	ELEVATION (Z), IN METERS	DISTANCE, IN METERS	CUMULATIVE DISTANCE, IN METERS
1	START	0	0	100		
2	CS	-5399.85	7719.85	64.815	0.00	0.00
3	CS	-5398.12	7724.08	63.032	4.57	4.57
4	CS	-5397.61	7725.51	62.864	1.52	6.09
5	CS	-5396.74	7727.65	63.014	2.31	8.40
6	CS	-5395.85	7729.78	63.817	2.31	10.71
7	CS	-5394.71	7732.46	63.471	2.91	13.62
8	CS	-5393.45	7735.45	63.533	3.24	16.86
9	CS	-5391.28	7738.45	63.305	3.70	20.57
10	CS	-5390.30	7740.76	63.153	2.51	23.07
11	CS	-5389.42	7743.17	62.222	2.57	25.64
12	CS	-5387.44	7747.41	61.313	4.68	30.32
13	CS	-5387.38	7747.52	61.118	0.13	30.44
14	CS	-5386.73	7748.90	60.843	1.53	31.97
15	CS	-5385.92	7750.72	60.781	1.99	33.97
16	CS	-5385.19	7752.16	60.742	1.61	35.58
17	CS	-5384.67	7753.11	60.838	1.09	36.66
18	CS	-5383.40	7755.73	61.478	2.91	39.58
19	CS	-5383.01	7756.92	62.468	1.25	40.83
20	CS	-5382.08	7759.06	63.384	2.33	43.16



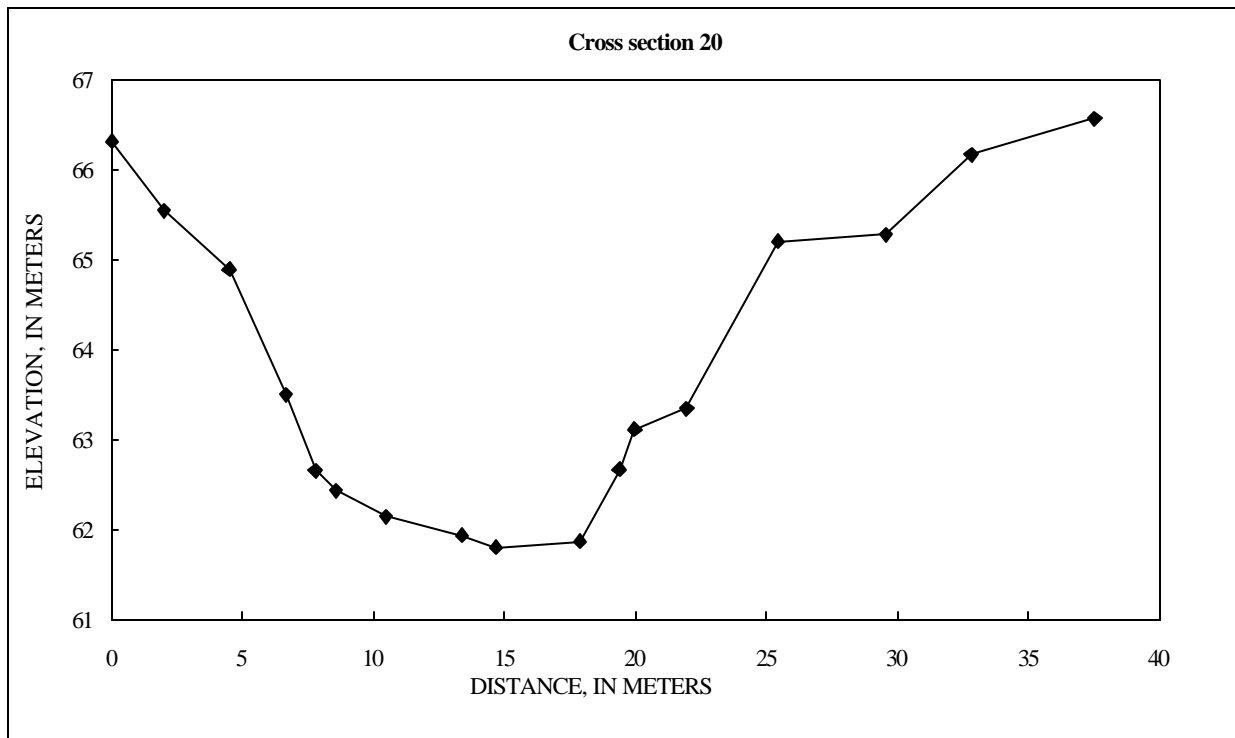
CROSS SECTION 22

SHOT #	PCODE	NORTHING (N)	EASTING (E)	ELEVATION (Z), IN METERS	DISTANCE, IN METERS	CUMULATIVE DISTANCE, IN METERS
1	START	0	0	100		
2	CS	-5092.84	7263.37	65.596	0.00	0.00
3	CS	-5091.72	7269.54	63.038	6.27	6.27
4	CS	-5092.65	7270.61	61.549	1.42	7.69
5	CS	-5092.38	7271.49	61.221	0.93	8.62
6	CS	-5092.18	7272.51	61.062	1.04	9.65
7	CS	-5091.42	7275.30	60.875	2.89	12.54
8	CS	-5091.05	7277.26	60.881	2.00	14.54
9	CS	-5090.71	7278.55	60.950	1.34	15.88
10	CS	-5090.43	7279.65	61.204	1.14	17.01
11	CS	-5090.13	7280.46	61.751	0.86	17.87
12	CS	-5089.29	7282.18	62.766	1.92	19.79
13	CS	-5089.39	7282.76	63.505	0.59	20.37
14	CS	-5087.58	7286.59	64.679	4.24	24.61
15	CS	-5086.96	7288.87	65.690	2.37	26.98



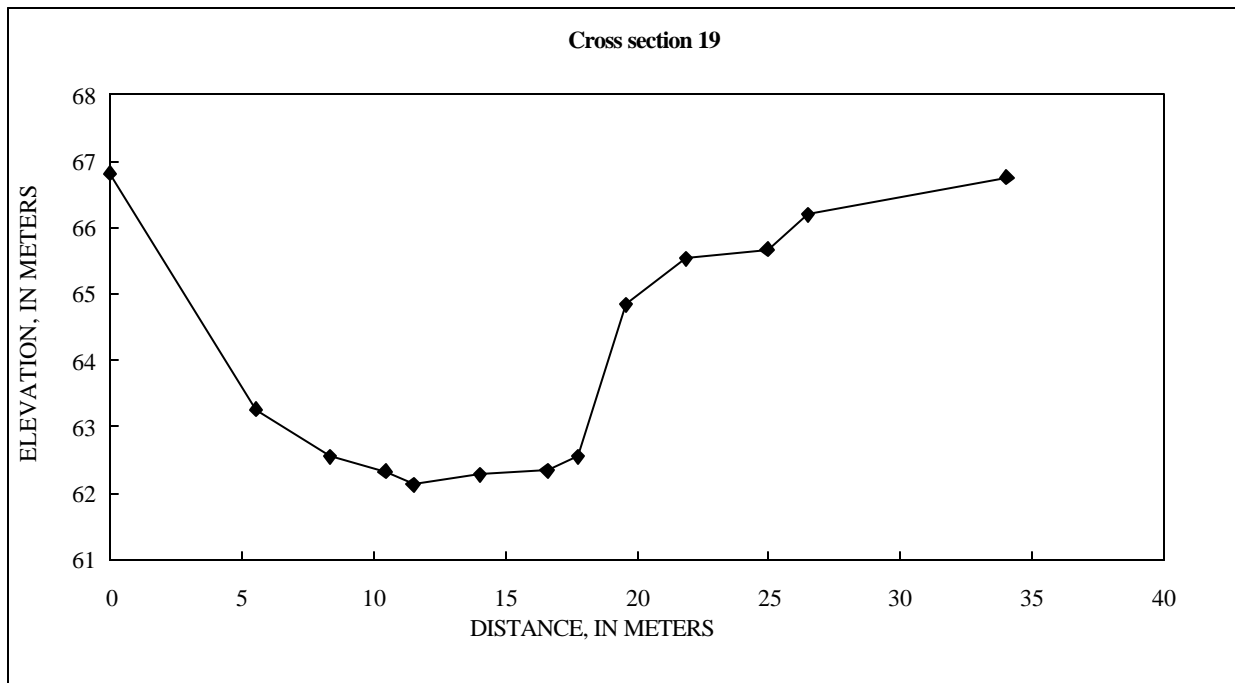
CROSS SECTION 20

SHOT #	PCODE	NORTHING (N)	EASTING (E)	ELEVATION (Z), IN METERS	DISTANCE, IN METERS	CUMULATIVE DISTANCE, IN METERS
1	START	0	0	100		
2	CS	-4790.60	7003.79	66.315	0.00	0.00
3	CS	-4788.82	7004.76	65.547	2.03	2.03
4	CS	-4786.57	7005.75	64.888	2.46	4.49
5	CS	-4784.58	7006.66	63.501	2.19	6.68
6	CS	-4783.57	7007.11	62.664	1.10	7.78
7	CS	-4782.90	7007.51	62.439	0.78	8.56
8	CS	-4781.27	7008.49	62.148	1.91	10.47
9	CS	-4778.76	7009.95	61.942	2.90	13.37
10	CS	-4777.60	7010.53	61.803	1.30	14.67
11	CS	-4774.82	7012.07	61.867	3.18	17.85
12	CS	-4773.42	7012.71	62.672	1.54	19.39
13	CS	-4772.97	7013.10	63.113	0.59	19.97
14	CS	-4771.22	7014.02	63.344	1.98	21.96
15	CS	-4768.15	7015.67	65.201	3.49	25.44
16	CS	-4764.63	7017.74	65.282	4.08	29.53
17	CS	-4761.80	7019.41	66.169	3.28	32.81
18	CS	-4757.57	7021.45	66.568	4.70	37.51



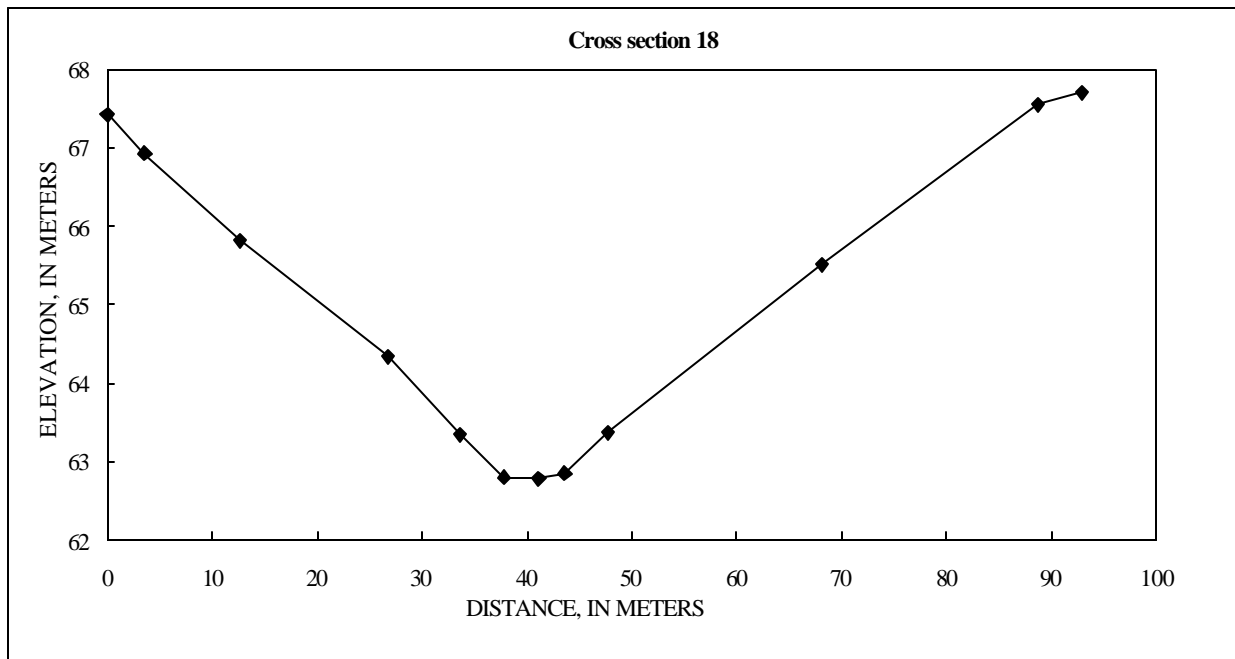
CROSS SECTION 19

SHOT #	PCODE	NORTHING (N)	EASTING (E)	ELEVATION (Z), IN METERS	DISTANCE, IN METERS	CUMULATIVE DISTANCE, IN METERS
1	START	0	0	100		
2	CS	-4247.43	6652.45	66.814	0.00	0.00
3	CS	-4250.72	6648.00	63.263	5.53	5.53
4	CS	-4252.96	6646.33	62.548	2.80	8.33
5	CS	-4254.28	6644.68	62.328	2.11	10.44
6	CS	-4255.16	6644.12	62.128	1.04	11.48
7	CS	-4257.16	6642.56	62.274	2.53	14.02
8	CS	-4258.80	6640.58	62.332	2.58	16.59
9	CS	-4259.53	6639.65	62.552	1.18	17.77
10	CS	-4260.96	6638.50	64.834	1.84	19.61
11	CS	-4262.73	6637.12	65.538	2.24	21.85
12	CS	-4265.09	6635.11	65.676	3.10	24.95
13	CS	-4266.19	6634.02	66.196	1.55	26.50
14	CS	-4271.53	6628.68	66.751	7.56	34.06



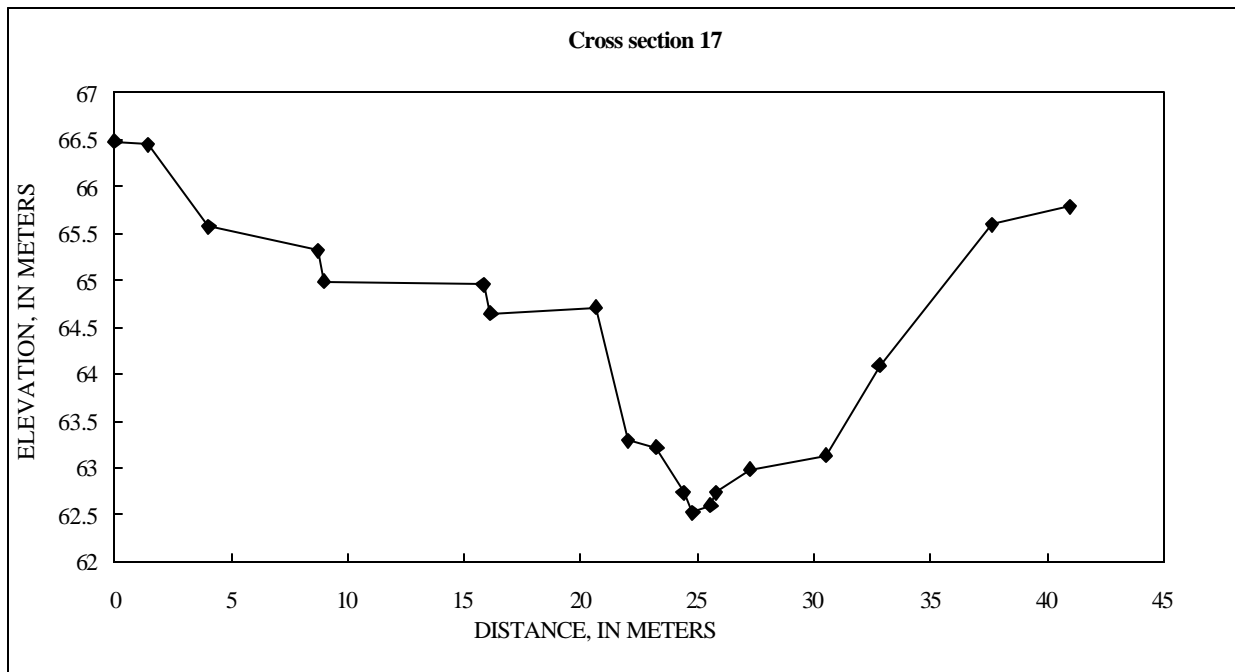
CROSS SECTION 18

SHOT #	PCODE	NORTHING (N)	EASTING (E)	ELEVATION (Z), IN METERS	DISTANCE, IN METERS	CUMULATIVE DISTANCE, IN METERS
1	START	0	0	100		
2	CS	-4146.07	6527.34	67.421	0.00	0.00
3	CS	-4149.10	6525.47	66.930	3.57	3.57
4	CS	-4157.30	6521.46	65.816	9.12	12.69
5	CS	-4170.03	6515.51	64.338	14.05	26.74
6	CS	-4176.02	6512.14	63.341	6.88	33.62
7	CS	-4179.54	6509.84	62.805	4.21	37.82
8	CS	-4182.38	6508.18	62.790	3.29	41.11
9	CS	-4184.43	6506.75	62.854	2.50	43.61
10	CS	-4187.76	6504.42	63.371	4.07	47.68
11	CS	-4204.67	6492.85	65.514	20.49	68.17
12	CS	-4221.81	6481.63	67.546	20.49	88.65
13	CS	-4225.39	6479.37	67.698	4.24	92.89



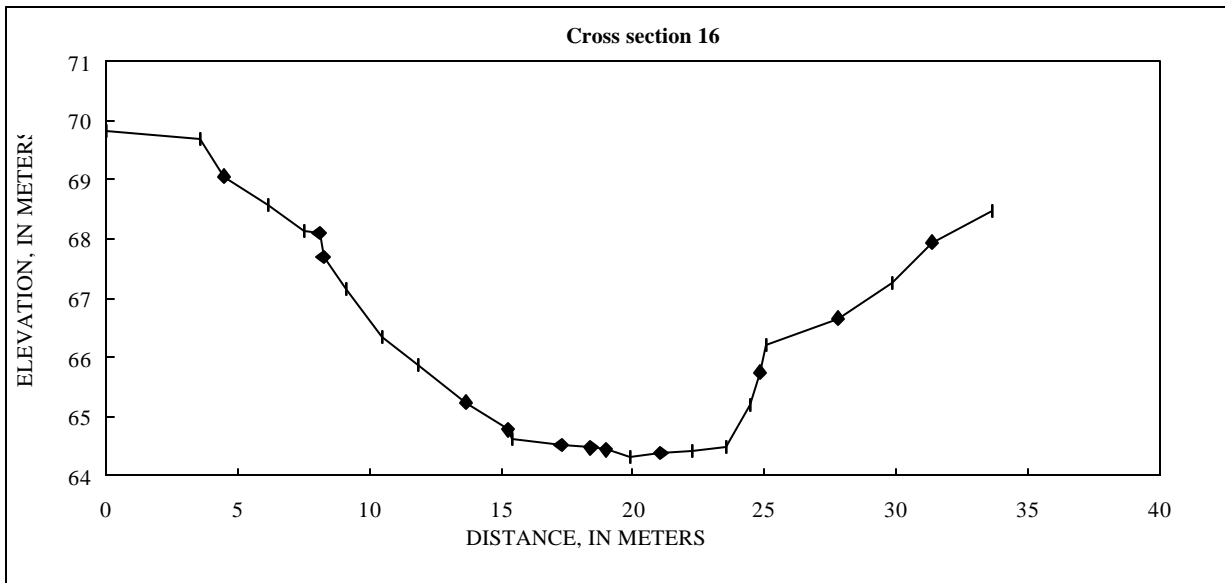
CROSS SECTION 17

SHOT #	PCODE	NORTHING (N)	EASTING (E)	ELEVATION (Z), IN METERS	DISTANCE, IN METERS	CUMULATIVE DISTANCE, IN METERS
1	START	0	0	100		
2	CS	-4070.95	6426.77	66.483	0.00	0.00
3	CS	-4071.60	6425.48	66.443	1.45	1.45
4	CS	-4073.05	6423.35	65.575	2.58	4.03
5	CS	-4075.06	6419.09	65.321	4.70	8.73
6	CS	-4075.17	6418.89	64.987	0.23	8.96
7	CS	-4078.73	6413.04	64.960	6.85	15.81
8	CS	-4078.83	6412.72	64.649	0.34	16.15
9	CS	-4080.98	6408.73	64.711	4.53	20.68
10	CS	-4081.90	6407.74	63.291	1.35	22.02
11	CS	-4082.49	6406.66	63.215	1.23	23.26
12	CS	-4083.01	6405.65	62.730	1.14	24.40
13	CS	-4083.31	6405.35	62.526	0.42	24.82
14	CS	-4083.86	6404.82	62.603	0.77	25.58
15	CS	-4083.93	6404.63	62.736	0.20	25.78
16	CS	-4084.91	6403.55	62.977	1.46	27.24
17	CS	-4087.01	6400.98	63.134	3.31	30.55
18	CS	-4088.43	6399.23	64.087	2.26	32.81
19	CS	-4090.52	6394.89	65.598	4.82	37.63
20	CS	-4092.35	6392.09	65.790	3.34	40.97



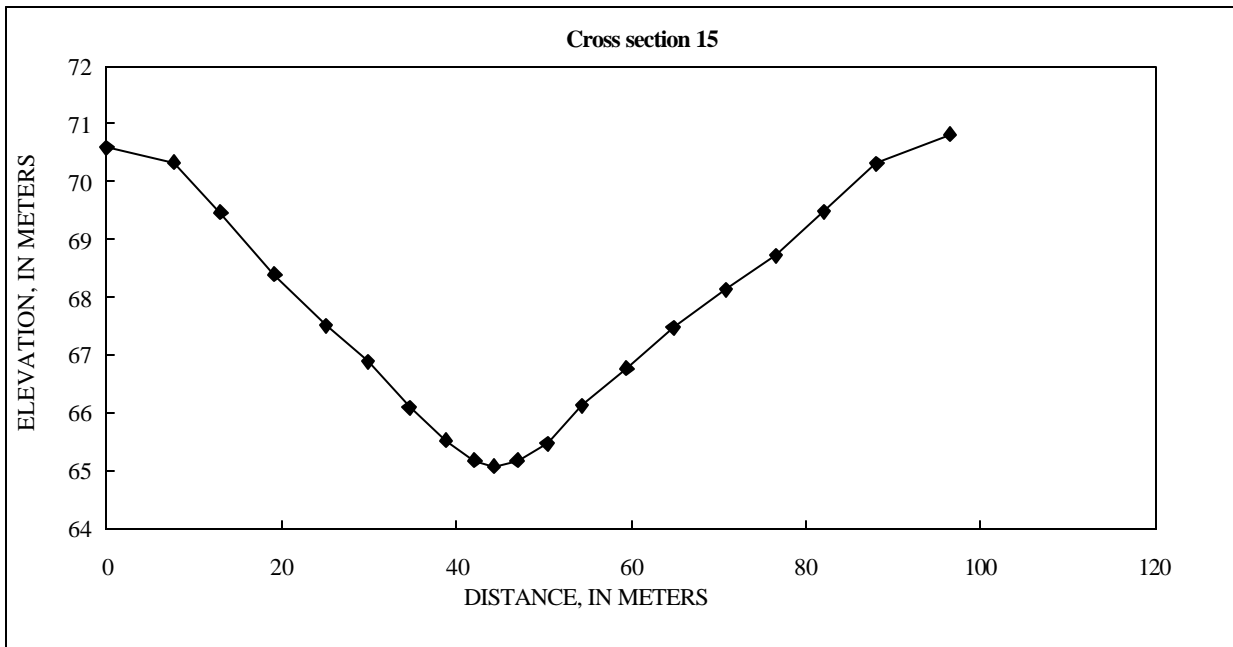
CROSS SECTION 16

SHOT #	PCODE	NORTHING (N)	EASTING (E)	ELEVATION (Z), IN METERS	DISTANCE, IN METERS	CUMULATIVE DISTANCE, IN METERS
1	START	0	0	100		
2	CS	-3631.21	5704.38	69.843	0.00	0.00
3	CS	-3631.51	5700.85	69.701	3.55	3.55
4	CS	-3631.76	5699.94	69.069	0.94	4.49
5	CS	-3631.41	5698.32	68.572	1.66	6.15
6	CS	-3631.14	5696.99	68.130	1.36	7.50
7	CS	-3630.97	5696.44	68.109	0.58	8.08
8	CS	-3630.88	5696.32	67.713	0.15	8.23
9	CS	-3630.85	5695.46	67.166	0.86	9.09
10	CS	-3630.72	5694.07	66.352	1.40	10.49
11	CS	-3630.82	5692.70	65.867	1.37	11.86
12	CS	-3630.85	5690.90	65.241	1.80	13.65
13	CS	-3630.92	5689.32	64.778	1.59	15.24
14	CS	-3630.90	5689.13	64.628	0.19	15.43
15	CS	-3630.95	5687.28	64.508	1.85	17.28
16	CS	-3630.93	5686.16	64.466	1.13	18.41
17	CS	-3630.91	5685.55	64.436	0.60	19.01
18	CS	-3630.83	5684.67	64.326	0.89	19.89
19	CS	-3630.88	5683.49	64.383	1.18	21.07
20	CS	-3630.85	5682.34	64.409	1.15	22.23
21	CS	-3630.73	5681.04	64.483	1.30	23.53
22	CS	-3631.09	5680.19	65.198	0.92	24.45
23	CS	-3631.10	5679.81	65.754	0.38	24.83
24	CS	-3631.14	5679.58	66.207	0.23	25.06
25	CS	-3632.15	5677.07	66.668	2.71	27.78
26	CS	-3632.24	5674.98	67.254	2.09	29.86
27	CS	-3632.00	5673.46	67.954	1.54	31.40
28	CS	-3631.83	5671.23	68.480	2.23	33.64



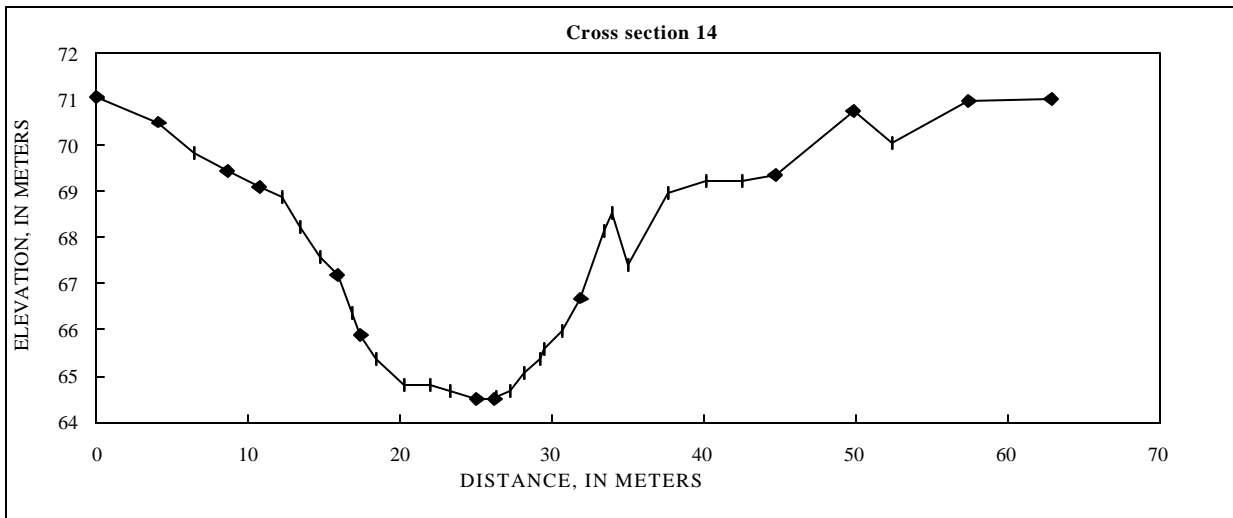
CROSS SECTION 15

SHOT #	PCODE	NORTHING (N)	EASTING (E)	ELEVATION (Z), IN METERS	DISTANCE, IN METERS	CUMULATIVE DISTANCE, IN METERS
1	START	0	0	100		
2	CS	-3185.29	5491.76	70.600	0.00	0.00
3	CS	-3191.65	5487.38	70.336	7.72	7.72
4	CS	-3195.69	5483.89	69.467	5.34	13.06
5	CS	-3200.06	5479.54	68.390	6.17	19.23
6	CS	-3204.23	5475.45	67.508	5.83	25.07
7	CS	-3207.70	5472.06	66.875	4.85	29.92
8	CS	-3210.80	5468.54	66.087	4.69	34.61
9	CS	-3213.50	5465.40	65.526	4.15	38.75
10	CS	-3215.49	5462.69	65.178	3.36	42.11
11	CS	-3216.58	5460.74	65.077	2.24	44.35
12	CS	-3218.24	5458.73	65.177	2.61	46.96
13	CS	-3220.32	5455.96	65.462	3.46	50.42
14	CS	-3222.81	5452.89	66.133	3.95	54.37
15	CS	-3225.59	5448.56	66.766	5.15	59.52
16	CS	-3228.51	5444.12	67.471	5.31	64.83
17	CS	-3231.96	5439.14	68.134	6.07	70.90
18	CS	-3234.88	5434.19	68.728	5.74	76.64
19	CS	-3237.91	5429.59	69.477	5.51	82.15
20	CS	-3241.32	5424.65	70.308	6.01	88.15
21	CS	-3246.50	5418.01	70.817	8.42	96.57



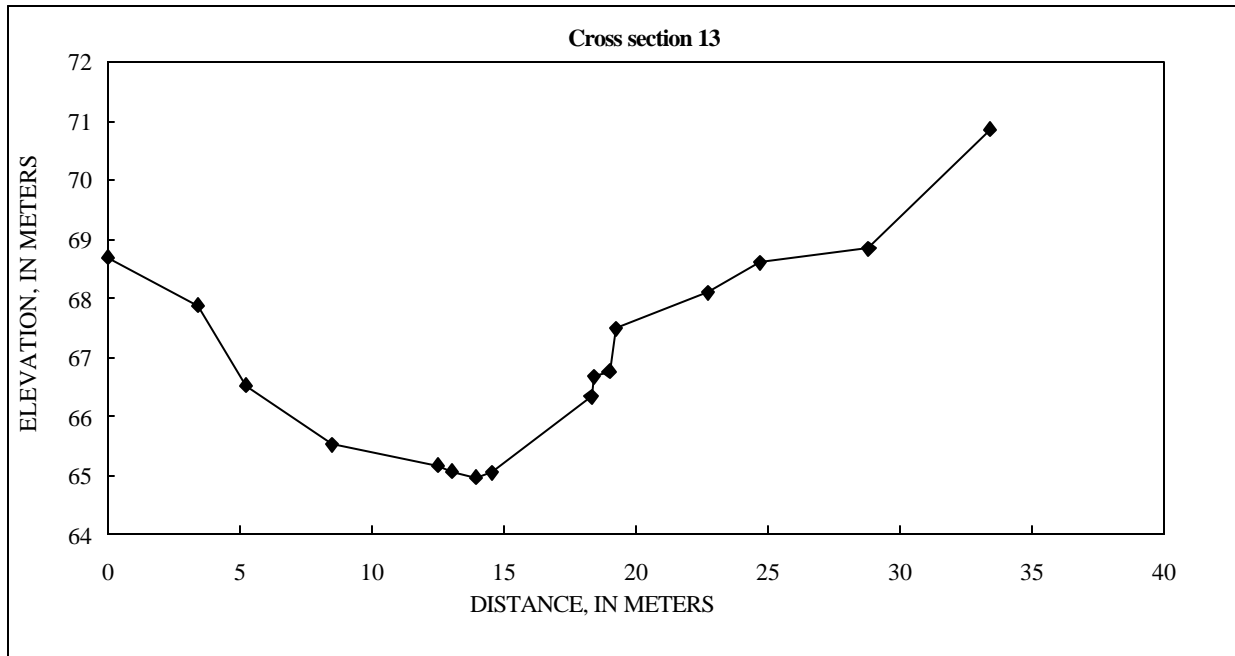
CROSS SECTION 14

SHOT #	PCODE	NORTHING (N)	EASTING (E)	ELEVATION (Z), IN METERS	DISTANCE, IN METERS	CUMULATIVE DISTANCE, IN METERS
1	START	0	0	100		
2	CS	-3097.34	5411.99	71.057	0.00	0.00
3	CS	-3100.06	5408.92	70.507	4.09	4.09
4	CS	-3101.78	5407.38	69.820	2.31	6.41
5	CS	-3103.41	5405.90	69.447	2.20	8.61
6	CS	-3104.83	5404.38	69.113	2.08	10.69
7	CS	-3105.72	5403.20	68.870	1.48	12.17
8	CS	-3106.56	5402.33	68.220	1.21	13.37
9	CS	-3107.33	5401.28	67.582	1.31	14.68
10	CS	-3108.05	5400.38	67.178	1.15	15.83
11	CS	-3108.73	5399.73	66.367	0.94	16.77
12	CS	-3108.83	5399.13	65.894	0.61	17.38
13	CS	-3109.48	5399.85	65.353	0.97	18.35
14	CS	-3110.32	5398.18	64.796	1.87	20.21
15	CS	-3111.11	5396.63	64.821	1.74	21.95
16	CS	-3111.97	5395.60	64.682	1.35	23.30
17	CS	-3113.15	5394.29	64.484	1.76	25.06
18	CS	-3113.73	5393.29	64.517	1.16	26.22
19	CS	-3113.79	5393.25	64.530	0.08	26.29
20	CS	-3114.43	5392.63	64.683	0.89	27.18
21	CS	-3115.01	5391.87	65.077	0.95	28.14
22	CS	-3115.84	5391.20	65.378	1.07	29.20
23	CS	-3115.88	5391.00	65.597	0.20	29.41
24	CS	-3116.72	5390.15	65.982	1.20	30.61
25	CS	-3117.44	5389.11	66.692	1.27	31.87
26	CS	-3117.88	5387.66	68.146	1.51	33.38
27	CS	-3118.10	5387.12	68.516	0.59	33.97
28	CS	-3118.10	5388.15	67.424	1.03	35.00
29	CS	-3119.56	5385.97	68.973	2.63	37.63
30	CS	-3121.09	5383.96	69.246	2.53	40.15
31	CS	-3122.41	5382.03	69.239	2.33	42.48
32	CS	-3123.66	5380.19	69.357	2.23	44.71
33	CS	-3125.39	5375.36	70.733	5.13	49.84
34	CS	-3125.47	5377.92	70.069	2.56	52.40
35	CS	-3127.33	5373.24	70.953	5.04	57.43
36	CS	-3130.50	5368.85	70.996	5.42	62.85



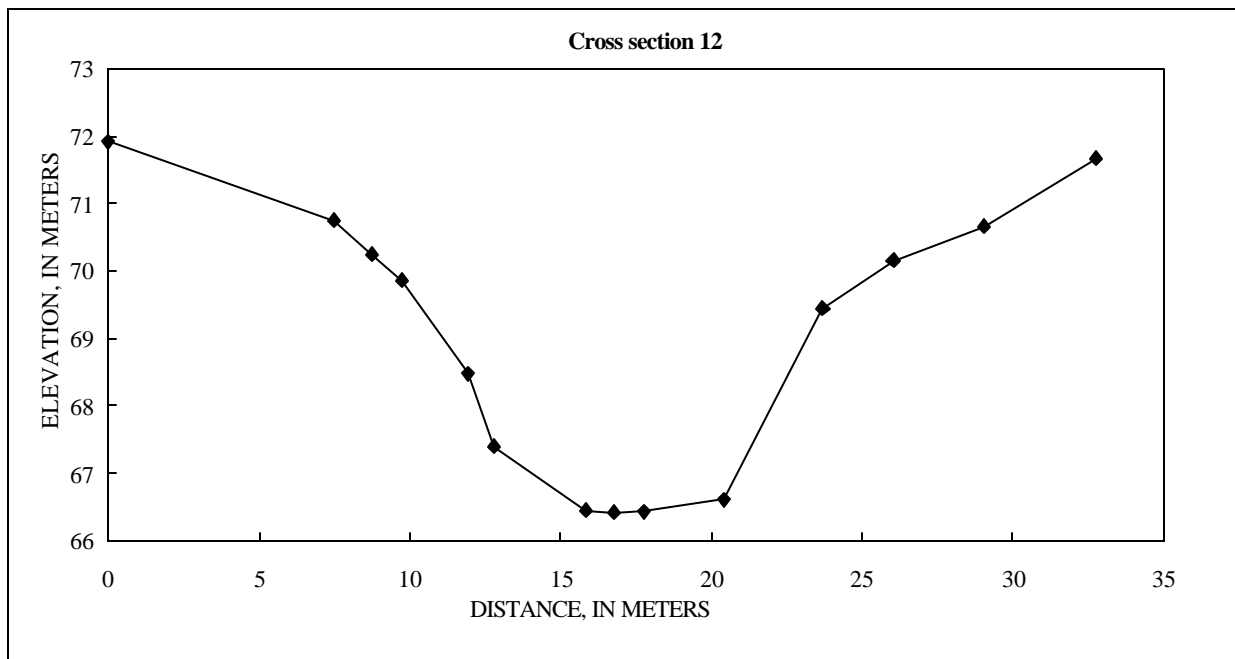
CROSS SECTION 13

SHOT #	PCODE	NORTHING (N)	EASTING (E)	ELEVATION (Z), IN METERS	DISTANCE, IN METERS	CUMULATIVE DISTANCE, IN METERS
1	START	0	0	100		
2	CS	-2696.35	4724.58	68.696	0.00	0.00
3	CS	-2699.76	4724.36	67.879	3.42	3.42
4	CS	-2701.55	4724.28	66.516	1.80	5.21
5	CS	-2704.82	4724.49	65.529	3.28	8.49
6	CS	-2708.82	4724.53	65.165	4.00	12.49
7	CS	-2709.35	4724.69	65.055	0.55	13.04
8	CS	-2710.22	4724.42	64.957	0.92	13.95
9	CS	-2710.81	4724.35	65.054	0.59	14.55
10	CS	-2714.56	4724.21	66.339	3.76	18.30
11	CS	-2714.69	4724.21	66.666	0.13	18.43
12	CS	-2715.24	4724.32	66.759	0.56	18.99
13	CS	-2715.51	4724.42	67.480	0.29	19.28
14	CS	-2719.00	4724.48	68.102	3.49	22.77
15	CS	-2720.97	4724.50	68.608	1.97	24.74
16	CS	-2724.84	4723.17	68.843	4.09	28.83
17	CS	-2729.43	4723.58	70.855	4.61	33.44



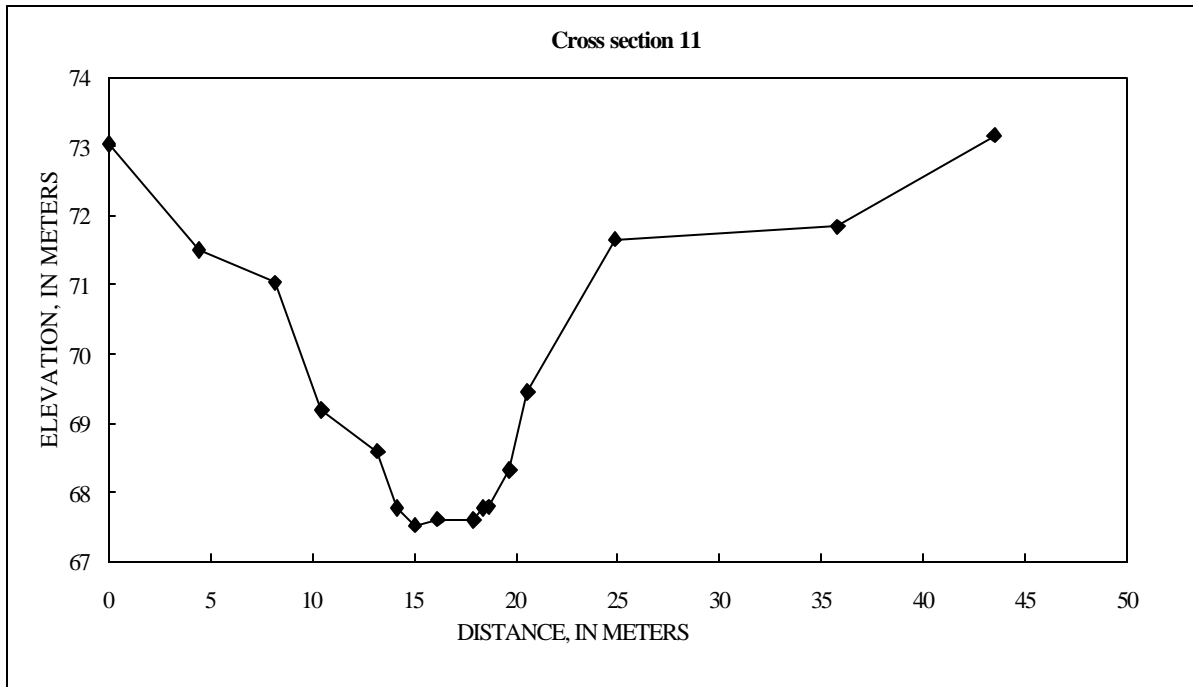
CROSS SECTION 12

SHOT #	PCODE	NORTHING (N)	EASTING (E)	ELEVATION (Z), IN METERS	DISTANCE, IN METERS	CUMULATIVE DISTANCE, IN METERS
1	START	0	0	100		
2	CS	-2117.37	4298.73	71.925	0.00	0.00
3	CS	-2123.82	4294.93	70.750	7.48	7.48
4	CS	-2124.81	4294.14	70.245	1.26	8.75
5	CS	-2125.72	4293.69	69.859	1.02	9.76
6	CS	-2127.62	4292.61	68.488	2.19	11.95
7	CS	-2128.39	4292.33	67.398	0.82	12.77
8	CS	-2131.07	4290.80	66.441	3.09	15.86
9	CS	-2131.89	4290.36	66.414	0.93	16.79
10	CS	-2132.72	4289.86	66.429	0.97	17.76
11	CS	-2135.05	4288.56	66.612	2.67	20.43
12	CS	-2138.02	4287.17	69.441	3.27	23.70
13	CS	-2140.15	4286.25	70.159	2.33	26.03
14	CS	-2142.77	4284.77	70.662	3.01	29.03
15	CS	-2146.19	4283.33	71.669	3.71	32.74



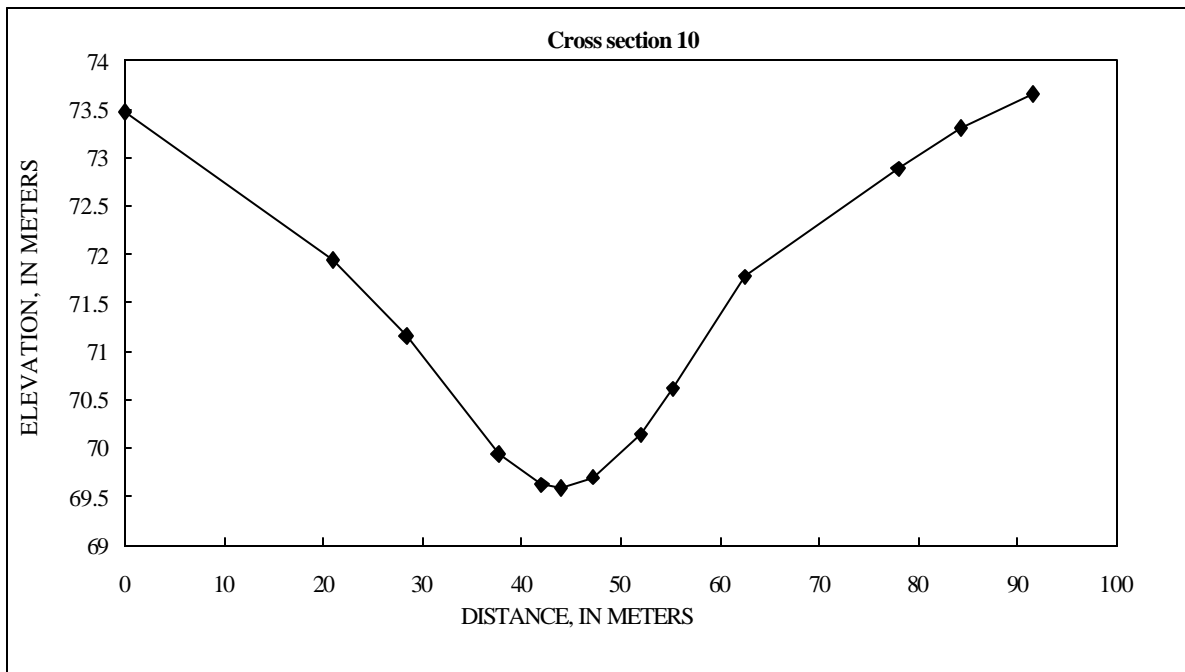
CROSS SECTION 11

SHOT #	PCODE	NORTHING (N)	EASTING (E)	ELEVATION (Z), IN METERS	DISTANCE, IN METERS	CUMULATIVE DISTANCE, IN METERS
1	START	0	0	100		
2	CS	-1828.73	3747.28	73.041	0.00	0.00
3	CS	-1832.93	3745.96	71.513	4.40	4.40
4	CS	-1836.44	3744.63	71.040	3.76	8.16
5	CS	-1838.70	3744.30	69.195	2.28	10.45
6	CS	-1841.42	3743.85	68.596	2.75	13.20
7	CS	-1842.23	3744.35	67.767	0.95	14.15
8	CS	-1843.08	3744.07	67.519	0.89	15.04
9	CS	-1844.19	3743.92	67.609	1.12	16.16
10	CS	-1845.93	3743.68	67.597	1.76	17.91
11	CS	-1846.41	3743.71	67.772	0.49	18.40
12	CS	-1846.65	3743.74	67.797	0.24	18.64
13	CS	-1847.69	3743.76	68.317	1.05	19.68
14	CS	-1848.16	3743.01	69.444	0.89	20.57
15	CS	-1852.18	3741.43	71.668	4.32	24.89
16	CS	-1862.51	3737.94	71.844	10.91	35.79
17	CS	-1869.62	3735.03	73.177	7.68	43.47



CROSS SECTION 10

SHOT #	PCODE	NORTHING (N)	EASTING (E)	ELEVATION (Z), IN METERS	DISTANCE, IN METERS	CUMULATIVE DISTANCE, IN METERS
1	START	-1777.28	3667.97	73.475	0.00	0.00
2	CS	-1794.44	3655.95	71.941	20.95	20.95
3	CS	-1800.88	3652.20	71.160	7.45	28.40
4	CS	-1809.28	3648.28	69.939	9.27	37.67
5	CS	-1813.38	3646.72	69.629	4.38	42.05
6	CS	-1815.11	3645.92	69.592	1.91	43.96
7	CS	-1818.00	3644.54	69.698	3.20	47.16
8	CS	-1822.46	3642.62	70.143	4.85	52.02
9	CS	-1825.33	3641.14	70.612	3.23	55.25
10	CS	-1831.50	3637.15	71.771	7.35	62.60
11	CS	-1845.24	3630.17	72.886	15.41	78.01
12	CS	-1850.90	3627.34	73.310	6.33	84.33
13	CS	-1857.16	3623.73	73.653	7.23	91.57
14	CS	-1777.28	3667.97	73.475	0.00	0.00



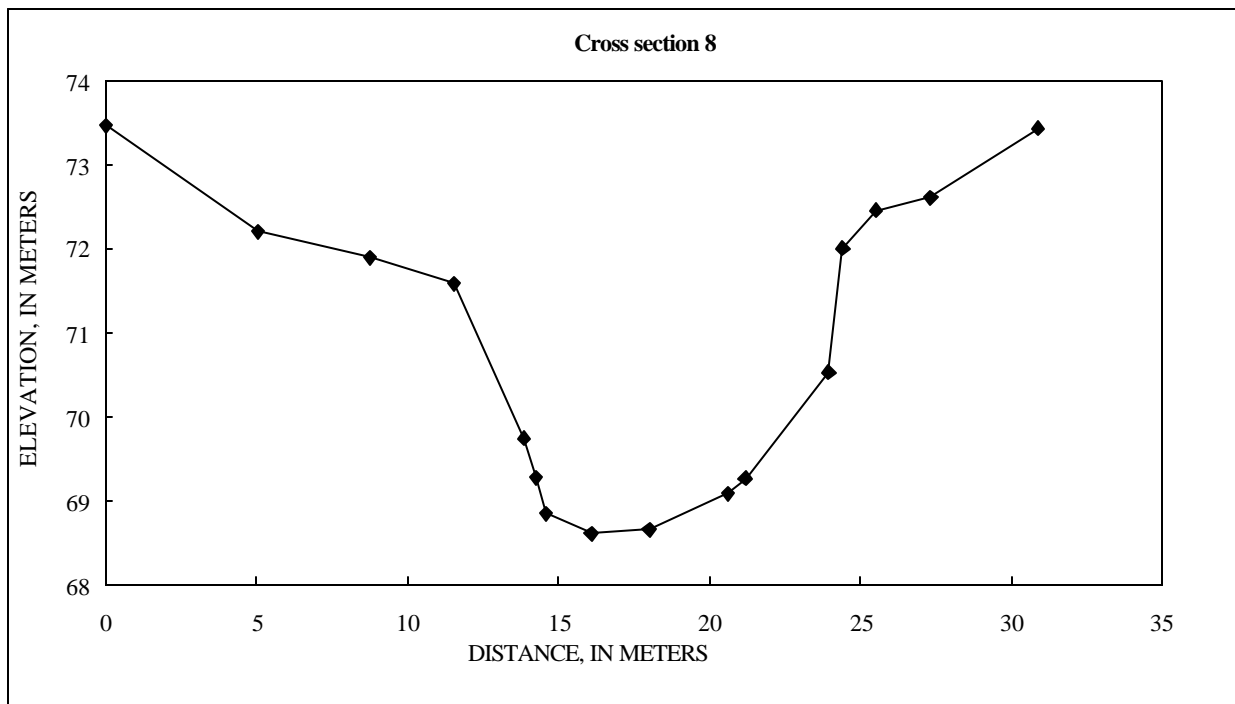
CROSS SECTION 9

SHOT #	PCODE	NORTHING (N)	EASTING (E)	ELEVATION (Z), IN METERS	DISTANCE, IN METERS	CUMULATIVE DISTANCE, IN METERS
1	START	0	0	100		
2	CS	-1745.14	3549.15	73.373	0.00	0.00
3	CS	-1749.29	3546.66	73.108	4.84	4.84
4	CS	-1751.86	3545.28	72.626	2.92	7.76
5	CS	-1753.07	3544.31	72.035	1.55	9.30
6	CS	-1757.02	3541.65	71.395	4.76	14.07
7	CS	-1757.13	3541.60	71.078	0.12	14.18
8	CS	-1758.34	3541.13	70.153	1.30	15.48
9	CS	-1758.67	3541.06	69.605	0.34	15.82
10	CS	-1758.83	3540.96	69.348	0.19	16.01
11	CS	-1760.17	3539.95	68.650	1.67	17.68
12	CS	-1760.89	3539.57	68.465	0.81	18.50
13	CS	-1764.98	3536.88	68.624	4.90	23.40
14	CS	-1766.01	3536.47	69.127	1.10	24.50
15	CS	-1766.55	3536.43	69.579	0.54	25.04
16	CS	-1766.56	3536.53	69.704	0.11	25.15
17	CS	-1768.84	3535.27	71.360	2.61	27.76
18	CS	-1770.18	3534.69	71.603	1.46	29.22
19	CS	-1772.72	3532.79	72.364	3.17	32.39
20	CS	-1777.23	3530.09	73.286	5.26	37.65



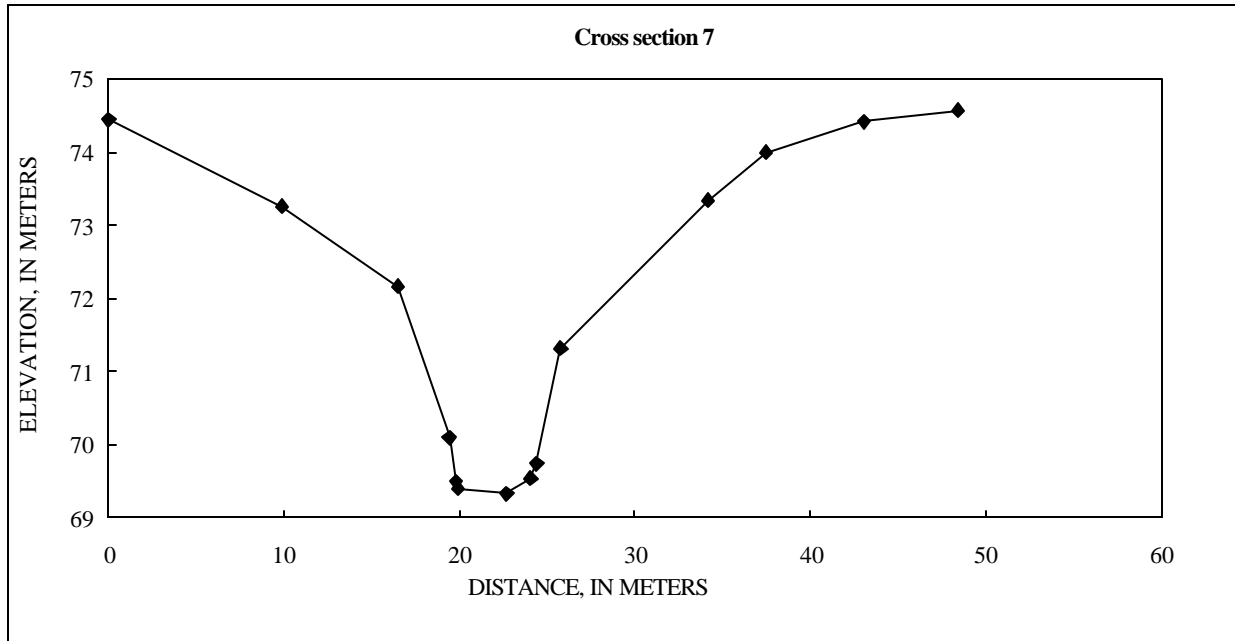
CROSS SECTION 8

SHOT #	PCODE	NORTHING (N)	EASTING (E)	ELEVATION (Z), IN METERS	DISTANCE, IN METERS	CUMULATIVE DISTANCE, IN METERS
1	START	0	0	100		
2	CS	-1486.84	2990.72	73.466	0.00	0.00
3	CS	-1491.88	2990.26	72.215	5.06	5.06
4	CS	-1495.33	2988.97	71.905	3.68	8.74
5	CS	-1497.92	2987.92	71.591	2.79	11.53
6	CS	-1500.19	2988.31	69.747	2.31	13.84
7	CS	-1500.59	2988.35	69.283	0.41	14.25
8	CS	-1500.91	2988.33	68.856	0.32	14.57
9	CS	-1502.36	2987.87	68.613	1.52	16.08
10	CS	-1504.09	2987.06	68.661	1.91	17.99
11	CS	-1506.46	2985.91	69.087	2.64	20.63
12	CS	-1507.01	2986.03	69.273	0.57	21.19
13	CS	-1509.64	2986.88	70.536	2.76	23.96
14	CS	-1509.65	2986.42	72.008	0.47	24.42
15	CS	-1510.69	2986.15	72.463	1.08	25.50
16	CS	-1512.49	2985.77	72.619	1.84	27.33
17	CS	-1515.95	2985.04	73.444	3.54	30.88



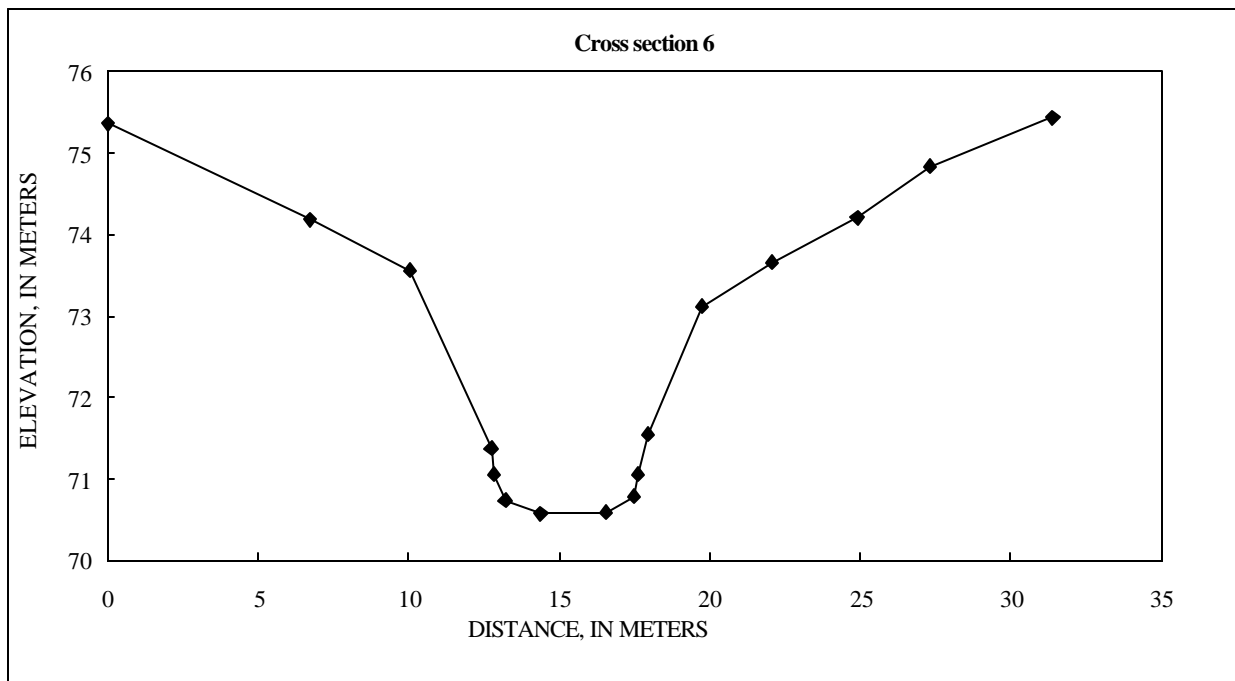
CROSS SECTION 7

SHOT #	PCODE	NORTHING (N)	EASTING (E)	ELEVATION (Z), IN METERS	DISTANCE, IN METERS	CUMULATIVE DISTANCE, IN METERS
1	START	0	0	100		
2	CS	-1268.72	2525.24	74.444	0.00	0.00
3	CS	-1277.40	2520.54	73.252	9.87	9.87
4	CS	-1283.43	2517.70	72.161	6.66	16.53
5	CS	-1285.64	2515.86	70.108	2.88	19.41
6	CS	-1285.99	2515.73	69.490	0.37	19.78
7	CS	-1286.10	2515.75	69.400	0.11	19.89
8	CS	-1288.87	2515.22	69.342	2.83	22.71
9	CS	-1290.10	2514.62	69.544	1.37	24.08
10	CS	-1290.41	2514.55	69.742	0.32	24.40
11	CS	-1290.75	2513.22	71.317	1.37	25.77
12	CS	-1298.54	2510.10	73.346	8.39	34.16
13	CS	-1301.62	2508.84	73.992	3.33	37.49
14	CS	-1306.76	2506.72	74.417	5.57	43.05
15	CS	-1311.57	2504.33	74.576	5.37	48.43



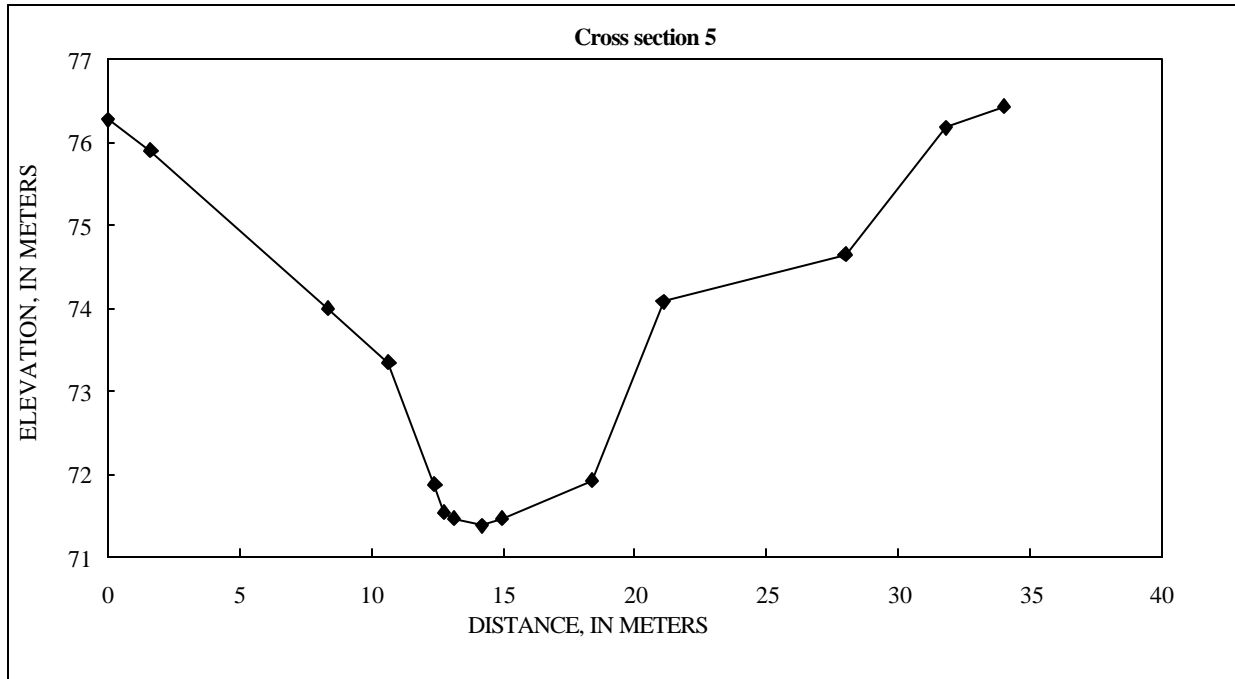
CROSS SECTION 6

SHOT #	PCODE	NORTHING (N)	EASTING (E)	ELEVATION (Z), IN METERS	DISTANCE, IN METERS	CUMULATIVE DISTANCE, IN METERS
1	START	0	0	100		
2	CS	-957.18	2036.10	75.367	0.00	0.00
3	CS	-962.27	2031.72	74.185	6.72	6.72
4	CS	-964.48	2029.22	73.557	3.33	10.05
5	CS	-966.38	2027.33	71.378	2.69	12.73
6	CS	-966.41	2027.24	71.056	0.09	12.83
7	CS	-966.69	2026.99	70.741	0.38	13.20
8	CS	-967.32	2025.98	70.582	1.19	14.39
9	CS	-968.54	2024.21	70.587	2.15	16.54
10	CS	-969.32	2023.73	70.784	0.92	17.46
11	CS	-969.50	2023.71	71.058	0.17	17.64
12	CS	-969.78	2023.55	71.542	0.32	17.95
13	CS	-971.02	2022.30	73.124	1.76	19.72
14	CS	-972.87	2020.88	73.654	2.34	22.06
15	CS	-975.03	2019.06	74.203	2.82	24.88
16	CS	-976.61	2017.23	74.839	2.42	27.30
17	CS	-979.30	2014.13	75.442	4.10	31.40



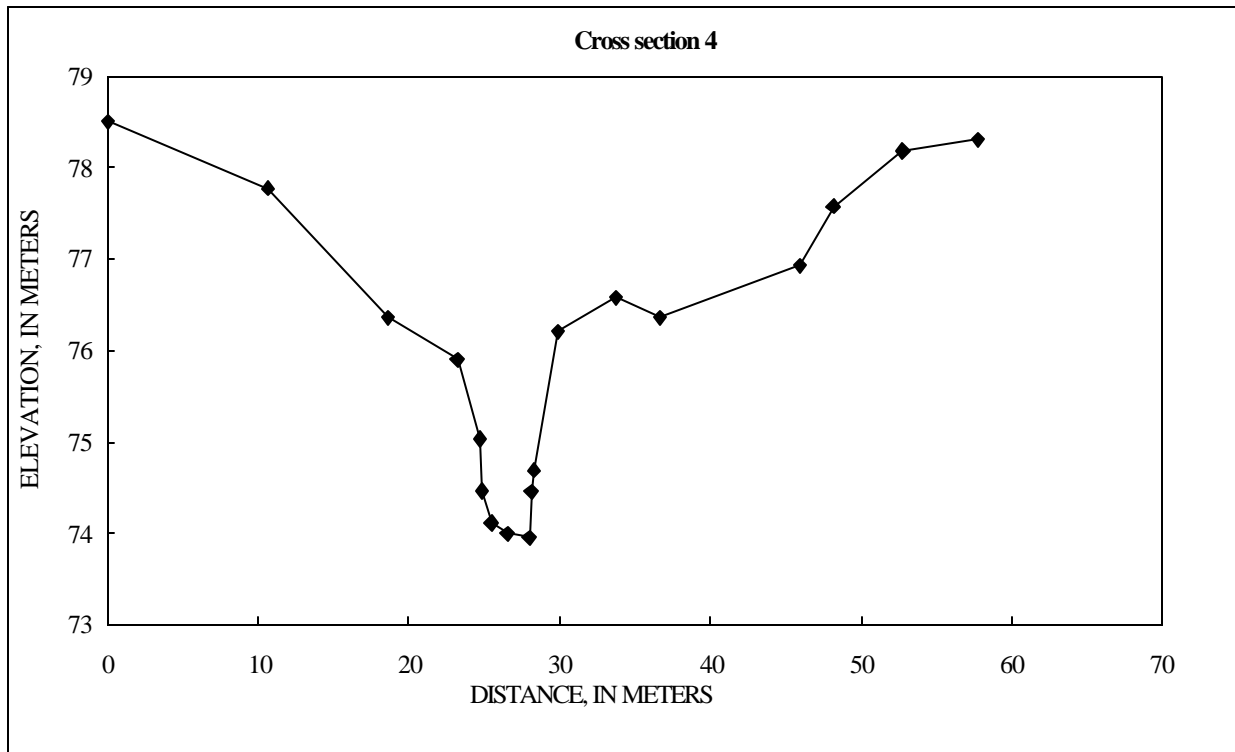
CROSS SECTION 5

SHOT #	PCODE	NORTHING (N)	EASTING (E)	ELEVATION (Z), IN METERS	DISTANCE, IN METERS	CUMULATIVE DISTANCE, IN METERS
1	START	0	0	100		
2	CS	-619.02	1751.42	76.275	0.00	0.00
3	CS	-620.59	1750.95	75.904	1.64	1.64
4	CS	-626.82	1748.40	73.997	6.73	8.37
5	CS	-628.78	1747.19	73.353	2.30	10.67
6	CS	-630.43	1746.68	71.879	1.73	12.40
7	CS	-630.77	1746.52	71.544	0.38	12.78
8	CS	-631.12	1746.41	71.465	0.36	13.14
9	CS	-631.98	1745.82	71.382	1.04	14.18
10	CS	-632.74	1745.79	71.474	0.77	14.95
11	CS	-636.13	1745.20	71.931	3.44	18.39
12	CS	-638.64	1744.21	74.084	2.70	21.08
13	CS	-644.93	1741.40	74.650	6.89	27.97
14	CS	-648.40	1739.79	76.186	3.82	31.80
15	CS	-650.31	1738.73	76.429	2.19	33.98



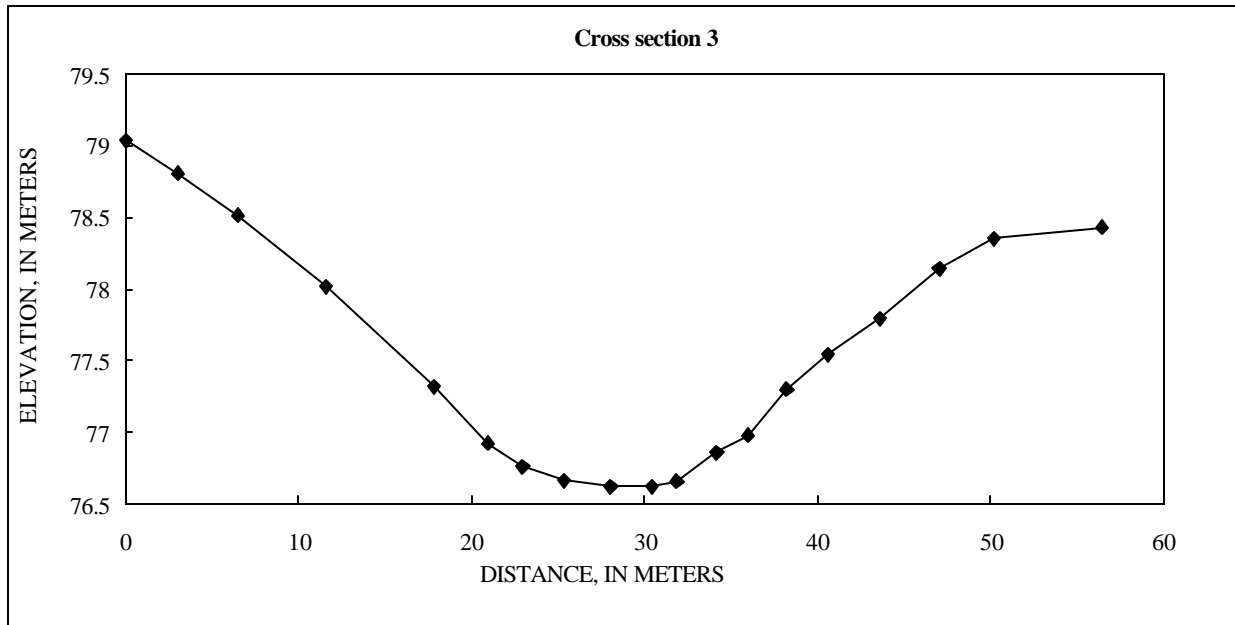
CROSS SECTION 4

SHOT #	PCODE	NORTHING (N)	EASTING (E)	ELEVATION (Z), IN METERS	DISTANCE, IN METERS	CUMULATIVE DISTANCE, IN METERS
1	START	0	0	100		
2	CS	-603.31	789.84	78.505	0.00	0.00
3	CS	-613.05	785.46	77.772	10.67	10.67
4	CS	-620.75	783.58	76.364	7.93	18.60
5	CS	-625.07	781.97	75.906	4.61	23.21
6	CS	-626.44	781.45	75.039	1.47	24.68
7	CS	-626.63	781.47	74.470	0.20	24.87
8	CS	-626.91	781.99	74.116	0.58	25.45
9	CS	-627.98	781.80	73.998	1.09	26.54
10	CS	-629.36	781.40	73.957	1.44	27.98
11	CS	-629.49	781.40	74.459	0.13	28.11
12	CS	-629.63	781.34	74.695	0.16	28.27
13	CS	-631.26	781.01	76.210	1.66	29.92
14	CS	-635.00	780.19	76.580	3.83	33.76
15	CS	-637.79	779.39	76.360	2.90	36.66
16	CS	-646.64	776.58	76.932	9.28	45.94
17	CS	-648.70	775.77	77.574	2.22	48.16
18	CS	-653.12	774.41	78.179	4.63	52.79
19	CS	-657.47	772.02	78.301	4.96	57.74



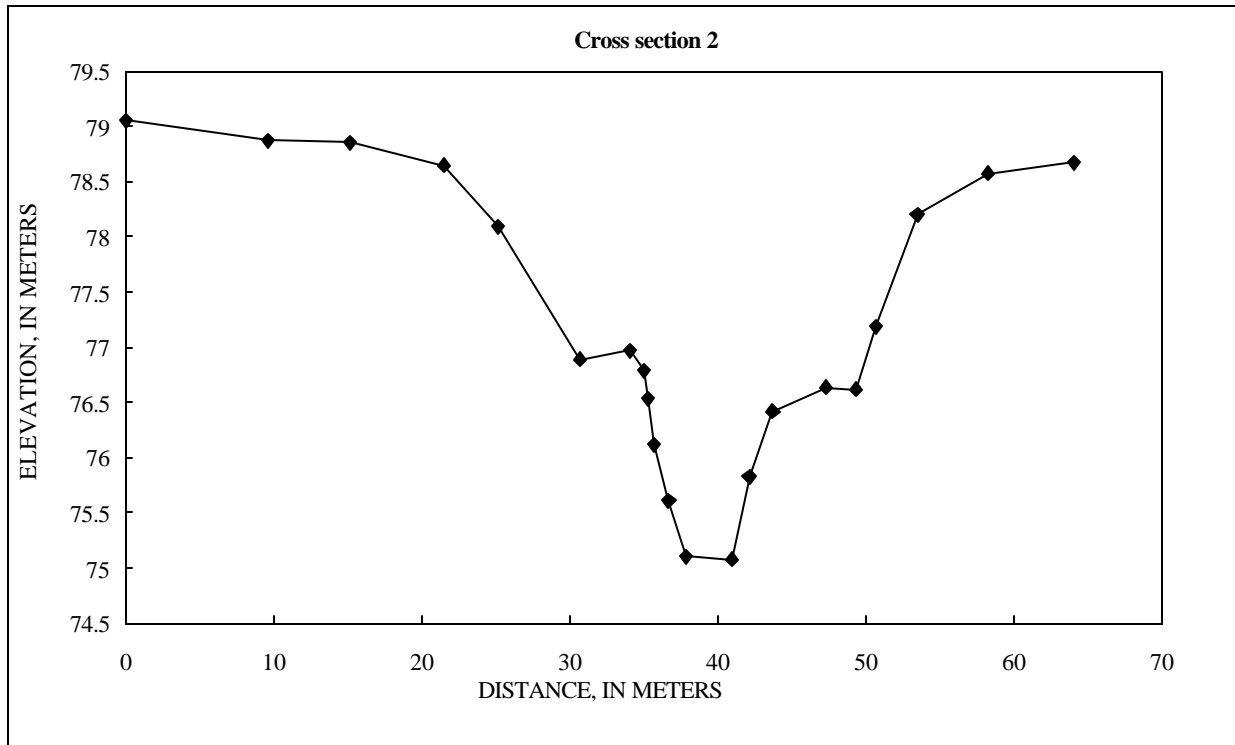
CROSS SECTION 3

SHOT #	PCODE	NORTHING (N)	EASTING (E)	ELEVATION (Z), IN METERS	DISTANCE, IN METERS	CUMULATIVE DISTANCE, IN METERS
1	START	0	0	100		
2	CS	-584.89	743.95	79.042	0.00	0.00
3	CS	-587.85	743.48	78.811	3.01	3.01
4	CS	-591.29	742.85	78.515	3.49	6.50
5	CS	-596.35	742.15	78.016	5.11	11.61
6	CS	-602.50	741.38	77.322	6.20	17.81
7	CS	-605.62	741.11	76.925	3.13	20.93
8	CS	-607.60	740.81	76.768	2.01	22.94
9	CS	-610.01	740.57	76.669	2.42	25.36
10	CS	-612.69	740.23	76.627	2.69	28.06
11	CS	-615.09	740.04	76.624	2.41	30.47
12	CS	-616.48	739.88	76.662	1.40	31.87
13	CS	-618.75	739.43	76.861	2.31	34.18
14	CS	-620.55	739.17	76.980	1.82	36.00
15	CS	-622.77	738.93	77.303	2.24	38.24
16	CS	-625.09	738.56	77.541	2.35	40.59
17	CS	-628.04	738.04	77.800	3.00	43.58
18	CS	-631.46	737.48	78.149	3.46	47.04
19	CS	-634.56	736.95	78.357	3.15	50.19
20	CS	-640.76	736.06	78.434	6.27	56.46



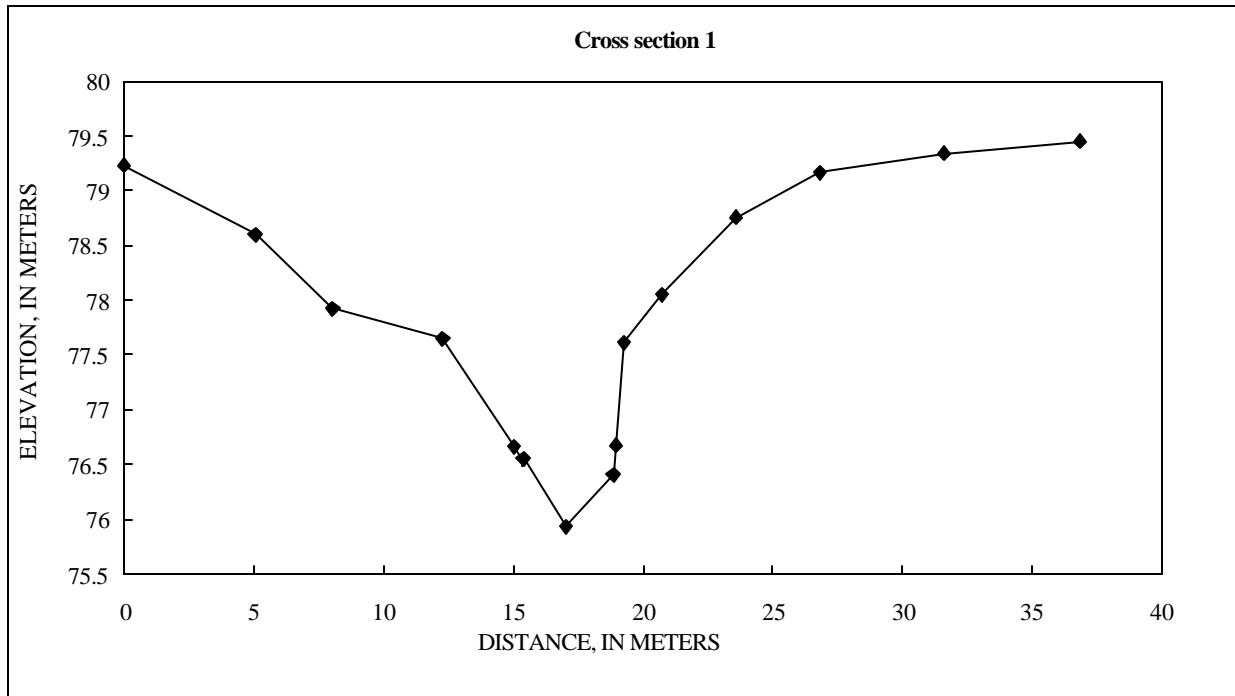
CROSS SECTION 2

SHOT #	PCODE	NORTHING (N)	EASTING (E)	ELEVATION (Z), IN METERS	DISTANCE, IN METERS	CUMULATIVE DISTANCE, IN METERS
1	START	0	0	100		
2	CS	-599.75	609.19	79.055	0.00	0.00
3	CS	-607.92	614.30	78.876	9.64	9.64
4	CS	-612.54	617.38	78.855	5.55	15.19
5	CS	-617.78	620.87	78.652	6.30	21.49
6	CS	-621.00	622.62	78.093	3.66	25.15
7	CS	-625.66	625.66	76.892	5.57	30.72
8	CS	-628.26	627.78	76.978	3.35	34.07
9	CS	-629.00	628.46	76.790	1.00	35.07
10	CS	-629.22	628.52	76.539	0.23	35.30
11	CS	-629.58	628.66	76.115	0.39	35.69
12	CS	-630.12	629.55	75.607	1.05	36.74
13	CS	-630.79	630.45	75.105	1.12	37.86
14	CS	-633.66	631.62	75.078	3.09	40.95
15	CS	-634.67	632.27	75.835	1.20	42.15
16	CS	-636.02	633.06	76.421	1.57	43.72
17	CS	-638.90	635.21	76.633	3.60	47.31
18	CS	-640.58	636.32	76.619	2.01	49.32
19	CS	-641.72	637.17	77.187	1.42	50.75
20	CS	-643.91	638.82	78.205	2.75	53.49
21	CS	-648.00	641.29	78.576	4.78	58.27
22	CS	-652.87	644.48	78.673	5.82	64.09



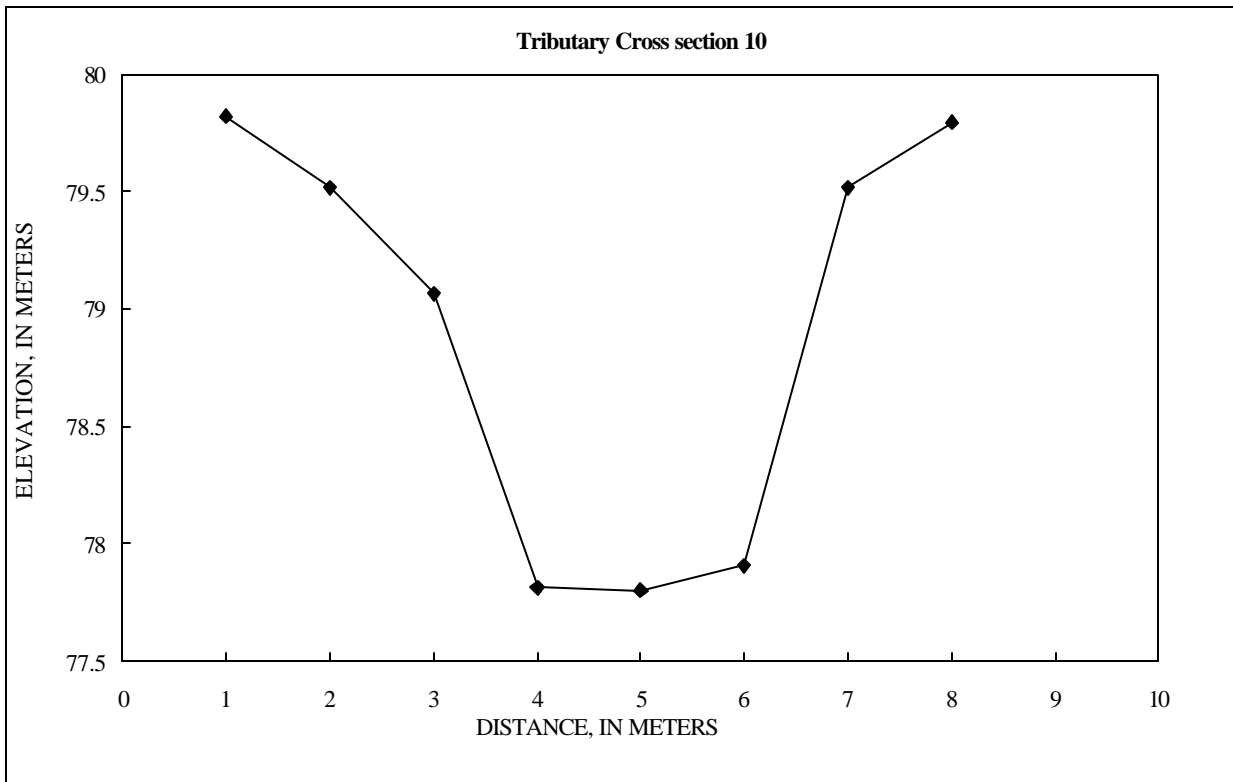
CROSS SECTION 1

SHOT #	PCODE	NORTHING (N)	EASTING (E)	ELEVATION (Z), IN METERS	DISTANCE, IN METERS	CUMULATIVE DISTANCE, IN METERS
1	START	0	0	100		
2	CS	-696.36	114.71	79.232	0.00	0.00
3	CS	-701.06	116.54	78.604	5.04	5.04
4	CS	-704.04	116.74	77.923	2.99	8.03
5	CS	-708.14	117.86	77.651	4.25	12.28
6	CS	-710.89	118.07	76.671	2.76	15.04
7	CS	-711.13	117.87	76.541	0.31	15.35
8	CS	-711.15	117.86	76.556	0.02	15.37
9	CS	-712.45	118.88	75.937	1.66	17.02
10	CS	-714.22	119.35	76.409	1.83	18.86
11	CS	-714.29	119.44	76.674	0.11	18.97
12	CS	-714.57	119.41	77.615	0.29	19.25
13	CS	-715.98	119.90	78.051	1.49	20.74
14	CS	-718.74	120.60	78.759	2.85	23.58
15	CS	-721.96	120.84	79.168	3.23	26.82
16	CS	-726.60	121.98	79.343	4.78	31.59
17	CS	-731.71	123.29	79.450	5.28	36.87



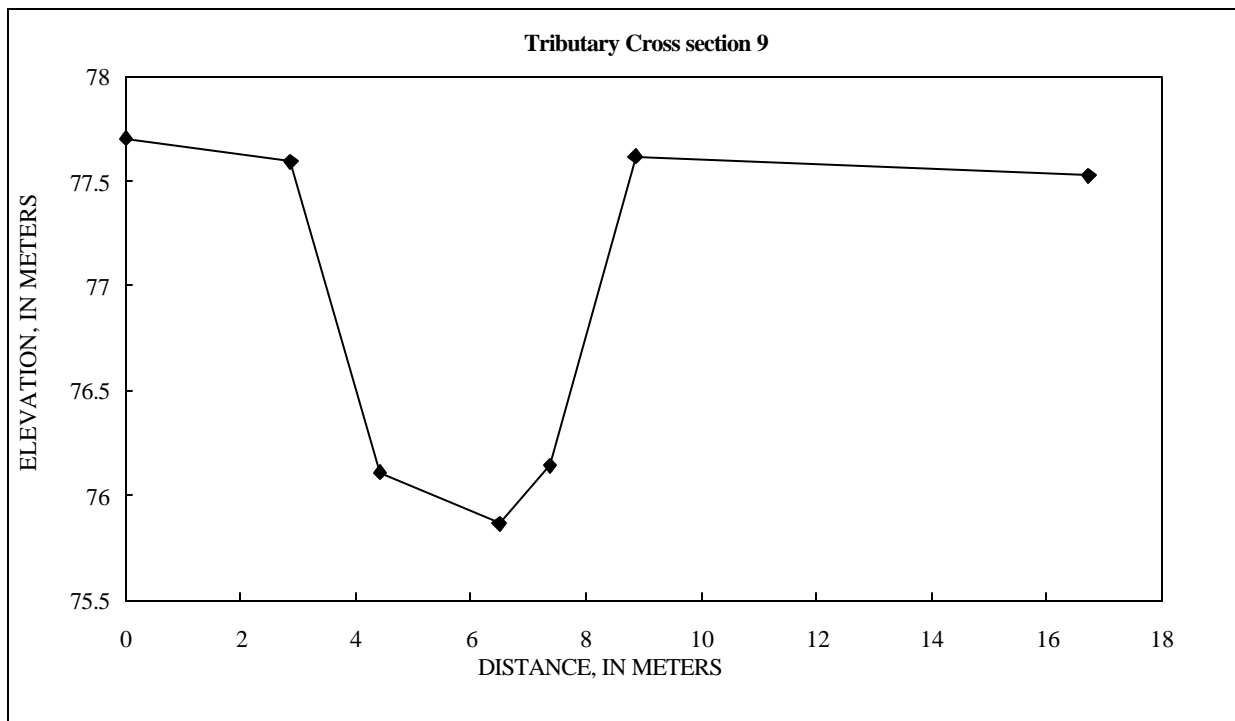
TRIBUTARY CROSS SECTION 10

SHOT #	PCODE	NORTHING (N)	EASTING (E)	ELEVATION (Z), IN METERS	DISTANCE, IN METERS	CUMULATIVE DISTANCE, IN METERS
1	START	0	0	100		
2	CS	1328.79	3208.90	80.131	0.00	0.00
3	CS	1358.53	3223.28	79.819	33.03	33.03
4	CS	1356.34	3222.01	79.519	2.53	35.56
5	CS	1351.54	3219.42	79.063	5.45	41.02
6	CS	1350.15	3219.34	77.814	1.39	42.41
7	CS	1348.78	3219.20	77.799	1.38	43.79
8	CS	1347.33	3218.53	77.906	1.60	45.39
9	CS	1345.60	3217.00	79.516	2.30	47.69



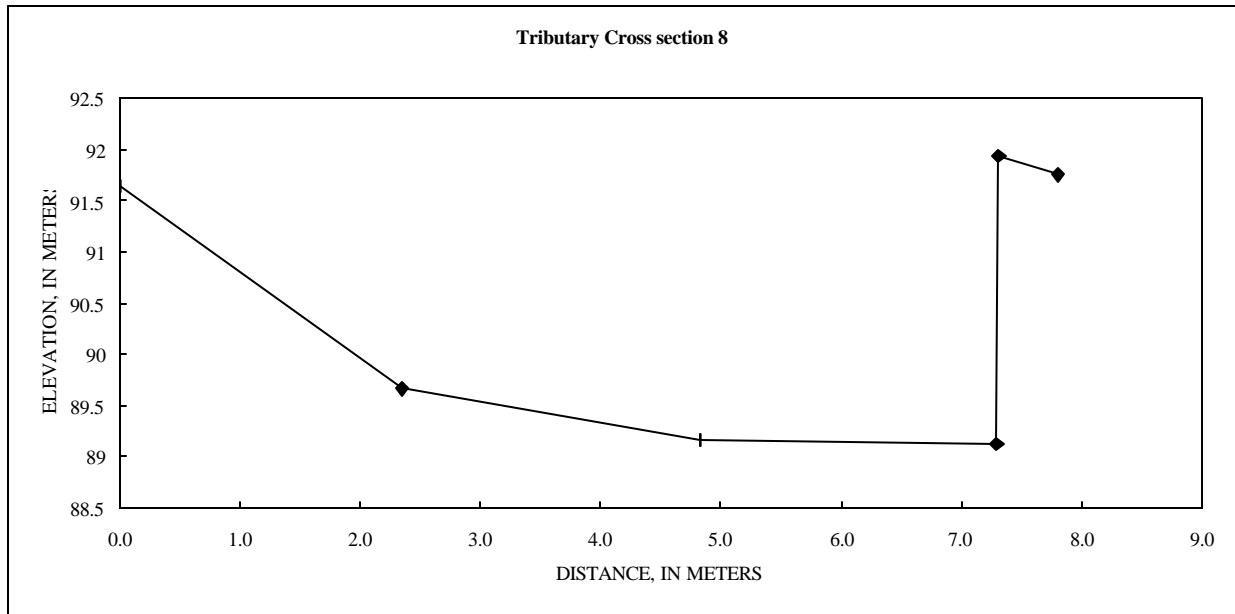
TRIBUTARY CROSS SECTION 9

SHOT #	PCODE	NORTHING (N)	EASTING (E)	ELEVATION (Z), IN METERS	DISTANCE, IN METERS	CUMULATIVE DISTANCE, IN METERS
1	START	0	0	100		
2	CS	684.56	3665.70	77.703	0.00	0.00
3	CS	683.44	3663.06	77.597	2.87	2.87
4	CS	682.11	3662.26	76.109	1.55	4.42
5	CS	681.84	3660.21	75.865	2.07	6.49
6	CS	681.79	3659.33	76.145	0.88	7.37
7	CS	681.49	3657.87	77.617	1.49	8.86
8	CS	676.84	3651.51	77.530	7.88	16.74



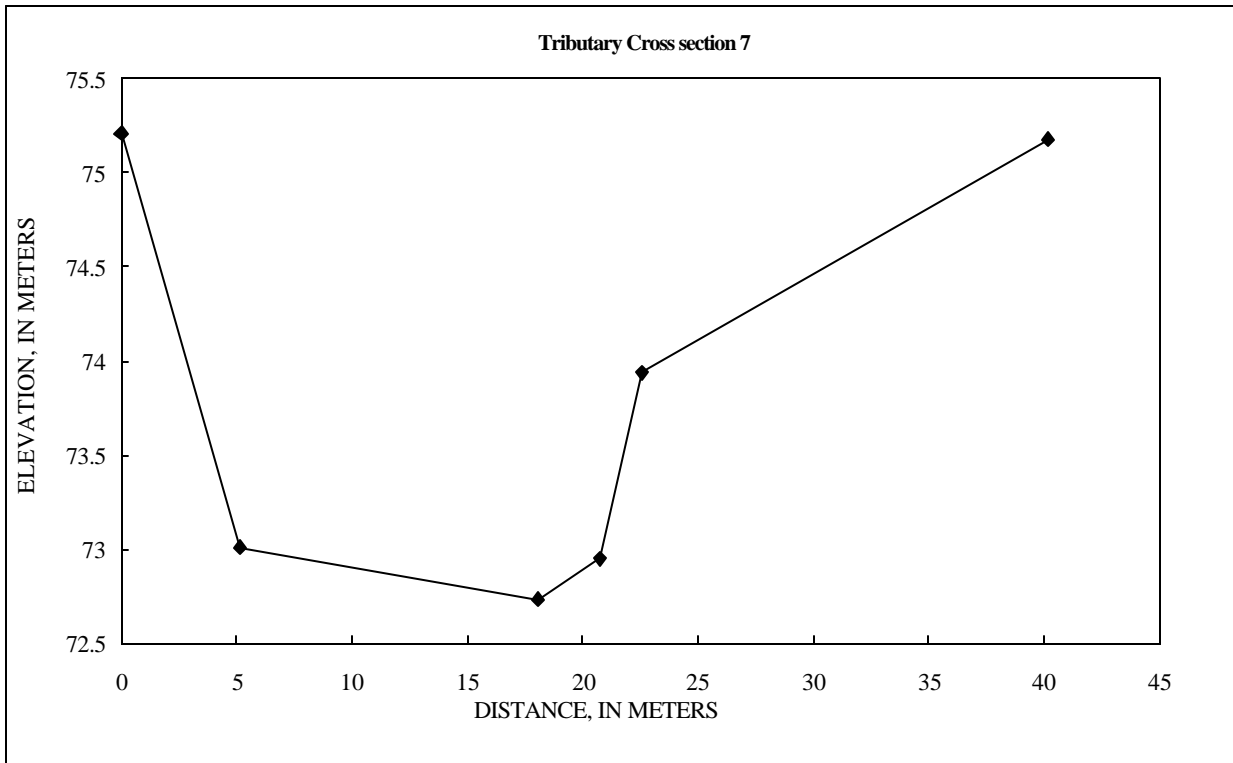
TRIBUTARY CROSS SECTION 8

SHOT #	PCODE	NORTHING (N)	EASTING (E)	ELEVATION (Z), IN METERS	DISTANCE, IN METERS	CUMULATIVE DISTANCE, IN METERS
1	START	0	0	100		
2	CS	305.56	3974.69	91.639	0.00	0.00
3	CS	303.36	3975.81	89.660	2.47	2.35
4	CS	302.73	3976.38	89.154	0.84	4.82
5	CS	300.52	3977.20	89.124	2.35	7.30
6	CS	299.32	3978.15	91.939	0.02	7.31
7	CS	299.03	3979.35	91.752	0.50	7.81



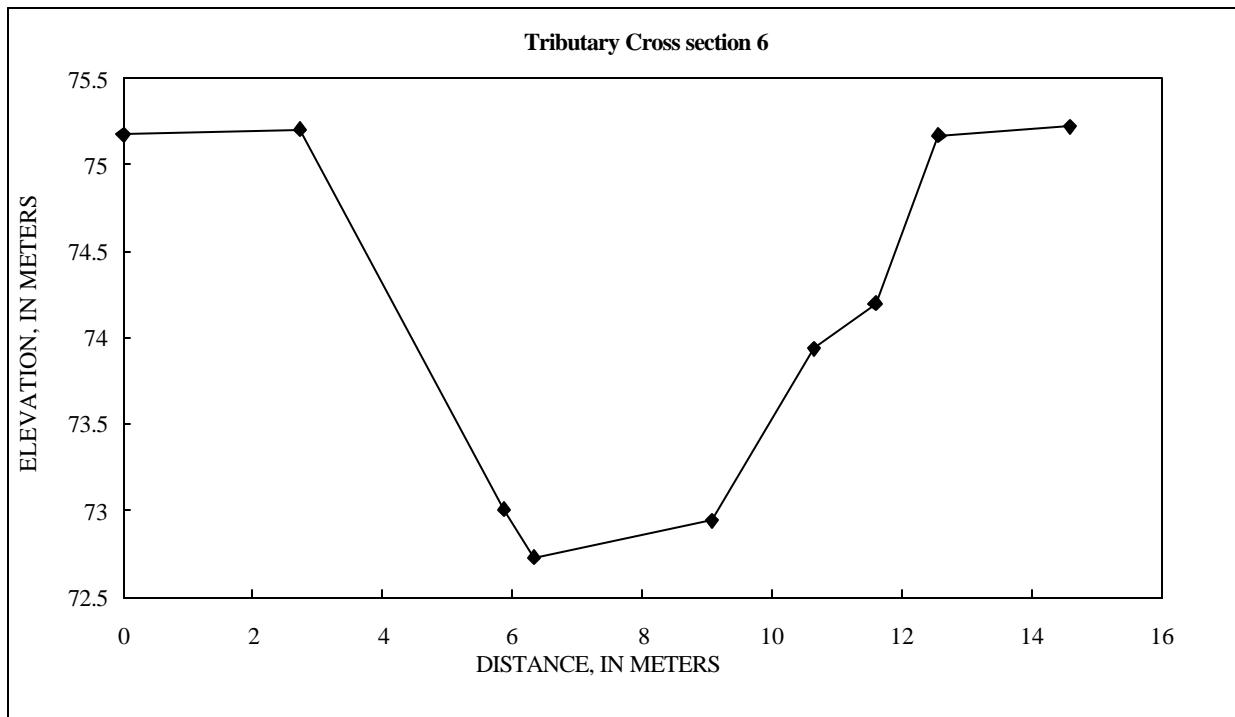
TRIBUTARY CROSS SECTION 7

SHOT #	PCODE	NORTHING (N)	EASTING (E)	ELEVATION (Z), IN METERS	DISTANCE, IN METERS	CUMULATIVE DISTANCE, IN METERS
1	START	0	0	100		
2	CS	236.61	4027.53	75.206	0.00	0.00
3	CS	238.39	4022.70	73.009	5.15	5.15
4	CS	244.36	4011.22	72.731	12.94	18.09
5	CS	245.40	4008.76	72.946	2.67	20.76
6	CS	246.13	4007.11	73.939	1.81	22.56
7	CS	228.51	4006.76	75.176	17.63	40.19



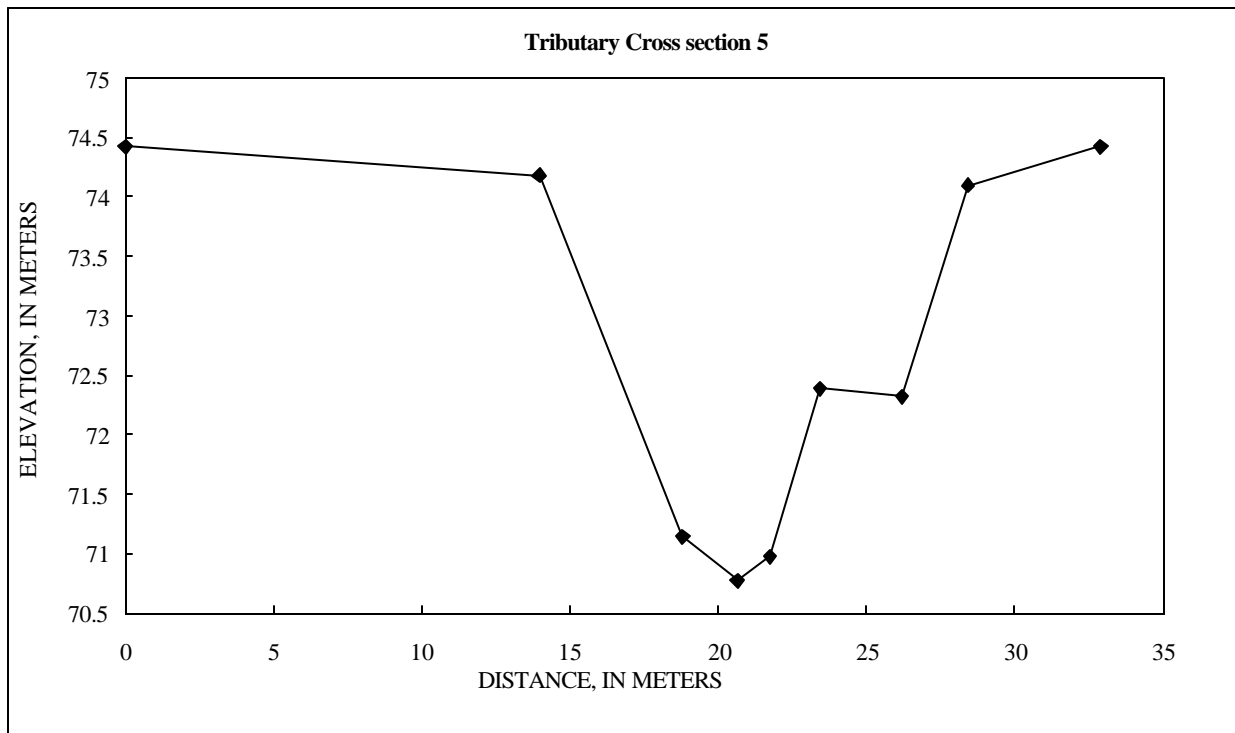
TRIBUTARY CROSS SECTION 6

SHOT #	PCODE	NORTHING (N)	EASTING (E)	ELEVATION (Z), IN METERS	DISTANCE, IN METERS	CUMULATIVE DISTANCE, IN METERS
1	START	0	0	100		
2	CS	-95.46	4112.34	75.176	0.00	0.00
3	CS	-94.09	4114.69	75.206	2.72	2.72
4	CS	-92.18	4117.21	73.009	3.16	5.88
5	CS	-91.96	4117.61	72.731	0.46	6.34
6	CS	-90.99	4120.18	72.946	2.75	9.09
7	CS	-89.94	4121.33	73.939	1.56	10.65
8	CS	-89.43	4122.12	74.200	0.94	11.58
9	CS	-88.78	4122.86	75.170	0.99	12.57
10	CS	-87.67	4124.55	75.222599	2.02	14.59



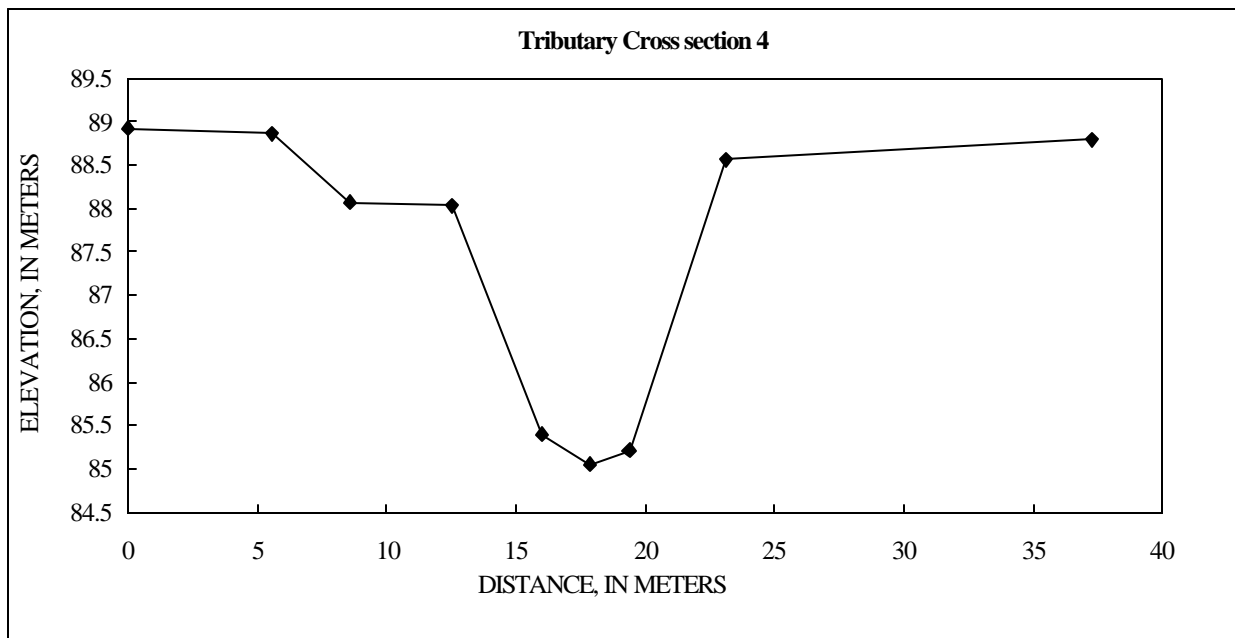
TRIBUTARY CROSS SECTION 5

SHOT #	PCODE	NORTHING (N)	EASTING (E)	ELEVATION (Z), IN METERS	DISTANCE, IN METERS	CUMULATIVE DISTANCE, IN METERS
1	START	0	0	100		
2	CS	-765.46	4289.70	74.428	0.00	0.00
3	CS	-774.00	4300.74	74.177	13.96	13.96
4	CS	-776.82	4304.67	71.148	4.83	18.79
5	CS	-777.94	4306.13	70.771	1.84	20.63
6	CS	-778.62	4307.00	70.975	1.11	21.74
7	CS	-779.66	4308.32	72.391	1.67	23.41
8	CS	-781.16	4310.63	72.325	2.76	26.17
9	CS	-782.00	4312.71	74.096	2.25	28.42
10	CS	-785.14	4315.88	74.428	4.47	32.89



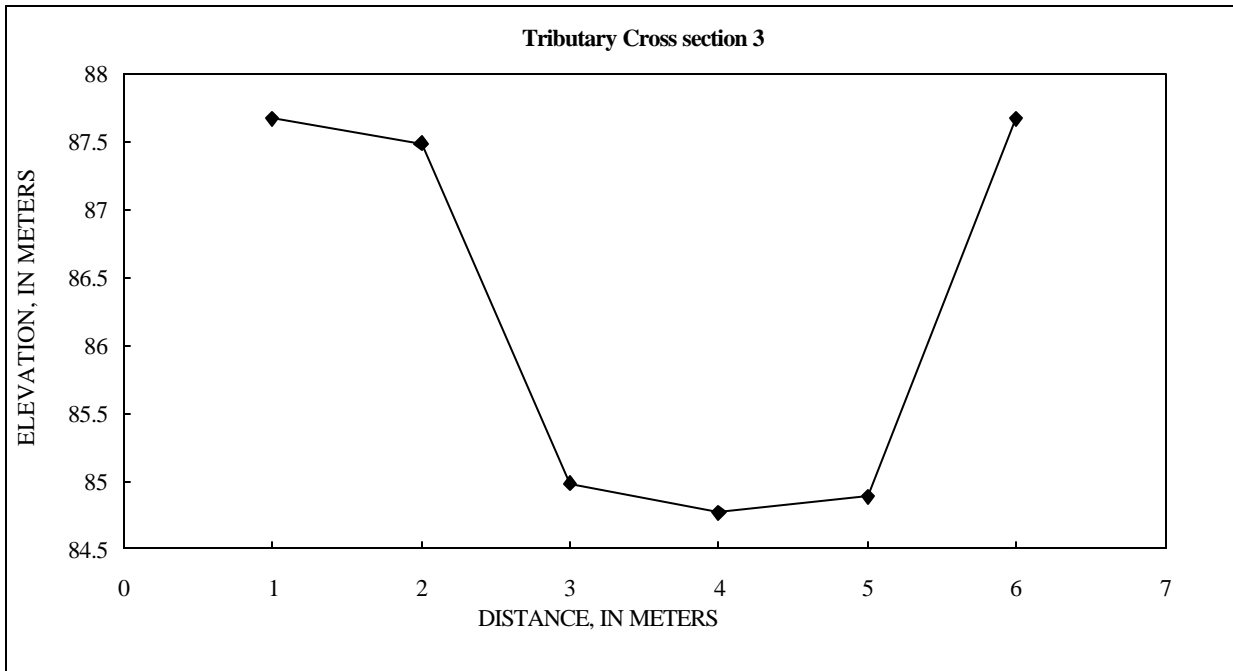
TRIBUTARY CROSS SECTION 4

SHOT #	PCODE	NORTHING (N)	EASTING (E)	ELEVATION (Z), IN METERS	DISTANCE, IN METERS	CUMULATIVE DISTANCE, IN METERS
1	START	0	0	100		
2	CS	-1314.46	4368.89	88.930	0.00	0.00
3	CS	-1316.77	4363.86	88.857	5.54	5.54
4	CS	-1318.23	4361.17	88.070	3.06	8.60
5	CS	-1319.42	4357.44	88.035	3.92	12.52
6	CS	-1321.37	4354.51	85.395	3.52	16.04
7	CS	-1322.04	4352.79	85.055	1.84	17.88
8	CS	-1322.59	4351.39	85.209	1.50	19.38
9	CS	-1323.37	4347.71	88.571	3.76	23.14
10	CS	-1328.66	4334.57	88.793	14.17	37.31



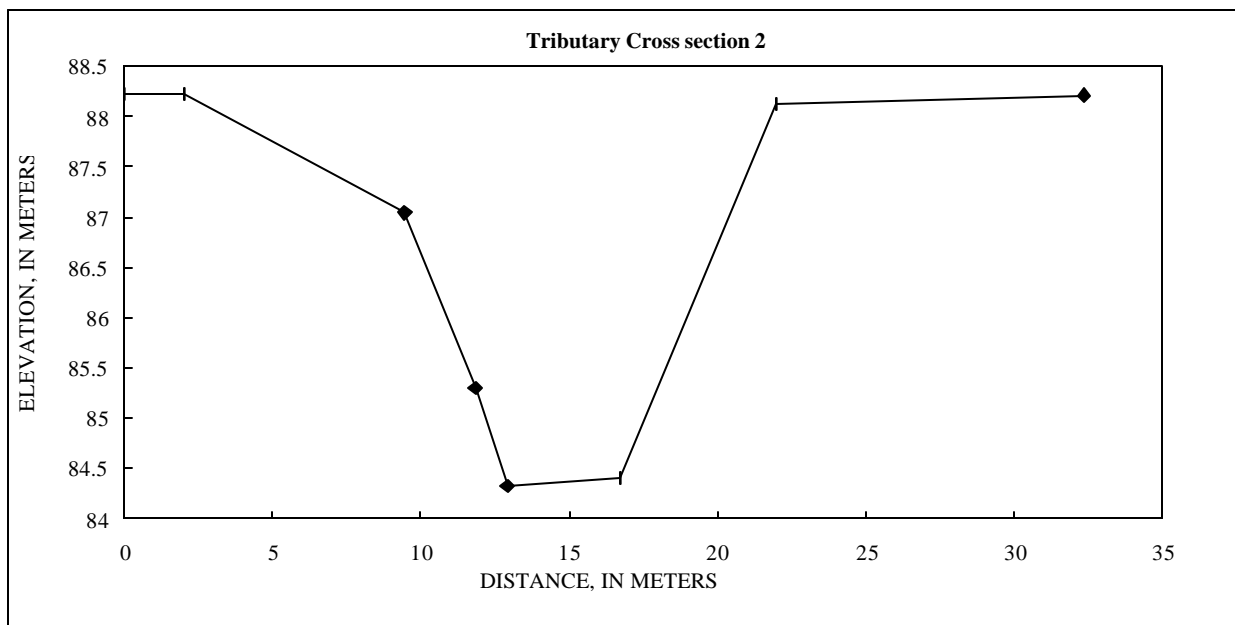
TRIBUTARY CROSS SECTION 3

SHOT #	PCODE	NORTHING (N)	EASTING (E)	ELEVATION (Z), IN METERS	DISTANCE, IN METERS	CUMULATIVE DISTANCE, IN METERS
1	START	0	0	100		
2	CS	-1644.12	4439.99	87.675	0.00	0.00
3	CS	-1644.35	4440.98	87.489	1.02	1.02
4	CS	-1644.32	4443.40	84.981	2.42	3.43
5	CS	-1644.06	4447.48	84.767	4.09	7.53
6	CS	-1643.86	4449.68	84.886		
7				87.675		20.00



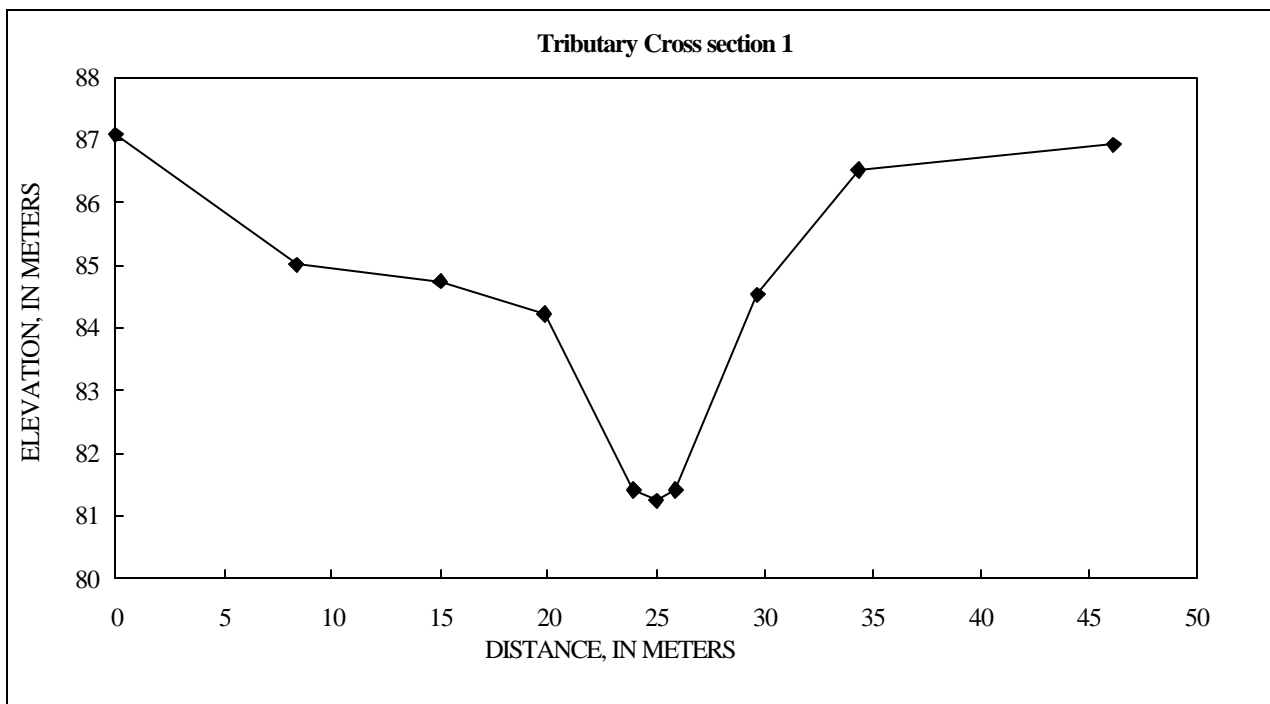
TRIBUTARY CROSS SECTION 2

SHOT #	PCODE	NORTHING (N)	EASTING (E)	ELEVATION (Z), IN METERS	DISTANCE, IN METERS	CUMULATIVE DISTANCE, IN METERS
1	START	0	0	100		
2	CS	-1710.94	4439.14	88.220	0.00	0.00
3	CS	-1710.39	4441.05	88.221	1.99	1.99
4	CS	-1709.82	4448.50	87.043	7.47	9.46
5	CS	-1708.59	4450.51	85.301	2.36	11.82
6	CS	-1708.16	4451.51	84.334	1.09	12.91
7	CS	-1707.70	4455.28	84.400	3.79	16.70
8	CS	-1706.46	4460.39	88.128	5.26	21.96
9	CS	-1706.46	4470.76	88.216	10.37	32.33

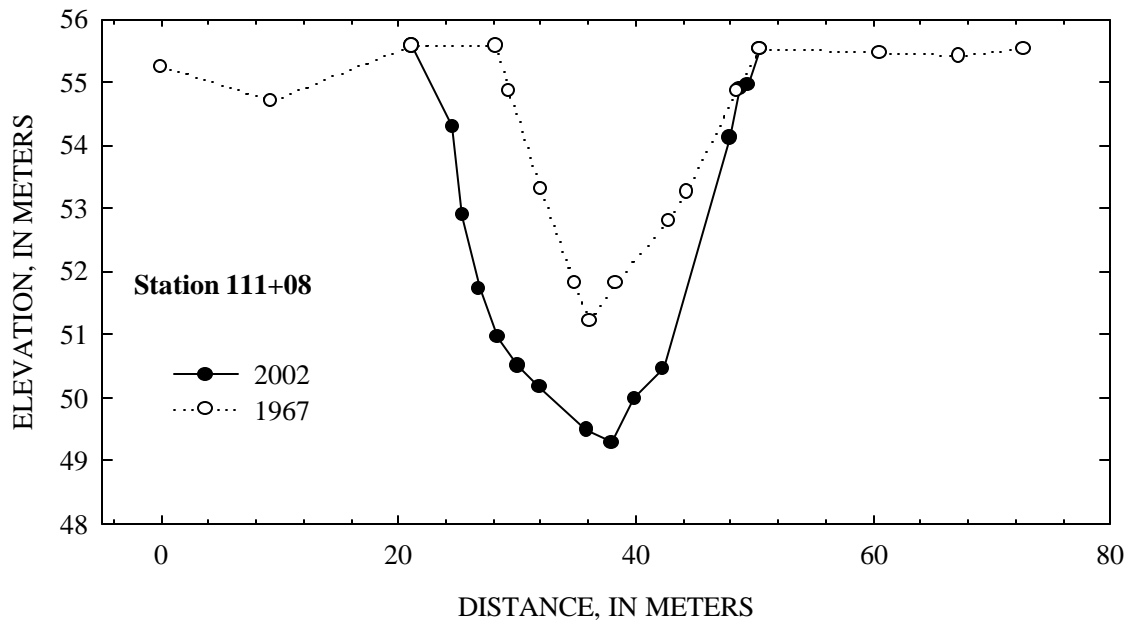
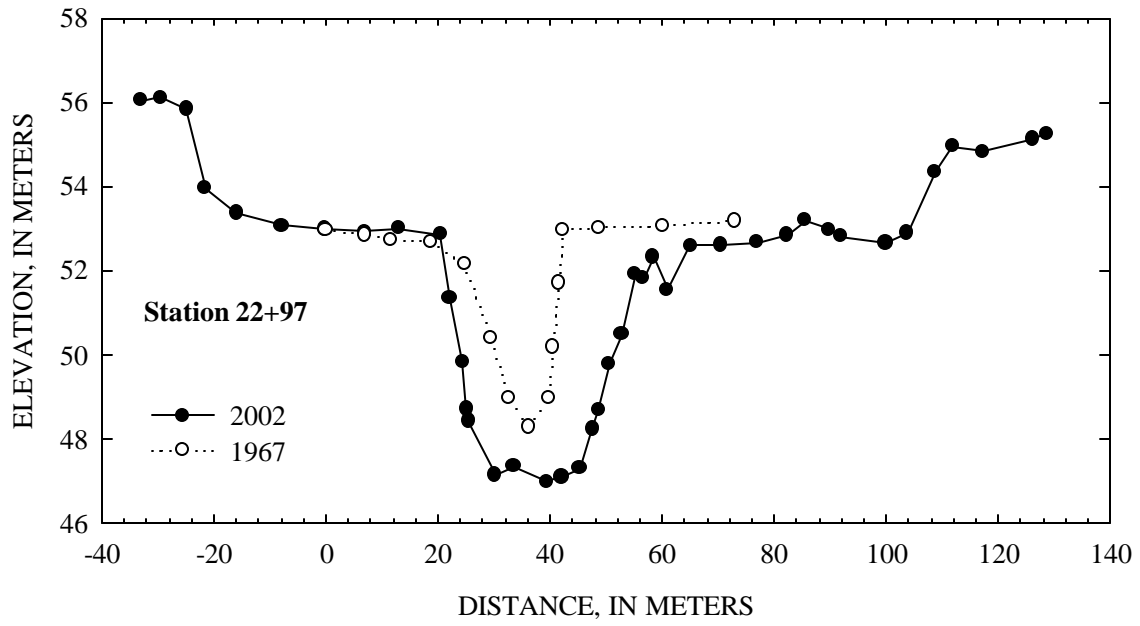


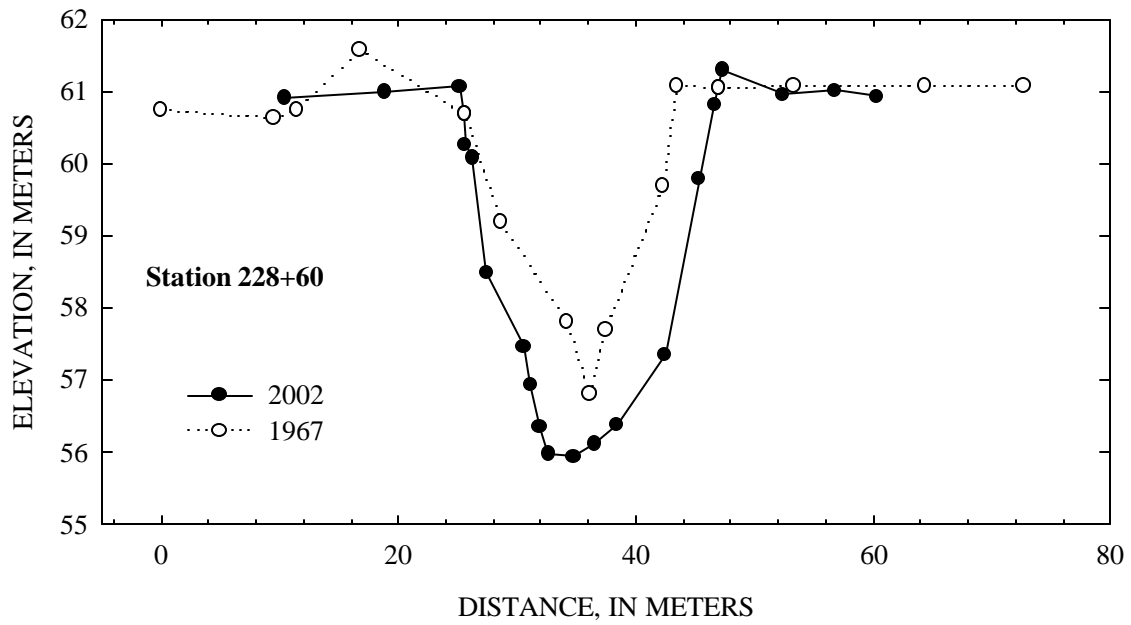
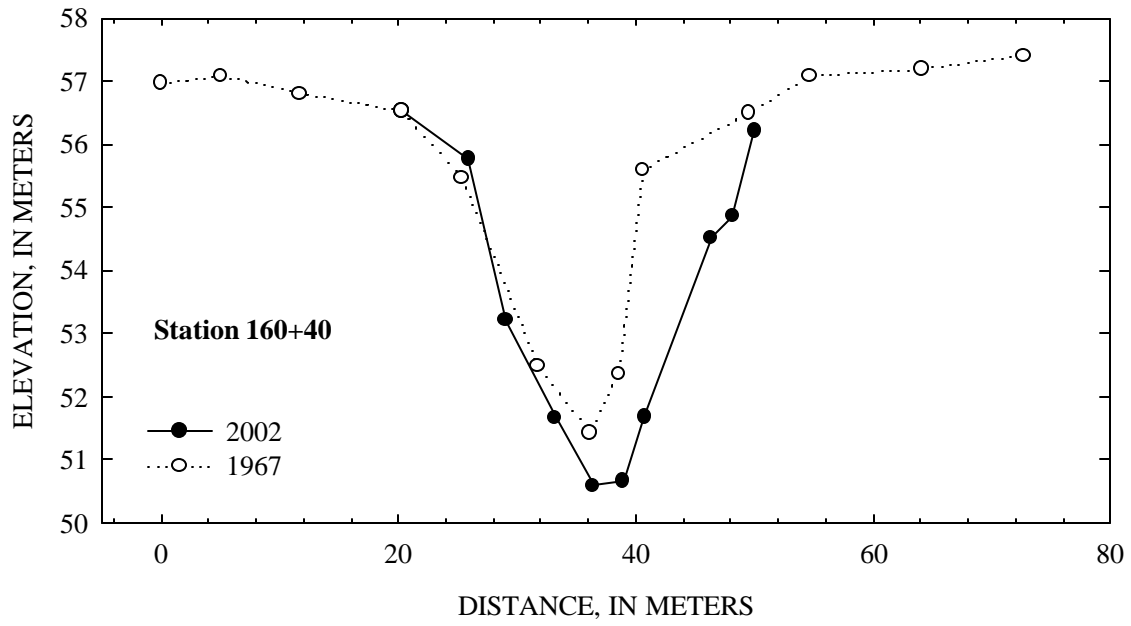
TRIBUTARY CROSS SECTION 1

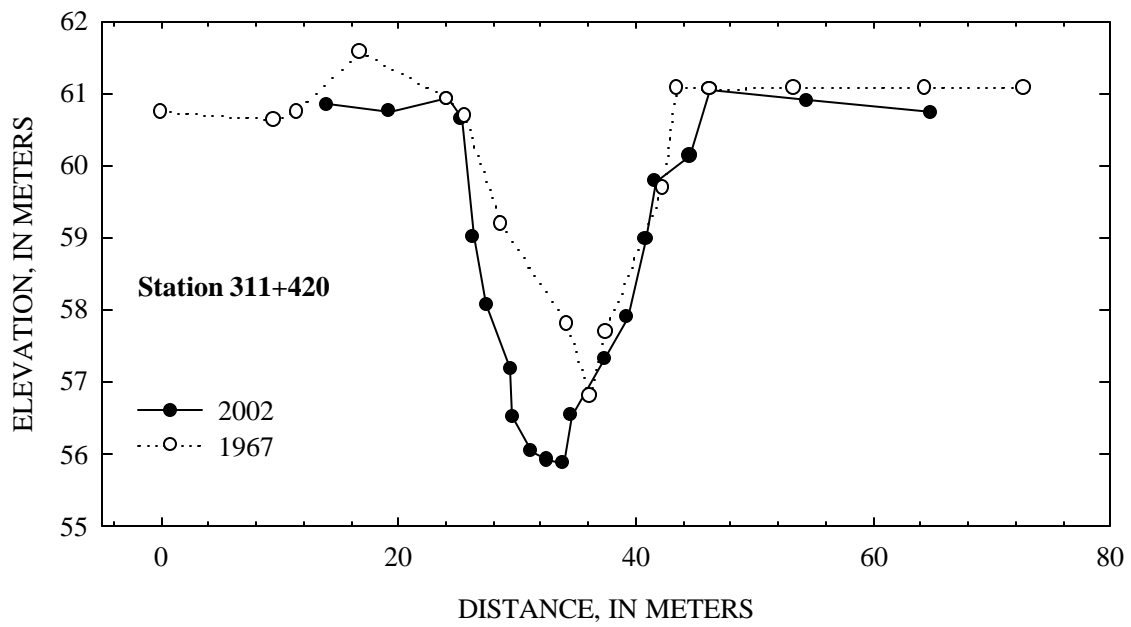
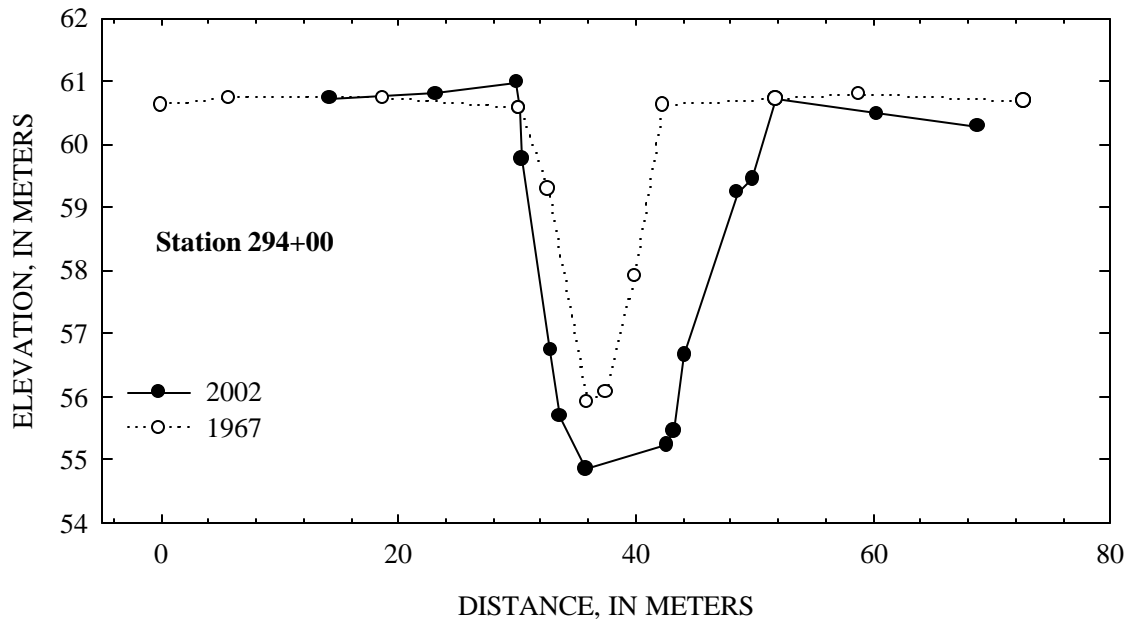
SHOT #	PCODE	NORTHING (N)	EASTING (E)	ELEVATION (Z), IN METERS	DISTANCE, IN METERS	CUMULATIVE DISTANCE, IN METERS
1	START	0	0	100		
2	CS	-2410.87	4558.92	87.082	0.00	0.00
3	CS	-2412.34	4567.12	85.011	8.33	8.33
4	CS	-2413.27	4573.74	84.747	6.69	15.02
5	CS	-2414.18	4578.47	84.225	4.82	19.83
6	CS	-2415.39	4582.39	81.409	4.10	23.94
7	CS	-2415.65	4583.43	81.241	1.07	25.01
8	CS	-2415.76	4584.32	81.408	0.90	25.91
9	CS	-2415.78	4588.10	84.526	3.78	29.69
10	CS	-2416.37	4592.75	86.515	4.68	34.37
11	CS	-2417.51	4604.48	86.924	11.78	46.16

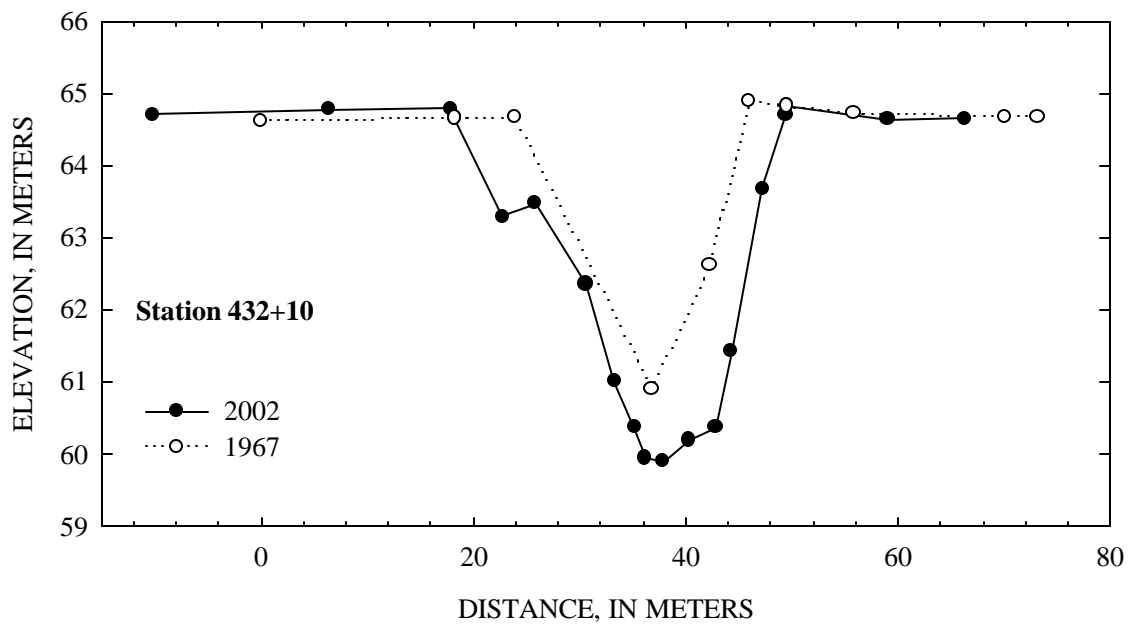
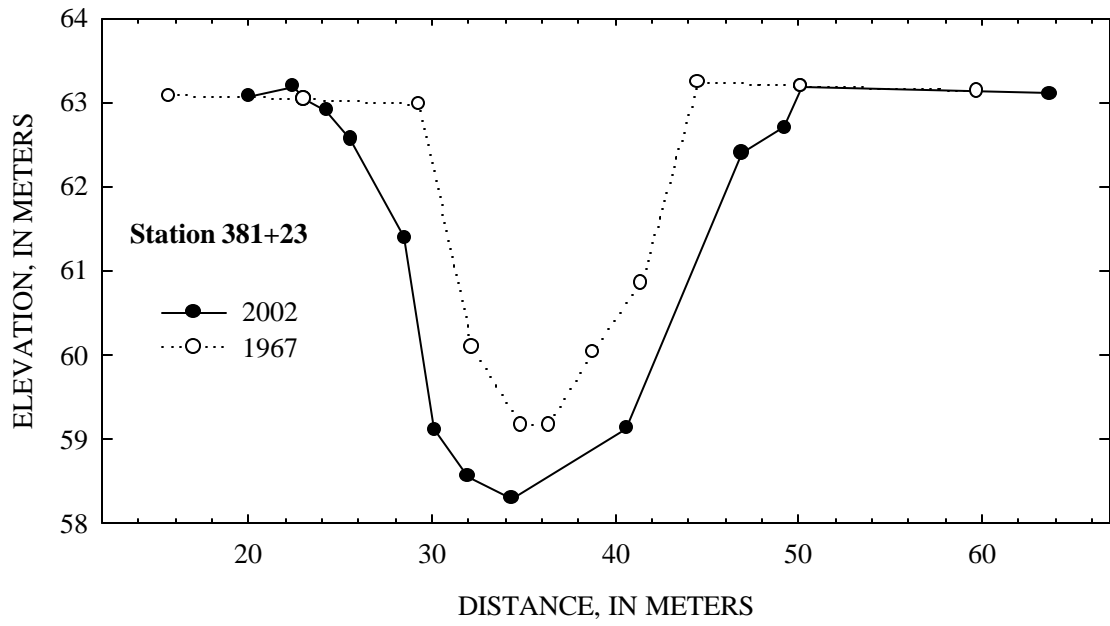


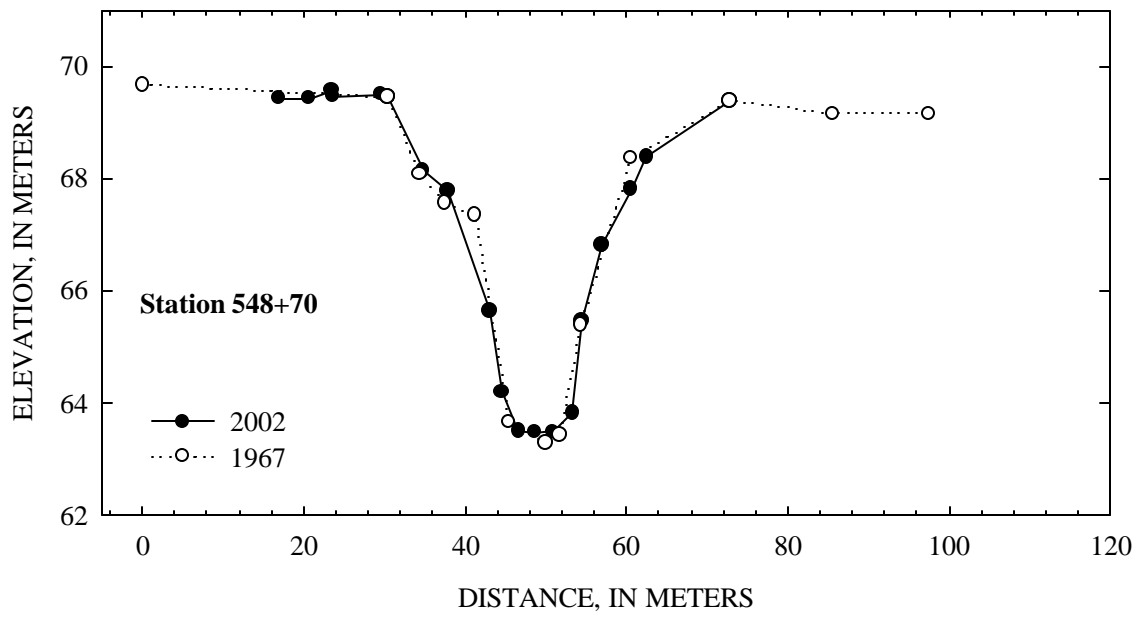
**APPENDIX B - COMPARISON OF 1967 AND 2002 MEASURED CROSS
SECTIONS**











**APPENDIX C: – SUMMARY OF SUSPENDED-SEDIMENT DATA FOR SITES IN THE
SOUTHEASTERN PLAINS (ECOREGION 65) USED TO DEVELOP REFERENCE
SEDIMENT-TRANSPORT CONDITIONS.**

Note: n = number of samples.

State	Station Number	n	Start date (yyyymmdd)	End date (yyyymmdd)	Q _{1.5} (m ³ /s)	Sediment load at Q _{1.5} (T/D)	Maximum sampled Q	Area (km ²)	Sediment yield at Q _{1.5} (T/D/km ²)
							(m ³ /s)		
AL	02343801	69	19821019	19940901	1208.4	1723	913.4	21263	0.08
AL	02369800	45	19841017	19950413	50.0	517	13.2	228	2.27
AL	02376500	87	19780118	19940908	163.0	812	81.6	1020	0.80
AL	02420000	355	19750121	19970306	2880.0	10355	7579.3	39073	0.27
AL	02423000	116	19891106	19970211	2908.0	16196	4858.5	44273	0.37
AL	02424590	104	19891106	19970211	448.0	12961	399.8	3833	3.38
AL	02427470	61	19891108	19940920	2128.8	11541	7468.3	51727	0.22
AL	02427511	57	19891108	19940920	2130.5	8510	3470.4	51789	0.16
AL	02429500	307	19731115	19980115	3285.0	31061	6024.6	56891	0.55
AL	02444157	168	19881021	19970110	980.0	7502	1790.7	15305	0.49
AL	02444500	168	19881021	19970110	1325.0	11280	5080.6	15394	0.73
AL	02447008	43	19890113	19940216	1122.2	22022	3886.8	18930	1.16
AL	02447010	42	19890113	19940216	1122.5	27384	1899.0	18938	1.45
AL	02449000	371	19750123	19930810	1774.0	18804	4719.7	22356	0.84
AL	02464035	56	19770825	19830422	23.7	986	33.3	44.4	22.22
AL	02465000	220	19790607	19950220	2665.0	19563	4386.6	12483	1.57
AL	02466031	91	19780314	19930810	969.5	3456	1732.4	15047	0.23
AL	02469525	126	19891107	19970124	1956.0	20569	5774.7	45289	0.45
AL	02469762	172	19741024	19960919	2021.7	21368	5441.6	47697	0.45
AL	02470040	135	19881122	19970123	2069.9	22706	61078.8	49497	0.46
AL	02479945	78	19920204	19950510	29.0	48	29.2	81.5	0.59
AL	02479948	35	19920204	19940803	16.0	-	1.9	23.9	-
AL	02479950	37	19920409	19941102	15.2	-	2.2	22.1	-
AL	02479980	64	19920408	19941102	17.0	100	6.6	20.9	4.78
AL	02480002	64	19920203	19950510	30.0	150	10.3	21.3	7.05
AL	323642087541 800	64	19870120	19970309	1167.9	22925	2357.1	20154	1.14
AL	323653087540 800	62	19870120	19970309	1167.8	35141	1976.7	20154	1.74
AL	323704087542 400	61	19870120	19970309	1167.8	13047	3720.3	20154	0.65
AL	325645088100 700	41	19890113	19940216	1122.2	23508	2348.8	18931	1.24
FL	02320500	146	19740117	19960112	378.0	378	1085.5	20408	0.02
FL	02326838	51	19930310	19960422	6.0	8	14.4	25.0	0.31
FL	02329000	127	19741101	19951212	157.0	270	283.2	2952	0.09
FL	02368000	123	19741107	19930902	175.0	361	170.7	1616	0.22
FL	02375500	125	19741024	19940908	869.0	4194	1093.9	9885	0.42
GA	02197830	43	19700401	19840705	84.0	132	297.1	1225	0.11
GA	02198000	135	19571221	19780228	72.0	104	218.8	1673	0.06
GA	02203000	37	19571222	19700402	92.0	68	102.7	1437	0.05
GA	02213000	217	19571216	19680718	638.0	10576	1249.3	5801	1.82
GA	02215100	55	19930304	19960522	43.0	96	41.4	422	0.23

State	Station Number	n	Start date	End date	Q _{1.5}	Sediment load at Q _{1.5}	Maximum sampled Q	Area	Sediment yield at Q _{1.5}
			(yyyymmdd)	(yyyymmdd)	(m ³ /s)	(T/D)	(m ³ /s)	(km ²)	(T/D/km ²)
GA	02215260	114	19601011	19610927	581.0	2294	1196.6	11551	0.20
GA	02215500	55	19580203	19940725	602.0	2009	2557.0	13415	0.15
GA	02223500	328	19610302	19711213	713.0	4218	1485.3	11395	0.37
GA	02225500	94	19580113	19840816	162.0	245	410.9	2875	0.09
GA	02316000	45	19580306	19760818	85.0	122	203.5	1717	0.07
GA	02317797	38	19930305	19960530	33.0	34	44.8	334	0.10
GA	02317830	41	19700325	19780726	61.0	109	70.0	539	0.20
GA	02318000	38	19590306	19610715	119.0	433	261.0	1494	0.29
GA	02318500	53	19930311	19970910	198.0	389	252.1	3833	0.10
GA	02341800	75	19771121	19840731	136.0	8154	263.7	886	9.21
GA	02349500	38	19571122	19940706	579.0	3535	1610.3	7511	0.47
GA	02350080	70	19930303	19950920	21.0	168	23.2	160	1.05
GA	02350600	57	19610301	19770826	55.0	97	52.2	510	0.19
GA	02352500	56	19610301	19690829	724.0	2464	1027.2	13752	0.18
GA	02353000	518	19610301	19970911	711.0	2153	2784.6	14866	0.14
GA	02353500	105	19581113	19940511	115.0	397	255.4	1606	0.25
GA	02356980	40	19930302	19950307	28.0	62	22.2	272	0.23
GA	02357000	43	19620406	19940708	89.0	157	355.4	1256	0.12
GA	02358000	1765	19740201	19970910	2071.0	3839	5663.7	44545	0.09
GA	02359000	119	19741121	19940907	117.0	191	194.1	2023	0.09
MD	01594000	355	19850905	19970915	70.0	5500	177.7	255	21.58
MD	01594440	629	19780130	19980805	109.0	1655	252.2	901	1.84
MD	01594526	291	19851009	19960924	36.0	1391	80.1	232	5.99
MD	01594670	288	19890314	19970916	6.0	25	9.2	24.3	1.05
MD	01594705	46	19890501	19901023	-	-	0.0	-	-
MD	01594710	427	19851008	19970916	4.0	400	6.3	8.44	47.38
MD	01594780	164	19860716	19940922	-	-	0.1	-	-
MS	02430000	94	19770608	19790927	49.6	650	96.0	173	3.75
MS	02430500	49	19881117	19970414	232.0	2731	22.0	798	3.42
MS	02430680	39	19881229	19970414	291.0	21662	71.0	339	63.85
MS	02430690	35	19881229	19950905	177.8	8877	51.1	388	8.39
MS	02431000	170	19740925	19980721	378.0	19000	1385.0	1585	11.99
MS	02431410	129	19881122	19950905	169.0	35628	225.0	173	205.5
MS	02433500	61	19890105	19980430	584.0	16489	1943.0	3175	5.19
MS	02436500	204	19740925	19950726	650.0	129237	719.0	1606	80.5
MS	02437500	88	19740926	19980429	614.0	13000	3200.0	5623	2.31
MS	02439400	71	19740926	19980429	476.0	2578	294.0	2067	1.25
MS	02441498	36	19890305	19970307	-	-	519.2	-	-
MS	02443500	65	19881115	19980428	376.0	1610	340.0	1852	0.87
MS	02448000	189	19740910	19950907	266.0	1300	422.0	1989	0.7
MS	02472373	45	19750120	19810812	501.9	153723	291.5	2696	4.02
MS	02472880	41	19771007	19810812	375.0	284249	124.9	1564	11.44
MS	02473260	51	19740909	19810812	674.7	676765	619.1	4685	4.56
MS	02473460	32	19760512	19791007	126.0	947	51.0	264	3.59

State	Station Number	n	Start date	End date	Q _{1.5}	Sediment load at Q _{1.5}	Maximum sampled Q	Area	Sediment yield at Q _{1.5}
			(yyyymmdd)	(yyyymmdd)	(m ³ /s)	(T/D)	(m ³ /s)	(km ²)	(T/D/km ²)
MS	02473490	41	19740910	19791007	208.1	4563	51.4	521	3.03
MS	02474740	43	19771006	19810812	845.0	11661	1832.4	7798	1.50
MS	02477492	43	19771006	19810813	641.8	178092	508.1	4268	2.71
MS	02478500	53	19740910	19810813	533.0	7617	983.0	6967	1.09
MS	02479020	154	19731127	19950629	1357.9	593477	3303.8	17300	0.82
MS	02479155	138	19731030	19960822	74.0	1722	105.0	136	12.64
MS	02479560	32	19851016	19930818	228.0	2222	170.0	1455	1.53
MS	02481510	49	19780106	19860723	247.0	3432	343.0	798	4.30
MS	03592800	37	19770608	19780201	101.0	2566	165.0	370	6.93
MS	07274235	94	19880422	19950510	37.7	520	20.0	21.4	52.94
MS	07274237	89	19880422	19950510	62.1	1121	17.8	54.4	24.51
MS	07274245	97	19880422	19950510	95.1	21974	62.2	121	120.4
MS	07274247	97	19880422	19950510	121.9	20000	118.0	192	104.2
MS	07274251	93	19880422	19950510	20.0	5000	14.5	5.83	833.3
MS	07274252	91	19871116	19970722	154.0	35000	461.0	251	139.4
MS	332030088212 200	36	19940211	19970307	700.4	2748	2526.4	14199	0.19
MS	332100088224 500	36	19940211	19970307	700.4	28530	444.2	14199	2.01
MS	332112088223 500	36	19940211	19970307	700.2	3567	2804.1	14195	0.25
MS	332751088261 000	36	19890305	19970307	631.4	5039	1932.3	11958	0.42
MS	332929088273 300	36	19890305	19970307	631.0	3351	2393.2	11945	0.28
NC	02080500	143	19750902	19951127	873.0	907	982.8	21713	0.04
NC	02081000	38	19741001	19761201	798.0	1083	916.2	22457	0.05
NC	02083000	31	19750903	19790907	102.0	550	157.1	1362	0.40
NC	02083500	198	19730828	19970219	324.0	1355	524.7	5654	0.24
NC	02083833	48	19930309	19961115	4.0	12	4.9	28.5	0.41
NC	02087570	96	19731221	19960913	216.0	2169	235.4	3123	0.69
NC	02089500	218	19730828	19980929	301.0	789	741.3	6972	0.11
NC	02090625	32	19730829	19780505	2.0	12	16.7	5.44	2.28
NC	02091500	172	19750904	19980929	89.0	191	159.4	1898	0.10
NC	02091700	38	19750824	19950607	33.0	98	86.3	242	0.41
NC	02102500	39	19731221	19830927	922.0	23984	1277.1	8971	2.67
NC	02102908	30	19750730	19790905	3.0	34	7.5	19.8	1.72
NC	02106000	34	19750825	19790907	19.0	17	47.2	240	0.07
NC	02106500	35	19750825	19840921	96.0	83	385.9	1751	0.05
NC	02106648	81	19770307	19810815	14.0	13	16.7	96.6	0.13
NC	02106681	92	19770307	19810815	16.0	73	25.0	125	0.58
NC	0210782005	101	19820813	19900809	6.0	6	16.0	21.5	0.28
NC	0210787855	102	19830915	19900809	4.0	5	8.1	15.5	0.34
NC	0210788875	104	19830915	19900809	9.0	8	38.3	52.1	0.16
NC	0210789100	105	19820813	19900809	9.0	9	39.1	58.5	0.15

State	Station Number	n	Start date	End date	Q _{1.5}	Sediment load at Q _{1.5}	Maximum sampled Q	Area	Sediment yield at Q _{1.5}
			(yyyymmdd)	(yyyymmdd)	(m ³ /s)	(T/D)	(m ³ /s)	(km ²)	(T/D/km ²)
NC	0210789120	98	19830915	19900809	13.0	13	54.7	91.9	0.14
NC	02129000	108	19730905	19860903	1737.0	7190	1679.7	17774	0.40
NC	02133500	30	19750730	19790907	28.0	16	67.7	474	0.03
SC	02131000	120	19771026	19950928	948.0	2662	1299.3	22868	0.12
SC	02135300	191	19730130	19960724	15.0	6	18.4	249	0.02
SC	02169500	38	19771027	19970909	1749.0	12636	1489.2	20330	0.62
SC	02169570	73	19951010	19980513	25.0	115	35.3	154	0.75
SC	02171500	45	19740116	19770913	407.0	713	554.2	38071	0.02
SC	02197300	144	19730214	19930928	9.0	4	32.5	256	0.02
TN	03593005	117	19750423	19940616	9515.0	13092	4822.4	84999	0.15
TN	07024300	39	19790725	19860912	75.0	2994	197.7	144	20.83
TN	07029410	53	19770303	19780503	74.0	4538	102.7	123	36.81
TN	07029425	45	19770303	19780503	349.0	11952	616.3	2675	4.47
TN	07029500	125	19770304	19950803	404.0	188	852.3	3833	0.05
VA	01668000	130	19771230	19941109	657.0	9415	1365.9	4133	2.28
VA	01673000	168	19741016	19990125	214.0	1056	416.4	2800	0.38
VA	01674500	114	19790410	19990127	79.0	134	102.8	1556	0.09
VA	02038700	54	19750813	19790227	-	-	3803.5	-	
VA	02041650	115	19771228	19990125	240.0	468	369.2	3481	0.13
VA	0204228301	82	19931205	19940617	0.1	1	0.0	0.005	100
VA	02047000	109	19771215	19960926	189.0	307	383.1	3680	0.08
VA	02052000	67	19790418	19930818	208.0	66	83.3	1935	0.03

APPENDIX D – UNIT CONVERSIONS

Quantity	From: Referenced Units	To: English Units	Multiply By:
Acceleration	m/s ²	ft/s ²	3.280840
Area	m ²	ft ²	10.76391
	km ²	mi ²	0.3861007
	ha	ac	2.471044
Concentration	mg/l	ppm	1.0
Density	kg/m ³	lb/ft ³	0.0624280
Erodibility Coefficient	cm ³ /(N· s)	ft ³ /(lb· s)	0.0001570874
	m ³ /(N· s)	ft ³ /(lb· s)	157.0874
Flow, volume	m ³ /s	ft ³ /s	35.31466
Length	mm	in.	0.03937008
	m	ft	3.280840
	km	mi	0.6213712
Mass	Tonne	Ton	1.102311
Mass per time	Tonne/d	Ton/d	1.102311
	Tonne/y	Ton/y	1.102311
Mass per time per length	Tonne/y/m	Ton/y/ft	0.3359844
	Tonne/y/km	Ton/y/mi	1.773998
Mass per time per area	Tonne/d/km ²	Ton/d/mi ²	2.854972
	Tonne/y/km ²	Ton/y/mi ²	2.854972
	Tonne/y/ha	Ton/y/ac	0.4460912
Pressure	Pa	lb/in. ² (psi)	0.0001450377
	kPa	lb/in. ² (psi)	0.1450377
Unit Weight	N/m ³	lb/ft ³	0.006365881
	kN/m ³	lb/ft ³	6.365881
Velocity, linear	mm/y	in/y	0.03937008
	m/s	ft/s	3.280840